



UNIL | Université de Lausanne

Unicentre

CH-1015 Lausanne

<http://serval.unil.ch>

---

Year : 2021

## Defining the mechanism of action in a novel class of anti-PD-1 antibodies

Joo Victor

Joo Victor, 2021, Defining the mechanism of action in a novel class of anti-PD-1 antibodies

Originally published at : Thesis, University of Lausanne

Posted at the University of Lausanne Open Archive <http://serval.unil.ch>

Document URN : urn:nbn:ch:serval-BIB\_6986325599052

### **Droits d'auteur**

L'Université de Lausanne attire expressément l'attention des utilisateurs sur le fait que tous les documents publiés dans l'Archive SERVAL sont protégés par le droit d'auteur, conformément à la loi fédérale sur le droit d'auteur et les droits voisins (LDA). A ce titre, il est indispensable d'obtenir le consentement préalable de l'auteur et/ou de l'éditeur avant toute utilisation d'une oeuvre ou d'une partie d'une oeuvre ne relevant pas d'une utilisation à des fins personnelles au sens de la LDA (art. 19, al. 1 lettre a). A défaut, tout contrevenant s'expose aux sanctions prévues par cette loi. Nous déclinons toute responsabilité en la matière.

### **Copyright**

The University of Lausanne expressly draws the attention of users to the fact that all documents published in the SERVAL Archive are protected by copyright in accordance with federal law on copyright and similar rights (LDA). Accordingly it is indispensable to obtain prior consent from the author and/or publisher before any use of a work or part of a work for purposes other than personal use within the meaning of LDA (art. 19, para. 1 letter a). Failure to do so will expose offenders to the sanctions laid down by this law. We accept no liability in this respect.



**UNIL** | Université de Lausanne

Faculté de biologie  
et de médecine

**Defining the mechanism of action in a novel class of anti-PD-1  
antibodies**

**Thèse de Doctorat en Sciences de la Vie (PhD)**

Présentée à la

Faculté de Biologie et Médecine

de l'Université de Lausanne

par

**Victor Joo**

MSc Immunology of Infectious Diseases

London School of Hygiene and Tropical Medicine, UK

**PhD Committee:**

Prof. François Bochud, Président

Prof. Giuseppe Pantaleo, Directeur de Thèse

Dr. Craig Fenwick, Co-directeur de Thèse

Prof. Margot Thome Miazza, Expert

Prof. Pedro Romero, Expert

Prof. Onur Boyman, External Expert

**Lausanne, January 2021**



UNIL | Université de Lausanne

Faculté de biologie  
et de médecine

**Ecole Doctorale**

**Doctorat ès sciences de la vie**

# Imprimatur

Vu le rapport présenté par le jury d'examen, composé de

<b>Président·e</b>	Monsieur	Prof.	François	<b>Bochud</b>
<b>Directeur·trice de thèse</b>	Monsieur	Prof.	Giuseppe	<b>Pantaleo</b>
<b>Co-directeur·trice</b>	Monsieur	Dr	Craig	<b>Fenwick</b>
<b>Expert·e·s</b>	Madame	Prof.	Margot	<b>Thome Miazza</b>
	Monsieur	Prof.	Pedro	<b>Romero</b>
	Monsieur	Prof.	Onur	<b>Boyman</b>

le Conseil de Faculté autorise l'impression de la thèse de

## **Monsieur Victor S Joo**

Master in Immunology of infectious diseases,  
London School of Hygiene and Tropical Medicine, Royaume-Uni

intitulée

## **Defining the mechanism of action in a novel class of anti-PD-1 antibodies**

Date de l'examen : 12 janvier 2021

Date d'émission de l'imprimatur : Lausanne, le 10 février 2021

pour le Doyen  
de la Faculté de biologie et de médecine

Prof. Niko GELDNER  
Directeur de l'Ecole Doctorale

## Table of Contents

<b>Acknowledgments</b> .....	<b>4</b>
<b>Abstract (in English)</b> .....	<b>5</b>
<b>Abstract (en Français)</b> .....	<b>6</b>
<b>List of Abbreviations</b> .....	<b>8</b>
<b>List of Figures</b> .....	<b>9</b>
<b>CHAPTER I: INTRODUCTION</b> .....	<b>10</b>
1.1 T cell activation and inhibition .....	10
1.1.1 Requirements of TCR engagement.....	10
1.1.2 Early T cell signaling.....	10
1.1.3 Formation of the immunological synapse.....	12
1.1.4 T cell signaling pathway .....	13
1.1.5 Downstream of the signaling cascade .....	14
1.1.6 Costimulation.....	16
1.1.7 Costimulatory receptors (Signal 2).....	16
1.1.8 Cytokines during T cell activation (Signal 3).....	19
1.1.9 Inhibition of T cell activation .....	19
1.1.10 Coinhibitory receptors .....	21
1.2 The PD-1 receptor.....	23
1.2.1 Expression and function of PD-1 .....	24
1.2.2 Ligands of PD-1 .....	26
1.2.3 PD-1 signaling pathway.....	27
1.2.4 T cell memory and exhaustion.....	28
1.3 Monoclonal antibodies .....	29
1.3.1 Characteristics of mAbs in immunotherapy .....	31
1.3.2 Fc $\gamma$ Receptors .....	32
1.3.3 Antibody effector function .....	32
1.3.4 Immunomodulatory antibodies .....	34
1.3.5 PD-1 antibodies .....	35
<b>CHAPTER II: RESULTS</b> .....	<b>40</b>
Paper I: Tumor Suppression of Novel Anti-PD-1 Antibodies Mediated Through CD28 Costimulatory Pathway.....	40
Paper II. T-cell exhaustion in HIV infection .....	41
Paper III. An Alternative Fc-mediated Mechanism of Regulating PD-1 Expression in Anti- PD-1 Therapy (Manuscript in preparation). .....	41

<b>CHAPTER III: DISCUSSION.....</b>	<b>43</b>
<b>CHAPTER IV: REFERENCES .....</b>	<b>51</b>
<b>ADDENDUM THESIS PROJECT.....</b>	<b>130</b>
<b>Abstract (in English).....</b>	<b>130</b>
<b>Abstract (en Français).....</b>	<b>131</b>
<b>List of Abbreviations.....</b>	<b>133</b>
<b>List of Figures.....</b>	<b>134</b>
<b>CHAPTER V: INTRODUCTION.....</b>	<b>135</b>
5.1 Influenza classification and epidemiology.....	135
5.2 Influenza viral proteins.....	136
5.3 Influenza replication cycle and pathogenesis.....	137
5.4 Influenza vaccines .....	138
5.5 Immune correlates of protection .....	139
5.6 Influenza vaccination in the elderly .....	141
<b>CHAPTER VI: RESULTS.....</b>	<b>142</b>
Paper I: Circulating CXCR3 <sup>+</sup> Tfh and Antigen-specific B cells Expand in Elderly individuals During Influenza Vaccination (Manuscript in preparation).....	142
<b>CHAPTER VII: DISCUSSION.....</b>	<b>143</b>
<b>CHAPTER VIII: REFERENCES .....</b>	<b>147</b>

## ACKNOWLEDGMENTS

---

I would like to thank, first and foremost, Professor Giuseppe Pantaleo for accepting me to do my PhD in his laboratory for all these remarkable years. Under his guidance, instruction, and insightful words of wisdom, I feel like I have learned much about the field of immunology and the research methodology. The Professor had also permitted me a large degree of freedom in the experimental design and hypothesis testing which allowed me to think more independently and critically and I am truly grateful for that.

I would also like to thank my thesis co-director, Dr. Craig Fenwick. He was instrumental in my day-to-day supervision and his guidance allowed me to progress to the completion of my degree. We have had countless, great discussions which became integral to the results of this work and I was very lucky to have been part of his group. Also, I would like to thank fellow group members Alex, Navina, Line, and Celine who have helped me critically along this journey with their technical support and who I have worked closely with over the years. I would like to thank other members of the laboratory for their friendship and support over these many years. I would first like to thank Dr. Alessandra Noto and Dr. Francesco Procopio, both of whom I have known personally since working at VGTI Florida over 8 years ago. You guys are family to me and I want to formally thank you for all your kindness at work or at home over these years that have inspired me to keep moving forward. I would also like to thank other members of the lab such as Antonio, Morgane, Madeleine, Erica, and Patricia for their help and support and for keeping my sanity in check. I would also like to thank the members of the VIC for their work in maintaining the samples and databases which I had frequently used and needed.

I would like to thank my family for their support and understanding during this journey: my parents Bae Seok and Meong Seon, my sister Rose, and my entire extended family in the US and Korea who have supported me with love and care throughout the years. In particular, I would like to thank my grandmother, Bong Sung Ham, who sadly passed away in April 2020 at the age of 95. My grandmother lived through Japanese colonial occupation, escaped from the North during the Korean War, endured the autocratic governments of the early Korean Republic, raised our entire extended family, and brought my immediate family to America for a better life. She had raised me since I was born and was my main inspiration for pursuing higher education. I stand here now at the end of my PhD because of her boundless love and guidance over all these years. Thank you, Grandma.

Finally, I would like to thank my wife, Young Sun Kim, for her incredible love, sacrifice, patience, and endless support. We have been through everything together and I would not be here today without her love and encouragement.

## ABSTRACT

---

**Background.** Despite the relative success of anti-PD-1 antibodies over the years in cancer immunotherapy, the mechanism of action beyond blockade of the ligand binding site remains inadequately defined. Given that anti-PD-1 therapy is effective in only a fraction of cancer patients, it is imperative to elucidate the mechanisms imparted by anti-PD-1 antibodies and how they are involved in restoring activity to functionally exhausted PD-1<sup>+</sup> memory T cells.

**Hypothesis.** The two hypotheses investigated are: 1) The novel non-blocking anti-PD-1 antibody discovered in our lab differs in its mechanism of action from the traditional blocking PD-1 antibodies, 2) Anti-PD-1 mediated downregulation contributes to the relief of T cell exhaustion and occurs through an antibody-Fc interaction with Fc $\gamma$ R expressing cells.

**Objectives.** The research plans are: 1) to develop an experimental strategy to evaluate the functional activity in primary, memory T cells responding to the anti-PD-1 therapies utilizing coinhibitory conditions with PD-L1 and 2) to identify the cell populations and associated determinants for anti-PD-1 mediated downregulation on primary, memory T cells.

**Experimental strategy.** 1) We used PBMCs isolated from chronically infected HIV<sup>+</sup> donors with high expression of PD-1 to measure the activation of key mediators of the T cell activation pathway. We were able to evaluate the restoration of phosphoprotein activity and calcium signaling to these functionally exhausted primary T cells at early timepoints when stimulated by CD3/CD28/PD-L1 and treated with anti-PD-1. 2) We isolated different fractions of the PBMC composition to determine if any effector cells were involved in PD-1 downregulation. Furthermore, we sought to establish a contact-based dependency test to determine which receptor was necessary for the anti-PD-1 downregulation effect.

**Results.** 1) We demonstrated that both blocking and non-blocking antibodies were able to restore T cell signaling but the non-blocking antibody restored significantly more Akt signaling and the combination of the two anti-PD-1 antibodies enhanced the restoration of Ca<sup>2+</sup> signaling dramatically. 2) Anti-PD-1 mediated downregulation was observed only in the presence of monocytes and CD64 was found to be the Fc $\gamma$ R with the highest impact for this effect.

**Conclusions.** 1) The non-blocking PD-1 antibody was shown to be effective in restoring T cell functionality and appeared to preferentially restore signaling through the CD28 associated pathway while the blocking PD-1 antibody exerted its effect over the TCR pathway. 2) The requirement for CD64 expressing monocytes was shown for the antibody-mediated downregulation of PD-1 on memory T cells.

## ABSTRACT (en Français)

---

**Contexte:** Malgré le succès relatif des anticorps anti-PD-1 au fil des années dans l'immunothérapie anticancéreuse, le mécanisme d'action au-delà du blocage du site de liaison du ligand reste mal défini. Étant donné que le traitement anti-PD-1 n'est efficace que chez une fraction des patients cancéreux, il est impératif d'élucider les mécanismes conférés par les anticorps anti-PD-1 et comment ils sont impliqués dans la restauration de l'activité de la mémoire PD-1<sup>+</sup> fonctionnellement épuisée T cellules.

**Hypothèse:** Les deux hypothèses étudiées sont: 1) Le nouvel anticorps anti-PD-1 non bloquant découvert dans notre laboratoire diffère dans son mécanisme d'action des anticorps bloquants traditionnels PD-1, 2) La régulation négative médiée par anti-PD-1 contribue à la soulagement de l'épuisement des cellules T et se produit par le biais d'une interaction anticorps-Fc avec les cellules exprimant Fc $\gamma$ R.

**Objectifs:** Les plans de recherche sont les suivants: 1) développer une stratégie expérimentale pour évaluer l'activité fonctionnelle des lymphocytes T mémoires primaires répondant aux thérapies anti-PD-1 utilisant des conditions co-inhibitrices avec PD-L1 et 2) pour identifier les populations cellulaires et les déterminants associés pour la régulation négative à médiation anti-PD-1 sur les lymphocytes T primaires à mémoire.

**Stratégie expérimentale:** 1) Nous avons utilisé des PBMC isolées de donneurs VIH + infectés de manière chronique avec une forte expression de PD-1 pour mesurer l'activation de médiateurs clés de la voie d'activation des lymphocytes T. Nous avons pu évaluer la restauration de l'activité des phosphoprotéines et la signalisation du calcium vers ces lymphocytes T primaires fonctionnellement épuisés à des moments précoces lorsqu'ils sont stimulés par CD3 / CD28 / PD-L1 et traités avec de l'anti-PD-1. 2) Nous avons isolé différentes fractions de la composition de PBMC pour déterminer si des cellules effectrices étaient impliquées dans la régulation négative de PD-1. En outre, nous avons cherché à établir un test de dépendance basé sur le contact pour déterminer quel récepteur était nécessaire pour l'effet de régulation négative anti-PD-1.

**Résultats:** 1) Nous avons démontré que les anticorps bloquants et non bloquants étaient capables de restaurer la signalisation des lymphocytes T, mais l'anticorps non bloquant a restauré significativement plus de signalisation Akt et la combinaison des deux anticorps anti-PD-1 a considérablement amélioré la restauration de la signalisation Ca<sup>2+</sup>. 2) une régulation négative à médiation anti-PD-1 a été observée uniquement en présence de monocytes et CD64 s'est avéré être le Fc $\gamma$ R avec l'impact le plus élevé pour cet effet.

**Conclusion:** 1) L'anticorps PD-1 non bloquant s'est avéré efficace pour restaurer la fonctionnalité des lymphocytes T et semblait restaurer préférentiellement la signalisation via la voie associée au CD28 tandis que l'anticorps bloquant PD-1 exerçait son effet sur la voie TCR. 2) L'exigence de monocytes exprimant CD64 a été montrée pour la régulation à la baisse médiée par les anticorps de PD-1 sur les cellules T mémoire.

## LIST OF ABBREVIATIONS

---

1. **TCR:** T cell receptor
2. **MHC:** major histocompatibility complex
3. **APC:** antigen-presenting cell
4. **PBMC:** Peripheral blood mononuclear cell
5. **CDR:** complementarity-determining region
6. **ITAM:** immune tyrosine-based activation motif
7. **ITIM:** immune tyrosine-based inhibitory motif
8. **ITSM:** immune tyrosine-based switch motif
9. **SMAC:** supramolecular activation cluster
10. **ZAP-70:** zeta-chain-associated protein kinase 70
11. **LAT:** linker for activation of T cells
12. **PLC $\gamma$ 1:** phospholipase C, gamma 1
13. **SLP-76:** SH2 domain containing leukocyte protein of 76kDa
14. **PIP2/3:** phosphatidylinositol 4,5-bisphosphate/triphosphate
15. **PI3K:** phosphoinositide 3-kinase
16. **Akt:** protein kinase B
17. **PDK1:** pyruvate dehydrogenase kinase 1
18. **ITK:** IL-2 inducible T cell kinase
19. **Lck:** lymphocyte-specific protein tyrosine kinase
20. **Erk:** extracellular signal-regulated kinase
21. **Csk:** C-terminal Src kinase
22. **NFAT:** nuclear factor of activated T cells
23. **NF- $\kappa$ B:** nuclear factor kappa-light-chain-enhancer of activated B cells
24. **AP-1:** activator protein 1
25. **CTLA-4:** cytotoxic T-lymphocyte-associated protein 4
26. **PD-1:** programmed cell death protein 1
27. **PD-L1:** programmed death ligand 1
28. **LAG-3:** lymphocyte-activation gene 3
29. **Tim-3:** T-cell immunoglobulin and mucin-domain containing-3
30. **SHP1/2:** Src homology region 2 domain-containing phosphatase 1/2
31. **SHIP1:** Src homology 2 domain containing inositol polyphosphate 5-phosphatase 1
32. **TSS:** transcription start sites
33. **TCF1:** transcription factor T cell factor 1
34. **IRF4:** interferon regulatory factor 4
35. **NR4A:** nuclear receptor subfamily 4 group A member 1
36. **Treg:** regulatory T cells
37. **ADCC:** antibody-dependent cellular cytotoxicity
38. **ADCP:** antibody-dependent cellular phagocytosis
39. **CDC:** complement-dependent cytotoxicity
40. **IgG:** immunoglobulin G
41. **mAb:** monoclonal antibody
42. **Fc $\gamma$ R:** Fc-gamma receptor
43. **IFN $\gamma$ :** Interferon gamma
44. **TNF- $\alpha$ :** Tumor necrosis factor alpha
45. **IL-2:** Interleukin-2
46. **TIL:** tumor infiltrating lymphocyte

## LIST OF FIGURES

---

**FIGURE 1:** T cell signaling pathway

**FIGURE 2:** Immunological synapse and associated receptors

**FIGURE 3:** Calcium flux and the NFAT pathway

**FIGURE 4:** CD28 costimulatory pathway

**FIGURE 5:** T cell anergy mediated by Cbl-b and T cell activation mediated by CD28

**FIGURE 6:** Coinhibitory receptors and their inhibitory functions.

**FIGURE 7:** Schematic of PD-1 and CTLA-4

**FIGURE 8:** T cell exhaustion pathway

**FIGURE 9:** Antibody structure and functional relationships.

**FIGURE 10:** IgG subclasses and their sites for allotype variation

## CHAPTER I: INTRODUCTION

---

Cancer immunotherapy has been revolutionized over the last decade. In 2018, the Nobel Prize in Medicine or Physiology was awarded to James Allison and Tasuku Honjo for their discovery of immune checkpoint inhibitors. The legacy behind these lifetime achievements is the culmination of decades of research in the foundations of T cell activation and inhibition that have built up our current knowledge. In this thesis, we will begin with an introduction on the fundamentals of T cell activation and inhibition before proceeding to a more in-depth focus on the PD-1 receptor itself and lastly, the current paradigm of monoclonal antibody therapy.

### 1.1 T cell activation and inhibition

#### 1.1.1 Requirements of TCR Engagement

The main principle of cell-mediated adaptive immunity lies within the breadth and specificity of the T cell response. It is estimated that  $10^{10}$  different T cell clonotypes are maintained in the human body at any given time, reflecting the vast diversity of antigen recognition[1]. The initiation of T cell activation is dependent on the specific recognition by a T cell receptor (TCR) to its corresponding peptide bound to a major histocompatibility complex (MHC) expressed by an antigen-presenting cell (APC)[2].

CD4<sup>+</sup> expressing T cells, also known as helper T cells, typically recognize peptides fragments of 12–16 amino acids that are processed through endocytosis or phagocytosis by professional APCs (dendritic cells, monocytes/macrophages, and B cells) and presented by MHC-II. CD8<sup>+</sup> expressing T cells, known as cytolytic or killer T cells, recognize 9-10 amino-acid cytosolically derived peptide fragments processed through the proteasome and presented by MHC-I, which can be expressed on all nucleated cells and platelets.

#### 1.1.2 Early T cell signaling

The TCR is comprised of an  $\alpha$  and  $\beta$  subunit (to a minor degree,  $\gamma$  and  $\delta$  subunits), both with variable and constant regions and containing no signaling motifs on its cytoplasmic tail. More specifically, antigen recognition is determined by 3 complementarity-determining regions (CDR) present on variable domain of both  $\alpha/\beta$  subunits with CDR3 representing the bulk of this interaction and the TCR repertoire being generated by V(D)J recombination during somatic T cell development[3].

The non-covalent association of the TCR with CD3 $\epsilon\delta$ , CD3 $\epsilon\gamma$ , and CD3 $\zeta\zeta$  chains on the plasma membrane form the TCR complex and these associated components contain the obligatory immune tyrosine-based activation motifs (ITAM) in their cytoplasmic domains that implement the TCR signal (**Fig. 1**) [4].

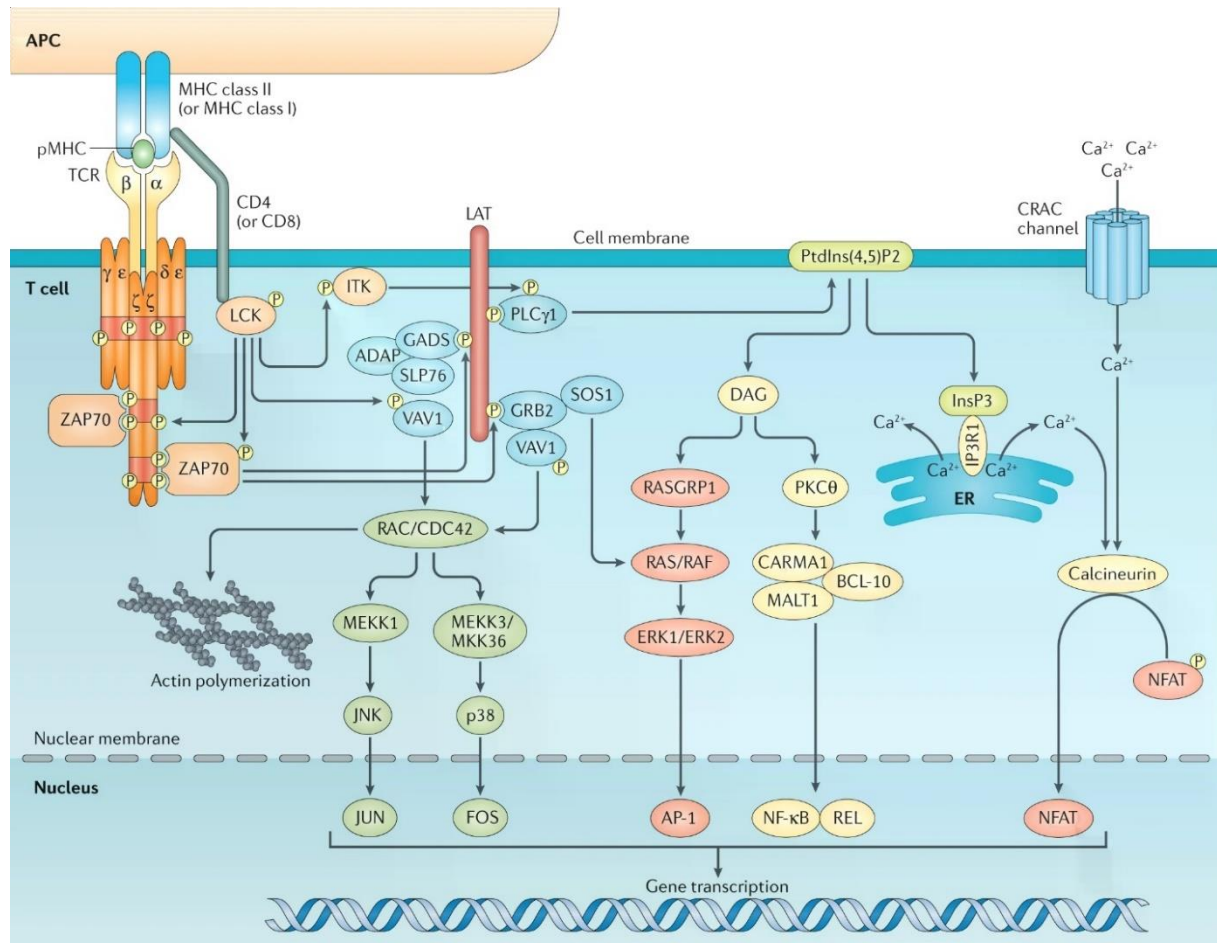


**Figure 1.** The T cell signaling pathway starting from antigen recognition to gene transcription. All major TCR pathways are shown. From Gaud G, Lesourne R, Love PE. *Nat Rev Immunol.* 2018 Aug;18(8):485-497.

The TCR-MHC binding is stabilized by the interaction of the MHC to either CD4 or CD8 coreceptors, which recruit the Src tyrosine kinase p65lck or Lck to concentrate intracellularly to the TCR complex and phosphorylate the associated CD3 signaling chains [5, 6]. Phosphorylation of CD3 $\zeta$  provides a binding site by its SH2 domain for ZAP-70 which then allows adjacent Lck/Fyn to phosphorylate ZAP-70 for catalytic activity and autophosphorylation [7]. The activated ZAP-70 subsequently leads to the formation of adaptor proteins such as LAT and SLP-76 that further recruits and propagates other phosphoproteins for the continuation of T cell signaling cascade [8].

### 1.1.3 Formation of the Immunological synapse

Before and during the initiation of the T cell activation, TCR microclusters form at the periphery which then serve as the site for initiating and sustaining TCR signals. These microclusters are formed upon TCR engagement through the merging of preexisting TCR nanoclusters that are distributed throughout the plasma membrane as multimeric complexes[9, 10]. It has been shown that memory T cells contain larger, linear clusters of TCR than naïve T cells, leading to enhanced sensitivity and a more rapid response upon antigen recognition[11]. These engaged microclusters move centripetally towards the center during the interaction between the T cell and APC and a highly ordered, specialized region called the immunological synapse (IS) is eventually formed[12, 13]. The IS represents the ~15nm gap between the T cell-APC conjugate formation and the structural organization of associated receptor-ligand activity and secretory molecules formed at the initiation and for the maintenance of T cell activation (Fig. 2)[14, 15].

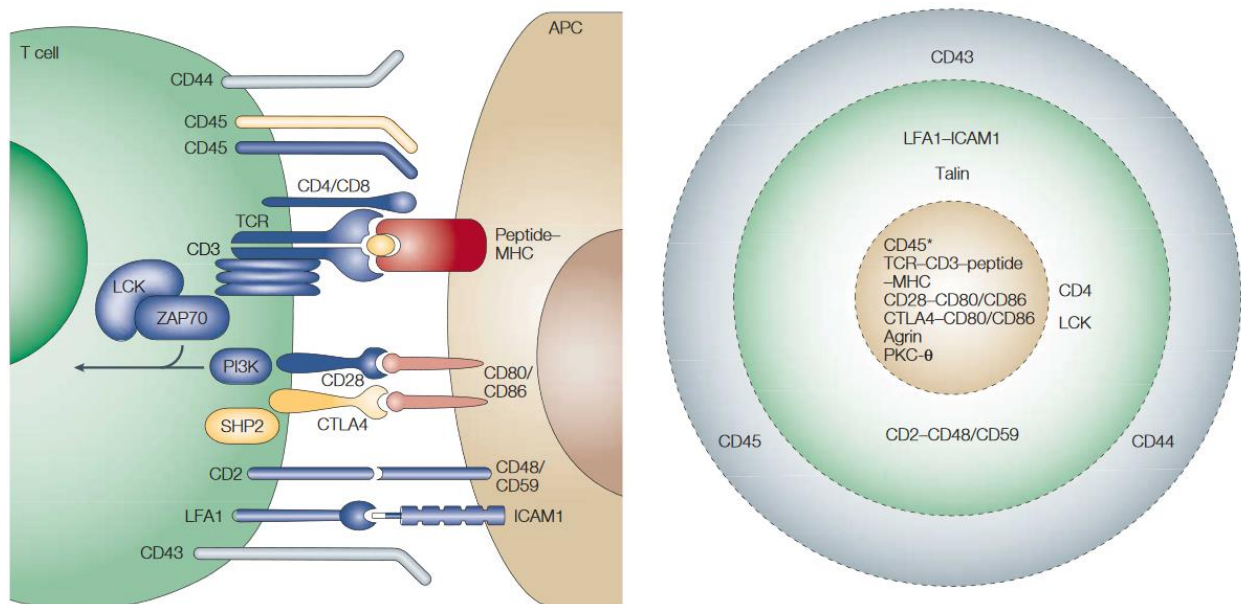


**Figure 2.** Immunological synapse and associated receptors. From Huppa JB, Davis MM. Nat Rev Immunol. 2003 Dec;3(12):973-83.

In its conventionally known form, the IS comprises of 3 concentric circles each denoted as a specific region of supramolecular activation clusters or SMAC - the center circle or c-SMAC (center-SMAC) which houses the TCR-MHC complexes and associated coreceptors such as CD28 or PD-1, its surrounding ring called the p-SMAC (peripheral-SMAC) containing adhesion molecules such as LFA-1 and CD43, and the outermost circle called the d-SMAC (distal-SMAC), which sterically segregates regulatory CD45 phosphatase receptors from TCR-

MHC activation site[15]. The c-SMAC itself can be further segregated into 2 components: the endo-cSMAC which contains the centermost TCR-enriched regions and the exo-cSMAC, a region surrounding the endo-cSMAC and which is TCR-poor, contains CD28 and PD-1 coreceptors, and acts as the site for exogenous secretory vesicles for cell-cell crosstalk[16].

These physical segregations provide spatial context into the contact interface between the T cell and APC as well as the cytoskeletal rearrangements and localization of signaling components that are necessary for T cell activation to occur.

#### **1.1.4 T cell signaling pathway**

Early TCR activation leads to the recruitment and phosphorylation of linker for activation of T cells (LAT) from the plasma membrane and subsynaptic vesicles. The transmembrane LAT protein contains a short extracellular region but a long cytoplasmic tail with multiple tyrosine residues that can be rapidly phosphorylated by ZAP-70 and further serves as binding sites for SH2 domain-containing proteins such as PLC $\gamma$ 1, Grb2, and Gads[17]. LAT also oligomerizes through the binding of Grb2 and Sos1 to form LAT microclusters, which act to amplify the TCR signaling cascade[18, 19].

Phosphorylated LAT recruits and binds to SH2-domain-containing leukocyte protein of 76 kDa (Slp76) via Gads and the docked SLP-76 further recruits more phosphoproteins such as Nck, ADAP, Vav, and Itk to the LAT complex, each recruited mediator acting on their own specific targets; for example, Vav – Rac/Cdc42 and ITK – PLC $\gamma$ 1[20, 21].

The resulting LAT/ SLP-76 complex is then bound by phospholipase C- $\gamma$ 1 (PLC $\gamma$ 1), which propagates TCR signaling through the hydrolyzation of phosphatidylinositol bisphosphate (PIP<sub>2</sub>) to generate diacylglycerol (DAG) and inositol trisphosphate (IP<sub>3</sub>)[22]. Subsequently, DAG recruits downstream phosphoproteins to the plasma membrane such as Ras-GRP (RAS guanyl nucleotide releasing protein) and protein kinase C- $\theta$  (PKC $\theta$ ) that activate Ras for MAPK signaling pathway[23].

Phosphatidylinositol 3-kinase (PI3K) consists of a heterodimer containing a regulatory p85/p55 and a catalytic p110 subunit[24]. The main function of activated PI3K is the inclusion of phosphate onto the 3'-OH of the inositol group in phosphoinositides such as PIP<sub>2</sub> and thereby producing PIP<sub>3</sub> secondary messengers[24]. These phosphorylated lipids are located on inner leaflet of the plasma membrane and directly bind phosphoproteins containing a pleckstrin homology (PH) domain such as Akt and PDK1. PI3K activity is critical for translocation of

Akt to the plasma membrane[25, 26]. PI3K mediated catalyzation of PIP3 causes conformational changes in Akt phosphorylation sites T308 and S473 to be open to the kinase activity of PDK1 and mTORC2, respectively[27, 28].

These signaling phosphoproteins interact with numerous partners and the abrogation or loss of any critical phosphoprotein mediator can catastrophically disrupt signaling through other effectors. However, not all phosphoproteins involved in T cell signaling are necessary due to overlapping or compensatory roles. For example, it has been shown that *Itk*-deficient T cells were capable of cytokine production and proliferation under antigen stimulation[29]. Yet, these interconnected redundancies are critical for coordinating the different pieces of the TCR signaling network to ultimately initiate gene transcription for T cell activation.

### **1.1.5 Downstream of the signaling cascade**

The targets downstream of the TCR signaling cascade are the transcription factors NFAT (nuclear factor of activated T cells), AP1 (activator protein 1), and NF- $\kappa$ B (nuclear factor- $\kappa$ B) which bind the promoter and activate the transcription of the IL-2 gene[23, 30].

NFAT activity is modulated by intracellular concentrations of  $\text{Ca}^{2+}$  ions (**Fig. 3**)[31-33]. The transcription factor NFAT (containing five members) at steady state remains heavily phosphorylated and retained in the cytoplasm. TCR activation modulates cytoplasmic  $\text{Ca}^{2+}$  levels through the activity of PLC $\gamma$ . Activated PLC $\gamma$  hydrolyzes PIP2 into IP<sub>3</sub> which enters the  $\text{Ca}^{2+}$ -permeable ion channel IP<sub>3</sub> receptors (IP<sub>3</sub>R) in the endoplasmic reticulum (ER) and subsequently leads to ER depletion of  $\text{Ca}^{2+}$ [34, 35].  $\text{Ca}^{2+}$  sensors stromal interaction molecule 1 and 2 (STIM 1/2) on the ER interact with Orai1 on the plasma membrane and generate a massive, sustained influx of  $\text{Ca}^{2+}$  into the cytoplasmic space. As intracellular  $\text{Ca}^{2+}$  levels increase, the dephosphorylation of NFAT is facilitated by calcineurin and calmodulin, leading to nuclear translocation. Furthermore, the nuclear import of NFAT is also regulated by PI3K as well as the Akt mediated inhibition of GSK-3 $\beta$ [36-38].

The activation and heterodimerization of c-Fos and c-Jun to produce AP-1 occurs downstream of three converging MAPK signaling pathways: JNK, p38, and Erk. The JNK and p38 pathways are initiated by activated Rac in response to cellular stress and share MAP3K mediators[39]. The Erk pathway is initiated by the association of active Ras with Raf leading to MKK1 and/or MKK2 activation[40]. The phosphorylation of c-Fos and c-Jun proteins as

well as the upregulation of c-Fos and c-Jun transcription are mediated by MAPK signaling pathways, leading to the generation of AP-1 dimers[23, 40].

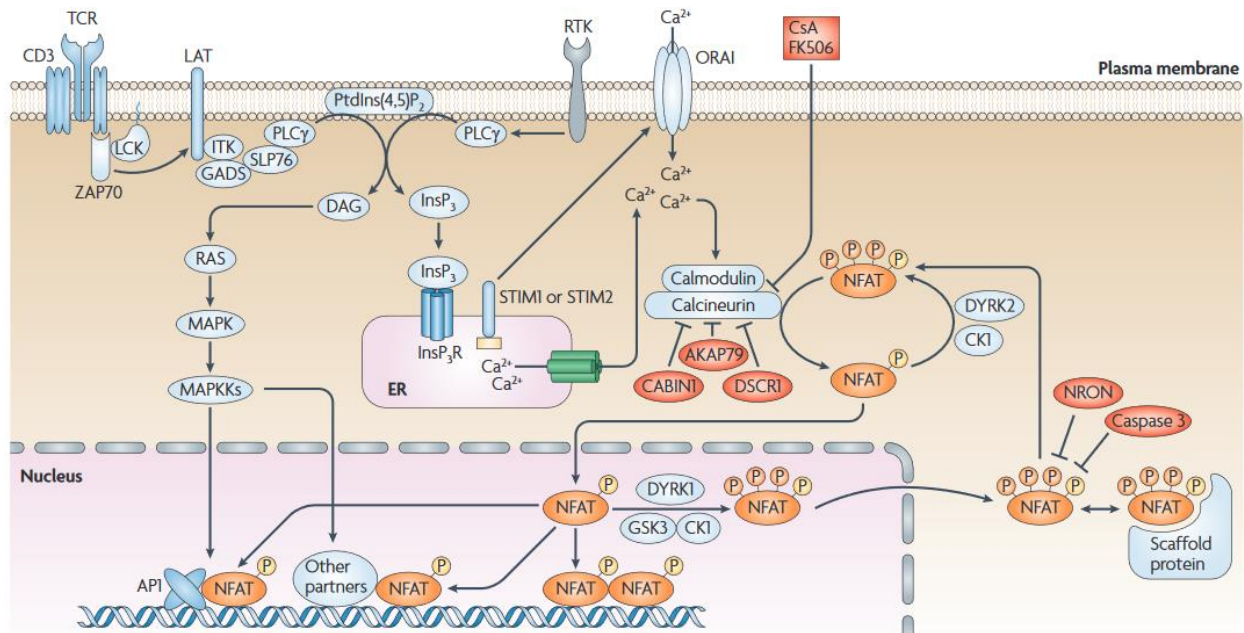


**Figure 3.** Calcium flux and the NFAT Pathway. From Müller MR, Rao A. Nat Rev Immunol. 2010 Sep;10(9):645-56.

The canonical pathway for NF- $\kappa$ B activation involves the degradation of protein inhibitor I $\kappa$ B by I $\kappa$ B kinase (IKK)[41]. The IKK complex is composed of catalytic IKK $\alpha$  and IKK $\beta$  subunits and regulatory subunit IKK $\gamma$ [42]. Like NFAT, NF- $\kappa$ B is present in the cytoplasmic space in an inactivated form typically as p50–RelA dimers bound by I $\kappa$ B. Following PKC $\theta$  activation, CARMA1 is phosphorylated, forming a complex with BCL10 and MALT1 (CBM complex), and MALT1 binds ubiquitin ligase TRAF6 for the polyubiquitination of MALT1 and BCL10[43, 44]. This ubiquitination motif causes IKK to be recruited and activated by TAK1, leading to the phosphorylation of I $\kappa$ B $\alpha$  for its proteasomal degradation and nuclear transport of NF- $\kappa$ B. The initiation of the PLC $\gamma$  pathway provides the substrates for the activation of both the NF- $\kappa$ B and NFAT pathways.

Beyond these established 3 transcription factors, numerous other transcription factors are involved in the differentiation program of T cell subtypes from antigen stimulation. Stronger TCR affinity results in increased expression of T-bet and BLIMP1, leading to the differentiation into effector CD8[45, 46]. The higher ratio of Eomes to T-bet and Bcl-6 expression from intermediate TCR signals dictates the formation of memory CD8[47]. In CD4, strong TCR stimulation is thought to prevent the early expression of IL-4, promote the generation of IFN $\gamma$ , and IL-12-dependent T-bet expression, polarizing CD4s towards Th1

subset[48]. On the other hand, lower levels of antigen seem to promote Th2 differentiation[49]. Reduced levels of CD28 coreceptor or low potency antigens have been shown to polarize CD4 into IL-17 producing Th17[48].

It is important to note that cell signaling does not occur as a one-way street; both positive feedforward and negative feedback loops regulate components of the signaling pathway. For example, Erk mediates phosphorylation on Lck Ser59 to prevent SHP1 binding and its subsequent inactivation, therefore sustaining Lck activity[50]. On the other hand, BCL10 is phosphorylated by components of IKK in order to be degraded through the ubiquitin-proteasomal pathway and reduce overall NF- $\kappa$ B activation[51]. TCR signaling, in parallel with signal modulation by costimulatory molecules, cytokines, chemokines, integrins, and metabolites drive T cells into distinct programs of activation, expansion, and differentiation of functionalized T cell subsets.

### **1.1.6 Costimulation**

T cell activation does not happen as a simplistic response of antigen recognition between the T cell and APC. Numerous coreceptors are involved in either enhancing or constraining the threshold for T cell responses. With the initial TCR-peptide-MHC engagement referred to as signal 1, the provision of costimulatory receptors to amplify that first signal is called signal 2 and the presence of cytokines enhancing T cell activation represents signal 3. A singular response of signal 1 leads to significantly reduced T cell responses, an anergic phenotype, or even cell death[52, 53]. It has been shown that the addition of signal 2 leads to dose-dependent increases in cell division and cell death responses[54]. In accordance with MHC expression, the ligands for costimulatory receptors are typically expressed by the same APCs which either constitutively express these ligands such as ICOS-L or are induced following exposure to an inflammatory environment (LPS, IFN $\gamma$ ) such as CD80 and CD86[55].

### **1.1.7 Costimulatory receptors (Signal 2)**

CD28 and the B7 family

The B7 family are a part of the larger Ig superfamily that encompass two costimulatory receptors CD28 and ICOS as well as their associated ligands, CD80 (B7-1) and CD86 (B7-2) for CD28 and ICOS-L for ICOS. Other B7 members - PD-1, BTLA and ligands PD-L1, PD-

L2, VISTA - represent the coinhibitory side of the B7 family and will be discussed in more detail in the later chapters.

The most fundamental and widely studied costimulatory receptor is CD28. Since its initial discovery as signal amplifier for anti-CD3 mediated T cell activation in 1986, CD28 has been found to drive a number of essential events in T cell activation via the modulation of phosphoprotein mediators and the production of key cytokines, chemokines, and survival signals necessary for the expansion and differentiation of T cells as well as the amplification of TCR signaling (**Fig. 4**)[56, 57]. The CD28 cytoplasmic tail contains a membrane proximal YMNM motif and a distal PYAP motif which binds through SH2/SH3 domain interactions with various phosphoprotein mediators such as p85 PI3K, Lck, and Grb2[57]. Furthermore, it has been shown that CD28 induced Rlp<sub>tr</sub> facilitates the recruitment of PKC $\theta$  and CARMA1 to the IS and that a single point mutation of Rlp<sub>tr</sub> resulted in a phenotype of CD28 signaling deficiency[58]. Most importantly, CD28 signaling is critical for NF- $\kappa$ B-mediated production of IL-2, leading to long-term expansion and the upregulation of Bcl-x<sub>L</sub> prosurvival factor for resistance to apoptosis[57, 59].

Costimulation by CD28 represents the most important pathway for the initial activation of naïve T cells and is constitutively expressed on resting CD4<sup>+</sup> and on 50-80% of CD8<sup>+</sup> T cells[60]. Chronic antigenic stimulation leads to downregulation of CD28 expression as a self-limiting negative feedback mechanism as well as the differentiation of antigen experienced memory T cells[61]. Furthermore, CD28 expression has been shown to decrease with age with up to 70% of CD4 and 95% of CD8 T cells being CD28<sup>-</sup> and is being used as a potential immunosenescence marker[62-64]. However, CD28 ligation is necessary as the starting point for naïve cells and in the recall response of memory T cells.

ICOS embodies the other costimulatory receptor of the B7 family and binds its own unique ligand, ICOS-L. Similar to CD28, ICOS shares a high degree of sequence homology and ICOS-L binding enhances the production of effector cytokines such as IL-4, IL-5, IFN $\gamma$ , and TNF $\alpha$ [65]. Unlike CD28, ICOS expression is not constitutively expressed and is induced under TCR and/or CD28 stimulation. Furthermore, ICOS signaling does not enhance IL-2 production but increases IL-10 production, indicating non-redundant roles with CD28 signaling[66].



### **1.1.8 Cytokines during T cell activation (Signal 3)**

The enhancement of TCR activation by secreted cytokines represent signal 3. Antigen-experienced memory T cells are able to respond to signal 3 (IL-2, IL-4, IL-7, IL-12, IL-15) alone and undergo proliferation and activation, but naive T cells can proliferate only in response to IL-7 in the absence of antigen. For naïve CD8, type I interferons and IL-12 has been shown for optimal expansion but not for the upregulation of anti-apoptotic genes[71]. Furthermore, these cytokines sustain the expression of CD25 (IL-2 receptor) leading to a greater IL-2 mediated proliferation via PI3K pathway[72]. For naïve CD4 activation, exogenous IL-1 has been shown to drive antigen-specific expansion and differentiation[73]. However, prior exposure to IL-2 in naïve CD4s were transiently abrogated in their ability to respond to antigen, indicating that timing is critical for optimal TCR stimulation[74].

### **1.1.9 Inhibition of T cell activation**

Negative feedback mechanisms

T cell activation is intrinsically modulated or attenuated by their incorporated feedback mechanisms within the TCR signaling pathway. The phosphorylation and dephosphorylation processes of TCR signaling molecules by inhibitory phosphoproteins affects the development of signaling complexes and influences the dissemination and magnitude of TCR signals.

Critical mediators of negative regulation at the signaling level are the protein tyrosine phosphatases (PTP) such as Src homology region 2 domain-containing phosphatase-1 (SHP1) and -2 (SHP2) which share a high sequence similarity, and Src homology 2 domain containing inositol polyphosphate 5-phosphatase 1 (SHIP1). PTPs are implicated in both positive and negative regulatory roles as well as in hematopoietic cell development. Within the context of TCR signaling, SHP1/2 dephosphorylate and deactivate both ZAP-70 and Lck, resulting in inactivation of the signaling cascade[75]. SHIP1 functions as an adaptor protein, enabling Dok1/2 anchoring to LAT for the regulation of ZAP-70 and AKT kinases as well as the removal of phosphate from PIP3 to attenuate PI3K signaling[76].

CD45 or protein tyrosine phosphatase receptor type C (PTPRC) is one of the most abundant transmembrane proteins on the T cell plasma membrane. CD45 plays both positive and negative regulatory roles and is required for TCR signaling for its activation of Lck [77, 78]. The dephosphorylation of Lck on the inhibitory C-terminal site (Tyr Y505) by CD45 has been shown to activate the Lck and enhance TCR responses. However, CD45 has also been

shown to associate and dephosphorylate the CD3  $\zeta$ -chains, indicating negative regulation of the TCR complex directly and the necessity for steric exclusion from the IS[79].

As a counterpart to the CD45 phosphatase, C-terminal Src kinase or Csk also inhibits TCR signaling by regulating Lck activity. Csk is notable for its phosphorylation of the Lck Y505 site, maintaining Lck conformation in an inactive form as well as its association with glycosphingolipid-enriched microdomains and phosphorylation of the inhibitory C-terminal tail of Fyn [80, 81].

PLC $\gamma$ 1 signaling can be regulated by diacylglycerol kinases (DGK) which generate phosphatidic acids through the phosphorylation of diacylglycerol and prevent PKC $\theta$  activity[82]. Both DGK $\alpha$  and DGK $\zeta$  act as crucial negative regulators downstream of the TCR and in Jurkat T cells, the silencing of DGK $\alpha$  or DGK $\zeta$  show increased TCR-induced signaling in Ras and PKC $\theta$  pathways leading to hyperproliferative responses [83].

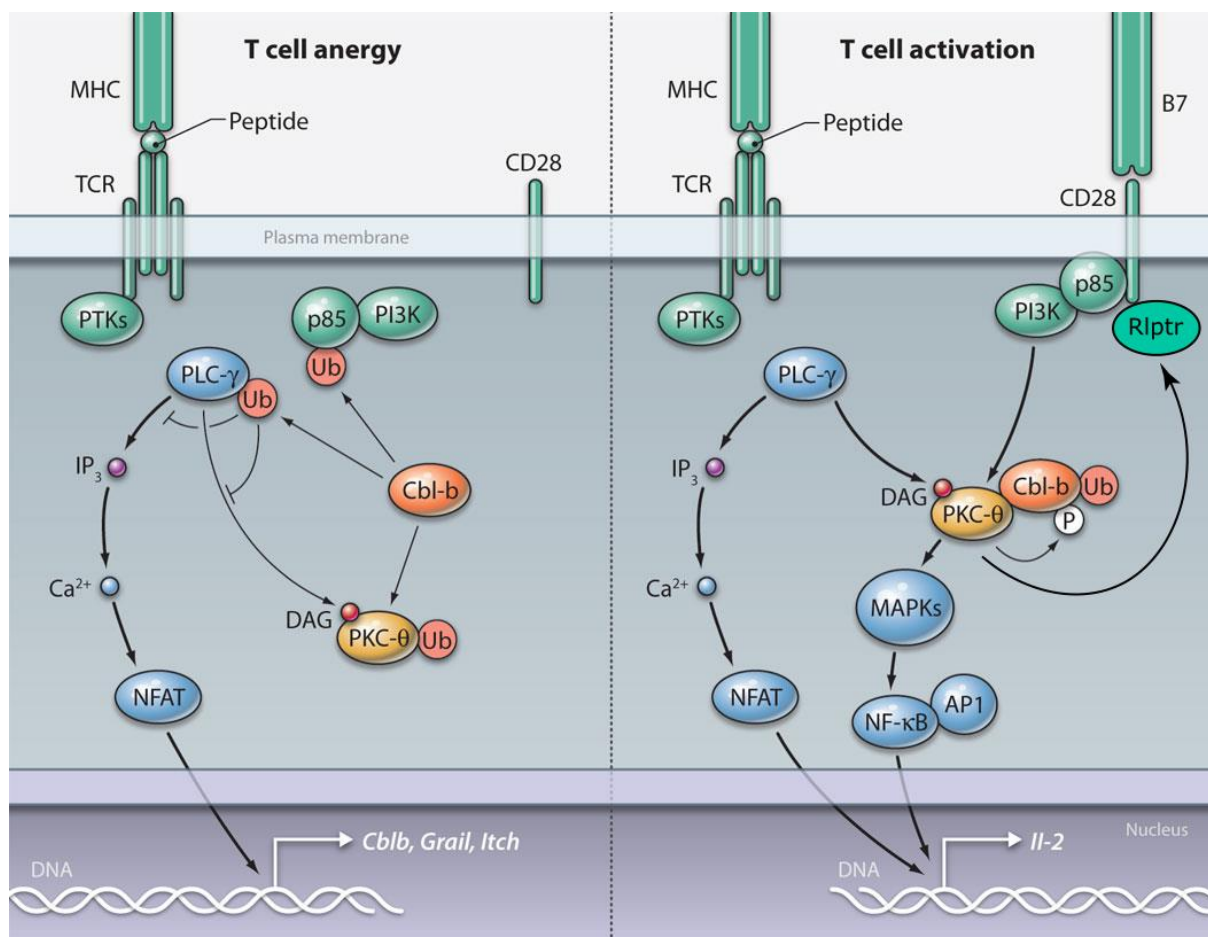


**Figure 5.** T cell energy mediated by Cbl-b and T cell activation mediated by CD28. Adapted from Schmitz ML. *Sci Signal*. 2009 Jun 23;2(76):pe38.

Numerous E3 ligases such as Cbl, Itch, and GRAIL are intermediaries of the ubiquitination-mediated degradation of TCR signaling components such as CD3 $\zeta$ , ZAP-70, PLC $\gamma$ 1, and PI3K (**Fig. 5**)[84]. More specifically, Cbl-b recognizes TCR signaling proteins for proteasomal degradation targeting Lck and ZAP-70 while Itch ubiquitinates Jun and reducing AP-1 activity[23]. Furthermore, both Cbl-b and Itch connect K33-linked ubiquitin chains to CD3 $\zeta$  and prevent the association of ZAP-70[85].

### 1.1.10 Coinhibitory receptors

The study of T cell coinhibitory receptors began with the discovery of cytotoxic T lymphocyte-associated antigen-4 (CTLA-4) in 1987 by the P. Golstein group as a receptor for B7 molecules that shared a high sequence similarity to CD28[86, 87]. Since this initial finding, many coinhibitory receptors such as BTLA, PD-1, LAG-3, TIGIT, and TIM-3 and others such as SLAM family members CD150 and 2B4 have been discovered and have ushered in a new era in the investigation for immunotherapeutics or more suitably called immune checkpoint blockade (**Fig. 6**).

CTLA-4 or CD152 is a CD28 family receptor that is present as a homodimer and has no intrinsic catalytic activity on its cytoplasmic tail. Given its similarity with CD28 as a homologue, it was not yet known in the early days whether CTLA-4 was a costimulatory or coinhibitory receptor. However, knockout studies of CTLA-4 showed that mice developed fatal lymphoproliferative disease with high lymphocyte infiltration and tissue destruction, revealing the role of CTLA-4 as a negative regulator or an immune checkpoint to maintain homeostasis[88]. Further experiments with CTLA-4 blockade showed increases in T cell proliferation and cytokine production, validating its role as a negative regulator of T cell activation[89, 90].

CTLA-4 also contains the YxxM motif similarly to CD28, but no agreement has been reached as to which potential inhibitory signaling components are involved[91]. Rather, the mechanism of action for CTLA-4 was found to occur by binding to the same ligands as CD28 with considerably higher affinity/ avidity and thereby sequestering CD28 ligands to impede a disproportionate immune response. The currently proposed model for CTLA-4 is trans-endocytosis, wherein CTLA-4 binds its ligands CD80 and CD86 on the APC to efficiently remove, internalize, and degrade those ligands[92]. This causes a physical, cell-extrinsic depletion of ligands for CD28 and as a result, an immunoregulatory mechanism for reduced CD28 signaling.

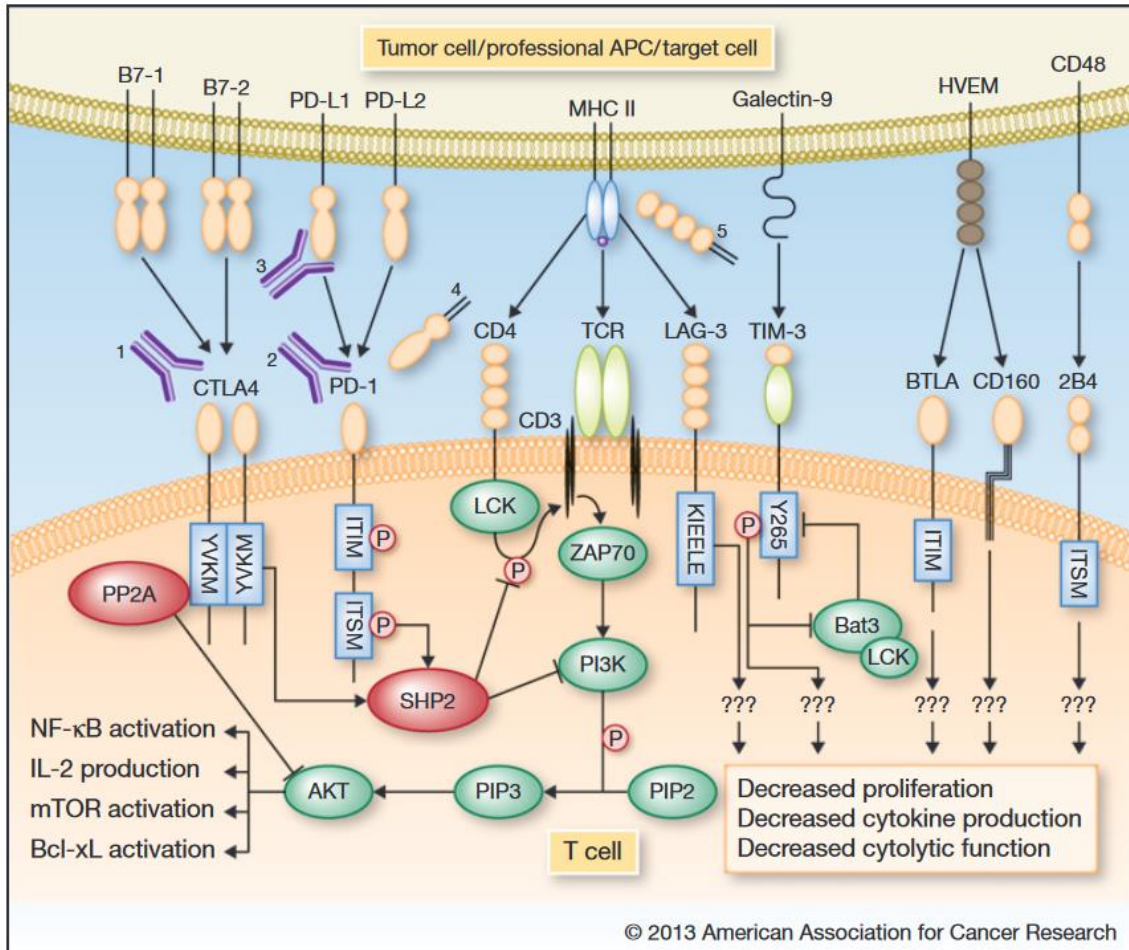


**Figure 6.** Coinhibitory receptors and their inhibitory functions. From Nirschl CJ, Drake CG. Clin Cancer Res. 2013 Sep 15;19(18):4917-24.

The coinhibitory B7 family is most notable for its coinhibitory receptor PD-1, which will be discussed more in the following chapter. Other more recently discovered B7 members, B7-H3 to B7-H7, are undergoing active research to characterize their functions and ligands given their impact in T cell suppression and have been found to be generally coinhibitory [93].

LAG-3 is a type I transmembrane protein with highly similar structural motifs with the CD4 receptor. Like CD4, LAG-3 also binds to MHC-II from APCs but with a much greater affinity. However, it has not been confirmed that inhibitory action occurs competitively with CD4 [94]. Instead, the unique signaling motif KIEELE has been found to be essential for inhibitory regulation of activated T cells [95]. The signaling partners that LAG-3 engages with in the intracellular domain are presently unknown. Nevertheless, the inhibitory function of LAG-3 has been clearly demonstrated in the suppression of T cell expansion and cytokine production through KO experiments with LAG-3<sup>+/-</sup> vs LAG-3<sup>-/-</sup> CD4<sup>+</sup> OT-II T cells [96].

A member of the TIM family of proteins, TIM-3 - which binds primarily to galectin-9 and to a lesser degree, CEACAM-1, phosphatidylserine, HMGB1 - does not contain inhibitory signaling motifs on its cytoplasmic tail[97]. In its inactive, unbound form, the Tyr residues on the cytoplasmic tail are constitutively occupied by HLA-B-associated transcript 3 (BAT3) and tyrosine kinase Fyn while inducibly bound by PI3K p85[97, 98]. Once TIM-3 binds its ligand, BAT3 is released from the cytoplasmic tail and various inhibitory effects are seen in the form of T cell anergy, disruption of stability in IS formation, and reduced T cell proliferation[99, 100].

Given the vast interest in recent times on coinhibitory receptors, new reports on functionality and mechanisms as well as novel targets are being uncovered regularly. We will now move onto the most well-known coinhibitory receptor of this decade and the main focus of this thesis, PD-1.

## 1.2 The PD-1 receptor

In 1992, a new coinhibitory receptor, programmed death-1 (PD-1 or CD279), was discovered by Y. Ishida and the T. Honjo group[101]. It was initially believed to be a gene regulating apoptosis in self-reactive immature T cells, hence the name programmed death. Over the next few years, the members of the Honjo group continued to further characterize the PD-1 receptor, uncovering its role in negative regulation mediated by SHP2 and in controlling autoimmunity[102-104].

PD-1 is a 288 amino acid, type 1 transmembrane protein that is encoded by the *Pdcd1* gene. It contains an Ig variable (IgV) extracellular domain, a transmembrane region, and a cytoplasmic tail that holds an immunoreceptor tyrosine-based inhibitory motif (ITIM) and an immunoreceptor tyrosine-based switch motif (ITSM) (**Fig. 7**)[105]. The role of PD-1 in adaptive immunity is critical; it serves to create a balance between T cell activation, tolerance, and autoimmunity. Gene knockout studies of PD-1 in mice has been associated with accelerated diabetes, excessive immunopathology and mortality in chronic infections as well as accelerated autoimmunity[106, 107]. Disrupting the PD-1 pathway can drastically affect the physiology and homeostasis of T cells. However, in the case for chronic infections and cancer, blockade of the PD-1 pathway serves as a way to increase functional activity against disease and as an immunotherapy.

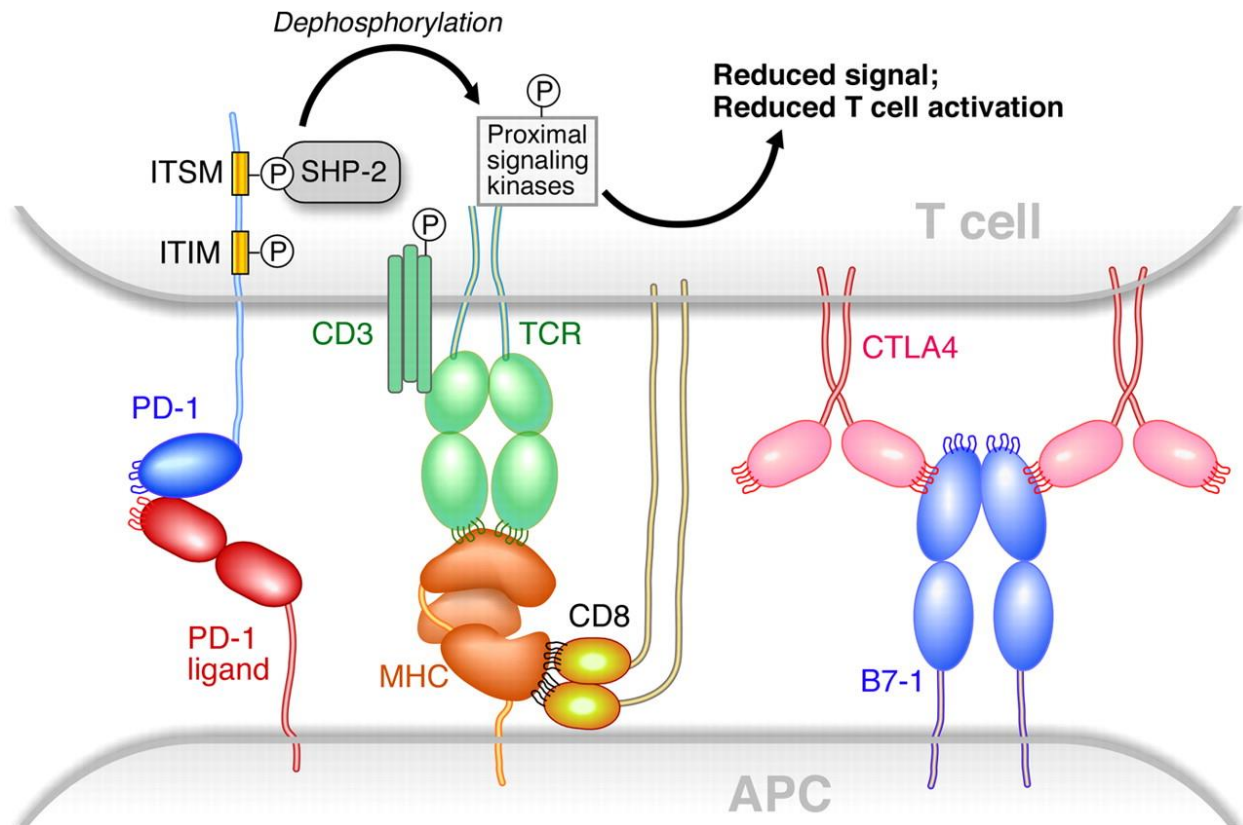


**Figure 7.** Schematic of PD-1 and CTLA-4. From Freeman GJ. Proc Natl Acad Sci USA. 2008 Jul 29;105(30):10275-6.

### 1.2.1 Expression and function of PD-1

PD-1 is typically expressed on T cells, B cells, monocytes, and some subsets of dendritic cells. Under antigen recognition, naïve T cells express PD-1 which is transiently expressed and decreases in the absence of antigen [108]. The constant presence of antigen such as chronic infections or cancer causes a prolonged PD-1 expression that is unable to cease and drives T cells towards an exhaustion phenotype [109]. Nevertheless, the expression of PD-1 alone on T cells is not a marker for exhaustion; many T cell subsets natively express PD-1 such as memory T cells, regulatory T cells, and T follicular helper cells [110].

Gene expression of PD-1 is tied to numerous transcription factors that are activated during T cell signaling. Two conserved regions, CR-B and CR-C, have been identified upstream of the transcription start site and are associated with the activation of Pdc1 [111]. NFATc1 (NFAT2) is necessary for the initial activation induced expression of PD-1 and binds strongly to the CR-C region. Numerous sites for NFATc1 binding have been uncovered, indicating that several NFATc1 transcription factors can drive Pdc1 [112]. AP-1 binding in the CR-B region and Notch signaling have been found to drive PD-1 expression as well [113, 114].

On the other hand, potential transcription factors that are involved in the inhibition of PD-1 expression are being investigated [115]. T-bet, which binds 500 bp upstream of the *Pdcd1* TSS, has been shown to repress expression of PD-1 but is insufficient on its own to completely negate PD-1 [115]. Blimp-1 has also been implicated as well in the loss of PD-1 expression following an acute infection and notably T<sub>fh</sub> cells, which are high in PD-1, express Bcl6 which antagonizes Blimp-1 expression [116, 117]. Interestingly, Blimp-1 expression is positively correlated with T cell exhaustion, suggesting unknown mechanisms or additional cofactors involved in PD-1 regulation [118].

The functional effects of PD-1 are well characterized and inhibit the proliferation, survival, cytokine production and release, and cytotoxicity of T cells [119]. More specific examples are the reduction of IL-2, IFN $\gamma$ , TNF- $\alpha$ , and IL-10 production, the reduction of proliferating CD4 and CD8, and the decrease in cytolytic capacity in CD8 for viral clearance [107, 120, 121].

PD-1 also is implicated in the development of regulatory T cells (Treg) as an indirect, cell-mediated means of negative regulation. PD-L1 was found to induce Tregs *in vitro* from naïve T cells shown as increased FoxP3 expression and enhanced immunosuppressive capabilities [122]. Overexpression of PD-L1 on T cells or K562 myeloid tumor cells were able to convert Tbet<sup>+</sup> Th1 cells into FoxP3<sup>+</sup> Tregs *in vivo* and the inhibition of PD-1 signaling stabilized Th1 differentiation [123]. Furthermore, PD-1 is able to reduce the threshold for TGF- $\beta$ -mediated conversion of Tregs [124]. Given the many immunosuppressive roles that Tregs play – sequestration of IL-2, depletion of costimulatory CD80/ CD86 on APCs, and the secretion of inhibitory cytokines such as TGF- $\beta$  and IL-10, the generation of Tregs represents another facet of PD-1 inhibitory function.

PD-1 also alters the metabolic profile of T cells by sustaining mitochondria activity and the diversion to fatty acid oxidation (FAO) and increased lipolysis while impairing glycolysis and glutaminolysis, thus creating a more oxidative environment [125]. Conventional proliferating T cells utilize glycolysis to sustain their growth and effector differentiation while memory T cells operate under FAO for survival [126]. This switch to FAO as well as the generation of spare respiratory capacity may enable the longevity of T cells receiving PD-1 signals by utilizing a fat-based metabolism. Furthermore, it has been shown that PD-1<sup>hi</sup> exhausted T cells have an accumulation of depolarized mitochondria and this mitochondrial dysregulation causes a loss of effector function and cell fitness [127].

### 1.2.2 Ligands of PD-1

The ligands of PD-1 are PD-L1 and PD-L2, which contain an N-terminal IgV and C-terminal IgC-like extracellular domain, a transmembrane domain, and a short cytoplasmic tail with very little sequence similarity to other B7 molecules[128]. PD-L1 is constitutively present on both hematopoietic cells, in particular, myeloid cells and non-hematopoietic tissue cells and can be further induced by external stimuli. On the other hand, PD-L2 is inducibly expressed on the surface of myeloid cells such as macrophages, B cells, dendritic cells, and mast cells. Furthermore, both PD-L1 and PD-L2 can be expressed by tumor cells and stroma[129].

The binding of PD-1 to its ligands involves the front  $\beta$  sheets of the interacting molecules (PD-L1 – GFCC, PD-L2 - AGFC strands) with contributions from the FG loops[130]. Although both PD-L1 and PD-L2 bind the same target, they have binding different mechanisms: PD-L2 has a higher binding affinity ( $K_d$ : ~83–143 nM) than PD-L1 ( $K_d$ : ~256–270 nM) from SPR studies and PD-L1 binding requires conformational changes to facilitate binding whereas PD-L2 binding to PD-1 is 1:1[131, 132]. However, given the abundance and basal constitutive expression of PD-L1 throughout the tissue compared to the restricted expression of PD-L2, PD-L1 represents the primary ligand for PD-1[129].

PD-L1 has other mechanisms of action to exert its inhibitory effects on T cell signaling. Soluble PD-L1 is released by PD-L1<sup>+</sup> cancer cells and found to retain its ability to bind and trigger apoptotic signals to T cells[133]. PD-L1 is also capable of binding to CD80 *in trans* but not CD86 and induce T cell anergy by this interaction[134]. Interestingly, it has recently been reported that the same CD80: PD-L1 interaction *in cis* on APCs prevents PD-1 signaling by reducing PD-L1 availability[135]. Furthermore, PD-L1 and PD-1 are also capable of binding *in cis* on APCs, adding another facet of dynamic regulation in T cell signaling[136].

For cancer prognosis, PD-L1 and/or PD-L2 are being investigated as predictors for cancer therapy outcome. In esophageal cancer, the expression of both PD-L1 and PD-L2 are associated with unfavorable prognosis for overall survival[137]. The presence of PD-L1<sup>+</sup> PD-L2<sup>+</sup> CD14<sup>+</sup> macrophages were also shown to have poor prognosis in hepatocellular carcinoma[138]. On the other hand, PD-L1 and/or PD-L2 expression in metastatic melanoma was shown to have an improved overall survival[139]. Also, PD-L1 expression but not PD-L2 was favorable for postoperative prognosis and longer disease-free survival in small lung cell carcinoma[140, 141].

### 1.2.3 PD-1 signaling pathway

As mentioned earlier in this chapter, the cytoplasmic tail of PD-1 contains two structural motifs: an ITIM (Y223) or (V/I/LxYxxL) and an ITSM(Y248) or (TxYxxL)[142]. Mutational studies on the motifs have uncovered that the inhibitory function of PD-1 is mediated by phosphorylation of the ITSM - which acts to recruit SHP1/SHP2 to facilitate the dephosphorylation and downregulation of downstream signaling pathways[121, 143, 144]. Furthermore, it was found that close proximity of PD-1 to CD3 or CD28 was necessary for T cell inhibition[143]. The ITIM was previously thought to not have any inhibitory effect on T cell activation but recent reports indicate that it may function to stabilize SHP2 by keeping an open conformational state[121, 145, 146].

Phosphorylation of PD-1 at the ITSM is upregulated by simultaneous TCR and PD-1 ligation[144]. PD-1 molecules are stabilized by PD-L1 binding and colocalize with CD28 in the c-SMAC, which brings its cytoplasmic domain in close proximity with both the TCR and CD28. The phosphorylation of PD-1 Y248 allows for the preferential recruitment and binding of SHP2 at its SH2 domain which becomes phosphorylated at its catalytic SH3 site and activated to exert its phosphatase activity. The primary targets of PD-1 are varied along the T cell activation pathway and many results have been confirmed; the question that remains is to verify whether PD-1 signaling differentially targets the TCR pathway components such as ZAP-70, Vav1, PLC $\gamma$ 1, Ras, Erk or the CD28 costimulatory pathway components such as PI3K, GSK-3b, Akt, CK2, PTEN or an assortment of both pathways[124, 147-151]. However, it is agreed that PD-1 receptor needs to be engaged by its ligand and brought into the proximity of the IS for its inhibitory function[121, 143].

The role of SHP1 in PD-1 signaling is less clear; it does not accumulate in the TCR microclusters nor does it effectively phosphorylate PD-1[143]. However, it has recently been found that SHP1 can compensate for the loss of SHP2 and reduce IL-2 production in Jurkat cell lines, despite a 10-fold preference for SHP2 by PD-1[152]. Furthermore, it has been recently discovered that SHP2 knockout in mice did not abrogate PD-1 signaling nor did it prevent the persistence of exhausted T cells in LCMV clone 13 chronic infection and these mice were shown to be responsive to anti-PD-1 therapy[153]. This indicates that other mediators of PD-1 signaling pathway have yet to be fully defined.

PD-1 signaling can be overridden by the presence of IL-2 as well as IL-7 and IL-15; cytokines that are able to induce STAT5 phosphorylation[154]. STAT5 activity is required for

the maintenance of IL-2RA expression and the uptake of IL-7 and IL-15 can enhance IL-2R expression as well as IL-2 responsiveness[155].

#### 1.2.4 T cell memory and exhaustion

Activated naïve T cells differentiate into effector T cells over a period of 1-2 weeks. The clonal expansion, tissue relocation, gain of effector functions as well as metabolic, transcriptional, and epigenetic reprogramming all represent the hallmarks of this effector phase[156]. With the resolution of inflammation and antigen clearance, activated T cells enter a contraction phase in which 90-95% of effector T cells will undergo apoptosis[157]. The few remaining T cells are, depending on the model, either memory precursor T cells derived from asymmetric division or effector T cells that will undergo epigenetic remodeling to develop into the memory T cell subset[156, 158]. These memory T cells can be broadly defined into subsets by phenotype, function, and location: central memory (T<sub>cm</sub>), effector memory (T<sub>em</sub>), tissue-resident memory (T<sub>rm</sub>), T stem cell memory (T<sub>scm</sub>)[159]. The memory T cells reduce much of their activity compared to effector T cells and traffic to their designated locations: lymphoid tissues (T<sub>scm</sub>/T<sub>cm</sub>), non-lymphoid tissues/blood (T<sub>em</sub>), barrier tissue sites such as skin, gut, and lungs (T<sub>rm</sub>)[160]. When reencountering antigen, these memory T cells are capable of rapid upregulation of effector functions and antigen-independent self-renewal through IL-7 and IL-15 uptake[160].

During chronic infections and cancer, the persistent exposure of antigen as well as inflammation causes a dysfunctional alteration in effector T cells called T cell exhaustion[161]. This term “exhaustion” is defined as a suboptimal response to pathogens or cancer cells marked by reduced effector functions such as decreased cytokine production and proliferative capacity as well as the upregulation of multiple coinhibitory such as PD-1, TIM-3, LAG-3 and an altered transcriptional program and epigenetic landscape[162].

The current model for the lineage of exhausted T cells starts at the point of T cell memory precursors, mediated by the upregulation of TOX, and adopting a profile of TCF1<sup>+</sup> PD-1<sup>+</sup> TIGIT<sup>+</sup> as exhausted T cells with their progeny being TCF1<sup>-</sup> PD-1<sup>+</sup> TIGIT<sup>+</sup> terminally exhausted T cells (**Fig. 8**)[163, 164]. The principal driver for exhaustion is chronic TCR signaling mediated primarily by NFAT and other transcription factors such as IRF4, BATF, NR4A, TOX which altogether upregulate inhibitory receptor expression and maintain the survival of exhausted T cells[165]. It is primarily thought that NFAT activation without AP-1

due to insufficient costimulatory conditions can induce the expression of NR4A and TOX and drive the exhaustion program [166].

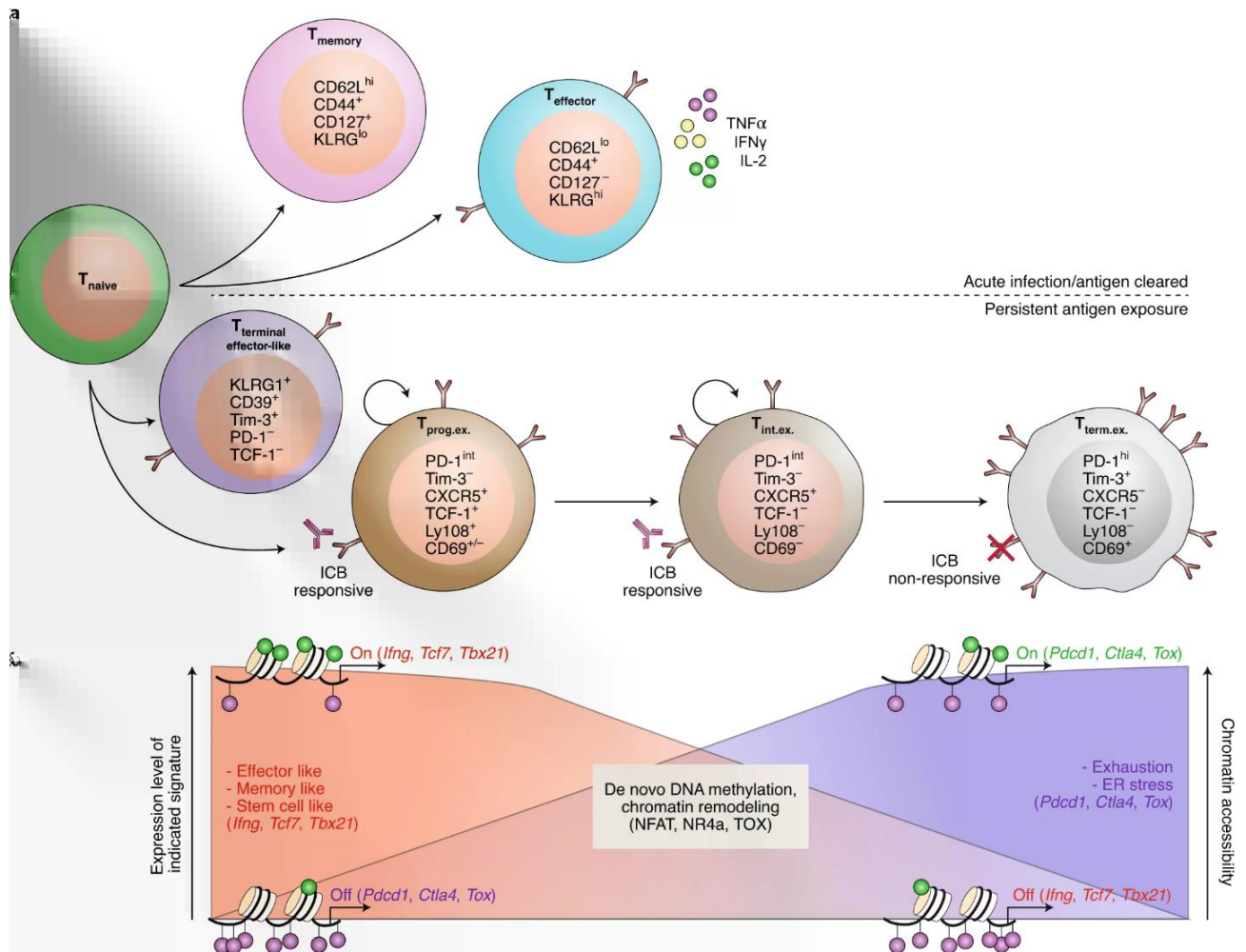


**Figure 8.** T cell exhaustion pathway. From Franco F, Jaccard A, Romero P, Yu YR, Ho PC. Nat Metab. 2020 Oct;2(10):1001-1012.

### 1.3 Monoclonal antibodies

Antibodies represent the humoral response of adaptive immunity and are characterized by their high degree of specificity and binding affinity to antigens. Moreover, monoclonal antibodies (mAbs) are antibodies that bind to the same antigenic epitope and are produced from a single B cell clone compared to polyclonal antibodies, which are generated against the same antigen but with multiple epitopes from different B cell clones. Ever since the development of the hybridoma technique in mice in 1975, research into as well as the utilization of monoclonal antibodies has grown tremendously, leading to the first licensed antibody for immunotherapy applications in humans - Orthoclone OKT3 for the treatment of acute transplant rejection in 1986 [167, 168]. As of December 2019, there are 79 FDA approved monoclonal antibodies in

the market targeting a wide range of human disease including cancers, autoimmune disorders, rheumatism, migraines, and infectious diseases[169].

The structure of an antibody is comprised of two identical heavy chains and two identical light chains linked together by a disulfide bond and can be partitioned into distinct functional domains: Fab (antigen-binding fragments), Fc (crystallizable fragment), and the hinge region, which connects the first two domains and aids antibodies in their flexibility for binding epitopes at distance and forming complexes (**Fig. 9**). The variable region (Fv) on the Fab contains the hypervariable regions folded as 3 loops of  $\beta$ -strands which are called complementarity-determining regions (CDRs)[170]. The combination of 3 CDRs from the heavy and light chains create the antigen binding site. The Fc region of the antibody is responsible for the binding and interaction with Fc receptors (FcR) for immune function. In humans, the five antibody classes are known as IgA, IgD, IgE, IgG, and IgM. Furthermore, IgA has two subclasses and the IgG has four subclasses[171].

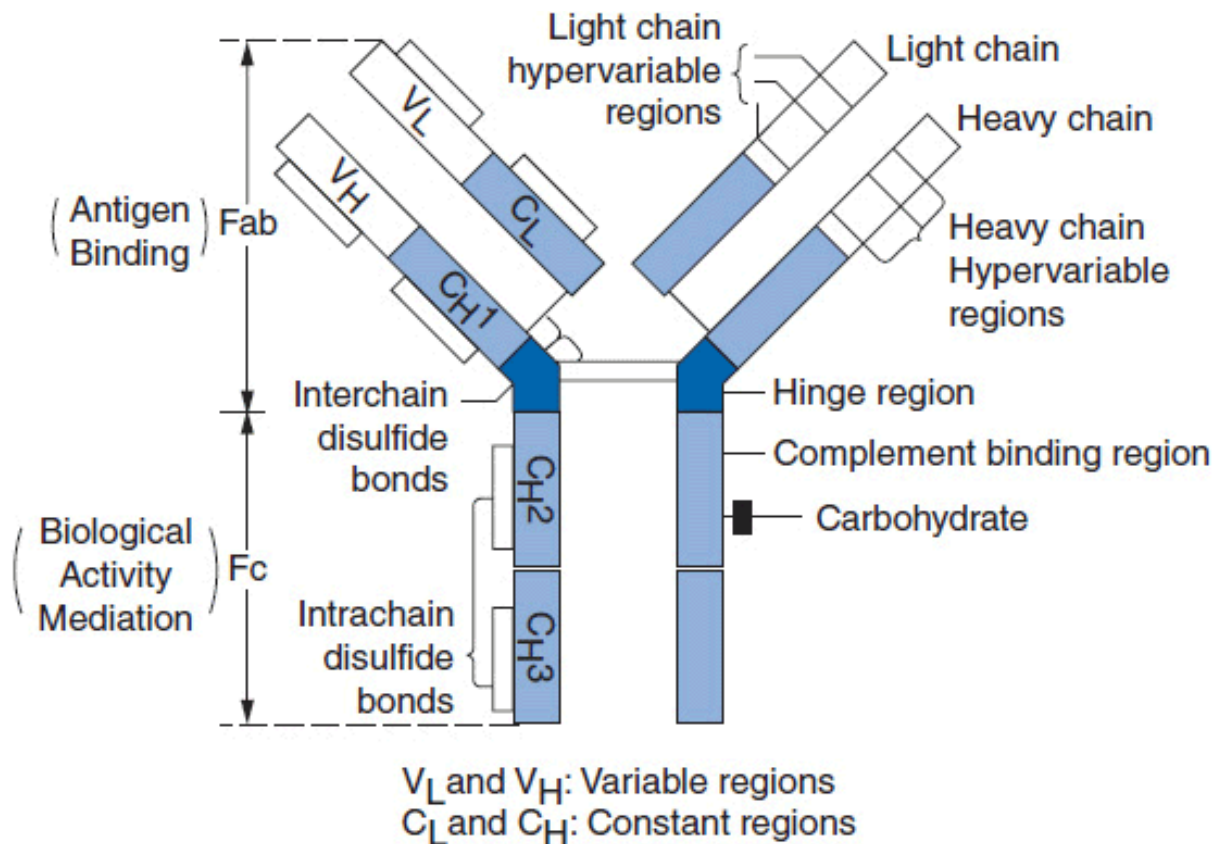


**Figure 9.** Antibody structure and functional relationships. From Wasserman RL, Capra, JD. In MI Horowitz, W Pigman (eds.), *The Glycoconjugates*, Academic Press, 1977, p. 323.

### 1.3.1 Characteristics of mAbs in immunotherapy

While a number of different antibody isotypes are possible, in practice, only the IgG isotype is used. The main reason is due to serum prevalence as well as longevity: the half-life of IgA, IgD, IgE, and IgM have been reported to be between 2-5 days, similar to the pharmacokinetics of serum proteins by renal filtration [172]. On the other hand, the IgG isotype has an approximate half-life of 21 days due to the FcRn (neonatal Fc receptor). The FcRn is expressed in the epithelium of the lungs and kidneys and binds tightly to the C<sub>H</sub>2–C<sub>H</sub>3 hinge region of pinocytosed IgG in the endosomal compartments and releases IgG at physiological pH upon recycling into the blood [173].

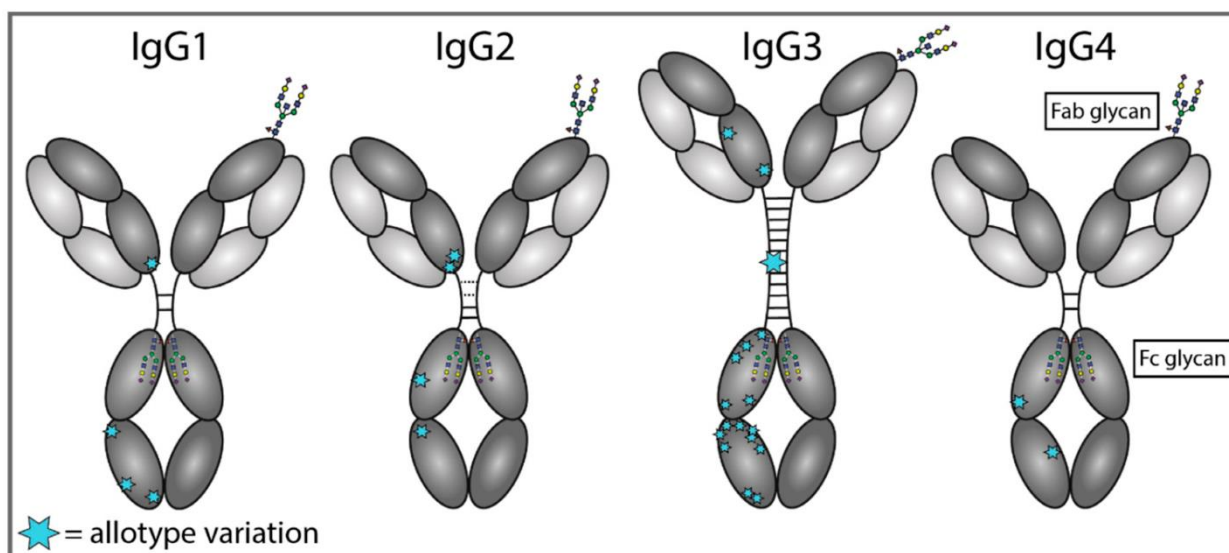


**Figure 10.** IgG subclasses and their sites for allotype variation. Adapted from de Taeve SW, Rispens T, Vidarsson G. *Antibodies (Basel)*. 2019;8(2):30. 2019 Apr 25.

Even amongst the IgG isotype, the majority of monoclonal antibodies used commercially are the IgG1 subtype (**Fig. 10**) [174]. IgG1 has excellent binding affinity as well as potent effector functions and historically has been used since the initial development of therapeutic antibodies. IgG2 and IgG4 have the least binding potential for the FcR and can be used when lack of effector function is warranted [174].

However, an FcR-independent agonistic activity was observed for the IgG2 subtype due to its alternating disulfide conformations in an anti-TNFR mAb, causing an aggregation of TNFR on the cell surface [175]. Specifically for the case of IgG4, Fab-arm exchange can occur wherein a heavy chain and the attached light chain from one IgG4 is switched with another, thus creating a bi-specific antibody [176]. This was remedied by a single mutation of the S228P which stabilized the disulfides in the core hinge region and prevented the formation of “half-molecules”. IgG3 has not been considered due to an increased likelihood for proteolysis from

an extensive hinge region and reduced half-life (~7 days) compared to other IgG subclasses[177].

### **1.3.2 Fc $\gamma$ Receptors**

The family of Fc receptors for IgG or Fc $\gamma$ R is expressed widely on hematopoietic cells and consists of Fc $\gamma$ RI (CD64), Fc $\gamma$ RIIa/b/c (CD32), and Fc $\gamma$ RIIIa/b (CD16) [178]. The expression of Fc $\gamma$ R is most commonly associated with innate immune effector cells such as monocytes/macrophages, dendritic cells (DC), neutrophils, basophils and mast cells. For lymphocytes, NK cells are notable for expressing only CD16 and B cells for the expression of CD32b with a small minority of both cell subsets expressing CD32c. [179, 180] T cells are not generally known to express any Fc receptors except for situational cases such as the expression of CD32a in HIV infected CD4 with high persistent levels of HIV-1 transcription[181, 182].

Each Fc $\gamma$ R has its own binding affinities and effector functions for each subclass of IgG. CD64 is a high-affinity Fc receptor that binds monomeric IgG and immune complexes with a high binding affinity for IgG1 and IgG4 and it is expressed on monocytes/macrophages, dendritic cells, and neutrophils[183]. CD32a and CD16a are both low affinity receptors that bind weakly to monomeric IgG but have higher affinity for IgG1 and IgG3 over IgG4 [178]. CD32b is an inhibitory Fc $\gamma$ R with weak binding affinity to all IgG subclasses that suppress B cell activation as well as type I interferon production by DCs[184]. An antibody–Fc $\gamma$ R interaction is influenced by several factors: the type of Fc $\gamma$ R bound, the effector cells expressing the receptor, cytokines that dictate differential levels of Fc $\gamma$ R expression, the IgG subclass and the degree of immune complex formation from the antibody binding[178].

### **1.3.3 Antibody effector functions**

The primary antibody function at its core level is the recognition and neutralization of antigen. Antibodies mediate the neutralization of toxins or microbial entry and replication and promote the clearance of antibody-opsinized foreign particles for uptake by phagocytotic cells[185]. In the context of cancer immunotherapy, antibodies are directed towards tumor antigens to cause cancer cell death through a variety of different ways. mAbs can induce cell death by blocking growth factor receptors (anti-EGFR), immunomodulation (anti-CTLA-4), agonistic (anti-TRAIL), and payload delivery with antibody-drug conjugates (inotuzumab ozogamicin)[186-189]. However, the other side of an antibody's mechanism of action lies in its effector functions mediated through its Fc domain.

### Antibody Dependent Cellular Cytotoxicity (ADCC)

ADCC is triggered by Fc $\gamma$ R expressing effector cells that recognize a target cell or particle that has been opsonized by antibodies. The primary effector cells for ADCC activity are NK cells through the binding of their highly expressed CD16a, although other cells such as monocytes/macrophages and granulocytes can also contribute to ADCC[180]. ADCC activity is mediated by cytotoxic granule release, generation of reactive oxygen species, and proinflammatory cytokines[190]. The binding of the antibody-Fc region to CD16a causes the polarization and exocytosis of perforin and granzymes in a calcium-dependent manner which causes pore formation by perforin, DNA fragmentation, and apoptosis by granzyme B[191].

In a study looking at cetuximab treatment and radiotherapy of head and neck cancer, high basal levels of both ADCC activity and EGFR expression were associated with higher probabilities of complete response and overall survival[192]. In another study, patients with a higher affinity polymorphism to IgG1 on CD16a (158V/F) achieved better clinical responses than those that did not in non-Hodgkin lymphoma when treated with rituximab[193].

### Antibody dependent cellular phagocytosis (ADCP)

ADCP is the process in which antibody opsonized particles or cells are removed through phagocytosis. It begins with the initial binding of antibody-Fc region to the Fc $\gamma$ R-expressing phagocyte followed by the receptor clustering and oligomerization of the Fc receptors[194]. This activates Fc $\gamma$ R signaling through the phosphorylation of associated ITAM by Src family kinases and drives the actin-mediated process of engulfment through Rac1 for the formation of the phagocytic cup and pseudopod extension around the target cell[195]. CD64, CD32a, CD16a, and CD16b are the phagocytic Fc $\gamma$ Rs that mediate ADCP and the main effector cells are macrophages, monocytes, NK cells, and neutrophils[196-199]. Recent studies using intravital microscopy have shown that ADCP is a major mechanism involved in the killing and removal of tumor cells[200, 201].

The role of ADCP in immunotherapy are further validated by studies on the blockade on anti-phagocytotic receptors such as the CD47/SIRP $\alpha$  axis. CD47 is an IgSF transmembrane protein that is constitutively expressed on all viable nucleated cells and red blood cells and binds to SIRP $\alpha$  receptors on macrophages[202]. It functions as a “don’t eat me” signal and has been shown to be overexpressed in some malignant cancers[203-205]. Blockade of this receptor has generated recent interest due to a potential combination therapy approach of blocking CD47 in tandem with anti-cancer immunotherapeutics. Xu, L et al. showed that

blockade of CD47 in parallel with a CD19/CD3-bispecific T cell engager blinatumomab led to significantly higher tumor volume reduction compared to each treatment alone in non-Hodgkin lymphoma grafted NOD/SCID mice[206]. In another study by Ring, N.G. et al., anti-SIRP $\alpha$  (KWAR23) in tandem with rituximab outperformed individual treatments in the tumor control of Burkitt's lymphoma in SRG (knockin of human Sirp $\alpha$ ) mice[207].

#### Complement-dependent cytotoxicity (CDC)

CDC represents one of the effector mechanisms for IgM and IgG antibodies. CDC is efficiently activated by human IgG1, IgG3, and IgM with weak activation from IgG2 and no activation from IgG4[208]. The reaction is started by C1q binding antibody complexed with antigen such as a pathogen or cancer cell which leads to the cleavage of complement cascade proteins through the classical complement pathway and ending with the formation of the membrane attack complex (MAC) for cell lysis[209]. Most mAbs approved for cancer immunotherapy are IgG1 subtype which has high activity for complement binding and activation.

Rituximab, which is used for B-cell malignancies, has been shown utilize complement to mediate anti-tumor function[210, 211]. Alemtuzumab, which is also used for B-cell malignancies, has been shown to increase CDC activity after combining treatment with ofatumumab[212]. However, tumor cells also express membrane bound complement regulators such as CD46, CD55, and CD59 which reduces the formation of the MAC and thereby cell lysis. These proteins are overexpressed in some tumor types and their upregulation is contributed to mAb resistance[213-215]. Targeted depletion of these complement regulators is being considered as a way to improve efficacy of anti-tumor mAbs[216, 217].

#### 1.3.4 Immunomodulatory antibodies

Checkpoint blockade inhibitors such as CTLA-4 and PD-1 fall under the immunodulatory antibody category as these antagonistic mAbs block or inhibit interaction with their ligands to enhance T cell responses and thereby modulate the immune system directly. By function, the IgG4 isotype represents the best candidate for these antibodies because of its minimal interaction with Fc receptors and diminished ADCC and CDC activity from myeloid and NK cells. Some immunomodulatory antibodies are targeted to activate costimulatory receptors such anti-GITR or anti-CD40 and represent an agonistic mechanism to enhance immunological responses[218, 219].

As the first checkpoint blockade inhibitor to enter the clinic in 2011 for the treatment of melanoma, anti-CTLA-4 antibody ipilimumab was designed to block CTLA-4 in its competitive binding for CD28 ligands, CD80 and CD86; thereby, allowing CD28 to continue signaling for T cell activation[220, 221]. The blockade of CTLA-4 signaling ultimately prolongs T cell activation via extended CD28 signaling and as a result, restores proliferative capacity and enhances T cell mediated effector functions[222].

Ipilimumab has shown strong durable responses for patients with stage 3 or stage 4 metastatic melanoma with median overall survival being 10 months in patients receiving ipilimumab plus gp100 versus 6.4 months in patients receiving gp100 alone[223]. Similarly, in a dual therapy of ipilimumab plus dacarbazine for metastatic melanoma, overall survival rates at 1, 2, and 3 years showed a significant benefit in dual therapy arm with 47.3%, 28.5%, and 20.8%, respectively, compared to the placebo plus dacarbazine arm, 36.3%, 17.9%, and 12.2%, respectively[224].

Interestingly, the anti-CTLA-4 antibody ipilimumab is an IgG1 antibody which would still retain Fc effector functions and in fact, one of the known mechanisms of action for ipilimumab is the cytotoxic depletion of inhibitory Tregs[225-227]. In a study by Roskopf, S. et al., substitution of IgG1 subclass to IgG4 on ipilimumab was found to increase proliferation and cytokine production in stimulated CD4<sup>+</sup> *ex vivo*, indicating potential adverse effects of ADCC induced by ipilimumab-IgG1[228]. However, tremelimumab - anti-CTLA-4 antibody in IgG2 format - has failed spectacularly over the years to pass phase III clinical trials[229]. It is believed that the IgG2, which does not bind efficiently FcγRs, represented a significant loss of cytotoxicity against Tregs which express higher levels of CTLA-4 than intratumoral T cells and therefore, a loss of one of the important mechanisms for anti-CTLA-4 therapy[229, 230].

### **1.3.5 PD-1 antibodies**

Although now commonly regarded in the field of cancer immunotherapy, it is important to remember that the anti-PD-1 antibodies, pembrolizumab and nivolumab, were only recently approved by the FDA in late 2014 for the treatment of melanoma, although anti-PD-1 antibodies have been under preclinical development since the mid-2000s[231]. Anti-PD-1 and anti-PD-L1 mAbs have now been tested and approved for the treatment of a variety of cancers such as non-small lung cancer, renal cell carcinoma, squamous cell carcinoma of head and neck, hepatocellular carcinoma, and more[232]. Currently, there are 3 FDA approved anti-PD-1

antibodies: pembrolizumab, nivolumab, and cemiplimab and there are also 3 FDA approved anti-PD-L1 antibodies: atezolizumab, avelumab, and durvalumab[233]. Ongoing research on PD-1/PD-L1 axis continues to reveal more information on the mechanisms and consequences of anti-PD-1 blockade.

The prolonged presence of antigen in cases of chronic infections or cancer leads to high PD-1 expression and an accumulation of T cells with an “exhausted” phenotype[107, 234]. Anti-PD-1 therapy aims to enhance T cell responses and restore attenuated T cell activity from exhaustion seen as functional increases in T cell proliferation, cytokine production, and cytolytic activity[120, 235]. Many cancer types overexpress PD-L1 and/or PD-L2 due to growth factors, hypoxia, or the presence of cytokines such as IFN $\gamma$ , IL-10, and/or TGF $\beta$  present in the tumor microenvironment; therefore, tumor infiltrating lymphocytes (TILs) become less effective in this immunosuppressive microenvironment, permitting the evasion and growth of cancer cells[236-238]. In this regard, PD-1 therapy has been shown to provide significant and durable objective responses in patients with certain types of cancers. In a phase III clinical trials for patients with advanced squamous-cell non–small-cell lung cancer, nivolumab or the standard docetaxel treatment arms were compared[239]. Median overall survival and response rates was found to be 9.2 months and 20% for nivolumab compared to 6.0 months and 9% for docetaxel. In another study for patients with advanced renal-cell carcinoma, the median overall survival and objective response rate was 25.0 months and 25% for nivolumab compared to 19.6 months and 5% for the standard treatment with everolimus[240]. Finally, in a phase III clinical trial for advanced melanoma, pembrolizumab was found to prolong progression free survival and overall survival while incurring less high-grade toxicity compared to ipilimumab[241]. There are numerous other reports and reviews on the efficacy of PD-1 therapy as a monotherapy or in combination with other drugs/ immunotherapeutics for the treatment of many different cancer types[233, 242-244].

The expression of PD-L1 on tumors is generally associated with poor prognosis for some cancer types[245]. In melanoma, PD-L1 expression defined a melanoma subset with distinct genetic and phenotypic features such as the upregulation of integrin  $\alpha$  subunits as well as increased aggressiveness and invasiveness [246]. For patients with completely resected stage I squamous cell carcinoma of the lung, a combination of no PD-L1 expression in tandem with low NLR (neutrophil to lymphocyte ratio) - a surrogate marker for immune activation, was shown to significantly predict positive recurrence-free survival and overall survival[247]. In patients with inoperable locally advanced non-small cell lung cancer undergoing concurrent

chemoradiotherapy, median progression free survival (PFS) was shown to be 19.9 months in patients without PD-L1 expression and 10.1 months in patients with PD-L1 expression[248]. In a univariate survival analysis of breast cancer cases, high expression of PD-L1 detected by immunohistochemistry had a significantly worse OS than PD-L1 negative breast cancer specimens [249]. However, some studies have also argued against the significance of PD-L1 expression as a biomarker for cancer prognosis, indicating that further biomarker analysis could include additional covariates such as tumor antigens, tumor mutation burden, or microRNA expression to better predict prognosis[250-254].

As mentioned in earlier chapters, PD-L1 expression on tumors, on the other hand, acts as a positive predictive marker for effective PD-1 therapy[255]. The FDA approved of intratumoral PD-L1 immunohistochemistry as a companion diagnostic for pembrolizumab in treatment of advanced NSCLC[256]. In the Keynote-040 trial for recurrent or metastatic head-and-neck squamous cell carcinoma, the proportion of patients with tumors expressing PD-L1 showed a higher objective response and progression-free survival than patients with PD-L1 negative tumors in the pembrolizumab treated group[257]. In the phase I study for in patients with advanced non-small-cell lung cancer treated with pembrolizumab, tumor expression of PD-L1 was correlated with enhanced likelihood of responses to pembrolizumab[258]. In the study by Jreige, M. et al., an inverse correlation was found with PD-L1 expression in tumor cells and the MMVR (ratio of metabolic to morphological lesion volumes)[259]. Furthermore, low expression of imaging marker MMVR with PD-L1 expression in tumors was correlated with radiological outcomes to PD-1 therapy.

There is no definitive evidence at the moment that indicates whether blockade against PD-1 or its ligand, PD-L1, is more effective or demonstrates higher functional activity than the other. However, meta-analysis studies have attempted to investigate this and their results show that anti-PD-1 therapy may be more effective than anti-PD-L1[260, 261]. In the meta-analysis review by Duan, J. et al., 19 randomized clinical trials across various tumor types were compared, involving a total of 11,379 patients, and found that anti-PD-1 therapy showed increased overall survival (HR: 0.75) and progression-free survival (HR: 0.73) compared to anti-PD-L1 therapy[261]. Furthermore, in two large phase I clinical studies against multiple advanced cancers, objective response rates for anti-PD-1 therapy were 27% for renal-cell cancer, 28% for melanoma, and 18% for non-small lung cancer while for anti-PD-L1 therapy, 12%, 17%, and 10%, respectively[262, 263]. In a comparison for anti-PD-1 vs anti-PD-L1 therapy in patients with advanced non-small cell lung cancer undergoing therapy with

nivolumab or atezolizumab (anti-PD-L1), anti-PD-L1 therapy was found to have significant gene expression changes in CD14<sup>+</sup> monocytes compared to T cells and differential gene analysis showed increases in inflammation-associated genes such as HBEGF, IL-1 $\beta$ , CXCL1/GRO $\alpha$ , CXCL2, and NLRP3, resulting in an inflammatory response from myeloid cells[264].

### Resistance to PD-1 therapy

Despite these successful improvements for cancer treatment by PD-1 therapy, the response rates from PD-1/PD-L1 inhibitors overall remains inadequate and have limited applications to certain cancer types. Furthermore, a significant proportion of patients undergoing PD-1 therapy remain partially responsive or unresponsive[265, 266]. Patients that are unresponsive to initial treatment with PD-1/PD-L1 therapy are known to have primary resistance while patients that showed a strong initial response but continued to develop progressive disease are known to have acquired resistance[265].

Primary resistance to PD-1 therapies includes insufficient T cell generation, infiltration, or exclusion which can be partially or wholly attributed to lowered immunogenicity of tumors[267]. In tumors that are not significantly differentiated from tissue of origin or have maintained low levels of mutational burden, a strong tumor antigen response is not effectively generated, resulting in the absence or low levels of CD8<sup>+</sup> [266]. Cancers such as pancreatic and prostate cancer have few somatic mutations and are resistant to PD-1 therapy[268]. The presence of immunosuppressive cells in the tumor microenvironment also greatly affects the outcome of PD-1 therapy. Intratumoral Treg, MDSC (myeloid derived suppressor cells), and TAM (tumor associated macrophages) are negatively associated with the efficacy of PD-1 therapy through the promotion of tumorigenesis, restriction of T cell responses, and the secretion of immunosuppressive cytokines and metabolites[269-271]. For acquired resistance to PD-1 therapy, failure of the relief of T cell exhaustion is considered to be a critical factor. PD-1 therapy restores the activity of hypofunctional exhausted CD8<sup>+</sup> T cells but epigenetic stability of the exhaustion phenotype limits the extent in which exhausted T cells can change to memory T cell state[272, 273]. A higher ratio of restored exhausted T cells to pretreatment tumor burden was correlated with higher clinical response to PD-1 therapy[274]. However, if the tumor burden/ antigen load remains high and the restored TILs remain unable to clear the tumor, the PD-1 treated T cells revert back to an exhaustion phenotype[273]. Compensatory coinhibitory signaling has also been observed in TILs upregulating LAG-3 and FCRL6

expression after relapse of initial treatment of PD-1 therapy in melanoma[275]. Cancer immunoediting can also increase neoantigen loss which may result in acquired anti-PD1 resistance due to the selective pressure of tumor subclones that can evade anti-tumor immunity after treatment[276]. Other mechanisms of primary and/or acquired resistance to PD-1 therapy are specific tumor mutations in B2M which affect antigen presentation by MHC-I and JAK1/2 resulting in the impairment of IFNGR signaling as well as upregulation of histone methyltransferase Ezh2 to reduce antigen processing mechanisms and immunogenicity. [277, 278].

Despite the significant advances made in the success of PD-1 therapy as well as the limitations, further understanding of the mechanisms of action in anti-PD-1 therapy within immunological settings are necessary to implement more effective approaches for improving the outcomes of cancer immunotherapy. In this thesis report, we aim to investigate the intrinsic properties of anti-PD-1 antibodies on their target memory T cell populations and to see if other alternative mechanisms play a role in restoring T cell responses.

## CHAPTER II: RESULTS

---

### **Paper I: Tumor suppression of novel anti-PD-1 antibodies mediated through CD28 costimulatory pathway**

Monoclonal antibodies against the PD-1 receptor block the PD-1-PD-L1 binding site. Although these commercialized PD-1 antibodies are now a standard line of treatment for a number of cancer types such as non-small cell lung cancer and advanced melanoma, only a fraction of these patients show significant, long-term clinical responses. Therefore, the work is needed to define the mechanisms of anti-PD-1 therapy in order to better address these limitations and pursue ways to improve them.

Our group had identified a high-affinity antagonistic mAb against PD-1 that does not block the PD-1-PD-L1 interaction site. Structural analysis by X-ray crystallography showed that the binding epitope for this non-blocking anti-PD-1 antibody (NB01b) lie on the opposite face of the PD-L1 binding site. Interestingly, we found that this non-blocking anti-PD-1 antibody was able to increase cytokine production (IFN $\gamma$ , TNF- $\alpha$ , and IL-10) and antigen-specific proliferation in T cells, similarly to blocking PD-1 antibodies.

We performed CD3/CD28 stimulation and PD-L1 coinhibition to investigate if any differential signaling pathways could be observed between the blocking (pembrolizumab) and non-blocking (NB01) anti-PD-1 antibodies. Both NB01 and pembrolizumab were capable of significantly restoring Akt S473 and PDK1 S241. We found that NB01 also restored Akt T308 and significantly more Akt S473 signaling compared to the pembrolizumab while pembrolizumab restored more Ca<sup>2+</sup> and NFAT signaling from PD-1 inhibitory signals.

Lastly, we found that that the coadministration of both pembrolizumab and NB01 was able to significantly enhance tumor clearance in an MC38 mice model compared to monotherapy.

These results show that blockade of the PD-1-PD-L1 interaction site is not necessary for an antagonistic effect and that anti-PD-1 antibodies binding different epitopes may exert different functional effects on T cell activation.

**Contribution:** My contributions for this paper were the development and implementation of the phosphorylation and calcium flux experiments as well as the analysis for these data. I have also written the results and materials and method sections regarding those experiments.

### **Paper II: T-cell exhaustion in HIV infection**

T cell responses are critical for the elimination of pathogens and cancer cells and T cell activation represents a process of antigen recognition, receptor costimulation, and signal termination. T cell activation leads to the control and elimination of pathogens but in the context of HIV, the presence of high levels of viral replication and lack of clearance to antigens creates a dysfunctional status called exhaustion. As a progressive condition, T cell exhaustion is correlated with the increasing loss of effector functions such as cytokine production and cytotoxic capacity in parallel with increased expression of coinhibitory receptors. We will review the role of T cell exhaustion in the progression of HIV, defects in T cell function in patients undergoing antiretroviral therapy, exhaustion markers that designate the HIV reservoir in latently infected cells, and targeted approaches to achieving a functional cure.

**Contribution:** My contribution for this review were the drafting and writing of the sections on immune signaling and negative regulators.

### **Paper III: An alternative Fc-mediated mechanism of regulating PD-1 expression in anti-PD-1 therapy (Manuscript under preparation)**

The blockade of PD-1 interaction with its ligands PD-L1 and PD-L2 is an important determinant in potentiating the antigen specific activation of PD-1<sup>+</sup> T cells; however, it is not clearly known if any other cell-extrinsic interactions are involved for anti-PD-1 therapy. We evaluated the kinetics of PD-1 antibody internalization and PD-1 receptor downregulation after an initial observation that PD-1 expression was decreasing with the treatment of anti-PD-1 on PD-1<sup>+</sup> memory T cells.

By using a pH-sensitive dye, pHrodo, conjugated to anti-PD-1 antibodies, we observed that PD-1 antibody internalization was more rapid, occurring over a few hours, compared to PD-1 receptor downregulation, a process which took over a 24-hour window. We then purified T cells and observed that the downregulation effect was significantly lost while PD-1 antibody internalization still occurred. Reconstitution of the CD3<sup>-</sup> and CD14<sup>+</sup> fractions restored this PD-

1 downregulation effect on memory T cells, indicating that monocytes were the likely mediators of this interaction.

A broad panel of compounds were tested to screen for inhibitors that could prevent PD-1 downregulation but not anti-PD-1 internalization in which dasatinib and 3-MA were found. Pulse-chase experiments with bound pHrodo-anti-PD-1 antibodies and unlabeled antibodies in the supernatant verified monocytes as the primary mediators of PD-1 downregulation. Furthermore, dasatinib-mediated inhibition of Fc $\gamma$ R activity on monocytes prevented the acquisition of PD-1 antibodies bound on the T cell surface.

To determine which Fc $\gamma$ R were involved in PD-1 downregulation, we transiently transfected 293T cells to express CD32a and CD64 cocultured with primary T cells. Here, we found that while both CD32a and CD64 were able to significantly downregulate PD-1 expression, CD64 represented the majority of this interaction and was significantly lower than CD32a.

Finally, we tested for the requirement of the Fc $\gamma$ R in restoring CD8<sup>+</sup> proliferation from antigen-specific stimulation using the standard format antibody vs F(ab')<sub>2</sub> variants. We found that standard format generated significantly higher amounts of antigen-specific CD8 than their respective F(ab')<sub>2</sub> variants. These results indicate that CD14<sup>+</sup> monocytes are necessary for the mAb mediated PD-1 downregulation on T cells via CD64 binding and that this interaction can enhance T cell functionality.

**Contribution:** My contributions were the design, implementation, and data analysis of all experiments except the IHC experiments as well as the drafting and writing of the original manuscript and creation of the figures.

## Chapter III: DISCUSSION

---

This PhD thesis is composed of two parts investigating anti-PD-1 mechanism of action: 1) The functional differences between a blocking and non-blocking antibody and 2) An Fc $\gamma$ R mediated downregulation of PD-1 with anti-PD-1 antibodies. The discussion will be split into 2 sections and each section will address the underlying hypothesis.

*Hypothesis 1: The novel non-blocking anti-PD-1 antibody differs in its mechanism of action from the traditional blocking PD-1 antibodies*

We isolated 5 out of 156 hybridoma clones selected for high-affinity antagonistic anti-PD-1 activity and that bound to PD-1 independently of PD-1-PD-L1 blockade. Competitive binding studies using a PD-1<sup>+</sup> Jurkat cell line and PD-1-PD-L1 interaction studies were done to confirm that these novel antibodies were unconditionally non-blocking of the PD-1-PD-L1 interaction, which was measured by simultaneous competitive binding with blocking PD-1 antibody and the candidate non-blocking PD-1 antibodies. This verified that the non-blocking PD-1 antibodies did not sterically interfere with PD-L1 binding to PD-1 nor did the binding cause a conformational change that would reduce PD-L1 binding affinity. The results from the hPD-1-NB01 Fab crystal structure as well as epitope mapping studies through the site-directed mutagenesis of PD-1 would later show that the non-blocking PD-1 mAb bound to an epitope on the opposite face of the PD-1-PD-L1 interaction site.

We also observed that both blocking and non-blocking anti-PD-1 antibodies similarly increased the proliferation of antigen-specific CD8 and significantly increased the IFN $\gamma$ , TNF- $\alpha$ , and IL-10 production. These results shed new insight on the necessity of a ligand blocking interaction for anti-PD-1 therapy. Additionally, we found that the combination of both blocking and non-blocking antibodies significantly enhanced both cytokine and proliferation profiles over the monotherapy alone, proving that both blocking and non-blocking anti-PD-1 antibodies can work in tandem to produce a synergistic effect.

Using an anti-CD3/ anti-CD28 with hPD-L1 for coinhibition, we saw that blocking (pembrolizumab) and non-blocking anti-PD-1 (NB01) antibodies relieved PD-1 inhibitory function by distinct pathways. Pembrolizumab was shown to have a higher effect in restoring Ca<sup>2+</sup> flux and NFAT expression while NB01 was more elevated in both Akt phosphosites,

indicative of the CD28 costimulatory pathway. Numerous studies have shown that components of the TCR and CD28 pathways are suppressed by PD-1 signaling[124, 149-151]. PD-1 ligation induces proximal phosphatase activity by SHP2 which affects TCR-associated kinases such as ZAP-70, Lck, and Erk1/2 as well as the phosphorylation of CD28 which leads downstream to the PI3K-Akt pathway. Anti-PD-1 blockade has been shown to reduce T cell exhaustion by preventing the recruitment of PD-1 into TCR microclusters[143, 151, 162].

The immunoprecipitation studies showed that pembrolizumab formed a physical interaction between PD-1 and CD28 along with cytoplasmically bound PI3K after T cell activation. This colocalization of PD-1 and CD28 indicates that even with PD-1 blockade, the PD-1 signalosome remains in close proximity to its CD28 target and would reduce the costimulatory signals nearby. On the other hand, NB01 did not significantly immunoprecipitate with CD28, which means that NB01 binding the opposite face of PD-1 causes a further segregation from CD28 and allows for increased CD28 signaling, which is consistent with our results on Akt phosphorylation. Our results also agree with Hui et al., who demonstrated that CD28 is the primary substrate for dephosphorylation through PD-1/SHP-2[151].

One aspect that could better understood is the visual confirmation of both blocking and non-blocking PD-1 antibodies and spatial resolution of their colocalization with CD28 and/or associated PI3K. Advancements in use of supported planar bilayers in conjunction with total internal reflection fluorescence microscopy (TIRFM) could help answer these questions. [279-281] Briefly, GPI-anchored proteins of interest such as ICAM-1, CD80, and antigen-specific MHC-I are incorporated into liposomes that will fuse with a glass surface and form a planar lipid bilayer[282]. Transgenic T cells specific for the MHC-I will be stimulated by the bilayers containing cognate peptide and in the presence or absence of blocking/ non-blocking PD-1 antibodies. Finally, the bilayer-T cell conjugate will be fixed and stained for proteins of interest. These experiments on PD-1 spatial localization were performed by T. Yokosuka et al. in their remarkable investigation of PD-1 recruitment of SHP2 at the IS and that anti-PD-L1 blockade interrupted the recruitment of PD-1[143]. In a similar fashion, we would like to investigate the different PD-1 antibodies and how the presence of bound PD-1 antibodies can change the kinetics in which CD28, PI3K, or TCR signaling components are differentially included during the formation of the IS for future experiments.

We also observed a lower amount of cytokine production from the NB01 compared to pembrolizumab given its limited effect on restoring the NFAT pathway. However, NB01 was shown to enhance antigen-specific proliferation when in combination with pembrolizumab, thereby engaging both the NFAT and NF- $\kappa$ B pathways. This led to the rationale that there could be a synergistic effect to substantially increase both T cell activation pathways with combination treatment of blocking and non-blocking antibodies.

Using the combination of blocking / non-blocking anti-PD-1, we observed increased CD8<sup>+</sup> proliferation, increased cytokine production and increased Ca<sup>2+</sup> mobilization compared to the monotherapy. Using two mouse tumor models established with immunogenic colon carcinoma MC38 cell line and highly aggressive and poorly immunogenic melanoma B16F10 cell line, it was shown that blocking and non-blocking anti-PD-1 antibodies had equivalent activity and in the MC38 study, the combination therapy significantly suppressed tumor growth, with a 2.4-fold increase for complete tumor control and a trend toward improved survival compared with anti-PD-1 monotherapies. In contrast, we did not observe significant, lasting anti-tumor activity in the B16F10 model for either the monotherapies nor the combination therapy. Limited antitumor effects in this study have been consistent with other studies using the B16F10 model for anti-PD-1 therapy given the rapid growth and tumor escape for this cell line[283-285]. It is likely that there was not enough time for anti-PD-1 antibodies to develop an impactful immune response with only two doses administered on day 7; however, the rapid growth of the B16F10 is unparalleled in comparison to human cancer. Another further investigation that could be added to the *in vivo* studies are the use of other tumor cell lines expressing different levels of PD-L1 such as: MCF-7 and MDA-MB-231, breast cancer cell lines with high levels of PD-L1 expression or A549 and HepG2, lung cancer and hepatocellular carcinoma cell lines with low PD-L1 expression[286]. While the outcome of PD-1 therapy is generally correlated with PD-L1 expression on the cancer cells, we could experimentally verify if this combination of blocking and non-blocking anti-PD-1 antibodies could also effectively reduce tumor size in PD-L1 low or negative tumors.

In this study, we have identified a novel class of non-blocking antagonistic anti-PD-1 antibodies that preferentially act on the CD28-PI3K-Akt costimulatory pathway. The combination of blocking and non-blocking anti-PD-1 antibodies produced a synergistic effect in restoring T cell functionality and an enhancement of anti-tumor activity. These results bring

new insight on the mechanisms by which different anti-PD-1 antibodies can differentially relieve PD-1 inhibitory signals and can provide novel strategies for cancer immunotherapy.

*Hypothesis 2: Anti-PD-1 mediated downregulation occurs through an interaction with FcγR expressing cells.*

In this study, we have shown that PD-1 antibody internalization and PD-1 surface downregulation occur as distinct processes. The internalization of anti-PD-1 antibodies in memory T cells was shown to be more rapidly induced and occurred regardless of the composition of its surrounding cells in a T cell intrinsic process. To our knowledge, this is the first reported study showing primary human T cells engaging in the active internalization of anti-PD-1 antibodies.

Even though antibody internalization could be attributed to intrinsic surface PD-1 receptor turnover, we did not observe any increases in surface PD-1 expression with MG132 inhibition of the proteasome compared to the no inhibitor control, indicating that proteasomal receptor degradation was not a factor in regulating PD-1 surface expression. This stood in contrast with a previous report that showed PD-1 surface expression increasing when the proteasomal degradation pathway was blocked [287]. However, the regulation of activation induced PD-1 expression under stimulation conditions compared to the PD-1 exhaustion profile on chronically infected, unstimulated memory T cells we used in this study may explain this disparity. Furthermore, when memory T cells were treated with bafilomycin A, we saw an increase in surface PD-1 expression which indicated that anti-PD-1 antibody binding directed the lysosomal degradation of the PD-1 receptor.

We observed that the downregulation of total surface PD-1 expression in memory T cells occurred more slowly with peak downregulation occurring between 24-48 hours and required the presence of Fc receptor expressing cells. Monocytes were shown to be the cell subset with the highest impact for the PD-1 downregulation effect within the PBMC composition and increased monocyte frequencies positively correlated with the degree of surface PD-1 downregulation. Several studies have shown that with monoclonal antibody therapies targeted against CD4, CD20, CD25, CD30, CD38, CTLA-4, and PD-L1, FcγR-expressing effector cells such as monocytes, macrophages, and granulocytes had a significant effect in downregulating

surface receptors by the crosslinking of the Fc domain of target antibody bound to its antigen and an FcγR *in trans* [227, 288-294]. The effects of anti-CD20 antibodies on downregulating surface CD20 expression has been heavily investigated over the past decade. The recent paper by Dahal, L. et al showed that the internalization and the downregulation of anti-CD20 antibodies occurred as separate processes whereby the downregulation of anti-CD20 on opsonized B cells occurred as a byproduct of phagocytotic events by macrophages in conditions where antibody internalization was not active [295]. Moreover, the authors found that obinutuzmab, a type II anti-CD20 antibody with low internalization capacity, had increased downregulation in primary CLL samples mediated by monocyte-derived macrophages. The culmination of these reports show that antibody mediated receptor downregulation represents an underappreciated but consistently observed effect that has the potential to dictate the outcomes in mAb therapies.

The availability of FcγR binding was shown to be critical in observing PD-1 downregulation as shown by the FcγR blockade experiments. The transfection studies revealed that the FcγR CD64 was primarily responsible for producing this effect. CD64 expression is mainly expressed on monocytes/macrophages and monocyte-derived DCs while inducible in neutrophils, eosinophils, and mast cells and therefore, the likely mediators of this interaction by homeostatic abundance would be the monocytic population [183]. In the work by Kreig, C, et al., higher frequencies of CD14<sup>+</sup> CD16<sup>-</sup> HLA-DR<sup>+</sup> CD64<sup>+</sup> monocytes were shown to be a positive indicator for anti-tumor responses in anti-PD-1 therapy measured by progression-free survival and overall survival in responders compared to non-responders in stage IV melanoma [296]. While the authors did not conclude on the mechanism that drove this finding, we believe that antibody induced PD-1 downregulation linked to higher monocytic frequencies may play a role in this observation.

In order to verify that the memory T cells affected by anti-PD-1 therapy had an exhausted profile, we added markers that defined exhaustion during the antigen-specific proliferation assays. We observed that the majority of the proliferating antigen-specific CD8<sup>+</sup> were TCF1<sup>-</sup> CD127<sup>-</sup> CD28<sup>-</sup> and CXCR3<sup>+</sup> CD39<sup>+</sup> CD244<sup>+</sup> Eomes<sup>hi</sup> in accordance with the current terminal T cell exhaustion model (data not shown)[162, 165]. We also observed that a smaller proportion (~5%) of proliferating CD8<sup>+</sup> were TCF1<sup>+</sup> which represented the precursor exhausted T cell phenotype[297]. This convincingly showed us that anti-PD-1 antibodies were

effective in restoring proliferative capacity in exhausted CD8<sup>+</sup>. However, we did not observe that significantly more TCF1<sup>+</sup> precursor exhausted T cells were preferentially expanded compared to TCF1<sup>-</sup> terminally exhausted T cells under anti-PD-1 treatment as shown in other works[297-300].

Interestingly, we observed that PD-1 downregulation on memory T cells reverted back to approximately ~30-50% of its initial expression after 48 hours when anti-PD-1 antibodies were removed from the supernatant (data not shown). The epigenetic stability of differentiated, exhausted T cells has been shown to be marginally remodeled after PD-1 blockade[273]. Genome-wide modifications such as Pdc1 locus DNA methylation, loss of inhibitory H3K9<sup>me3</sup>/ H3K27<sup>me3</sup> histone marks, and upregulation of activator FoxO1 leads to a high, consistent expression of PD-1 in exhausted T cells even after the removal of antigen presence[109, 301-303]. PD-1 blockade does not completely reprogram exhausted T cells to the memory or effector phenotype and is seen as the lack of durable response in presence of antigen[273].

Another observation was that despite the effect of PD-1 downregulation reaching up to a ~90% reduction of PD-1 expression on total memory CD4<sup>+</sup> and CD8<sup>+</sup>, we did not observe a complete loss of PD-1 surface expression. Preliminary studies did not show any differences in downregulation between T cell memory subsets CM, EM, and TM, indicating that other classifications for a T cell subset resistant to PD-1 downregulation are warranted. Future investigations could possibly include mass cytometry to phenotype this unaffected population more thoroughly by including a combination of exhaustion markers, adhesion markers, and transcription factors or by RNA-seq on sorted PD-1<sup>+</sup> T cells vs PD-1<sup>-</sup> after anti-PD-1 treatment to understand the transcriptional differences between the memory T cells that are permissive to PD-1 downregulation or not. If this loss of PD-1 downregulation effect on the unaffected subset can be associated with persistence of a particular T cell exhaustion phenotype, this could potentially be another mechanism for anti-PD-1 therapy resistance[304].

There have been previous reports that show that PD-1 antibodies are affected by Fc-FcγR interactions and other groups have evaluated the detrimental effects of PD-1 antibodies binding to Fc receptors on macrophages within the tumor microenvironment. Lo Russo et al. showed that Fc-FcR interactions with nivolumab aided in tumor progression in SCID mice with patient-

derived xenografts from NSLC hyperprogressive patients [305]. Furthermore, Arlauckas and colleagues showed reduced treatment efficacy with anti-PD-1 transfer and uptake by macrophages in C57BL6/J mice with MC38 murine adenocarcinoma [306]. In both studies, while the specific Fc receptors involved were not clearly explicated, experiments with Fc receptor blockade or deglycosylated/Fab<sub>2</sub> antibodies showed tumor size reduction in their *in vivo* model. This stood in contrast with our results which showed a significantly increased functional recovery of memory T cells when using the complete mAb over its respective deglycosylated or Fab<sub>2</sub> variant. A possible explanation for this discrepancy would be the type of macrophages that make up the tumor microenvironment in an *in vivo* model. The phenotype of tumor-associated macrophages (TAM) in the tumor milieu is governed by the presence of cytokines and growth factors that regulate differential expression levels of CD64 as well as M1/M2 polarization. Interestingly, increasing levels of inflammatory IFN $\gamma$  or anti-inflammatory IL-10 have both been shown to drive CD64 expression on tissue macrophages which indicates that both anti- and pro-tumorigenic responses can produce effector myeloid cells capable of downregulating PD-1 expression on T cells [183]. Nonetheless, a higher M1-/M2-like ratio has been shown for various cancer types to be a predictor for better prognosis [307-309]. The role of macrophages within the tumor microenvironment remains contentious and the depletion of existing anti-tumor macrophages may be detrimental to controlling tumor burden. A more conciliatory approach would be the reprogramming TAMs to a more proinflammatory phenotype such as the use of CD40 agonists, anti-MACRO or PI3K $\gamma$  antagonists in parallel with anti-PD-1 therapy which would be able to increase anti-tumor effects of tissue resident macrophages while increasing CD64 expression and mediating PD-1 downregulation [310, 311]. The limitation of our study was the use of an *ex vivo* system with monocytes as the primary mediator of this interaction and thereby, losing the effect of tumor polarized macrophages and the cytokine composition of the tumor microenvironment. However, the use of human anti-PD-1 antibodies with human primary cells in our study represents a simpler yet relevant model to reveal the possible human Fc-FcR interactions in PD-1 therapy that can be further investigated.

The results presented here shows the relevance of an alternative, FcR mediated mechanism by which PD-1 antibodies can downregulate the expression of PD-1 on memory T cells, regardless of a ligand blocking interaction. While all PD-1 antibodies tested were able to effectively internalize, the downregulation of the PD-1 receptor itself was reliant on CD64 expressing

monocytes, leading to implications for the prediction of efficacy in anti-PD-1 therapy. Thus, our findings emphasize the necessity of understanding the interactions of PD-1 mAb therapy within a complete immunological setting and further investigations are needed to fully clarify the influence of CD64 and other potential FcRs as well as the immune cell subsets that express them, for PD-1 therapy in clinical settings.

## Chapter IV: REFERENCES

1. Lythe, G., et al., *How many TCR clonotypes does a body maintain?* J Theor Biol, 2016. **389**: p. 214-24.
2. Smith-Garvin, J.E., G.A. Koretzky, and M.S. Jordan, *T cell activation*. Annu Rev Immunol, 2009. **27**: p. 591-619.
3. Pasqual, N., et al., *Quantitative and qualitative changes in V-J alpha rearrangements during mouse thymocytes differentiation: implication for a limited T cell receptor alpha chain repertoire*. J Exp Med, 2002. **196**(9): p. 1163-73.
4. Call, M.E., et al., *The organizing principle in the formation of the T cell receptor-CD3 complex*. Cell, 2002. **111**(7): p. 967-79.
5. Rudd, C.E., et al., *The CD4 receptor is complexed in detergent lysates to a protein-tyrosine kinase (pp58) from human T lymphocytes*. Proc Natl Acad Sci U S A, 1988. **85**(14): p. 5190-4.
6. Barber, E.K., et al., *The CD4 and CD8 antigens are coupled to a protein-tyrosine kinase (p56lck) that phosphorylates the CD3 complex*. Proc Natl Acad Sci U S A, 1989. **86**(9): p. 3277-81.
7. Thome, M., et al., *Syk and ZAP-70 mediate recruitment of p56lck/CD4 to the activated T cell receptor/CD3/zeta complex*. J Exp Med, 1995. **181**(6): p. 1997-2006.
8. Zhang, W., et al., *LAT: the ZAP-70 tyrosine kinase substrate that links T cell receptor to cellular activation*. Cell, 1998. **92**(1): p. 83-92.
9. Alarcon, B., et al., *T-cell antigen-receptor stoichiometry: pre-clustering for sensitivity*. EMBO Rep, 2006. **7**(5): p. 490-5.
10. Hashimoto-Tane, A., et al., *Micro-adhesion rings surrounding TCR microclusters are essential for T cell activation*. J Exp Med, 2016. **213**(8): p. 1609-25.
11. Castro, M., et al., *Receptor Pre-Clustering and T cell Responses: Insights into Molecular Mechanisms*. Front Immunol, 2014. **5**: p. 132.
12. Bunnell, S.C., et al., *T cell receptor ligation induces the formation of dynamically regulated signaling assemblies*. J Cell Biol, 2002. **158**(7): p. 1263-75.
13. Yi, J., et al., *TCR microclusters form spatially segregated domains and sequentially assemble in calcium-dependent kinetic steps*. Nat Commun, 2019. **10**(1): p. 277.
14. Monks, C.R., et al., *Three-dimensional segregation of supramolecular activation clusters in T cells*. Nature, 1998. **395**(6697): p. 82-6.
15. Dustin, M.L., *The immunological synapse*. Cancer Immunol Res, 2014. **2**(11): p. 1023-33.
16. Onnis, A. and C.T. Baldari, *Orchestration of Immunological Synapse Assembly by Vesicular Trafficking*. Front Cell Dev Biol, 2019. **7**: p. 110.
17. Wang, H., et al., *ZAP-70: an essential kinase in T-cell signaling*. Cold Spring Harb Perspect Biol, 2010. **2**(5): p. a002279.
18. Kortum, R.L., et al., *The ability of Sos1 to oligomerize the adaptor protein LAT is separable from its guanine nucleotide exchange activity in vivo*. Sci Signal, 2013. **6**(301): p. ra99.
19. Balagopalan, L., et al., *Plasma membrane LAT activation precedes vesicular recruitment defining two phases of early T-cell activation*. Nat Commun, 2018. **9**(1): p. 2013.
20. Balagopalan, L., et al., *The LAT story: a tale of cooperativity, coordination, and choreography*. Cold Spring Harb Perspect Biol, 2010. **2**(8): p. a005512.
21. Balagopalan, L., et al., *The linker for activation of T cells (LAT) signaling hub: from signaling complexes to microclusters*. J Biol Chem, 2015. **290**(44): p. 26422-9.

22. Shim, E.K., S.H. Jung, and J.R. Lee, *Role of two adaptor molecules SLP-76 and LAT in the PI3K signaling pathway in activated T cells*. J Immunol, 2011. **186**(5): p. 2926-35.
23. Huse, M., *The T-cell-receptor signaling network*. J Cell Sci, 2009. **122**(Pt 9): p. 1269-73.
24. Fruman, D.A., et al., *The PI3K Pathway in Human Disease*. Cell, 2017. **170**(4): p. 605-635.
25. Franke, T.F., et al., *The protein kinase encoded by the Akt proto-oncogene is a target of the PDGF-activated phosphatidylinositol 3-kinase*. Cell, 1995. **81**(5): p. 727-36.
26. Alessi, D.R. and P. Cohen, *Mechanism of activation and function of protein kinase B*. Curr Opin Genet Dev, 1998. **8**(1): p. 55-62.
27. Alessi, D.R., et al., *Characterization of a 3-phosphoinositide-dependent protein kinase which phosphorylates and activates protein kinase Balpha*. Curr Biol, 1997. **7**(4): p. 261-9.
28. Sarbassov, D.D., et al., *Phosphorylation and regulation of Akt/PKB by the rictor-mTOR complex*. Science, 2005. **307**(5712): p. 1098-101.
29. Conley, J.M., M.P. Gallagher, and L.J. Berg, *T Cells and Gene Regulation: The Switching On and Turning Up of Genes after T Cell Receptor Stimulation in CD8 T Cells*. Front Immunol, 2016. **7**: p. 76.
30. Spolski, R., P. Li, and W.J. Leonard, *Biology and regulation of IL-2: from molecular mechanisms to human therapy*. Nat Rev Immunol, 2018. **18**(10): p. 648-659.
31. Vaeth, M. and S. Feske, *NFAT control of immune function: New Frontiers for an Abiding Trooper*. F1000Res, 2018. **7**: p. 260.
32. Serafini, A.T., et al., *Isolation of mutant T lymphocytes with defects in capacitative calcium entry*. Immunity, 1995. **3**(2): p. 239-50.
33. Timmerman, L.A., et al., *Rapid shuttling of NF-AT in discrimination of Ca<sup>2+</sup> signals and immunosuppression*. Nature, 1996. **383**(6603): p. 837-40.
34. Foskett, J.K., et al., *Inositol trisphosphate receptor Ca<sup>2+</sup> release channels*. Physiol Rev, 2007. **87**(2): p. 593-658.
35. Jayaraman, T., et al., *Regulation of the inositol 1,4,5-trisphosphate receptor by tyrosine phosphorylation*. Science, 1996. **272**(5267): p. 1492-4.
36. Xue, L., et al., *Inhibition of PI3K and calcineurin suppresses chemoattractant receptor-homologous molecule expressed on Th2 cells (CRTH2)-dependent responses of Th2 lymphocytes to prostaglandin D(2)*. Biochem Pharmacol, 2007. **73**(6): p. 843-53.
37. Chow, W., G. Hou, and M.P. Bendeck, *Glycogen synthase kinase 3beta regulation of nuclear factor of activated T-cells isoform c1 in the vascular smooth muscle cell response to injury*. Exp Cell Res, 2008. **314**(16): p. 2919-29.
38. Yoeli-Lerner, M., et al., *Akt/protein kinase b and glycogen synthase kinase-3beta signaling pathway regulates cell migration through the NFAT1 transcription factor*. Mol Cancer Res, 2009. **7**(3): p. 425-32.
39. Huang, G., L.Z. Shi, and H. Chi, *Regulation of JNK and p38 MAPK in the immune system: signal integration, propagation and termination*. Cytokine, 2009. **48**(3): p. 161-9.
40. Rincon, M., R.A. Flavell, and R.J. Davis, *Signal transduction by MAP kinases in T lymphocytes*. Oncogene, 2001. **20**(19): p. 2490-7.
41. Israel, A., *The IKK complex, a central regulator of NF-kappaB activation*. Cold Spring Harb Perspect Biol, 2010. **2**(3): p. a000158.
42. Paul, S. and B.C. Schaefer, *A new look at T cell receptor signaling to nuclear factor-kappaB*. Trends Immunol, 2013. **34**(6): p. 269-81.

43. Thome, M., *CARMA1, BCL-10 and MALT1 in lymphocyte development and activation*. Nat Rev Immunol, 2004. **4**(5): p. 348-59.
44. Juilland, M. and M. Thome, *Holding All the CARDS: How MALT1 Controls CARMA/CARD-Dependent Signaling*. Front Immunol, 2018. **9**: p. 1927.
45. Daniels, M.A. and E. Teixeiro, *TCR Signaling in T Cell Memory*. Front Immunol, 2015. **6**: p. 617.
46. Hosokawa, H. and E.V. Rothenberg, *Cytokines, Transcription Factors, and the Initiation of T-Cell Development*. Cold Spring Harb Perspect Biol, 2018. **10**(5).
47. Knudson, K.M., et al., *Low-affinity T cells are programmed to maintain normal primary responses but are impaired in their recall to low-affinity ligands*. Cell Rep, 2013. **4**(3): p. 554-65.
48. Bhattacharyya, N.D. and C.G. Feng, *Regulation of T Helper Cell Fate by TCR Signal Strength*. Front Immunol, 2020. **11**: p. 624.
49. Tubo, N.J. and M.K. Jenkins, *TCR signal quantity and quality in CD4(+) T cell differentiation*. Trends Immunol, 2014. **35**(12): p. 591-596.
50. Poltorak, M., et al., *TCR activation kinetics and feedback regulation in primary human T cells*. Cell Commun Signal, 2013. **11**: p. 4.
51. Lobry, C., et al., *Negative feedback loop in T cell activation through I $\kappa$ B kinase-induced phosphorylation and degradation of Bcl10*. Proc Natl Acad Sci U S A, 2007. **104**(3): p. 908-13.
52. Appleman, L.J. and V.A. Boussiotis, *T cell anergy and costimulation*. Immunol Rev, 2003. **192**: p. 161-80.
53. Van Parijs, L., A. Ibraghimov, and A.K. Abbas, *The roles of costimulation and Fas in T cell apoptosis and peripheral tolerance*. Immunity, 1996. **4**(3): p. 321-8.
54. Heinzl, S., et al., *A Myc-dependent division timer complements a cell-death timer to regulate T cell and B cell responses*. Nat Immunol, 2017. **18**(1): p. 96-103.
55. Chen, L. and D.B. Flies, *Molecular mechanisms of T cell co-stimulation and co-inhibition*. Nat Rev Immunol, 2013. **13**(4): p. 227-42.
56. Martin, P.J., et al., *A 44 kilodalton cell surface homodimer regulates interleukin 2 production by activated human T lymphocytes*. J Immunol, 1986. **136**(9): p. 3282-7.
57. Esensten, J.H., et al., *CD28 Costimulation: From Mechanism to Therapy*. Immunity, 2016. **44**(5): p. 973-88.
58. Liang, Y., et al., *The lymphoid lineage-specific actin-uncapping protein Rltpr is essential for costimulation via CD28 and the development of regulatory T cells*. Nat Immunol, 2013. **14**(8): p. 858-66.
59. Boise, L.H., et al., *CD28 costimulation can promote T cell survival by enhancing the expression of Bcl-XL*. Immunity, 1995. **3**(1): p. 87-98.
60. Riley, J.L. and C.H. June, *The CD28 family: a T-cell rheostat for therapeutic control of T-cell activation*. Blood, 2005. **105**(1): p. 13-21.
61. Mou, D., et al., *CD28 negative T cells: is their loss our gain?* Am J Transplant, 2014. **14**(11): p. 2460-6.
62. Miller, J., et al., *Two pathways of costimulation through CD28*. Immunol Res, 2009. **45**(2-3): p. 159-72.
63. Vallejo, A.N., *CD28 extinction in human T cells: altered functions and the program of T-cell senescence*. Immunol Rev, 2005. **205**: p. 158-69.
64. Aiello, A., et al., *Immunosenescence and Its Hallmarks: How to Oppose Aging Strategically? A Review of Potential Options for Therapeutic Intervention*. Front Immunol, 2019. **10**: p. 2247.
65. van Berkel, M.E. and M.A. Oosterwegel, *CD28 and ICOS: similar or separate costimulators of T cells?* Immunol Lett, 2006. **105**(2): p. 115-22.

66. Wikenheiser, D.J. and J.S. Stumhofer, *ICOS Co-Stimulation: Friend or Foe?* Front Immunol, 2016. **7**: p. 304.
67. Locksley, R.M., N. Killeen, and M.J. Lenardo, *The TNF and TNF receptor superfamilies: integrating mammalian biology.* Cell, 2001. **104**(4): p. 487-501.
68. Buchan, S.L., A. Rogel, and A. Al-Shamkhani, *The immunobiology of CD27 and OX40 and their potential as targets for cancer immunotherapy.* Blood, 2018. **131**(1): p. 39-48.
69. Ward-Kavanagh, L.K., et al., *The TNF Receptor Superfamily in Co-stimulating and Co-inhibitory Responses.* Immunity, 2016. **44**(5): p. 1005-19.
70. Weinkove, R., et al., *Selecting costimulatory domains for chimeric antigen receptors: functional and clinical considerations.* Clin Transl Immunology, 2019. **8**(5): p. e1049.
71. Curtsinger, J.M. and M.F. Mescher, *Inflammatory cytokines as a third signal for T cell activation.* Curr Opin Immunol, 2010. **22**(3): p. 333-40.
72. Valenzuela, J., C. Schmidt, and M. Mescher, *The roles of IL-12 in providing a third signal for clonal expansion of naive CD8 T cells.* J Immunol, 2002. **169**(12): p. 6842-9.
73. Ben-Sasson, S.Z., et al., *IL-1 acts directly on CD4 T cells to enhance their antigen-driven expansion and differentiation.* Proc Natl Acad Sci U S A, 2009. **106**(17): p. 7119-24.
74. Sckisel, G.D., et al., *Out-of-Sequence Signal 3 Paralyzes Primary CD4(+) T-Cell-Dependent Immunity.* Immunity, 2015. **43**(2): p. 240-50.
75. Lorenz, U., *SHP-1 and SHP-2 in T cells: two phosphatases functioning at many levels.* Immunol Rev, 2009. **228**(1): p. 342-59.
76. Srivastava, N., R. Sudan, and W.G. Kerr, *Role of inositol poly-phosphatases and their targets in T cell biology.* Front Immunol, 2013. **4**: p. 288.
77. Furlan, G., et al., *Phosphatase CD45 both positively and negatively regulates T cell receptor phosphorylation in reconstituted membrane protein clusters.* J Biol Chem, 2014. **289**(41): p. 28514-25.
78. Courtney, A.H., et al., *CD45 functions as a signaling gatekeeper in T cells.* Sci Signal, 2019. **12**(604).
79. Hui, E. and R.D. Vale, *In vitro membrane reconstitution of the T-cell receptor proximal signaling network.* Nat Struct Mol Biol, 2014. **21**(2): p. 133-42.
80. Vang, T., et al., *Activation of the COOH-terminal Src kinase (Csk) by cAMP-dependent protein kinase inhibits signaling through the T cell receptor.* J Exp Med, 2001. **193**(4): p. 497-507.
81. Rossy, J., D.J. Williamson, and K. Gaus, *How does the kinase Lck phosphorylate the T cell receptor? Spatial organization as a regulatory mechanism.* Front Immunol, 2012. **3**: p. 167.
82. Singh, B.K. and T. Kambayashi, *The Immunomodulatory Functions of Diacylglycerol Kinase zeta.* Front Cell Dev Biol, 2016. **4**: p. 96.
83. Avila-Flores, A., et al., *Predominant contribution of DGKzeta over DGKalpha in the control of PKC/PDK-1-regulated functions in T cells.* Immunol Cell Biol, 2017. **95**(6): p. 549-563.
84. Hu, H. and S.C. Sun, *Ubiquitin signaling in immune responses.* Cell Res, 2016. **26**(4): p. 457-83.
85. O'Leary, C.E., E.L. Lewis, and P.M. Oliver, *Ubiquitylation as a Rheostat for TCR Signaling: From Targeted Approaches Toward Global Profiling.* Front Immunol, 2015. **6**: p. 618.
86. Brunet, J.F., et al., *A new member of the immunoglobulin superfamily--CTLA-4.* Nature, 1987. **328**(6127): p. 267-70.

87. Harper, K., et al., *CTLA-4 and CD28 activated lymphocyte molecules are closely related in both mouse and human as to sequence, message expression, gene structure, and chromosomal location*. J Immunol, 1991. **147**(3): p. 1037-44.
88. Tivol, E.A., et al., *Loss of CTLA-4 leads to massive lymphoproliferation and fatal multiorgan tissue destruction, revealing a critical negative regulatory role of CTLA-4*. Immunity, 1995. **3**(5): p. 541-7.
89. Krummel, M.F. and J.P. Allison, *CD28 and CTLA-4 have opposing effects on the response of T cells to stimulation*. J Exp Med, 1995. **182**(2): p. 459-65.
90. Walunas, T.L., C.Y. Bakker, and J.A. Bluestone, *CTLA-4 ligation blocks CD28-dependent T cell activation*. J Exp Med, 1996. **183**(6): p. 2541-50.
91. Rowshanravan, B., N. Halliday, and D.M. Sansom, *CTLA-4: a moving target in immunotherapy*. Blood, 2018. **131**(1): p. 58-67.
92. Qureshi, O.S., et al., *Trans-endocytosis of CD80 and CD86: a molecular basis for the cell-extrinsic function of CTLA-4*. Science, 2011. **332**(6029): p. 600-3.
93. Ni, L. and C. Dong, *New B7 Family Checkpoints in Human Cancers*. Mol Cancer Ther, 2017. **16**(7): p. 1203-1211.
94. Andrews, L.P., et al., *LAG3 (CD223) as a cancer immunotherapy target*. Immunol Rev, 2017. **276**(1): p. 80-96.
95. Workman, C.J., K.J. Dugger, and D.A. Vignali, *Cutting edge: molecular analysis of the negative regulatory function of lymphocyte activation gene-3*. J Immunol, 2002. **169**(10): p. 5392-5.
96. Workman, C.J. and D.A. Vignali, *The CD4-related molecule, LAG-3 (CD223), regulates the expansion of activated T cells*. Eur J Immunol, 2003. **33**(4): p. 970-9.
97. Wolf, Y., A.C. Anderson, and V.K. Kuchroo, *TIM3 comes of age as an inhibitory receptor*. Nat Rev Immunol, 2020. **20**(3): p. 173-185.
98. Lee, J., et al., *Phosphotyrosine-dependent coupling of Tim-3 to T-cell receptor signaling pathways*. Mol Cell Biol, 2011. **31**(19): p. 3963-74.
99. Rangachari, M., et al., *Bat3 promotes T cell responses and autoimmunity by repressing Tim-3-mediated cell death and exhaustion*. Nat Med, 2012. **18**(9): p. 1394-400.
100. Clayton, K.L., et al., *T cell Ig and mucin domain-containing protein 3 is recruited to the immune synapse, disrupts stable synapse formation, and associates with receptor phosphatases*. J Immunol, 2014. **192**(2): p. 782-91.
101. Ishida, Y., et al., *Induced expression of PD-1, a novel member of the immunoglobulin gene superfamily, upon programmed cell death*. EMBO J, 1992. **11**(11): p. 3887-95.
102. Nishimura, H., et al., *Development of lupus-like autoimmune diseases by disruption of the PD-1 gene encoding an ITIM motif-carrying immunoreceptor*. Immunity, 1999. **11**(2): p. 141-51.
103. Nishimura, H., et al., *Autoimmune dilated cardiomyopathy in PD-1 receptor-deficient mice*. Science, 2001. **291**(5502): p. 319-22.
104. Okazaki, T., et al., *PD-1 immunoreceptor inhibits B cell receptor-mediated signaling by recruiting src homology 2-domain-containing tyrosine phosphatase 2 to phosphotyrosine*. Proc Natl Acad Sci U S A, 2001. **98**(24): p. 13866-71.
105. Boussiotis, V.A., *Molecular and Biochemical Aspects of the PD-1 Checkpoint Pathway*. N Engl J Med, 2016. **375**(18): p. 1767-1778.
106. Wang, J., et al., *Establishment of NOD-Pdcd1<sup>-/-</sup> mice as an efficient animal model of type I diabetes*. Proc Natl Acad Sci U S A, 2005. **102**(33): p. 11823-8.
107. Barber, D.L., et al., *Restoring function in exhausted CD8 T cells during chronic viral infection*. Nature, 2006. **439**(7077): p. 682-7.
108. Agata, Y., et al., *Expression of the PD-1 antigen on the surface of stimulated mouse T and B lymphocytes*. Int Immunol, 1996. **8**(5): p. 765-72.

109. Youngblood, B., et al., *Chronic virus infection enforces demethylation of the locus that encodes PD-1 in antigen-specific CD8(+) T cells*. *Immunity*, 2011. **35**(3): p. 400-12.
110. Sharpe, A.H. and K.E. Pauken, *The diverse functions of the PD1 inhibitory pathway*. *Nat Rev Immunol*, 2018. **18**(3): p. 153-167.
111. Bally, A.P., J.W. Austin, and J.M. Boss, *Genetic and Epigenetic Regulation of PD-1 Expression*. *J Immunol*, 2016. **196**(6): p. 2431-7.
112. Austin, J.W., et al., *STAT3, STAT4, NFATc1, and CTCF regulate PD-1 through multiple novel regulatory regions in murine T cells*. *J Immunol*, 2014. **192**(10): p. 4876-86.
113. Xiao, G., et al., *Activator protein 1 suppresses antitumor T-cell function via the induction of programmed death 1*. *Proc Natl Acad Sci U S A*, 2012. **109**(38): p. 15419-24.
114. Mathieu, M., et al., *Notch signaling regulates PD-1 expression during CD8(+) T-cell activation*. *Immunol Cell Biol*, 2013. **91**(1): p. 82-8.
115. Kao, C., et al., *Transcription factor T-bet represses expression of the inhibitory receptor PD-1 and sustains virus-specific CD8+ T cell responses during chronic infection*. *Nat Immunol*, 2011. **12**(7): p. 663-71.
116. Lu, P., et al., *Blimp-1 represses CD8 T cell expression of PD-1 using a feed-forward transcriptional circuit during acute viral infection*. *J Exp Med*, 2014. **211**(3): p. 515-27.
117. Johnston, R.J., et al., *Bcl6 and Blimp-1 are reciprocal and antagonistic regulators of T follicular helper cell differentiation*. *Science*, 2009. **325**(5943): p. 1006-10.
118. Shin, H., et al., *A role for the transcriptional repressor Blimp-1 in CD8(+) T cell exhaustion during chronic viral infection*. *Immunity*, 2009. **31**(2): p. 309-20.
119. Riley, J.L., *PD-1 signaling in primary T cells*. *Immunol Rev*, 2009. **229**(1): p. 114-25.
120. Freeman, G.J., et al., *Engagement of the PD-1 immunoinhibitory receptor by a novel B7 family member leads to negative regulation of lymphocyte activation*. *J Exp Med*, 2000. **192**(7): p. 1027-34.
121. Chemnitz, J.M., et al., *SHP-1 and SHP-2 associate with immunoreceptor tyrosine-based switch motif of programmed death 1 upon primary human T cell stimulation, but only receptor ligation prevents T cell activation*. *J Immunol*, 2004. **173**(2): p. 945-54.
122. Francisco, L.M., et al., *PD-L1 regulates the development, maintenance, and function of induced regulatory T cells*. *J Exp Med*, 2009. **206**(13): p. 3015-29.
123. Amarnath, S., et al., *The PDL1-PD1 axis converts human TH1 cells into regulatory T cells*. *Sci Transl Med*, 2011. **3**(111): p. 111ra120.
124. Patsoukis, N., et al., *Selective effects of PD-1 on Akt and Ras pathways regulate molecular components of the cell cycle and inhibit T cell proliferation*. *Sci Signal*, 2012. **5**(230): p. ra46.
125. Patsoukis, N., et al., *PD-1 alters T-cell metabolic reprogramming by inhibiting glycolysis and promoting lipolysis and fatty acid oxidation*. *Nat Commun*, 2015. **6**: p. 6692.
126. Howie, D., et al., *The Role of Lipid Metabolism in T Lymphocyte Differentiation and Survival*. *Front Immunol*, 2017. **8**: p. 1949.
127. Yu, Y.R., et al., *Disturbed mitochondrial dynamics in CD8(+) TILs reinforce T cell exhaustion*. *Nat Immunol*, 2020. **21**(12): p. 1540-1551.
128. Escors, D., et al., *The intracellular signalosome of PD-L1 in cancer cells*. *Signal Transduct Target Ther*, 2018. **3**: p. 26.
129. Qin, W., et al., *The Diverse Function of PD-1/PD-L Pathway Beyond Cancer*. *Front Immunol*, 2019. **10**: p. 2298.

130. Lin, D.Y., et al., *The PD-1/PD-L1 complex resembles the antigen-binding Fv domains of antibodies and T cell receptors*. Proc Natl Acad Sci U S A, 2008. **105**(8): p. 3011-6.
131. Youngnak, P., et al., *Differential binding properties of B7-H1 and B7-DC to programmed death-1*. Biochem Biophys Res Commun, 2003. **307**(3): p. 672-7.
132. Ghiotto, M., et al., *PD-L1 and PD-L2 differ in their molecular mechanisms of interaction with PD-1*. Int Immunol, 2010. **22**(8): p. 651-60.
133. Frigola, X., et al., *Identification of a soluble form of B7-H1 that retains immunosuppressive activity and is associated with aggressive renal cell carcinoma*. Clin Cancer Res, 2011. **17**(7): p. 1915-23.
134. Park, J.J., et al., *B7-H1/CD80 interaction is required for the induction and maintenance of peripheral T-cell tolerance*. Blood, 2010. **116**(8): p. 1291-8.
135. Sugiura, D., et al., *Restriction of PD-1 function by cis-PD-L1/CD80 interactions is required for optimal T cell responses*. Science, 2019. **364**(6440): p. 558-566.
136. Zhao, Y., et al., *Antigen-Presenting Cell-Intrinsic PD-1 Neutralizes PD-L1 in cis to Attenuate PD-1 Signaling in T Cells*. Cell Rep, 2018. **24**(2): p. 379-390 e6.
137. Okadome, K., et al., *Prognostic and clinical impact of PD-L2 and PD-L1 expression in a cohort of 437 oesophageal cancers*. Br J Cancer, 2020. **122**(10): p. 1535-1543.
138. Yasuoka, H., et al., *Increased both PD-L1 and PD-L2 expressions on monocytes of patients with hepatocellular carcinoma was associated with a poor prognosis*. Sci Rep, 2020. **10**(1): p. 10377.
139. Obeid, J.M., et al., *PD-L1, PD-L2 and PD-1 expression in metastatic melanoma: Correlation with tumor-infiltrating immune cells and clinical outcome*. Oncoimmunology, 2016. **5**(11): p. e1235107.
140. Toyokawa, G., et al., *Favorable Disease-free Survival Associated with Programmed Death Ligand 1 Expression in Patients with Surgically Resected Small-cell Lung Cancer*. Anticancer Res, 2016. **36**(8): p. 4329-36.
141. Takamori, S., et al., *Prognostic Impact of PD-L2 Expression and Association with PD-L1 in Patients with Small-cell Lung Cancer*. Anticancer Res, 2018. **38**(10): p. 5903-5907.
142. Boussiotis, V.A., P. Chatterjee, and L. Li, *Biochemical signaling of PD-1 on T cells and its functional implications*. Cancer J, 2014. **20**(4): p. 265-71.
143. Yokosuka, T., et al., *Programmed cell death 1 forms negative costimulatory microclusters that directly inhibit T cell receptor signaling by recruiting phosphatase SHP2*. J Exp Med, 2012. **209**(6): p. 1201-17.
144. Bardhan, K., et al., *Phosphorylation of PD-1-Y248 is a marker of PD-1-mediated inhibitory function in human T cells*. Sci Rep, 2019. **9**(1): p. 17252.
145. Peled, M., et al., *Affinity purification mass spectrometry analysis of PD-1 uncovers SAP as a new checkpoint inhibitor*. Proc Natl Acad Sci U S A, 2018. **115**(3): p. E468-E477.
146. Marasco, M., et al., *Molecular mechanism of SHP2 activation by PD-1 stimulation*. Sci Adv, 2020. **6**(5): p. eaay4458.
147. Sheppard, K.A., et al., *PD-1 inhibits T-cell receptor induced phosphorylation of the ZAP70/CD3zeta signalosome and downstream signaling to PKCtheta*. FEBS Lett, 2004. **574**(1-3): p. 37-41.
148. Mizuno, R., et al., *PD-1 Primarily Targets TCR Signal in the Inhibition of Functional T Cell Activation*. Front Immunol, 2019. **10**: p. 630.
149. Patsoukis, N., et al., *PD-1 increases PTEN phosphatase activity while decreasing PTEN protein stability by inhibiting casein kinase 2*. Mol Cell Biol, 2013. **33**(16): p. 3091-8.
150. Parry, R.V., et al., *CTLA-4 and PD-1 receptors inhibit T-cell activation by distinct mechanisms*. Mol Cell Biol, 2005. **25**(21): p. 9543-53.

151. Hui, E., et al., *T cell costimulatory receptor CD28 is a primary target for PD-1-mediated inhibition*. *Science*, 2017. **355**(6332): p. 1428-1433.
152. Celis-Gutierrez, J., et al., *Quantitative Interactomics in Primary T Cells Provides a Rationale for Concomitant PD-1 and BTLA Coinhibitor Blockade in Cancer Immunotherapy*. *Cell Rep*, 2019. **27**(11): p. 3315-3330 e7.
153. Rota, G., et al., *Shp-2 Is Dispensable for Establishing T Cell Exhaustion and for PD-1 Signaling In Vivo*. *Cell Rep*, 2018. **23**(1): p. 39-49.
154. Carter, L., et al., *PD-1:PD-L inhibitory pathway affects both CD4(+) and CD8(+) T cells and is overcome by IL-2*. *Eur J Immunol*, 2002. **32**(3): p. 634-43.
155. Bennett, F., et al., *Program death-1 engagement upon TCR activation has distinct effects on costimulation and cytokine-driven proliferation: attenuation of ICOS, IL-4, and IL-21, but not CD28, IL-7, and IL-15 responses*. *J Immunol*, 2003. **170**(2): p. 711-8.
156. Farber, D.L., N.A. Yudanin, and N.P. Restifo, *Human memory T cells: generation, compartmentalization and homeostasis*. *Nat Rev Immunol*, 2014. **14**(1): p. 24-35.
157. Ahmed, R. and D. Gray, *Immunological memory and protective immunity: understanding their relation*. *Science*, 1996. **272**(5258): p. 54-60.
158. Youngblood, B., et al., *Effector CD8 T cells dedifferentiate into long-lived memory cells*. *Nature*, 2017. **552**(7685): p. 404-409.
159. Kumar, B.V., T.J. Connors, and D.L. Farber, *Human T Cell Development, Localization, and Function throughout Life*. *Immunity*, 2018. **48**(2): p. 202-213.
160. Jameson, S.C. and D. Masopust, *Understanding Subset Diversity in T Cell Memory*. *Immunity*, 2018. **48**(2): p. 214-226.
161. McLane, L.M., M.S. Abdel-Hakeem, and E.J. Wherry, *CD8 T Cell Exhaustion During Chronic Viral Infection and Cancer*. *Annu Rev Immunol*, 2019. **37**: p. 457-495.
162. Wherry, E.J. and M. Kurachi, *Molecular and cellular insights into T cell exhaustion*. *Nat Rev Immunol*, 2015. **15**(8): p. 486-99.
163. Buchholz, V.R. and D.H. Busch, *Back to the Future: Effector Fate during T Cell Exhaustion*. *Immunity*, 2019. **51**(6): p. 970-972.
164. Galletti, G., et al., *Two subsets of stem-like CD8(+) memory T cell progenitors with distinct fate commitments in humans*. *Nat Immunol*, 2020. **21**(12): p. 1552-1562.
165. Blank, C.U., et al., *Defining 'T cell exhaustion'*. *Nat Rev Immunol*, 2019. **19**(11): p. 665-674.
166. Seo, H., et al., *TOX and TOX2 transcription factors cooperate with NR4A transcription factors to impose CD8(+) T cell exhaustion*. *Proc Natl Acad Sci U S A*, 2019. **116**(25): p. 12410-12415.
167. Kohler, G. and C. Milstein, *Continuous cultures of fused cells secreting antibody of predefined specificity*. *Nature*, 1975. **256**(5517): p. 495-7.
168. Leavy, O., *Therapeutic antibodies: past, present and future*. *Nat Rev Immunol*, 2010. **10**(5): p. 297.
169. Lu, R.M., et al., *Development of therapeutic antibodies for the treatment of diseases*. *J Biomed Sci*, 2020. **27**(1): p. 1.
170. Al-Lazikani, B., A.M. Lesk, and C. Chothia, *Standard conformations for the canonical structures of immunoglobulins*. *J Mol Biol*, 1997. **273**(4): p. 927-48.
171. Kretschmer, A., et al., *Antibody Isotypes for Tumor Immunotherapy*. *Transfus Med Hemother*, 2017. **44**(5): p. 320-326.
172. Waldmann, T.A. and W. Strober, *Metabolism of immunoglobulins*. *Prog Allergy*, 1969. **13**: p. 1-110.
173. Roopenian, D.C. and S. Akilesh, *FcRn: the neonatal Fc receptor comes of age*. *Nat Rev Immunol*, 2007. **7**(9): p. 715-25.

174. Irani, V., et al., *Molecular properties of human IgG subclasses and their implications for designing therapeutic monoclonal antibodies against infectious diseases*. Mol Immunol, 2015. **67**(2 Pt A): p. 171-82.
175. Beers, S.A., M.J. Glennie, and A.L. White, *Influence of immunoglobulin isotype on therapeutic antibody function*. Blood, 2016. **127**(9): p. 1097-101.
176. van der Neut Kolfschoten, M., et al., *Anti-inflammatory activity of human IgG4 antibodies by dynamic Fab arm exchange*. Science, 2007. **317**(5844): p. 1554-7.
177. Carter, P.J., *Potent antibody therapeutics by design*. Nat Rev Immunol, 2006. **6**(5): p. 343-57.
178. Bruhns, P., *Properties of mouse and human IgG receptors and their contribution to disease models*. Blood, 2012. **119**(24): p. 5640-9.
179. Patel, K.R., J.T. Roberts, and A.W. Barb, *Multiple Variables at the Leukocyte Cell Surface Impact Fc gamma Receptor-Dependent Mechanisms*. Front Immunol, 2019. **10**: p. 223.
180. Nimmerjahn, F. and J.V. Ravetch, *Fc gamma receptors as regulators of immune responses*. Nat Rev Immunol, 2008. **8**(1): p. 34-47.
181. Noto, A., et al., *CD32(+) and PD-1(+) Lymph Node CD4 T Cells Support Persistent HIV-1 Transcription in Treated Aviremic Individuals*. J Virol, 2018. **92**(20).
182. Darcis, G., et al., *CD32(+)CD4(+) T Cells Are Highly Enriched for HIV DNA and Can Support Transcriptional Latency*. Cell Rep, 2020. **30**(7): p. 2284-2296 e3.
183. Swisher, J.F. and G.M. Feldman, *The many faces of Fc gamma RI: implications for therapeutic antibody function*. Immunol Rev, 2015. **268**(1): p. 160-74.
184. Smith, K.G. and M.R. Clatworthy, *Fc gamma RIIB in autoimmunity and infection: evolutionary and therapeutic implications*. Nat Rev Immunol, 2010. **10**(5): p. 328-43.
185. Lu, L.L., et al., *Beyond binding: antibody effector functions in infectious diseases*. Nat Rev Immunol, 2018. **18**(1): p. 46-61.
186. Sunada, H., et al., *Monoclonal antibody against epidermal growth factor receptor is internalized without stimulating receptor phosphorylation*. Proc Natl Acad Sci U S A, 1986. **83**(11): p. 3825-9.
187. Egen, J.G., M.S. Kuhns, and J.P. Allison, *CTLA-4: new insights into its biological function and use in tumor immunotherapy*. Nat Immunol, 2002. **3**(7): p. 611-8.
188. Greer, Y.E., et al., *MEDI3039, a novel highly potent tumor necrosis factor (TNF)-related apoptosis-inducing ligand (TRAIL) receptor 2 agonist, causes regression of orthotopic tumors and inhibits outgrowth of metastatic triple-negative breast cancer*. Breast Cancer Res, 2019. **21**(1): p. 27.
189. Ricart, A.D., *Antibody-drug conjugates of calicheamicin derivative: gemtuzumab ozogamicin and inotuzumab ozogamicin*. Clin Cancer Res, 2011. **17**(20): p. 6417-27.
190. Rajasekaran, N., et al., *Enhancement of antibody-dependent cell mediated cytotoxicity: a new era in cancer treatment*. Immunotargets Ther, 2015. **4**: p. 91-100.
191. de Saint Basile, G., G. Menasche, and A. Fischer, *Molecular mechanisms of biogenesis and exocytosis of cytotoxic granules*. Nat Rev Immunol, 2010. **10**(8): p. 568-79.
192. Lattanzio, L., et al., *Elevated basal antibody-dependent cell-mediated cytotoxicity (ADCC) and high epidermal growth factor receptor (EGFR) expression predict favourable outcome in patients with locally advanced head and neck cancer treated with cetuximab and radiotherapy*. Cancer Immunol Immunother, 2017. **66**(5): p. 573-579.
193. Cartron, G., et al., *Therapeutic activity of humanized anti-CD20 monoclonal antibody and polymorphism in IgG Fc receptor Fc gamma RIIIa gene*. Blood, 2002. **99**(3): p. 754-8.

194. Flannagan, R.S., V. Jaumouille, and S. Grinstein, *The cell biology of phagocytosis*. Annu Rev Pathol, 2012. **7**: p. 61-98.
195. Zent, C.S. and M.R. Elliott, *Maxed out macs: physiologic cell clearance as a function of macrophage phagocytic capacity*. FEBS J, 2017. **284**(7): p. 1021-1039.
196. Herter, S., et al., *Glycoengineering of therapeutic antibodies enhances monocyte/macrophage-mediated phagocytosis and cytotoxicity*. J Immunol, 2014. **192**(5): p. 2252-60.
197. Matlawska-Wasowska, K., et al., *Macrophage and NK-mediated killing of precursor-B acute lymphoblastic leukemia cells targeted with a-fucosylated anti-CD19 humanized antibodies*. Leukemia, 2013. **27**(6): p. 1263-74.
198. Vermi, W., et al., *slan(+) Monocytes and Macrophages Mediate CD20-Dependent B-cell Lymphoma Elimination via ADCC and ADCP*. Cancer Res, 2018. **78**(13): p. 3544-3559.
199. Campbell, K.S., A.D. Cohen, and T. Pazina, *Mechanisms of NK Cell Activation and Clinical Activity of the Therapeutic SLAMF7 Antibody, Elotuzumab in Multiple Myeloma*. Front Immunol, 2018. **9**: p. 2551.
200. Montalvao, F., et al., *The mechanism of anti-CD20-mediated B cell depletion revealed by intravital imaging*. J Clin Invest, 2013. **123**(12): p. 5098-103.
201. Gul, N., et al., *Macrophages eliminate circulating tumor cells after monoclonal antibody therapy*. J Clin Invest, 2014. **124**(2): p. 812-23.
202. Zhang, W., et al., *Advances in Anti-Tumor Treatments Targeting the CD47/SIRPalpha Axis*. Front Immunol, 2020. **11**: p. 18.
203. Zhao, H., et al., *CD47 Promotes Tumor Invasion and Metastasis in Non-small Cell Lung Cancer*. Sci Rep, 2016. **6**: p. 29719.
204. Majeti, R., et al., *CD47 is an adverse prognostic factor and therapeutic antibody target on human acute myeloid leukemia stem cells*. Cell, 2009. **138**(2): p. 286-99.
205. Chao, M.P., R. Majeti, and I.L. Weissman, *Programmed cell removal: a new obstacle in the road to developing cancer*. Nat Rev Cancer, 2011. **12**(1): p. 58-67.
206. Xu, L., et al., *CD47/SIRPalpha blocking enhances CD19/CD3-bispecific T cell engager antibody-mediated lysis of B cell malignancies*. Biochem Biophys Res Commun, 2019. **509**(3): p. 739-745.
207. Ring, N.G., et al., *Anti-SIRPalpha antibody immunotherapy enhances neutrophil and macrophage antitumor activity*. Proc Natl Acad Sci U S A, 2017. **114**(49): p. E10578-E10585.
208. Lucisano Valim, Y.M. and P.J. Lachmann, *The effect of antibody isotype and antigenic epitope density on the complement-fixing activity of immune complexes: a systematic study using chimaeric anti-NIP antibodies with human Fc regions*. Clin Exp Immunol, 1991. **84**(1): p. 1-8.
209. Nesargikar, P.N., B. Spiller, and R. Chavez, *The complement system: history, pathways, cascade and inhibitors*. Eur J Microbiol Immunol (Bp), 2012. **2**(2): p. 103-11.
210. Kennedy, A.D., et al., *Rituximab infusion promotes rapid complement depletion and acute CD20 loss in chronic lymphocytic leukemia*. J Immunol, 2004. **172**(5): p. 3280-8.
211. Racila, E., et al., *A polymorphism in the complement component C1qA correlates with prolonged response following rituximab therapy of follicular lymphoma*. Clin Cancer Res, 2008. **14**(20): p. 6697-703.
212. Baig, N.A., et al., *Complement dependent cytotoxicity in chronic lymphocytic leukemia: ofatumumab enhances alemtuzumab complement dependent cytotoxicity and reveals cells resistant to activated complement*. Leuk Lymphoma, 2012. **53**(11): p. 2218-27.

213. Liu, M., et al., *Membrane-bound complement regulatory proteins are prognostic factors of operable breast cancer treated with adjuvant trastuzumab: a retrospective study*. *Oncol Rep*, 2014. **32**(6): p. 2619-27.
214. Liu, J., et al., *The complement inhibitory protein DAF (CD55) suppresses T cell immunity in vivo*. *J Exp Med*, 2005. **201**(4): p. 567-77.
215. Watson, N.F., et al., *Expression of the membrane complement regulatory protein CD59 (protectin) is associated with reduced survival in colorectal cancer patients*. *Cancer Immunol Immunother*, 2006. **55**(8): p. 973-80.
216. Macor, P., et al., *In vivo targeting of human neutralizing antibodies against CD55 and CD59 to lymphoma cells increases the antitumor activity of rituximab*. *Cancer Res*, 2007. **67**(21): p. 10556-63.
217. Mamidi, S., et al., *Lipoplex mediated silencing of membrane regulators (CD46, CD55 and CD59) enhances complement-dependent anti-tumor activity of trastuzumab and pertuzumab*. *Mol Oncol*, 2013. **7**(3): p. 580-94.
218. Bulliard, Y., et al., *Activating Fc gamma receptors contribute to the antitumor activities of immunoregulatory receptor-targeting antibodies*. *J Exp Med*, 2013. **210**(9): p. 1685-93.
219. van Hooren, L., et al., *Sunitinib enhances the antitumor responses of agonistic CD40-antibody by reducing MDSCs and synergistically improving endothelial activation and T-cell recruitment*. *Oncotarget*, 2016. **7**(31): p. 50277-50289.
220. Leach, D.R., M.F. Krummel, and J.P. Allison, *Enhancement of antitumor immunity by CTLA-4 blockade*. *Science*, 1996. **271**(5256): p. 1734-6.
221. Wang, X.Y., et al., *Blockade of cytotoxic T-lymphocyte antigen-4 as a new therapeutic approach for advanced melanoma*. *Expert Opin Pharmacother*, 2011. **12**(17): p. 2695-706.
222. Peggs, K.S., et al., *Principles and use of anti-CTLA4 antibody in human cancer immunotherapy*. *Curr Opin Immunol*, 2006. **18**(2): p. 206-13.
223. Hodi, F.S., et al., *Improved survival with ipilimumab in patients with metastatic melanoma*. *N Engl J Med*, 2010. **363**(8): p. 711-23.
224. Robert, C., et al., *Ipilimumab plus dacarbazine for previously untreated metastatic melanoma*. *N Engl J Med*, 2011. **364**(26): p. 2517-26.
225. Wing, K., et al., *CTLA-4 control over Foxp3+ regulatory T cell function*. *Science*, 2008. **322**(5899): p. 271-5.
226. Arce Vargas, F., et al., *Fc Effector Function Contributes to the Activity of Human Anti-CTLA-4 Antibodies*. *Cancer Cell*, 2018. **33**(4): p. 649-663 e4.
227. Simpson, T.R., et al., *Fc-dependent depletion of tumor-infiltrating regulatory T cells co-defines the efficacy of anti-CTLA-4 therapy against melanoma*. *J Exp Med*, 2013. **210**(9): p. 1695-710.
228. Roskopf, S., et al., *CTLA-4 antibody ipilimumab negatively affects CD4(+) T-cell responses in vitro*. *Cancer Immunol Immunother*, 2019. **68**(8): p. 1359-1368.
229. Comin-Anduix, B., H. Escuin-Ordinas, and F.J. Ibarrondo, *Tremelimumab: research and clinical development*. *Onco Targets Ther*, 2016. **9**: p. 1767-76.
230. Takeuchi, Y. and H. Nishikawa, *Roles of regulatory T cells in cancer immunity*. *Int Immunol*, 2016. **28**(8): p. 401-9.
231. Berman, D., et al., *The development of immunomodulatory monoclonal antibodies as a new therapeutic modality for cancer: the Bristol-Myers Squibb experience*. *Pharmacol Ther*, 2015. **148**: p. 132-53.
232. Sun, L., et al., *Clinical efficacy and safety of anti-PD-1/PD-L1 inhibitors for the treatment of advanced or metastatic cancer: a systematic review and meta-analysis*. *Sci Rep*, 2020. **10**(1): p. 2083.

233. Vaddepally, R.K., et al., *Review of Indications of FDA-Approved Immune Checkpoint Inhibitors per NCCN Guidelines with the Level of Evidence*. *Cancers (Basel)*, 2020. **12**(3).
234. Hirano, F., et al., *Blockade of B7-H1 and PD-1 by monoclonal antibodies potentiates cancer therapeutic immunity*. *Cancer Res*, 2005. **65**(3): p. 1089-96.
235. Brown, J.A., et al., *Blockade of programmed death-1 ligands on dendritic cells enhances T cell activation and cytokine production*. *J Immunol*, 2003. **170**(3): p. 1257-66.
236. Taube, J.M., et al., *Colocalization of inflammatory response with B7-h1 expression in human melanocytic lesions supports an adaptive resistance mechanism of immune escape*. *Sci Transl Med*, 2012. **4**(127): p. 127ra37.
237. Jiang, X., et al., *Role of the tumor microenvironment in PD-L1/PD-1-mediated tumor immune escape*. *Mol Cancer*, 2019. **18**(1): p. 10.
238. Chen, L., et al., *Metastasis is regulated via microRNA-200/ZEB1 axis control of tumour cell PD-L1 expression and intratumoral immunosuppression*. *Nat Commun*, 2014. **5**: p. 5241.
239. Brahmer, J., et al., *Nivolumab versus Docetaxel in Advanced Squamous-Cell Non-Small-Cell Lung Cancer*. *N Engl J Med*, 2015. **373**(2): p. 123-35.
240. Motzer, R.J., et al., *Nivolumab versus Everolimus in Advanced Renal-Cell Carcinoma*. *N Engl J Med*, 2015. **373**(19): p. 1803-13.
241. Robert, C., et al., *Pembrolizumab versus Ipilimumab in Advanced Melanoma*. *N Engl J Med*, 2015. **372**(26): p. 2521-32.
242. Guo, L., et al., *Clinical and Recent Patents Applications of PD-1/PD-L1 Targeting Immunotherapy in Cancer Treatment-Current Progress, Strategy, and Future Perspective*. *Front Immunol*, 2020. **11**: p. 1508.
243. Wakabayashi, G., et al., *Development and clinical applications of cancer immunotherapy against PD-1 signaling pathway*. *J Biomed Sci*, 2019. **26**(1): p. 96.
244. Zhang, J.Y., et al., *PD-1/PD-L1 Based Combinational Cancer Therapy: Icing on the Cake*. *Front Pharmacol*, 2020. **11**: p. 722.
245. Chen, J., et al., *Regulation of PD-L1: a novel role of pro-survival signalling in cancer*. *Ann Oncol*, 2016. **27**(3): p. 409-16.
246. Massi, D., et al., *PD-L1 marks a subset of melanomas with a shorter overall survival and distinct genetic and morphological characteristics*. *Ann Oncol*, 2014. **25**(12): p. 2433-2442.
247. Tashima, Y., et al., *Prognostic impact of PD-L1 expression in correlation with neutrophil-to-lymphocyte ratio in squamous cell carcinoma of the lung*. *Sci Rep*, 2020. **10**(1): p. 1243.
248. Vrankar, M., et al., *PD-L1 expression can be regarded as prognostic factor for survival of non-small cell lung cancer patients after chemoradiotherapy*. *Neoplasma*, 2018. **65**(1): p. 140-146.
249. Muenst, S., et al., *Expression of programmed death ligand 1 (PD-L1) is associated with poor prognosis in human breast cancer*. *Breast Cancer Res Treat*, 2014. **146**(1): p. 15-24.
250. Sorensen, S.F., et al., *PD-L1 Expression and Survival among Patients with Advanced Non-Small Cell Lung Cancer Treated with Chemotherapy*. *Transl Oncol*, 2016. **9**(1): p. 64-69.
251. Vigneron, N., *Human Tumor Antigens and Cancer Immunotherapy*. *Biomed Res Int*, 2015. **2015**: p. 948501.
252. Verderio, P., et al., *Developing miRNA signatures: a multivariate prospective*. *Br J Cancer*, 2016. **115**(1): p. 1-4.

253. Nair, M., S.S. Sandhu, and A.K. Sharma, *Cancer molecular markers: A guide to cancer detection and management*. Semin Cancer Biol, 2018. **52**(Pt 1): p. 39-55.
254. Martinez-Usatorre, A., et al., *MicroRNA-155 Expression Is Enhanced by T-cell Receptor Stimulation Strength and Correlates with Improved Tumor Control in Melanoma*. Cancer Immunol Res, 2019. **7**(6): p. 1013-1024.
255. Jiang, Y., et al., *Progress and Challenges in Precise Treatment of Tumors With PD-1/PD-L1 Blockade*. Front Immunol, 2020. **11**: p. 339.
256. Topalian, S.L., et al., *Mechanism-driven biomarkers to guide immune checkpoint blockade in cancer therapy*. Nat Rev Cancer, 2016. **16**(5): p. 275-87.
257. Cohen, E.E.W., et al., *Pembrolizumab versus methotrexate, docetaxel, or cetuximab for recurrent or metastatic head-and-neck squamous cell carcinoma (KEYNOTE-040): a randomised, open-label, phase 3 study*. Lancet, 2019. **393**(10167): p. 156-167.
258. Garon, E.B., et al., *Pembrolizumab for the treatment of non-small-cell lung cancer*. N Engl J Med, 2015. **372**(21): p. 2018-28.
259. Jreige, M., et al., *(18)F-FDG PET metabolic-to-morphological volume ratio predicts PD-L1 tumour expression and response to PD-1 blockade in non-small-cell lung cancer*. Eur J Nucl Med Mol Imaging, 2019. **46**(9): p. 1859-1868.
260. Tartarone, A., et al., *Anti-PD-1 versus anti-PD-L1 therapy in patients with pretreated advanced non-small-cell lung cancer: a meta-analysis*. Future Oncol, 2019. **15**(20): p. 2423-2433.
261. Duan, J., et al., *Use of Immunotherapy With Programmed Cell Death 1 vs Programmed Cell Death Ligand 1 Inhibitors in Patients With Cancer: A Systematic Review and Meta-analysis*. JAMA Oncol, 2020. **6**(3): p. 375-384.
262. Topalian, S.L., et al., *Safety, activity, and immune correlates of anti-PD-1 antibody in cancer*. N Engl J Med, 2012. **366**(26): p. 2443-54.
263. Brahmer, J.R., et al., *Safety and activity of anti-PD-L1 antibody in patients with advanced cancer*. N Engl J Med, 2012. **366**(26): p. 2455-65.
264. Bar, N., et al., *Differential effects of PD-L1 versus PD-1 blockade on myeloid inflammation in human cancer*. JCI Insight, 2020. **5**(12).
265. Liu, D., R.W. Jenkins, and R.J. Sullivan, *Mechanisms of Resistance to Immune Checkpoint Blockade*. Am J Clin Dermatol, 2019. **20**(1): p. 41-54.
266. Lei, Q., et al., *Resistance Mechanisms of Anti-PD1/PDL1 Therapy in Solid Tumors*. Front Cell Dev Biol, 2020. **8**: p. 672.
267. Le, D.T., et al., *Mismatch repair deficiency predicts response of solid tumors to PD-1 blockade*. Science, 2017. **357**(6349): p. 409-413.
268. Schumacher, T.N. and R.D. Schreiber, *Neoantigens in cancer immunotherapy*. Science, 2015. **348**(6230): p. 69-74.
269. Highfill, S.L., et al., *Disruption of CXCR2-mediated MDSC tumor trafficking enhances anti-PD1 efficacy*. Sci Transl Med, 2014. **6**(237): p. 237ra67.
270. Gabrilovich, D.I., S. Ostrand-Rosenberg, and V. Bronte, *Coordinated regulation of myeloid cells by tumours*. Nat Rev Immunol, 2012. **12**(4): p. 253-68.
271. Arce Vargas, F., et al., *Fc-Optimized Anti-CD25 Depletes Tumor-Infiltrating Regulatory T Cells and Synergizes with PD-1 Blockade to Eradicate Established Tumors*. Immunity, 2017. **46**(4): p. 577-586.
272. Philip, M., et al., *Chromatin states define tumour-specific T cell dysfunction and reprogramming*. Nature, 2017. **545**(7655): p. 452-456.
273. Pauken, K.E., et al., *Epigenetic stability of exhausted T cells limits durability of reinvigoration by PD-1 blockade*. Science, 2016. **354**(6316): p. 1160-1165.
274. Huang, A.C., et al., *T-cell invigoration to tumour burden ratio associated with anti-PD-1 response*. Nature, 2017. **545**(7652): p. 60-65.

275. Johnson, D.B., et al., *Tumor-specific MHC-II expression drives a unique pattern of resistance to immunotherapy via LAG-3/FCRL6 engagement*. JCI Insight, 2018. **3**(24).
276. O'Donnell, J.S., M.W.L. Teng, and M.J. Smyth, *Cancer immunoeediting and resistance to T cell-based immunotherapy*. Nat Rev Clin Oncol, 2019. **16**(3): p. 151-167.
277. Patel, S.J., et al., *Identification of essential genes for cancer immunotherapy*. Nature, 2017. **548**(7669): p. 537-542.
278. Zingg, D., et al., *The Histone Methyltransferase Ezh2 Controls Mechanisms of Adaptive Resistance to Tumor Immunotherapy*. Cell Rep, 2017. **20**(4): p. 854-867.
279. Bertolet, G. and D. Liu, *The Planar Lipid Bilayer System Serves as a Reductionist Approach for Studying NK Cell Immunological Synapses and Their Functions*. Methods Mol Biol, 2016. **1441**: p. 151-65.
280. Lee, K.H., et al., *T cell receptor signaling precedes immunological synapse formation*. Science, 2002. **295**(5559): p. 1539-42.
281. Xiong, W., et al., *Immunological Synapse Predicts Effectiveness of Chimeric Antigen Receptor Cells*. Mol Ther, 2018. **26**(4): p. 963-975.
282. Dustin, M.L., et al., *Supported planar bilayers for study of the immunological synapse*. Curr Protoc Immunol, 2007. **Chapter 18**: p. Unit 18 13.
283. Chen, S., et al., *Combination of 4-1BB agonist and PD-1 antagonist promotes antitumor effector/memory CD8 T cells in a poorly immunogenic tumor model*. Cancer Immunol Res, 2015. **3**(2): p. 149-60.
284. Woods, D.M., et al., *HDAC Inhibition Upregulates PD-1 Ligands in Melanoma and Augments Immunotherapy with PD-1 Blockade*. Cancer Immunol Res, 2015. **3**(12): p. 1375-85.
285. Zamarin, D., et al., *PD-L1 in tumor microenvironment mediates resistance to oncolytic immunotherapy*. J Clin Invest, 2018. **128**(11): p. 5184.
286. Zheng, Y., Y.C. Fang, and J. Li, *PD-L1 expression levels on tumor cells affect their immunosuppressive activity*. Oncol Lett, 2019. **18**(5): p. 5399-5407.
287. Meng, X., et al., *FBXO38 mediates PD-1 ubiquitination and regulates anti-tumour immunity of T cells*. Nature, 2018. **564**(7734): p. 130-135.
288. Beum, P.V., et al., *Binding of rituximab, trastuzumab, cetuximab, or mAb T101 to cancer cells promotes trogocytosis mediated by THP-1 cells and monocytes*. J Immunol, 2008. **181**(11): p. 8120-32.
289. Beum, P.V., et al., *Loss of CD20 and bound CD20 antibody from opsonized B cells occurs more rapidly because of trogocytosis mediated by Fc receptor-expressing effector cells than direct internalization by the B cells*. J Immunol, 2011. **187**(6): p. 3438-47.
290. Zhang, Y., et al., *Daclizumab reduces CD25 levels on T cells through monocyte-mediated trogocytosis*. Mult Scler, 2014. **20**(2): p. 156-64.
291. Vogel, S., et al., *Antibody induced CD4 down-modulation of T cells is site-specifically mediated by CD64(+) cells*. Sci Rep, 2015. **5**: p. 18308.
292. Nakashima, M., et al., *Trogocytosis of ligand-receptor complex and its intracellular transport in CD30 signalling*. Biol Cell, 2018. **110**(5): p. 109-124.
293. Krejcik, J., et al., *Monocytes and Granulocytes Reduce CD38 Expression Levels on Myeloma Cells in Patients Treated with Daratumumab*. Clin Cancer Res, 2017. **23**(24): p. 7498-7511.
294. Dahan, R., et al., *FcgammaRs Modulate the Anti-tumor Activity of Antibodies Targeting the PD-1/PD-L1 Axis*. Cancer Cell, 2015. **28**(3): p. 285-95.
295. Dahal, L.N., et al., *Shaving Is an Epiphenomenon of Type I and II Anti-CD20-Mediated Phagocytosis, whereas Antigenic Modulation Limits Type I Monoclonal Antibody Efficacy*. J Immunol, 2018. **201**(4): p. 1211-1221.

296. Krieg, C., et al., *High-dimensional single-cell analysis predicts response to anti-PD-1 immunotherapy*. Nat Med, 2018. **24**(2): p. 144-153.
297. Miller, B.C., et al., *Subsets of exhausted CD8(+) T cells differentially mediate tumor control and respond to checkpoint blockade*. Nat Immunol, 2019. **20**(3): p. 326-336.
298. Utzschneider, D.T., et al., *T Cell Factor 1-Expressing Memory-like CD8(+) T Cells Sustain the Immune Response to Chronic Viral Infections*. Immunity, 2016. **45**(2): p. 415-27.
299. Siddiqui, I., et al., *Intratumoral Tcf1(+)PD-1(+)CD8(+) T Cells with Stem-like Properties Promote Tumor Control in Response to Vaccination and Checkpoint Blockade Immunotherapy*. Immunity, 2019. **50**(1): p. 195-211 e10.
300. Martinez-Usatorre, A., et al., *Enhanced Phenotype Definition for Precision Isolation of Precursor Exhausted Tumor-Infiltrating CD8 T Cells*. Front Immunol, 2020. **11**: p. 340.
301. Staron, M.M., et al., *The transcription factor FoxO1 sustains expression of the inhibitory receptor PD-1 and survival of antiviral CD8(+) T cells during chronic infection*. Immunity, 2014. **41**(5): p. 802-14.
302. McPherson, R.C., et al., *Epigenetic modification of the PD-1 (Pdc1) promoter in effector CD4(+) T cells tolerized by peptide immunotherapy*. Elife, 2014. **3**.
303. Utzschneider, D.T., et al., *T cells maintain an exhausted phenotype after antigen withdrawal and population reexpansion*. Nat Immunol, 2013. **14**(6): p. 603-10.
304. Nowicki, T.S., S. Hu-Lieskovan, and A. Ribas, *Mechanisms of Resistance to PD-1 and PD-L1 Blockade*. Cancer J, 2018. **24**(1): p. 47-53.
305. Lo Russo, G., et al., *Antibody-Fc/FcR Interaction on Macrophages as a Mechanism for Hyperprogressive Disease in Non-small Cell Lung Cancer Subsequent to PD-1/PD-L1 Blockade*. Clin Cancer Res, 2019. **25**(3): p. 989-999.
306. Arlauckas, S.P., et al., *In vivo imaging reveals a tumor-associated macrophage-mediated resistance pathway in anti-PD-1 therapy*. Sci Transl Med, 2017. **9**(389).
307. De Henau, O., et al., *Overcoming resistance to checkpoint blockade therapy by targeting PI3Kgamma in myeloid cells*. Nature, 2016. **539**(7629): p. 443-447.
308. Cao, W., et al., *Macrophage subtype predicts lymph node metastasis in oesophageal adenocarcinoma and promotes cancer cell invasion in vitro*. Br J Cancer, 2015. **113**(5): p. 738-46.
309. Maccio, A., et al., *Role of M1-polarized tumor-associated macrophages in the prognosis of advanced ovarian cancer patients*. Sci Rep, 2020. **10**(1): p. 6096.
310. DeNardo, D.G. and B. Ruffell, *Macrophages as regulators of tumour immunity and immunotherapy*. Nat Rev Immunol, 2019. **19**(6): p. 369-382.
311. Cassetta, L. and J.W. Pollard, *Targeting macrophages: therapeutic approaches in cancer*. Nat Rev Drug Discov, 2018. **17**(12): p. 887-904.

ARTICLE

# Tumor suppression of novel anti-PD-1 antibodies mediated through CD28 costimulatory pathway

Craig Fenwick<sup>1</sup>, Juan-Luis Loredó-Varela<sup>3\*</sup>, Victor Joo<sup>1\*</sup>, Céline Pellaton<sup>1</sup>, Alex Farina<sup>1</sup>, Navina Rajah<sup>1</sup>, Line Esteves-Leuenberger<sup>1</sup>, Thibaut Decaillon<sup>1</sup>, Madeleine Suffiotti<sup>1</sup>, Alessandra Noto<sup>1</sup>, Khalid Ohmiti<sup>1</sup>, Raphael Gottardo<sup>4</sup>, Winfried Weissenhorn<sup>3</sup>, and Giuseppe Pantaleo<sup>1,2</sup>

**Classical antagonistic antibodies (Abs) targeting PD-1, such as pembrolizumab and nivolumab, act through blockade of the PD-1-PDL-1 interaction. Here, we have identified novel antagonistic anti-PD-1 Abs not blocking the PD-1-PDL-1 interaction. The nonblocking Abs recognize epitopes on PD-1 located on the opposing face of the PDL-1 interaction and overlap with a newly identified evolutionarily conserved patch. These nonblocking Abs act predominantly through the CD28 coreceptor. Importantly, a combination of blocking and nonblocking Abs synergize in the functional recovery of antigen-specific exhausted CD8 T cells. Interestingly, nonblocking anti-PD-1 Abs have equivalent antitumor activity compared with blocker Abs in two mouse tumor models, and combination therapy using both classes of Abs enhanced tumor suppression in the mouse immunogenic tumor model. The identification of the novel nonblocker anti-PD-1 Abs and their synergy with classical blocker Abs may be instrumental in potentiating immunotherapy strategies and antitumor activity.**

## Introduction

The programmed cell death 1 receptor (PD-1) is the master regulator of T cells through the suppression of T cell activation following the binding to its primary ligand, programmed death ligand 1 (PDL-1; [Trautmann et al., 2006](#); [Tumeh et al., 2014](#); [Pauken and Wherry, 2015](#); [Wherry and Kurachi, 2015](#)). The proposed mechanism by which PD-1 acts as an immune checkpoint inhibitor includes recruitment of the SHP-2 phosphatase into the vicinity of the TCR complex, resulting in dephosphorylation of membrane proximal signaling proteins, including CD3 $\zeta$ , ZAP70, and PLC- $\gamma$ 1 ([Sheppard et al., 2004](#); [Yokosuka et al., 2012](#)). The PD-1-SHP-2 complex also acts on the CD28 costimulatory receptor and the associated PI3K and AKT signaling pathway needed for optimal T cell activation and survival ([Parry et al., 2005](#); [Patsoukis et al., 2012](#)). These dynamics have been observed in fluorescence microscopy imaging studies where PD-1 exists in microclusters on the cell surface and is recruited along with SHP-2 phosphatase into the immunological synapse to suppress phosphorylation events during TCR activation ([Chemnitz et al., 2004](#); [Sheppard et al., 2004](#); [Yokosuka et al., 2012](#); [Wherry and Kurachi, 2015](#)). Two recent studies have also indicated that anti-PD-1-mediated tumor-suppressive activity is primarily dependent of the CD28 costimulatory receptor ([Hui et al., 2017](#); [Kamphorst et al., 2017](#)).

Monoclonal antibodies (Abs) acting through PD-1 blockade represent a major breakthrough in oncology, showing significant clinical success in the treatment of several types of cancer, including advanced melanoma, non-small cell lung cancer, and head and neck squamous cell carcinoma ([Baitsch et al., 2011](#); [Mellman et al., 2011](#); [Topalian et al., 2012](#); [Hamid et al., 2013](#); [Rizvi et al., 2015](#); [Sharma and Allison, 2015](#); [Callahan et al., 2016](#)). Despite these successes, only ~30–40% of patients show a response to anti-PD-1 immunotherapy, and only a fraction of these show a durable clinical response. These limitations highlight the need for a better understanding of the mechanism by which anti-PD-1 Abs act and for the identification of new therapies that synergize to improve the response rate and/or breadth of cancers that can be treated.

The objective of the present study was to identify novel antagonist Abs with more potent antitumor activity and/or acting through a mechanism independent of the PD-1-PDL-1 blockade. A panel of Ab clones binding with high affinity to diverse epitopes on PD-1 was generated and profiled for antagonistic activity in recovering antigen (Ag)-specific CD8 T cells from functional exhaustion. A novel class of anti-PD-1 Ab was identified that was not blocking the PD-1-PDL-1 interaction with antagonistic activity comparable to pembrolizumab and nivolumab. Antagonistic activity of the novel

<sup>1</sup>Service of Immunology and Allergy, Department of Medicine, Lausanne University Hospital, University of Lausanne, Lausanne, Switzerland; <sup>2</sup>Swiss Vaccine Research Institute, Lausanne University Hospital, University of Lausanne, Lausanne, Switzerland; <sup>3</sup>University Grenoble Alpes, Commissariat à l’Energie Atomique, Centre National de la Recherche Scientifique, Institut de Biologie Structurale, Grenoble, France; <sup>4</sup>Division of Public Health Sciences, Fred Hutchinson Cancer Research Center, Seattle, WA.

\*J.-L. Loredó-Varela and V. Joo contributed equally to this paper; Correspondence to Giuseppe Pantaleo: [giuseppe.pantaleo@chuv.ch](mailto:giuseppe.pantaleo@chuv.ch).

© 2019 Fenwick et al. This article is distributed under the terms of an Attribution–Noncommercial–Share Alike–No Mirror Sites license for the first six months after the publication date (see <http://www.rupress.org/terms/>). After six months it is available under a Creative Commons License (Attribution–Noncommercial–Share Alike 4.0 International license, as described at <https://creativecommons.org/licenses/by-nc-sa/4.0/>).

anti-PD-1 Abs was determined by evaluating their ability to recover proliferation and/or to potentiate cytokine production of exhausted Ag-specific CD8 T cells. Biochemical and structural studies demonstrated that these Abs bound to the opposite face of the PD-1 protein relative to the PD-1-PDL-1 interaction site. In mechanistic studies, nonblocking anti-PD-1 Abs act predominantly through the CD28 coreceptor that restores signaling through the AKT-NF- $\kappa$ B pathway and leads to T cell proliferation and survival. Consisted with nonblocking anti-PD-1 Abs acting through a distinct mechanism of action, combinations of nonblocking and blocking anti-PD-1 Abs synergize to recover the functional activity of exhausted Ag-specific CD8 T cell in vitro and resulted in significantly enhanced antitumor activity in the MC38 immunogenic in vivo mouse tumor model.

## Results

### Characterization of a diverse panel of anti-PD-1 Abs binding different epitopes on PD-1

An immunization campaign with human PD-1 was launched in mice, and over 2,000 hybridoma clones were generated and screened in a Luminex assay for binding to recombinant human PD-1. Forty different Ab families with subnanomolar affinity were selected based on (1) possessing low nanomolar binding affinity for cell-surface PD-1, (2) competitive binding profile with a commercially available anti-PD-1 Ab that acted as a surrogate assay to identify blocking Abs of the PD-1-PDL-1 interaction, and (3) heavy-chain complementarity-determining region (CDR) variable region. Anti-PD-1 Abs were further screening to assess both the ability to block the PD-1-PDL-1 interaction in a Luminex biochemical assay and recover Ag-specific CD8 T cells from functional exhaustion. Therefore, the simultaneous use of a functional assay allowed also for the selection of anti-PD-1 Abs with antagonistic activity independent of PD-1-PDL-1 blockade.

The antagonistic, immune-enhancing activity of the novel anti-PD-1 Abs was evaluated in a highly standardized CFSE proliferation assay measuring the recovery of Ag-specific proliferation in blood mononuclear cells from chronically infected viremic HIV patients. HIV-specific CD8 T cells are instrumental to evaluate the ability of anti-PD-1 Abs to recover T cells from functional exhaustion because of the expression of high levels of PD-1 and poor proliferation in response to Ag-specific stimulation (Barber et al., 2006; Day et al., 2006; Trautmann et al., 2006; Zhang et al., 2007). Stimulation of blood mononuclear cells with HIV-derived peptides followed by 6 d in culture led to an increase in CFSE-low CD8 T cells that have undergone proliferation. However, the addition of two classical PDL-1-blocking anti-PD-1 Abs (e.g., pembrolizumab or nivolumab) led to an enhanced level of proliferation relative to the peptide alone control, thus indicating that both anti-PD-1 Abs recover CD8 T cells from exhaustion (Fig. 1, A and B). Validation studies have shown that proliferating CD8 T cells following pembrolizumab treatment were HIV specific, as indicated by pentamer MHC-HIV peptide complex staining. On the basis of the functional activity in this proliferation assay, 10 novel anti-PD-1 Abs showed potency similar to a pembrolizumab, which has been

used as a benchmark control (Fig. 1 B). Anti-PD-1 Ab clones of interest had antagonistic activity that was also replicated using blood mononuclear cells from five different HIV-infected donors having CD8 T cells specific to seven different HIV-derived peptides (Fig. 1, A and B; and Figs. S1 and S2).

We then investigated whether the newly identified antagonistic anti-PD-1 Abs act through PD-1-PDL-1 blockade, as with pembrolizumab and nivolumab. Initial profiling in an Ab competitive binding assay was consistent with two clones binding to a different epitope than the PDL-1 blocking Abs. A Luminex biochemical protein-protein interaction assay was established to test the novel Abs and directly determine PDL-1 binding to a preformed Ab-PD-1 complex. The 135C12 and 136B4 immune-enhancing anti-PD-1 Abs with distinct heavy- and light-chain CDR regions induced only a minor 1.5- to 3-fold reduced affinity of the PDL-1 protein for PD-1 (Fig. 2 A). In contrast, 137F2, which bound competitively to PD-1 with a blocking anti-PD-1 Ab, completely prevented binding of PDL-1 to PD-1-coated beads at all concentrations tested. It is important to underscore that out of the 156 Ab clones with high affinity for PD-1, only 3.2% corresponded to nonblocking Abs with antagonistic activity. The remaining Abs with antagonistic activity (Fig. 1 B) were tested in a PD-1-PDL-1 protein interaction screening assay, and all blocked the PD-1-PDL-1 interaction (Fig. 2 B).

The PD-1-PDL-1 blockade and the CFSE assay results clearly indicate that 135C12 and 136B4 represent novel anti-PD-1 Abs that may exert antagonistic activity independent of blockade of the PD-1-PDL-1 interaction. For these reasons, the two novel nonblocking anti-PD-1 Abs were advanced for more in-depth profiling along with 137F2 blocking Ab, which displayed an improved immune-enhancing activity in our in vitro functional assay relative to pembrolizumab. The CDR sequences for the 135C12 and 137F2 mouse IgG1 Abs were also transferred into a human IgG4 Ab with a panel of constant region clones screened to identify humanized Abs with subnanomolar affinity for cell-surface PD-1. These humanized clones were renamed NB01 for the nonblocking 135C12 Ab and B01 for the blocking 137F2 Ab.

### Binding epitopes of antagonistic anti-PD-1 Abs that do not block the PD-1-PDL-1 interaction

Binding epitopes for the three prioritized Abs were then mapped by monitoring binding to a panel of PD-1 proteins expressed with amino acid substitutions at solvent accessible residues of the extracellular domain (Fig. S3 A). Transiently transfected HeLa cells expressed mutant or wild-type forms of PD-1 and allowed for comparative Ab binding to cell-surface PD-1 by flow cytometry (Fig. 2 C). Discrete amino acid substitutions in PD-1 resulted in a loss in binding for selected Abs. Pembrolizumab and 137F2 Abs both mapped to regions previously identified as being important for PDL-1 binding to PD-1 (Lázár-Molnár et al., 2008; Lin et al., 2008), but binding of nonblocking antagonistic Abs was unaffected by these substitutions. 135C12 and 136B4 Ab binding was almost completely disrupted with either M18 (L41A/V43T/S137A/L138A/R139T substitutions) or M32 (D105A substitution) PD-1 constructs, respectively, which are situated on the opposite face to the PD-1 interaction with either PDL-1 or PDL-2. As a

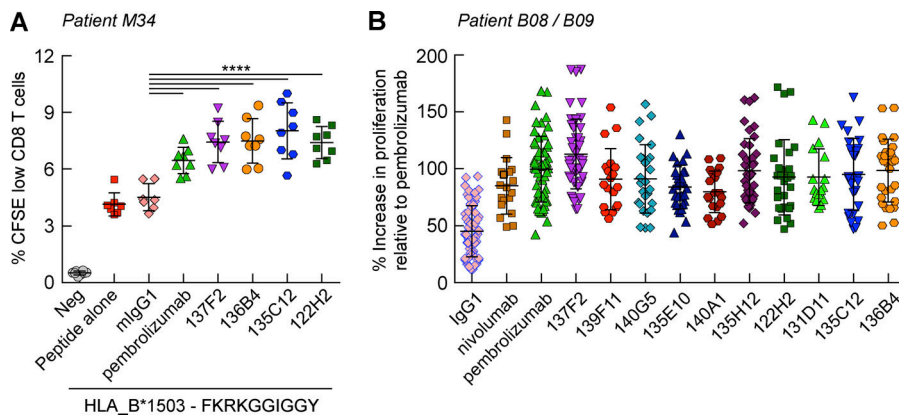


**Figure 1. Anti-PD-1 Abs significantly enhance proliferation of Ag-specific exhausted CD8 T cells.** (A) Recovery of proliferation in HIV-specific CD8 T cells following stimulation with an HIV-derived peptide. Results from a representative experiment are shown and expressed as the percentage of CFSE-low CD8 T cells. 8–10 replicates were performed for each experimental condition. (B) Cumulative results from multiple CFSE experiments ( $n = 2-6$ ) are shown for the 10 anti-PD-1 Abs identified with antagonistic properties similar to pembrolizumab. Results have been generated assessing the proliferation of CD8 T cells specific to three HIV-derived peptides (FLGKIWPSYK restricted by A\*0201 and RLRPGGKKK or RMRGAHTNDVK restricted by A\*0301) in patients B08 and B09. For com-

parative purposes across multiple assays and the different anti-PD-1 Abs, the level of proliferation in the pembrolizumab-treated samples was set as a 100% reference. Pembrolizumab was used as a positive control, while untreated (Neg) or mouse IgG1 isotype control Ab was used as a negative control in each experiment. Graphs show the mean  $\pm$  SD. \*\*\*\*,  $P < 0.0001$  for all anti-PD-1 Abs relative to the IgG1 control (unpaired  $t$  test with Welch's correction).

further evaluation of Ab-binding characteristics, competitive binding studies were performed with a PD-1-expressing Jurkat cell line. Saturating the PD-1 receptor with the 137F2 blocking Ab prevented cell staining with pembrolizumab, nivolumab, and B01 (humanized 137F2) but did not prevent staining with NB01 (humanized 135C12). Conversely, cell-surface PD-1 saturated with either 135C12 or 136B4 non-blocking Abs had no impact on the binding of pembrolizumab, nivolumab, or B01 Abs to PD-1. Both 135C12 and 136B4 Abs prevented the binding of NB01, the humanized version of the mouse 135C12 Ab (Fig. 2 D), indicating that these Abs bind overlapping epitopes on PD-1. These studies show that antagonistic blocking and nonblocking Abs of the PD-1-PDL-1 interaction can bind to cell-surface PD-1 simultaneously.

To complete the molecular details of the binding epitope of the newly generated PDL-1 nonblocker Abs, the structure of the NB01a (135C12) Fab in complex with hPD-1 was solved at a resolution of 2.2 Å (Table S1). The NB01a Fab binds at the opposite side of the PDL-1-binding site (Fig. 2 E) with interacting residues on PD-1 confirming our mapping studies performed with the 135C12 Ab. The overall structure of hPD-1 fits previously published structures (Zak et al., 2015). Superposition of the  $\alpha$  atoms of hPD-1 in complex with the NB01a Fab and hPD-1 in complex with hPDL-1 (Protein Data Bank [PDB] accession no. 4ZQK) showed no overlap of the binding footprints for NB01a and hPDL-1, indicating that they can bind PD-1 simultaneously (Fig. 2 E). One potential clash was noted between the hPDL-1 side chains E60/D61 and  $V_L$  residues S52/S65 of NB01a; however, these side chains may adopt different rotamers in solution, thereby allowing concomitant binding of hPDL-1 and NB01a to hPD-1. Consequently, the affinity of PDL-1 for hPD-1 in the presence of 135C12/NB01 may be slightly reduced, as observed in the biochemical binding data (Fig. 2 A). It was important to determine whether the four predicted N-glycosylation sites on PD-1 were interfering with NB01 Ab binding. However, the modeling of these sites shows that glycosylation at N49, N58, N74, and N116 does not overlap with the bind epitopes of NB01 or 136B4 Abs and would not interfere with Ab interaction with PD-1 (Fig. 2 F).

The epitope mapping and structural studies both revealed that Ab binding to a specific region of PD-1 on the opposing face of the PDL-1-PDL-2 interaction site resulted in an antagonistic functional activity (Fig. 1 and Fig. 2, C and E). Interestingly, sequence alignment across five species revealed that despite a low 52.3% identity with human PD-1, conserved regions throughout the sequence come together to form a highly conserved patch on PD-1 (Fig. S3 B) that is partially overlapping with the binding epitopes of both 135C12 (NB01 hIgG4) and 136B4 Abs (P1 patch in Fig. 2 F).

Structural models of hPD-1-NB01a Fab with either pembrolizumab (PDB accession no. 5GGS) or nivolumab (PDB accession no. 5GGR) were also generated and clearly show that NB01a can bind hPD-1 simultaneously with either PDL-1 blocking Ab (Fig. 2 G; Lee et al., 2016). This model is consistent with our Ab competitive binding studies (Fig. 2 D).

### Nonblocking and blocking anti-PD-1 Abs synergize in recovering Ag-specific CD8 T cells from exhaustion

Given that nonblocking anti-PD-1 Abs can bind simultaneously to cell-surface PD-1 with blocking Abs such as pembrolizumab, an important question is whether the simultaneous binding results in a synergistic potentiation of their antagonistic activity. This was addressed by testing combinations of blocking and nonblocking Abs in the in vitro functional recovery exhaustion assay. Studies presented in Fig. 3 show a significant increase in the recovery of proliferation of HIV-specific CD8 T cells when NB01a was used in combination of either pembrolizumab or B01 with 155% and 158% proliferating cells, respectively, relative to single Abs. These increases in proliferation were observed with the 135C12 mouse IgG1 variants of NB01 and several different humanized IgG4 clones (Fig. S2, A–D). It is important to underscore that this enhanced proliferation was beyond levels that could be achieved by higher Ab concentrations or with combinations of two blocking Abs that did not lead to enhancements in the recovery of proliferation (Fig. S2, E and F).

To further determine the biological activity of the two classes of anti-PD-1 Abs, the synergistic effect of the combination of blocking and nonblocking anti-PD-1 Abs was

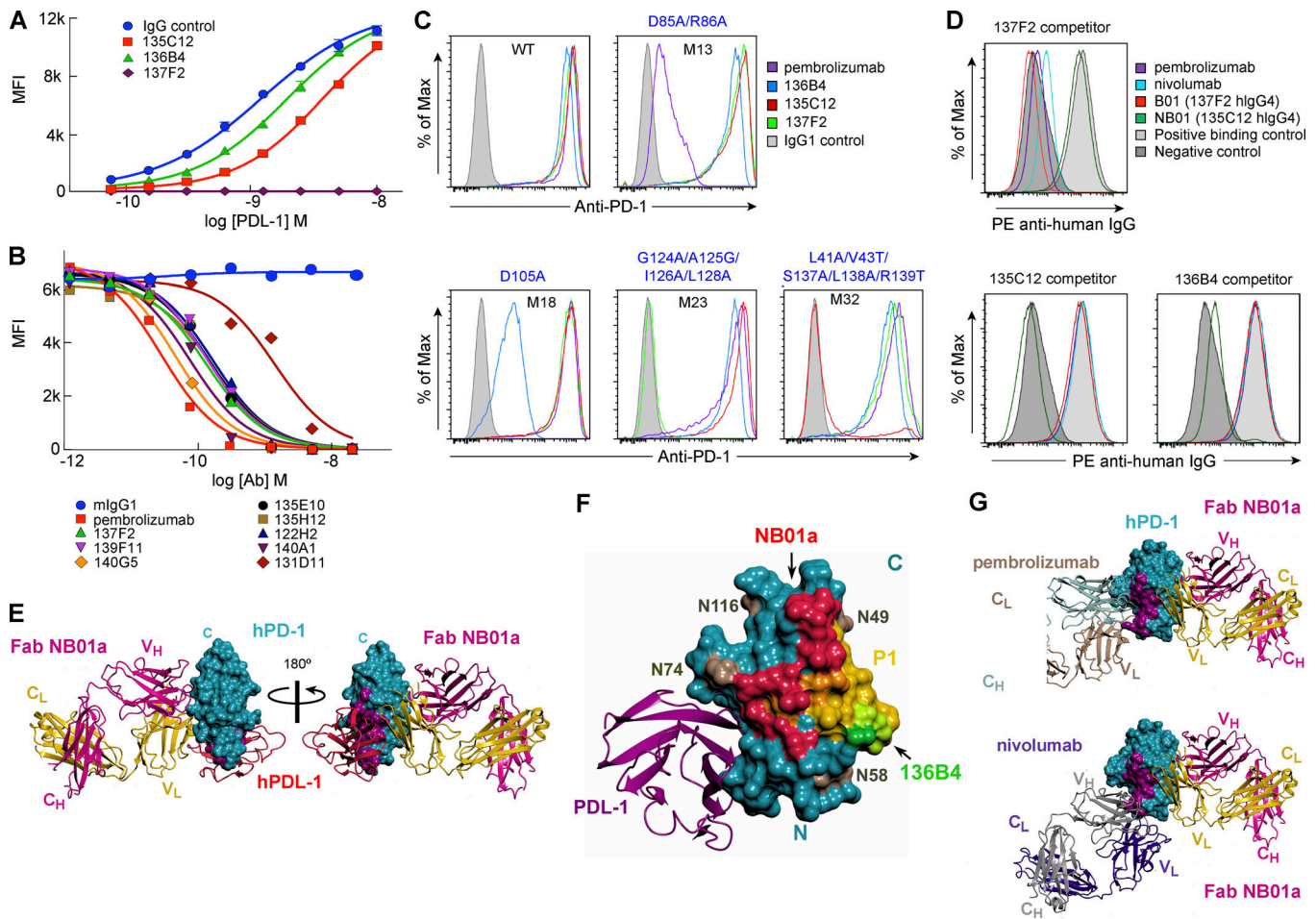


**Figure 2. Epitope mapping and structural studies of the prioritized anti-PD-1 Ab clones. (A)** Ability of anti-PD-1 Abs to block the PD-1-PDL-1 interaction in a Luminex biochemical assay. PD-1-coated beads were incubated in the presence or absence of a competitor anti-PD-1 Ab, and then beads were stained with different concentrations of biotin-labeled PDL-1 protein. Data ( $n = 2$ ) are mean  $\pm$  SD. MFI, mean fluorescence intensity. **(B)** Potency of anti-PD-1 Abs in blocking the PD-1-PDL-1 interaction in a Luminex biochemical assay. PD-1-coated beads were incubated with a fixed concentration of PDL-1 equivalent to the half-maximal inhibitory concentration value for the PD-1-PDL-1 interaction in this assay. The PD-1-PDL-1 complex, bound at 50% in equilibrium, was then treated with increasing concentrations of anti-PD-1 Ab to determine if they were capable of completely disrupting the PD-1-PDL-1 interaction with pembrolizumab used as a positive blocking Ab control. **(C)** Epitope mapping by site directed mutagenesis of PD-1. Defined epitopes were identified for anti-PD-1 Abs that were either blocking or nonblocking of the PD-1-PDL-1 interaction using HeLa cells transfected with expression vectors encoding PD-1 with substitutions at solvent accessible residues. Amino acid substitutions in PD-1 are indicated in blue lettering above each histogram. Representative data are shown for  $n = 3$  experiments. **(D)** Ab competitive binding studies for cell-surface PD-1. Jurkat PD-1 cells were incubated with excess of 137F2, 135C12, or 136B4 mouse Abs and then stained with a minimal concentration of the indicated humanized anti-PD-1 Abs ( $n = 3$ ). **(E)** hPD-1 and NB01a Fab (humanized version of the mouse 135C12 Ab) complexes were purified by size-exclusion chromatography and crystallized. Crystals diffracted to 2.2 Å resolution, and the structure was solved by molecular replacement. The structure reveals that the binding site of NB01a is adjacent to residues in purple involved in the PD-1 interaction with either PDL-1 or PDL-2. The CC' loop (residues 70–74) of hPDL-1 is disordered and indicated as a dashed line. Loops connecting  $\beta$  strands BC (57–63), C'D (84–92), and FG (127–133) were also disordered. Strands are named following the canonical designation. Ca superpositioning of the hPD-1 present in the NB01a Fab and hPDL-1 (PDB accession no. 4ZQK) complexes show that NB01a Fab and PDL-1 bind distinct nonoverlapping sites on PD-1. **(F)** Mapping of variable residues between human PD-1 and monkey, dog, horse, mouse, and rat PD-1 revealed an evolutionarily conserved patch (P1) on the opposite face of PD-1 from the PDL-1 or PDL-2 interaction site (yellow, orange, and light green colored residues). The P1 patch overlaps with the binding epitopes for the 135C12/NB01 (orange residues) and 136B4 (light green residues) antagonistic Abs that are nonblocking of PD-1-PDL-1. Residues N49, N58, N74, and N116 that are predicted N-linked glycosylation sites are shown in brown on the PD-1 model to be excluded from the P1 patch, 135C12/NB01, and 136B4 Ab binding epitopes. **(G)** Ca superpositioning of hPDL-1 coordinates of the NB01a complex with pembrolizumab (PDB accession no. 5GG5) and the nivolumab (PDB accession no. 5GGR) confirms that NB01a Fab binding to PD-1 does not interfere with the binding of either pembrolizumab or nivolumab anti-PD-1 Abs. hPDL-1 is shown as a ribbon diagram in E and F, with the hPDL-1 binding surface (PDB accession no. 4ZQK) colored in purple in G.

assessed on the production of cytokines. For these purposes, blood mononuclear cells from eight chronically infected viremic HIV individuals were stimulated with the specific antigenic peptides. Cells treated with anti-PD-1 Ab combinations released significantly higher levels of IFN $\gamma$ , TNF $\alpha$ , and IL-10

relative to antigenic peptide alone treatments (Fig. 3 B). Additionally, results across the different donors showed that Ab combination treatment lead to IFN $\gamma$  production with significantly higher levels than either blocking or nonblocking anti-PD-1 monotherapy treatments alone.

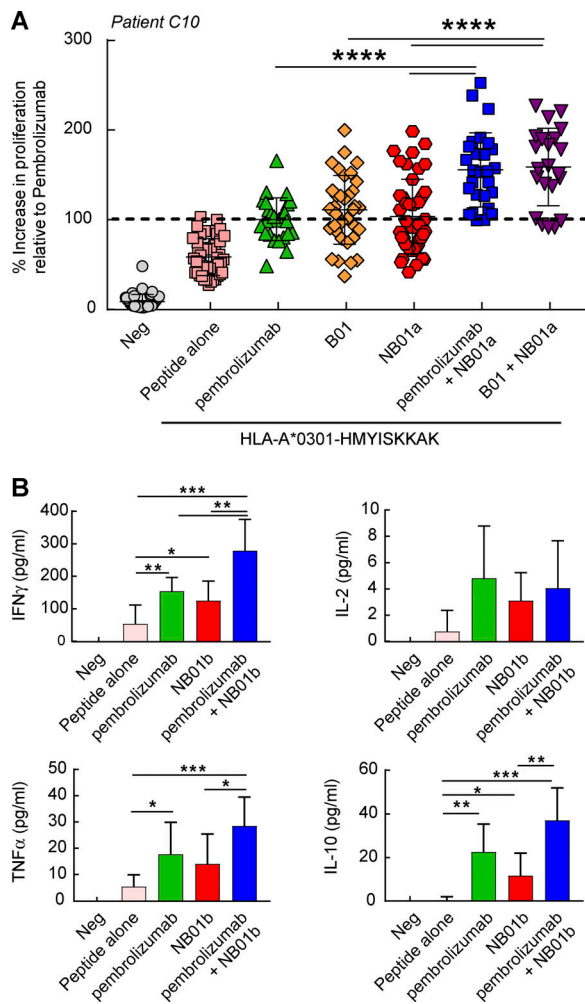


**Figure 3. Blocking and nonblocking anti-PD-1 Ab combinations synergize in recovering both the proliferation and functional activity of exhausted Ag-specific CD8 T cells.** (A) Cumulative results (three to six experiments) of the recovery of the proliferation of HIV-specific CD8 T cells after treatment with single and/or the combination of blocking and/or nonblocking anti-PD-1 Abs. Results are expressed as the percentage of CFSE-low CD8 T cells, and 8–10 replicates were performed for each experimental condition. (B) Recovery of T cell functionality evaluated by measuring cytokine levels of IFN $\gamma$ , IL-2, TNF $\alpha$ , and IL-10 in the cell medium following an Ag-specific CD8 T cell stimulation. Cumulative results are shown using the PBLs from six to eight different viremic HIV-positive donors. Untreated samples (Neg) were used as a negative control in each experiment. Data represent mean  $\pm$  SD. \*,  $P < 0.036$ ; \*\*,  $P < 0.0079$ ; \*\*\*,  $P < 0.0009$ ; \*\*\*\*,  $P < 0.0001$  (unpaired *t* test with Welch's correction).

**Nonblocking anti-PD-1 Abs act predominantly through the CD28 costimulatory receptor to promote the AKT-NF- $\kappa$ B pathway**

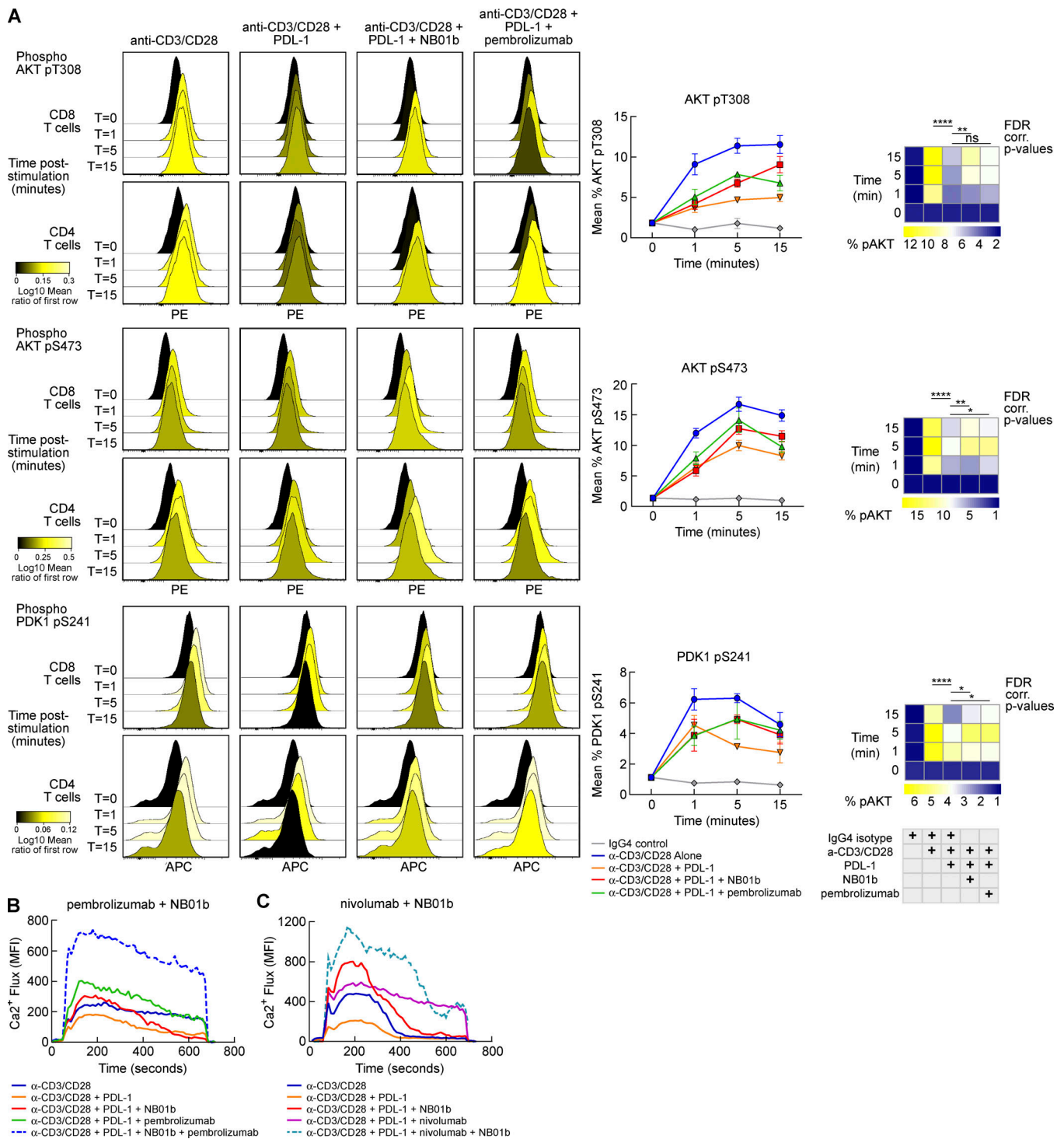
Mechanism-of-action studies with anti-PD-1 Abs were then investigated using phosphoflow intracellular staining of proteins important to the T cell signaling cascade. Blood mononuclear cells from a viremic HIV-positive donor were used for these signaling studies with 60–63% of memory T cells expressing the PD-1 exhaustion marker. T cell stimulation with anti-CD3/CD28 Abs induced a temporal increase in protein phosphorylation that was proximal to (ZAP70, SLP76, and Lck/Src) and downstream

of (AKT, PDK1, PLC $\gamma$ 1, NF- $\kappa$ B, ERK1/2, p38, and CREB) the TCR complex. T cell signaling was suppressed with human PDL-1 Fc fusion protein when added before the anti-CD3/CD28 stimulation. Importantly, this protocol using exhausted primary T cells identified the same canonical pathways reported for PDL-1-PD-1 mediated suppression of T cell activation using immunoblotting techniques that were performed with cell lines or in vitro stimulated T cell to augment PD-1 expression (Patsoukis et al., 2012; Yokosuka et al., 2012). T cell stimulation in the presence of PDL-1 resulted in statistically significant reduced phosphorylation of ZAP70 and Lck394/Src 1 min after stimulation and ERK1/2, AKT, and PDK1 5–15 min after stimulation (Figs. 4 A and S4).

Pretreatment of cells with NB01b or pembrolizumab partially restored phosphorylation of PDK1-pS242, AKT-pT308, and AKT-pS473 when stimulated with anti-CD3/CD28 in the presence of PDL-1 Fc protein. A trend toward recovery was also observed with ERK1/2, ZAP70, and LCK394/Src phosphorylation levels; however, these levels did not reach statistical significance. Anti-PD-1 Ab-mediated rescue was not evident for AKT at the earliest time point evaluated, but phosphorylation levels gradually built to a significant increase at 5 and 15 min for both PDK1 and AKT (Fig. 4 A). This increased phosphorylation was more statistically significant for the nonblocking anti-PD-1 Ab compared with pembrolizumab-treated cells, which also had a trend toward lower phospho-AKT levels 15 min after stimulation. This pathway is directly downstream of the CD28 costimulatory receptor, which was previously reported to be necessary for the antitumor activity of blocking anti-PD-1 Abs (Hui et al., 2017). These results are consistent with a mechanism whereby anti-PD-1 Ab therapy prevents the PDL-1-mediated recruitment of a phosphatase to the PDK1-AKT complex. Prolonged phosphorylation and activation of the PDK1-AKT complex would lead to increased T cell survival, trafficking and effector function.

An important aspect of T cell stimulation is the rapid increase in cytoplasmic levels of calcium (Ca<sup>2+</sup>) released from intracellular stores and through the opening of the plasma membrane calcium release-activated channels. This Ca<sup>2+</sup> release helps to propagate the T cell activation signal, including NFAT activation and cytoskeletal rearrangement. Similar to the phospho-flow experiments, stimulation of exhausted PD-1<sup>+</sup> T cells in the presence of a PDL-1 Fc fusion protein led to reduced levels of intracellular Ca<sup>2+</sup> relative to an anti-CD3/CD28 Ab stimulation control (Fig. 4, B and C). Pretreatment of cells with either blocking (pembrolizumab or nivolumab) or nonblocking NB01b anti-PD-1 Abs restored Ca<sup>2+</sup> mobilization to levels observed in cells stimulated in the absence of PDL-1 Fc protein. Importantly, combinations of NB01b and either pembrolizumab (Fig. 4 B) or nivolumab (Fig. 4 C) before T cell stimulation in the presence of PDL-1 resulted in a synergistic increase in Ca<sup>2+</sup> levels. This Ca<sup>2+</sup> mobilization was more intense and gave area under the curve values more than twofold higher compared with the anti-CD3/CD28 stimulation condition.

To provide insights on the mechanistic differences in the effect of blocking and nonblocking anti-PD-1 Abs, the two classes of Abs were further probed by immunoprecipitation (IP) of PD-1 expressed on a Jurkat cell line stably expressing high levels of PD-1. Cells were unstimulated or stimulated with anti-



CD3/CD28 Abs and then the PD-1 receptor and associated cellular complex was coprecipitated with NB01b, pembrolizumab or a combination of NB01b and pembrolizumab Abs covalently coupled to beads. In stimulated cells, pembrolizumab effectively pulled down a PD-1 complex that included CD28, SHP-2, PI3K, and phosphorylated Src (Fig. 5 A). In contrast, although NB01b pulled down equivalent levels of PD-1 and the PD-1-associated SHP-2 compared with pembrolizumab, there were significantly lower levels of CD28 receptor and PI3K in the nonblocking anti-PD-1 Ab IP complex (Fig. 5, A and B). AKT was weakly immunoprecipitated with the PD-1 complex, but there was a trend toward higher levels of AKT pulled down with pembrolizumab compared with the NB01b Ab. IPs performed with pembrolizumab- and NB01b-coated beads resulted in reduced levels of CD28 being coprecipitated with PD-1 relative to the pembrolizumab-alone IP (Fig. 5 B). In the above experiments, recruitment of PD-1 in the immunological synapsis after anti-CD3/CD28 stimulation occurred in the absence of PDL-1 engagement. To explain how the recruitment of PD-1 occurs in the absence of PDL-1 engagement, in control experiments, IPs were performed using biotinylated pembrolizumab and NB01b not coupled to beads. These experiments showed that uncoupled Abs did not pull down the CD28 in either the presence or absence of stimulation (Fig. 5 C). Therefore, these control experiments indicate that aggregation induced by the anti-PD-1 Abs coupled to beads deliver to PD-1 a signal similar to the engagement of PDL-1 and promote recruitment of PD-1 to the CD28 costimulatory receptor following T cell activation as shown in Fig. 5 B.

Taken together, these results indicate that PD-1 is recruited to the CD28 costimulatory receptor upon T cell activation and that this complex is unaffected by the blocking with pembrolizumab anti-PD-1 Ab. Importantly, nonblocking Abs such as NB01b inhibit the formation of the PD-1 complex that includes CD28. This would effectively reduce the recruitment of the SHP-2 phosphatase to the CD28 costimulatory receptor and its associated intracellular kinases that includes PI3K, the upstream activator of AKT (Parry et al., 2005; Patsoukis et al., 2012).

Given that the CD28 costimulatory receptor contributes to T cell activation through enhanced signaling of the AKT-NF- $\kappa$ B pathways and TCR stimulation acts strongly through the NFAT pathway, anti-PD-1 Abs were tested in NF- $\kappa$ B and NFAT reporter assays. A Jurkat-PD-1 T cell line stably expressing luciferase under the control of a NFAT promoter was transiently transfected with the NanoLuc NF- $\kappa$ B reporter plasmid in order to monitor the activation of both pathways in the same cells. Experiments using this cell line were designed to evaluate the potency of blocking anti-PD-1 Abs, and stimulation was achieved through coculture of Jurkat PD-1 cells with 293T cells coexpressing a membrane-associated anti-CD3 TCR activator and the PDL-1 receptor. Pretreating Jurkat PD-1 cells with the blocking pembrolizumab anti-PD-1 Ab before stimulation effectively relieved the PD-1-PDL-1-mediated suppression of the NFAT reporter by 6.4-fold in this assay relative to an IgG4 control Ab, while the NB01b nonblocking anti-PD-1 Ab resulted in low to no NFAT activation (Fig. 5 D). In contrast, parallel evaluation of the NF- $\kappa$ B pathway showed that both blocking and nonblocking

anti-PD-1 Abs significantly relieved PD-1-mediated suppression of the NF- $\kappa$ B promoter following TCR-mediated activation (1.7-fold and 2.4-fold relative to an IgG4 isotope control, respectively; Fig. 5 D). Consistent with the functional data (Fig. 3, A and B) and Ca<sup>2+</sup> flux studies (Fig. 4, B and C), combination of blocking and nonblocking anti-PD-1 Abs result in a significant increase in NFAT activation relative to single anti-PD-1 Ab treatments given alone.

Taken together, signaling and IP studies show that classical blocking and antagonistic nonblocking anti-PD-1 Abs act through distinct mechanisms in relieving T cell exhaustion. Both Ab classes are shown to act on pathways linked to PD-1-mediated suppression of T cell activation. However, blocking Abs have a more pronounced effect on the NFAT pathway, while nonblocking Abs act predominantly through the CD28 coreceptor that promotes the AKT-NF- $\kappa$ B pathway and leads to T cell proliferation and survival.

### In vivo efficacy of nonblocking anti-PD-1 Abs

The antagonistic activity of PDL-1 nonblocking Abs and the synergistic effect observed in vitro provided the scientific rationale to determine the ability of nonblocking Abs alone or in combination with blocking Abs in suppressing tumor growth in vivo. The in vivo efficacy of the NB01b antagonistic nonblocking Ab was then evaluated in the PD-1 HuGEMM in vivo tumor model (Lute et al., 2005; Huang et al., 2017). HuGEMM mice were genetically engineered to express a chimeric human/mouse PD-1 protein with the majority of the ectodomain (residues 26–146) encoded by the human PD-1 protein. Mice successfully engrafted with tumors formed from the PDL-1-high MC38 colon adenocarcinoma cell line were randomly ascribed to give the same average tumor volumes for the different arms of the study with the indicated treatments administered twice weekly (Fig. 6 A). The nonblocking NB01b Ab administered at 10 mg/kg effectively suppressed tumor growth similar to pembrolizumab (clinical Ab batch) or nivolumab administered at the same dose in three separate studies (Fig. 6, B–D and F). We then determined whether the antitumor activity was enhanced by combining NB01b and either pembrolizumab or nivolumab. Mice that were coadministered with NB01b and pembrolizumab or nivolumab at a dose of 5 mg/kg of each Ab, for a total dose of 10 mg/kg, had more potent suppression in tumor growth relative to either Ab dosed alone (Fig. 6, E and F). A global analysis of three separate studies was performed where mice were treated with NB01b, pembrolizumab, and nivolumab monotherapies or combination therapies consisting of NB01b with either pembrolizumab or nivolumab. This analysis showed that the combination of blocking and nonblocking anti-PD-1 Abs was associated with a significantly greater suppression of tumor growth throughout the study. In modeling the cubic root-transformed tumor volumes as a function of time and Ab therapy using a mixed-effects statistical framework (Fig. 6 F), it can be seen that Ab combination therapy had a significant reduction in tumor volume over time compared with the anti-PD-1 monotherapy arms in the studies ( $P = 0.00045$ ). Importantly, the proportion of mice with complete control of tumor growth, having a smaller tumor volume at the end of the study compared

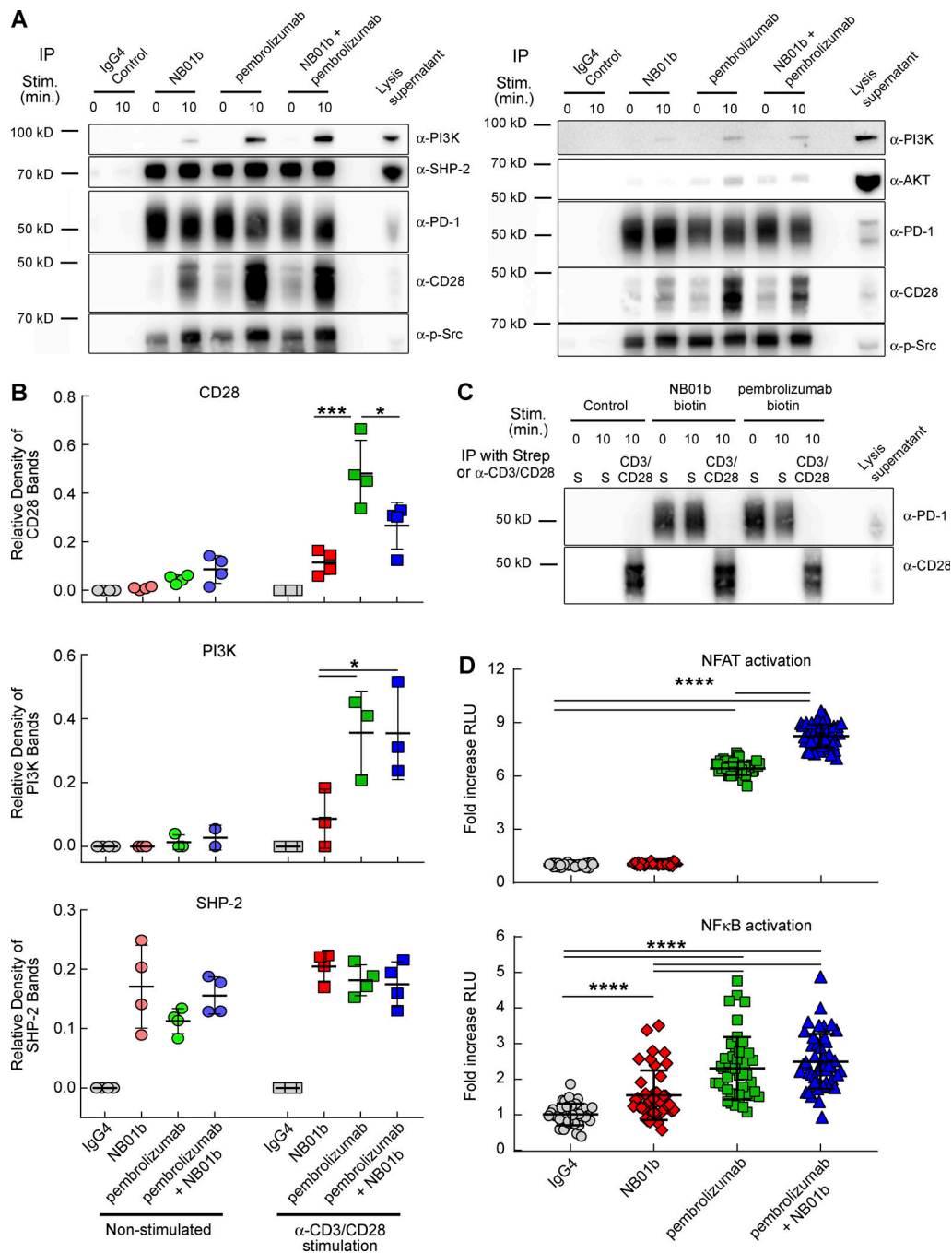
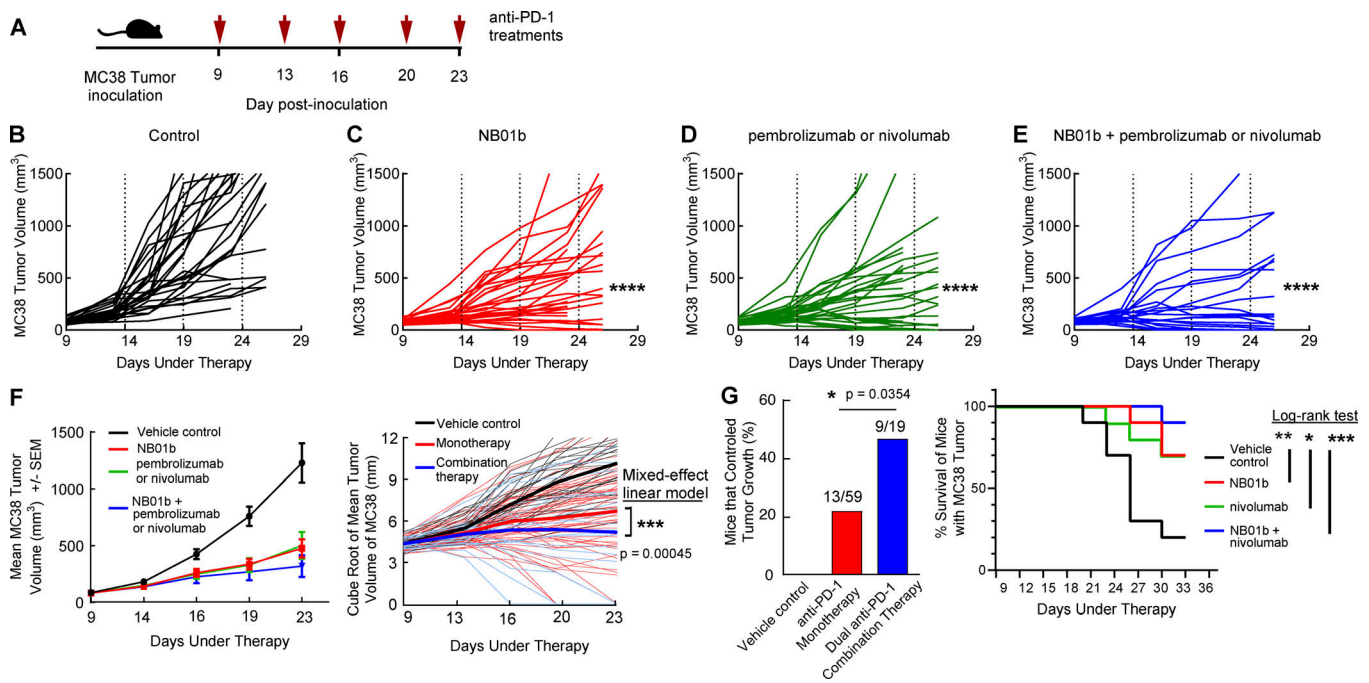


Figure 5. **Nonblocking anti-PD-1 Abs act primarily through the CD28 costimulatory receptor-associated pathway.** (A) IPs for two representative experiments are shown where the PD-1 receptor and associated protein complex were immunoprecipitated with NB01b, pembrolizumab, or a combination of NB01b and pembrolizumab in nonstimulated and anti-CD3/CD28 Ab-stimulated Jurkat PD-1 cells. In stimulated cells, pembrolizumab coprecipitated high levels of PD-1, CD28, SHP-2, PI3K, and the phosphorylated form of Src (p-Src) with the PD-1 complex. (B) NB01b pulled down equivalent levels of PD-1, SHP-2, and p-Src, but significantly reduced levels of CD28 and PI3K were observed in three or four separate experiments. AKT was only weakly pulled down in the PD-1 complex (A; right blot); however, there was a trend toward higher levels of AKT being immunoprecipitated with pembrolizumab compared with NB01b. (C) Control IPs performed by preincubating cells with either biotinylated pembrolizumab or NB01b before T cell stimulation shows that PD-1 pulled down with streptavidin (S) does not constitutively form a complex with CD28. Similarly, IPs performed with anti-CD3/CD28 coated beads show a strong pull-down of CD28 without detectable levels of associated PD-1. (D) The nonblocking anti-PD-1 Ab NB01b showed weak to no activation of the NFAT promoter in a Jurkat PD-1 luciferase reporter cell line when stimulated with 293T cells coexpressing a TCR activator and the PDL-1 receptor. Pretreatment of Jurkat PD-1 cells with the blocking anti-PD-1 Ab pembrolizumab strongly promoted NFAT activation. In contrast, both NB01b and pembrolizumab relieved PD-1-mediated suppression of NF-κB activation. Graphs show the mean ± SD and are representative of two independent experiments. \*,  $P < 0.045$ ; \*\*\*,  $P < 0.001$ ; \*\*\*\*,  $P < 0.0001$  (unpaired t test with Welch's correction). RLU, relative luminescence units.



**Figure 6. Enhancement of tumor clearance by the combination of blocking and nonblocking anti-PD-1 Abs in the PD-1 HuGEMM in vivo MC38 tumor model.** (A) Experimental scheme. (B–E) Mice successfully engrafted with the MC38 tumor cell line were treated twice weekly with PBS control (B), NB01b (C), pembrolizumab or nivolumab (D), or a combination of NB01b with either pembrolizumab or nivolumab (E), with tumor volumes measured in parallel. A collective analysis of three separate studies with  $n = 9–10$  mice per arm per study is presented in A–D. P values determined by pairwise comparison using a mixed-effect linear model showed that all Ab arms of the study had reduced tumor growth compared with the vehicle control arm. (F) Suppression of tumor volume in mice engrafted with PDL-1–high MC38 cell line with either single or the combination of blocking and nonblocking anti-PD-1 Abs. Blocking (pembrolizumab or nivolumab) and nonblocking (NB01b) anti-PD-1 Ab monotherapies exerted equivalent suppression of tumor growth and mean percent tumor inhibition. Modeling of the cubic root transformed tumor volume in three separate studies as a function of time demonstrated a statistically significant reduction in tumor volume over time for the anti-PD-1 combination therapy relative to anti-PD-1 monotherapies. (G) Combination anti-PD-1 Ab therapy significantly enhanced the proportion of mice that controlled tumor growth (9 out of 19 mice) relative to Ab monotherapies (13 out of 59 mice). Survival analysis for a study performed using NB01b and nivolumab, with statistical differences determined using the log-rank test. Graphs show the mean  $\pm$  SEM, unless otherwise indicated. \*,  $P = 0.0223$ ; \*\*,  $P < 0.008$ ; \*\*\*,  $P = 0.0005$ ; \*\*\*\*,  $P < 0.0001$ .

with the initial day of anti-PD-1 therapy, was 47% (9 out of 19 mice) in the combination treatment group (NB01b plus pembrolizumab or nivolumab) Abs as compared with 22% (13 out of 59) in the anti-PD-1 Ab monotherapy treatment groups (Fig. 6 G;  $P = 0.0354$ ). In a study that was extended to 33 d after MC38 inoculation, mouse survival was significantly improved for the combination therapy arm relative to vehicle control–treated mice (Fig. 6 G;  $P = 0.0005$ ). The significance of this extended survival was greater for the combination therapy relative to either NB01b or nivolumab monotherapies administered alone (Fig. 6 G, 0.0079 and 0.0223, respectively).

In a second in vivo study, PD-1 HuGEMM mice were subcutaneously implanted with the highly aggressive and poorly immunogenic wild-type B16F10 cell line (Kuzu et al., 2015; Kokolus et al., 2017). B16F10 tumor, which is engrafted subcutaneously, is characterized by a very fast growth and generation of rapid lung metastasis. As for the MC38 tumor model, mice were dosed twice weekly with blocking pembrolizumab, nonblocking NB01b, and/or the combination of both blocker/nonblocker Abs (Fig. 7 A). Suppression of tumor growth in the active groups versus the vehicle control untreated group was similar (Fig. 7, B–E). Although the suppression of tumor growth was significant ( $P < 0.008$ ) in the active groups, the effect was transient and

associated with rapid escape of the tumor. Furthermore, significant prolonged mouse survival was observed in the active groups as compared with the vehicle control group as determined using a log-rank statistical test (Fig. 7 F).

## Discussion

Here, we report the identification of a novel class of antagonistic anti-PD-1 Abs acting independently of PDL-1 blockade. These Abs were rare among hybridoma clone–producing Abs with high affinity for PD-1 (3.2% of 156 clones), which may partially explain why this novel anti-PD-1 Ab class has eluded discovery until now. Given the prevailing theory that PD-1–PDL-1 blockade is an important element needed for relieving T cell exhaustion, we performed several different lines of investigation to validate that our novel anti-PD-1 Abs were truly nonblocking of the PD-1–PDL-1 interaction.

Protein-to-protein (PD-1–PDL-1) interaction studies, together with competitive binding studies using the Jurkat PD-1 stable cell line, provided evidence that 135C12 or 136B4 nonblocking Abs interfere neither with the PD-1–PDL-1 interaction nor with the simultaneous binding of blocking Abs to PD-1 expressed at the cell surface. These results indicate that

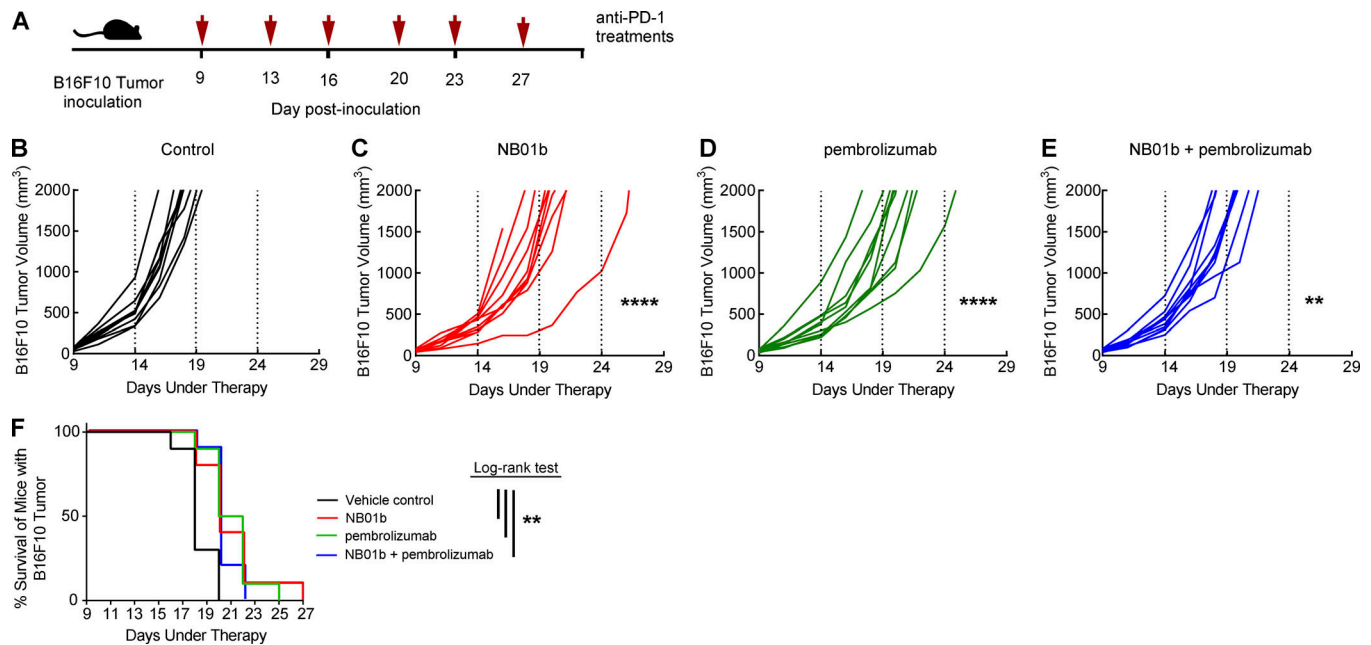


**Figure 7. Blocking and nonblocking anti-PD-1 Abs suppress tumor growth and prolong survival of mice implanted with B16F10 cells in the PD-1 HuGEMM in vivo tumor model. (A)** Experimental scheme. **(B–E)** Mice successfully engrafted with the poorly immunogenic B16F10 tumor cell line were treated twice weekly with PBS control (B), NB01b (C), pembrolizumab (D), or a combination of NB01b and pembrolizumab (E), with tumor volumes measured in parallel in the treatment ( $n = 10$  mice) and control (vehicle;  $n = 10$  mice) groups. P values determined by pairwise comparison using a mixed-effect linear model showed that blocking (pembrolizumab), nonblocking (NB01b), and combination anti-PD-1 Ab therapies had reduced tumor volume growth relative to the vehicle control. **(F)** Survival analysis with statistical difference determined using the log-rank test. Graphs show the mean  $\pm$  SEM. \*\*,  $P = 0.008$ ; \*\*\*\*,  $P < 0.0001$ .

nonblocking anti-PD-1 Abs do not sterically interfere with PDL-1 binding to PD-1 and do not exert a conformational change to the PD-1 protein that would significantly reduce its affinity for the PDL-1 ligand, and they exclude the possibility that either conformational or posttranslational differences occur between recombinant PD-1 and the cell-surface PD-1 receptor.

Epitope mapping studies performed through PD-1 site-directed mutagenesis together with the hPD-1-NB01a Fab crystal structure have shown that the novel two nonblocking anti-PD-1 Abs with antagonistic activity both bind PD-1 on different epitopes located on the opposing face of PD-1 relative to the PDL-1 interaction site. Importantly, we discovered that this novel functional active region of PD-1 recognized by nonblocking Abs overlaps with a patch of PD-1 residues that are highly conserved across six different species. Evolutionary conservation of this region suggests that PD-1 is under a selective pressure to preserve this site, which could be explained by the site being functionally implicated in PD-1 signaling or potentially through interaction with an alternate ligand from PDL-1–PDL-2. The fact that 135C12/NB01 and 136B4 Abs both overlap with an edge of this conserved site on PD-1 indicates that steric blocking of an alternate ligand and/or a complex formed with CD28 may represent the most likely hypothesis.

Consistent with blocking and nonblocking Abs both exerting distinct immune-enhancing functional activity through PD-1, combination therapy using the two classes of anti-PD-1 resulted in synergistic functional recovery of Ag-specific CD8 T cells from exhaustion.

Mechanism-of-action studies demonstrated that blocking and nonblocking anti-PD-1 Abs relieve PD-1 mediated T cell exhaustion through distinct effects on the TCR and CD28 related signaling cascades. We have provided evidence that the blocking Abs have a more pronounced effect on the NFAT pathway, while nonblocking Abs act predominantly through the CD28 coreceptor that promotes the AKT-NF- $\kappa$ B pathway. Previous studies (Patsoukis et al., 2012, 2013; Yokosuka et al., 2012; Hui et al., 2017) have indicated that PD-1 exerts its suppressive effects on T cell activation through PDL-1-mediated recruitment of PD-1 into the immunological synapse. This recruitment brings the PD-1-associated SHP-2 phosphatase into contact with the TCR-associated kinases, including ZAP70, Lck/Src, and ERK1/2, thus resulting in dephosphorylation of these kinases and dampening the intensity and duration of the T cell-specific activation. Blocking anti-PD-1 and anti-PDL-1 Abs relieve T cell exhaustion by preventing this recruitment of PD-1 into the TCR complex (Chemnitz et al., 2004; Sheppard et al., 2004; Yokosuka et al., 2012; Wherry and Kurachi, 2015; Hui et al., 2017; Kamphorst et al., 2017). Interestingly, our IP studies performed with the blocking anti-PD-1 Ab pembrolizumab showed that a complex formed between PD-1 and CD28 upon T cell activation. This indicates that elevated levels of PD-1 on a T cell may suppress TCR activation by a second mechanism, whereby PD-1 forms a cis complex with the CD28 costimulatory receptor. This colocalization would bring CD28-associated intracellular kinases essential for T cell costimulation into contact with

PD-1-associated SHP-2 phosphatase, resulting in a reduced costimulatory effect. In contrast, IPs performed with the non-blocking anti-PD-1 NB01b show significantly lower levels of a PD-1-CD28 complex after T cell activation. Taken together, our results support the model that in binding PD-1 on the opposing face of the PDL-1 interaction site, NB01b disrupts the inhibitory close-contact complex that forms between PD-1 and CD28 on activated T cells. The importance of this PD-1-CD28 interaction may explain the evolutionary conservation of the residues on PD-1 overlapping with the binding site of the nonblocking Abs. Our results are also consistent with Hui et al., who recently demonstrated that CD28 is the primary substrate for dephosphorylation through PD-1/SHP-2, leading to T cell suppression (Hui et al., 2017).

The distinct mechanism of nonblocking anti-PD-1 Abs may also help rationalize our *in vitro* functional data, where there is a trend toward lower cytokine production with NB01b compared with pembrolizumab. Since nonblocking Abs have a more limited effect on restoring PD-1-mediated suppression of the NFAT-Ca<sup>2+</sup> flux pathways, one would predict a reduced enhancement in cytokine production. Conversely, the more pronounced effect of nonblocking anti-PD-1 Abs on the AKT-NF- $\kappa$ B pathway is consistent with the enhanced proliferation observed when used in combination with blocking anti-PD-1 Abs.

The finding that blocker and nonblocker Abs act through distinct mechanisms explains the synergistic effect observed both *in vitro* and *in vivo* studies in combining the two classes of Abs. We have provided three lines of evidence in *in vitro* studies on the synergistic effect using a combination of blocking and nonblocking anti-PD-1 Abs: (1) increased Ag-specific CD8 T cell proliferation, (2) increased cytokine production in response to Ag-specific stimulation, and (3) enhanced intracellular Ca<sup>2+</sup> mobilization following anti-CD3/CD28 stimulation in the presence of PDL-1 suppression.

The immunotherapy with anti-PD-1 Abs is a major breakthrough in the fight against cancer, and anti-PD-1 therapy using pembrolizumab or nivolumab achieves a 20–50% objective response rate depending upon the type of cancer and the selection of criteria used for determining the percentage of PDL-1-expressing tumor cells (Carbognin et al., 2015; Gandini et al., 2016). Many patients have only a partial response to treatment, and a variable proportion of patients (depending on the type of cancer) experience recurrence of the tumor. Therefore, it has become clear that the potentiation of the antitumor activity of blocker anti-PD-1 Abs and the development of combinations of immunotherapy strategies are urgently needed. In addition to combination of anti-PD-1 Abs with anti-CTLA-4 (Larkin et al., 2015), combination therapies with Abs targeting other immune checkpoint inhibitors have entered clinical development.

In the present study, we have shown in two *in vivo* mouse tumor models that the novel nonblocking anti-PD-1 Abs have an antitumor activity equal to the conventional blocking Abs such as pembrolizumab. We have validated the results using the immunogenic colon carcinoma MC38 cell line and the highly aggressive and poorly immunogenic melanoma B16F10 cell line. Of note, in the MC38 studies, combination therapy using both classes of anti-PD-1 Abs significantly suppressed tumor growth

(74%) and was associated with a 2.4-fold increase in mice with complete tumor control and a trend toward improved survival relative to anti-PD-1 monotherapies.

The antitumor activity in the B16F10 model observed with anti-PD-1 monotherapy using either blocking or nonblocking Abs was inferior and transient as compared with MC38 model. The limited antitumor effect observed in our study is consistent with previous studies (Chen et al., 2015; Woods et al., 2015; Zamarin et al., 2018) in the B16F10 tumor model using anti-PD-1 treatment. Along the same line, combination of blocking and nonblocking Abs did not provide an additional therapeutic advantage in the poorly immunogenic B16F10 model. This may be attributed to the exceptionally rapid growth of the B16F10 cells, where tumor volume was >1,000 mm<sup>3</sup> in 70% of mice in the vehicle control arm by day 7 after initiation of anti-PD-1 therapy. Because of the rapid tumor escape, there is likely not sufficient time to develop a fully competent immune response and allow for the combined anti-PD-1 treatment to enhance tumor suppression, since only two doses of the combined treatment were administered by day 7. It should be underscored that this high rate of tumor growth in the B16F10 mouse tumor model is not representative of tumor development in humans.

In conclusion, we report the identification of a novel class of antagonistic anti-PD-1 Abs acting independently of PDL-1 blockade and acting through the CD28-AKT-NF- $\kappa$ B costimulatory pathway. These nonblocking anti-PD-1 Abs synergize with the classical blocker anti-PD-1 and are associated with an improvement of antitumor activity. These results provide important advances in the biology and function of PD-1 and may open new avenues for enhanced antitumor activity.

## Materials and methods

### Abs

Novel mouse anti-PD-1 Abs were isolated from the media of hybridoma cell lines and tested for binding to human PD-1 protein in the Luminex assay described below. For hybridomas that produced Abs with affinity < 1 nM, RNA was extracted using the Rneasy micro kit (Qiagen) followed by cDNA synthesis with the Cellsdirect 1-step QRT-PCR kit (Thermo Fisher Scientific) using the mouse Ig-Primer set (EMD Biosciences). The heavy-chain CDR region for each hybridoma was PCR amplified using the mouse Ig-Primer sets and then sequenced using the Applied Biosystems 3500 Genetic Analyzer sequencer (Thermo Fisher Scientific) with sequences described in a patent application (Pantaleo and Fenwick, 2016). Prioritized clones were expressed from 200 ml of hybridoma cells with the monoclonal Abs purified from the cell medium using a protein A column (Thermo Fisher Scientific) with Abs eluted with a 100 mM glycine buffer pH 3.0 into a 1 M Tris-HCl eluate at pH 8.0. Abs were dialyzed twice against PBS, concentrated using a JumboSep centrifuge filter with a 3-kD molecular weight cutoff (Pall Laboratories) and sterile filtered with a Millex GP 0.22  $\mu$ m filter (Millipore). Prior to anti-PD-1 Ab evaluation in the *in vitro* functional recovery assay, Abs were tested with the Food and Drug Administration-licensed Endosafe-PTS kit (Charles River Laboratory), and all had low endotoxin levels at <5 EU per mg of protein.

Humanized Abs of the 135C12 and 137F2 mouse clones were produced by GenScript with the Deluxe Antibody Humanization Service and using a framework assembly method. Briefly, frameworks of different human germlines with high sequence identities for each of the mouse anti-PD-1 Abs were selected and assembled using overlapping PCR. The resulting libraries of humanized Fabs with different framework sequences and encoding the mouse Ab CDR sequences for either 135C12 or 137F2 were then used to generate a phage display library encoding panels of humanized Fabs. Panning the library against the human PD-1 Fc fusion protein (R&D Systems) allowed for the enrichment of binding constructs and individual clones were screened for affinity using a phage ELISA assay. The FASEBA screen (fast screening for expression, biophysical properties, and affinity) was employed to identify Fab fragments that expressed well and had good biophysical properties, with candidate clones ranked based on their dissociation rate after binding to the PD-1 Fc fusion protein in a Biacore T200 assay (GE Healthcare). Candidate sequences with low-binding off rates were transferred into a proprietary vector at GenScript to produce the humanized anti-PD-1 Abs with an IgG4 Fc region that encoded a serine 228 to proline substitution in the hinge region to help prevent *in vivo* Fab arm exchange. High-affinity humanized clones NB01a, NB01b, and NB01c were identified for the 135C12 Ab and B01 for the 137F2 Ab. Pembrolizumab and nivolumab used in the *in vitro* functional studies were produced by GenScript using codon-optimized genes to express IgG4 Abs. A clinical lot of pembrolizumab was used in the *in vivo* mouse studies and was obtained through the Hospitalier Universitaire Vaudois.

The following Abs were used in flow cytometry and Luminex binding studies: allophycocyanin (APC)-H7-conjugated anti-CD3 (clone SK7), Pacific blue-, FITC-, or PE-CF594-conjugated anti-CD4 (clone RPA-T4), anti-CD8 Pacific blue (clone RPA-T8) Abs (Becton Dickinson); PE-labeled goat anti-mouse IgG secondary, PE-labeled F(ab')<sub>2</sub>-goat anti-mouse IgG secondary Ab, and mouse IgG1 isotype control (P3.6.2.8.1; eBioscience); PE-labeled goat anti-human IgG secondary Ab (Invitrogen); human IgG4 Isotype control Ab (ET904; Eureka Therapeutics); anti-PD-1 Ab (clone EH12.2H7) and PE-labeled streptavidin (BioLegend) and energy-coupled dye (phycoerythrin-Texas red conjugate)-conjugated anti-CD45RA (clone 2H4; Beckman Coulter).

Phospho-flow and Ca<sup>2+</sup> signaling studies were performed with the following Abs: CD3 Alexa Fluor 700 (UCHT1; BD), CD4 Qdot 605 (S3.5; Thermo Fisher Scientific), CD8 APC-eFluor780 (RPA-T8; eBioscience), CD8 PerCP-Cy5.5 (SK1; BD), and CD45RA Brilliant violet 650 (HII100; BioLegend) was used for surface T cell characterization. For PD-1 staining of humanized mAbs, goat anti-human PE secondary (Thermo Fisher Scientific) was used. For intracellular phosphoprotein staining, ZAP70 pY319 PE-Cy7 (17A/P-ZAP70; BD), Erk1/2 pT202/pY204 PE-CF594 (20A; BD), SLP76 pY128 Alexa Fluor 488 (J141-668.36.58; BD), p38 pT180/pY182 PE-CF594 (36/p38; BD), PLCγ1 pY783 (27/PLC; BD), AKT pS473 Brilliant violet 421(M89-61; BD), AKT pT308 PE (J1-223.371, BD), PDK1 pS241 Alexa Fluor 647 (J66-653.44.17; BD), NF-κB p65 pS529 Alexa Fluor 488 (K10-895.12.50;

BD), CREB pS133 PE (J151-21; BD), Src pY418 Alexa Fluor 488 (K98-37; BD), Lck505 pY505 Alexa Fluor 647 (4/LCK-Y505; BD), and S6 pS235/236 PE-Cy7 (D57.2.2E; Cell Signaling Technology) were used. For stimulation conditions, anti-CD3 (OKT3; BD), anti-CD28 (CD28.2; BD), and goat anti-mouse secondary Ab (Jackson ImmunoResearch) was used. Recombinant Fc chimeric PDL-1 protein (R&D Systems) was resuspended in PBS and used for suppression experiments. Fluo-4 AM (Thermo Fisher Scientific) was used for calcium flux experiments.

Immunoblot studies were performed with the Abs against PD-1 (D4W23), CD28 (D2Z4E), PI3K (19H8), and pSRC (D49G4) from Cell Signaling Technology and against SHP-2 (79) and AKT (M89-61) from BD Biosciences. Detection of primary Abs used the anti-mouse IgG or the anti-rabbit IgG HRP-linked Abs (catalog numbers 58802 and 7074, respectively; Cell Signaling Technology).

### Cell culture

Peripheral blood mononuclear cells were cultured in Roswell Park Memorial Institute (RPMI) medium and HeLa cells in DMEM (GIBCO BRL Life Technologies), each containing 10% heat-inactivated FBS or 6% human serum as indicated (both from Institut de Biotechnologies Jacques Boy), 100 IU/ml penicillin, and 100 μg/ml streptomycin (Bio Concept). Incubation of cells was performed at 37°C with 5% CO<sub>2</sub>.

### HIV-positive donors, ethics statement, and cell isolation

The present study was approved by the Institutional Review Board of the Centre Hospitalier Universitaire Vaudois, and all individuals gave written informed consent. Blood mononuclear cells used in the *in vitro* functional assay were obtained following leukapheresis performed on eight HIV-positive donors that were chronically infected based on virological and clinical profiles (Vajpayee et al., 2005). Blood mononuclear cells were isolated as previously described (Perreau and Kremer, 2005) and cryopreserved in liquid nitrogen.

### Luminex binding assay

The human PD-1 Fc fusion protein (R&D Systems) was conjugated to Bio-Plex magnetic beads (Bio-Rad) according to the manufacturer's protocol and used in a primary screen for anti-PD-1 Ab binding affinity. Ab serial dilutions were incubated with PD-1 Fc-coated beads for 2 h with bound mouse Ab detected using a PE-labeled anti-mouse IgG secondary in a Luminex binding assay. In the competitive binding assay performed with a commercial anti-PD-1 Ab, PD-1 Fc-conjugated Bio-Plex beads were preincubated with one of the novel anti-PD-1 Ab clones. A biotinylated clone EH12.2H7 anti-PD-1 Ab was then added to the beads and incubated for 2 h before staining for the bound commercial Abs with PE-labeled streptavidin. Competitive Ab binding to PD-1 results in a reduction in mean fluorescence intensity relative to biotinylated EH12.2H7 Ab binding in the absence of a competitor Ab. Beads were analyzed on a FLEXMAP 3D or Luminex 100 instrument (Luminex Corporation).

The PD-1-PDL-1 biochemical protein-protein interaction assay was performed by preincubating PD-1 Fc coated Bio-Plex

beads in the presence of 20 nM of anti-PD-1 Ab (clones 137F2, 135C12, and 136B4) or a mouse IgG1 isotype control for 1 h. Duplicate samples of biotinylated PD-L1 Fc protein (R&D Systems) were added in a concentration range from 0.08 to 10 nM to the preformed Ab-PD-1 complex and incubated for a further 4 h before removing unbound PDL-1 and staining beads with PE-labeled streptavidin. In a variation of this assay to identify blocking Abs, PD-1 Fc-coated Bio-Plex beads were preincubated for 1 h with up to 20 nM anti-PD-1 Ab followed by a 4-h incubation with 1.25 nM biotinylated PDL-1 protein, a concentration that gave half-maximal binding to the PD-1-coated beads in the absence of Ab competitor. Bound PDL-1 was stained with PE-labeled streptavidin and measured with the Luminex 100 instrument.

### Ab epitope mapping studies

The pReceiver-M67 vector encoding the open reading frame the PDCD1 gene (GeneCopoeia) was used to express human PD-1, and vectors encoding the amino acid substitutions in PD-1 listed in Fig. S4 were generated using the Q5 Site-Directed Mutagenesis Kit (New England Biolabs) according to the manufacturer's protocol. These PD-1 expression vectors together with an enhanced GFP pcDNA3 construct (Addgene) were used to transiently transfect HeLa cells using the FuGENE 6 transfection reagent (Promega). Following a 2-d incubation at 37°C, the adherent HeLa cells were detached from the plates with a stream of PBS and labeled with the Aqua LIVE/DEAD staining kit (Thermo Fisher Scientific). Ab binding to wild-type or mutant forms of PD-1 was performed in parallel by incubating the different transfected cell samples with 2 µg/ml of the indicated mouse anti-PD-1 Ab followed by a PE-labeled F(ab')<sub>2</sub>-goat anti-mouse IgG secondary Ab. Binding of pembrolizumab to the transiently transfected HeLa cells expressing the different PD-1 constructs was detected using PE-labeled goat anti-human IgG secondary Ab. Flow cytometry analysis of the samples was performed on an LSR II (Becton Dickinson) with Ab binding for the different wild-type and mutant PD-1 constructs evaluated for the live, enhanced GFP-expressing HeLa cells. Flow cytometry histogram results presented are representative of two to four independent experiments.

### Ab binding to cell-surface PD-1 and a competitive binding assay

A Jurkat cell line stably transfected to express high levels of human PD-1 (BPS Biosciences) was used to evaluate Ab binding affinity to cell-surface PD-1. These cells were incubated with different Ab concentrations, washed, stained with a PE-labeled anti-mouse or anti-human secondary Ab, and analyzed by flow cytometry. Percent detection of PD-1 positive cells was determined for each Ab concentration and binding affinities were determined with the GraphPad Prism7 software using a non-linear curve-fitting analysis.

Competitive binding between different anti-PD-1 Ab clones to Jurkat PD-1 cells was performed by adding saturating amounts (40 µg/ml) mouse IgG1 competitor Ab (137F2, 135C12, or 136B4) with cells incubated for 30 min followed by 1 µg/ml of the indicated human IgG4 anti-PD-1 Abs. The PE-labeled goat

anti-human IgG secondary Ab was used to detect the levels of human anti-PD-1 Abs binding to cell-surface PD-1 in the presence of competitor. Maximal binding to the Jurkat PD-1 cells was equivalent for all human anti-PD-1 Abs, and the positive control in each graph is shown for pembrolizumab staining.

### Functional exhaustion CFSE proliferation assay

Cryopreserved blood mononuclear cells from a patient with chronic HIV infection were thawed and resuspended in RPMI medium containing 20% FBS, washed with 37°C PBS, and rested in RPMI medium with 10% FBS overnight. The following morning, cells were washed twice with 37°C PBS and then incubated with 20 µM CFSE (Invitrogen) at 37°C for 7 min in the dark. The staining was quenched with the addition of FBS at a final concentration of 10% and then washed twice with RPMI medium. An aliquot of CFSE-stained blood mononuclear cells was set aside for the negative control samples, and the remaining peripheral blood mononuclear cells were batch stimulated with the addition of the indicated HIV antigenic peptide (GPT) to give a final concentration of 1.11 µg/ml. Peptide-stimulated and nonstimulated cells were then distributed into 48-well plates at 10<sup>6</sup> cells per well in 900 µl. Replicates of 8–10 wells were prepared for each condition tested. Abs tested were prepared in a 10× stock in RPMI + 6% human serum, then 100 µl was added to the appropriate wells to have a final peptide concentration of 1 µg/ml and final Ab concentration of 5 µg/ml unless otherwise indicated. As additional controls, a mouse IgG1 or human IgG4 isotype control Ab at a final concentration of 5 µg/ml was included in most experiments, and one well of cells was stimulated with staphylococcal enterotoxin B as a positive control for the induction of cellular proliferation. All samples within the 48-well plates were then returned to the 37°C, 5% CO<sub>2</sub> incubator for 6 d.

On the sixth day, the cells were harvested from wells and washed with warm PBS, as before. The cells were then labeled with Aqua viability stain and incubated with an Ab cocktail containing anti-CD3 APC Cy7, anti-CD4 PE CF 594, and anti-CD8 Pacific blue. The samples were then analyzed by flow cytometry on the LSR II SORP four-laser (405, 488, 532, and 633 nm) instrument. The five different chronic HIV-infected patients used for the CFSE proliferation assay studies were B08, B09, C10, M34, and M114.

### Assessment of cytokine production

Cryopreserved blood mononuclear cells from eight different HIV-infected donors (B08, B09, C10, M34, M114, B02, M24, and M46) were used in studies monitoring cytokine production following Ag-specific stimulations in the presence and absence of anti-PD-1 Abs. The protocol for HIV antigenic peptide stimulations is the same as described above for the proliferation assay with the omission of the CFSE cell staining. Following a 3-d incubation in culture, cell medium supernatants were assessed for levels of INF-γ, TNF-α, IL-2, and IL-10 by Luminex assay using a ProcartaPlex custom human 4-plex kit (Thermo Fisher Scientific) according the manufacturer's protocol with measurements performed on the Luminex 100 instrument.

### Purification of hPD1 and the hPD-1–Fab NB01a complex

The expression of hPD-1 33–150 (UniProt Q15116), cloned into pET-24d (kindly provided by Krzysztof M. Zak and Tad A. Holak; Faculty of Biochemistry, Biophysics, and Biotechnology, Jagiellonian University, Krakow, Poland), was induced with 1 mM isopropyl  $\beta$ -D-1-thiogalactopyranoside for 5 h at 37°C in *Escherichia coli* BL21 (DE3) cells, and the protein purification protocol was adapted from Zak et al. (2015). Briefly, induced cells were lysed by sonication with recovery of the inclusion bodies by centrifugation at 20,000 rpm. The inclusion bodies were resuspended in 50 mM Tris, pH 8.0, 6 M guanidine hydrochloride, 200 mM NaCl, and 20 mM  $\beta$ -mercaptoethanol before drop-wise dilution into ice-cold refolding buffer containing 0.1 M Tris-HCl, pH 8.0, 0.4 M L-arginine, 2 mM EDTA, 2 mM reduced glutathione, and 0.2 mM oxidized glutathione. Overnight refolding at 4°C was followed by dialysis and sample loading onto HiTrap Q HP and HiTrap SP FF columns (GE Healthcare). The flow through was concentrated and run in a Superdex 200 10/300 size-exclusion chromatography (GE Healthcare) column.

(Fab)<sub>2</sub> and Fab species were generated by digestion of the NB01a IgG4 with the FabRICATOR protease at 4°C overnight according to the manufacturer's protocol with the Fc domain removed using a Protein A affinity column (Thermo Fisher Scientific). (Fab)<sub>2</sub> were reduced to Fab with the addition of 2 mM dithiothreitol. Complexes were assembled by mixing hPD-1 with the Fab or reduced (Fab)<sub>2</sub> NB01a species in a 1.5:1 molar ratio. After 45 min of incubation at room temperature, the complexes were loaded onto a size-exclusion chromatography Superdex 200 10/300 column equilibrated with 10 mM Tris HCl, 70 mM NaCl, and 2 mM dithiothreitol. Fractions in which the complex eluted were concentrated down to 4.3 mg/ml.

### Data collection, processing, and refinement of the x-ray structure

X-ray data were collected at the European Synchrotron Radiation Facility (ESRF), Grenoble, France, at the ID29 beamline (Table S1). Data were collected at a wavelength of 0.97625 Å with a crystal to detector distance of 398.81 mm and a 0.15° rotation of the crystal to complete a total rotation of 150°. The data were processed with XDS (Kabsch, 2010) using the resolution range 65.49–2.2 Å. The structure of the complex was solved by molecular replacement in Phaser MR (McCoy et al., 2007; Read and McCoy, 2011; Z-score 14.9) using hPD-1 in complex with hPD-L1 (PDB accession no. 4ZQK) and a model built in Phenix using coordinates from Fab BL3-6 (PDB accession no. 4Q9Q; Huang et al., 2014), which exhibits high sequence homology with Fab NB01a (90% and 73% with the heavy and light chains, respectively) as search models. The model of the complex was refined in Phenix (Adams et al., 2010) and Refmac5 (Murshudov et al., 2011) and adjusted manually in Coot (Emsley and Cowtan, 2004) to values of  $R_{\text{factor}} = 0.2120$  and  $R_{\text{free}} = 0.2760$ . The software Contact, part of the CCP4 suite like Phaser MR and REFMAC5 (Winn et al., 2011) and PDBePISA (Krissinel and Henrick, 2007), were used to identify contacts in the binding interface. Structure representations were prepared using CCP4mg (McNicholas et al., 2011). The data for this study are available under PDB accession no. 6HIG.

### Modeling of the hPD-1–136B4Fv interaction

The model of 136B4 was built using Phenix software and the aligned sequences of 136B4 and the Fv from PDB file 1DZB (Åy et al., 2000), which shares 63% identity with 136B4. In addition to the high sequence identity, this PDB file was selected because it comprises an Fv, which is expected to adopt a similar fold to 136B4. Subsequently, models for the light and heavy chains were searched on the PDB to model the CDRs. The heavy and light chains from PDB files 1MVU and 4M61 (Stanfield and Eilat, 2014) share 79% and 96% of identity with those from 136B4, respectively, and the length of the CDR is comparable. The CDR segments were built into the model provided by Phenix software using Coot.

### Phosphoprotein signaling by flow cytometry

Blood mononuclear cells from a viremic HIV-positive donor were incubated with 20  $\mu$ g/ml of pembrolizumab, NB01b, or IgG4 isotype control for 30 min at 37°C. PDL-1 Fc fusion protein was then added to the indicated test conditions at 20  $\mu$ g/ml for an additional 30 min. For all conditions except the IgG4 control, anti-CD3/CD28 Ab stimulation was performed at 5  $\mu$ g/ml of each Ab and cross-linked with an anti-mouse secondary Ab at 50  $\mu$ g/ml to initiate T cell activation. Cells were incubated at 37°C for various time points (1, 5, and 15 min) and fixed immediately with 2% formaldehyde in PBS at 37°C for 10 min to stop the reaction. Blood mononuclear cells were washed and stained for CD3, CD4, CD8, and CD45RA T cell surface markers at room temperature for 20 min. Following cell permeabilization in chilled 70% methanol for 30 min, intracellular staining with various phosphoproteins was performed. The stained cells were washed and fixed once more in 2% formaldehyde in PBS before FACS acquisition. The percentage of positive phosphoproteins was determined at the different time points following stimulation by applying a global positive gate using the time 0 sample for each experiment as reference.

### Calcium flux

Blood mononuclear cells were washed in PBS and incubated with 1  $\mu$ M of Fluo-4 AM for 15 min at room temperature. Cells were then washed again and incubated with an anti-CD4/CD8 Ab cocktail for T cell markers. Blood mononuclear cells were washed once more and resuspended in RPMI medium. NB01b, pembrolizumab, and/or nivolumab anti-PD-1 Abs were incubated at 10  $\mu$ g/ml for 30 min at 37°C and PD-L1 protein was incubated at 5  $\mu$ g/ml for an additional 30 min before the samples were stimulated with the same anti-CD3/CD28 Ab protocol described above and directly analyzed by FACS acquisition. Calcium flux from TCR stimulation was measured in real time for 10 min before ending the reaction with the addition of 2 mM EDTA, which was acquired for a further 1 min.

### Immunoprecipitation of the cellular PD-1 protein complex

Immunoprecipitation studies used Dynabeads M-450 Epoxy beads (Thermo Fisher Scientific) covalently coupled with either anti-PD-1 or IgG4 control Abs according to the manufacturer's protocol. For each condition, 10 million Jurkat cells stably expressing PD-1 (BPS Bioscience) were either left

unstimulated or stimulated with biotinylated anti-CD3 (5 µg/ml; OKT3; eBioscience) and anti-CD28 (5 µg/ml; CD28.2; eBioscience) then aggregated with the addition of 50 µg/ml of avidin (Invitrogen). Ab-coated beads were added directly and cells were incubated at 37°C for 10 min. Cell membranes were then lysed with ice cold PBS containing 1% Triton X-100, protease inhibitor cocktail (Complete; Roche) and a phosphatase inhibitor cocktail followed by a 15-min incubation on ice with frequent mixing. Magnetic beads were attracted to the side of each tube with a magnet and washed three times with cell lysis buffer and then once with lysis buffer without detergent. Immune complexes analyzed by Western blot had proteins separated on a NuPAGE 10% Bis-Tris gel (Invitrogen) and then transferred onto nitrocellulose (Bio-Rad). Immunoblotting was performed by staining with the primary Ab overnight at 4°C followed by washing steps and then incubation with the HRP-conjugated secondary Ab and detection with the Pierce ECL Western blotting substrate (Thermo Fisher Scientific) in accordance with the manufacturer's protocol. Blots were imaged with the Fusion FX Vilber Lourmat camera (Witec), and the density of individual bands was evaluated using ImageJ software.

#### Jurkat PD-1 NFAT and NF-κB reporter assays

The Jurkat PD-1 NFAT reporter assay was performed according to the manufacturer's protocol with minor modifications (BPS Bioscience). 2 d before performing the assay, Jurkat PD-1 NFAT cells were transiently transfected with the NanoLuc reporter vector with an NF-κB response element (Promega) using the Fugene 6 transfection reagent (Promega). Preparation of the activator cells involved transient cotransfection of 293T cells with the TCR activator and PDL-1 expression vectors using the Fugene 6 transfection reagent. The following day, cells were resuspended and seeded at 60–70% confluence in wells of a 96-well plate and then incubated for 5 h to allow cell adherence. The NanoLuc transfected Jurkat PD-1 NFAT reporter cells were added at 100,000 cells per well in the absence or presence of the indicated Abs. The NFAT and NF-κB activation was measured 18 h later using the Nano-Glo Dual-luciferase Reporter assay system (Promega) on the Synergy H1 Hybrid Multi-Mode Microplate Reader (BioTek Instruments).

#### Mouse tumor model

The *in vivo* tumor model studies using PD-1 HuGEMM mice (background: C57BL/6) were performed at CrownBio (Taicang, China) in three separate MC38 studies and one B16F10 tumor study. Each mouse was inoculated subcutaneously at the right hind flank with 10<sup>6</sup> MC38 cells or 10<sup>5</sup> B16F10 cells. Mice with successfully engrafted tumors of the desired size were enrolled in the studies with 10 mice per arm with mean tumor volumes of 82, 84, and 85 mm<sup>3</sup> for the first, second, and third MC38 tumor study, respectively. Mice enrolled for the B16F10 study had mean tumor volumes of 65.1 mm<sup>3</sup> for the 10 mice per arm of the study. Mice were administered the indicated Abs at a concentration of 0.9 to 1.0 mg/ml in PBS or a sterile PBS vehicle control at twice weekly intervals over the course of the study. All *in vivo* therapies used a total dose of 10 mg/kg Ab apart from the

combination therapy arm of the B16F10 study, where 10 mg/kg of pembrolizumab and NBO1b were administered. Tumor volumes were measured twice weekly in two dimensions using a caliper, and the volume was expressed in cubic millimeters using the formula  $V = 0.5 a \times b^2$ , where  $a$  and  $b$  are the long and short diameters of the tumor, respectively. Body weight was also measured twice weekly. Mice that controlled MC38 tumor growth had a decrease in tumor volume at the end of the study relative to the start, just before initiating Ab therapy. The protocol and any amendments or procedures involving the care and use of animals in this study were reviewed and approved by the Institutional Animal Care and Use Committee of CrownBio before conduct. During the study, the care and use of animals was conducted in accordance with the regulations of the Association for Assessment and Accreditation of Laboratory Animal Care.

#### Statistical analyses

Statistical significance (P values) between two sample conditions in the *in vitro* functional assay was obtained using two-tailed unpaired *t* tests with a Welch correction to account for samples with nonequivalent standard deviations. In the mouse study, a mixed-effects linear model, modeling the volume (after cubic-root transformation) as a function of group, time, and their interaction, was used to test whether the combination therapy had lower mean volume over time than any single therapy. Our model allows for a group-specific slope, taking into account the correlation within mice across time (due to the repeated measurements) and using a mice-specific random effect, which is common for such studies (Galecki and Burzykowski, 2013). The cubic-root transformation was used to stabilize the variance and make the data more normally distributed. It is also a natural transformation for volume measurements as the scale is easily interpretable. Since the original unit is a volume expressed in cubic millimeters, the transformed unit is a length expressed in millimeters. The cube-root transformation is often used to model volume data (Matthews et al., 1990; Gallegos et al., 1996; Mandonnet et al., 2003). Using our model, we tested the null hypothesis that the slope of the combination therapy is equal to the slope of the anti-PD-1 monotherapies alone versus the alternative that the slope is smaller using a two-sided test. In our model, the slope can be interpreted as the rate of increase of the mean tumor diameter over time.

#### Online supplemental material

Fig. S1 shows the enhanced proliferation of Ag-specific exhausted CD8 T cells in the presence of a panel of prioritized anti-PD-1 Abs. Fig. S2 shows four separate experiments where blocking and nonblocking anti-PD-1 Ab combinations synergize in recovering the proliferation of exhausted Ag-specific CD8 T cells. Fig. S3 shows a PD-1 sequence map of the mutations used for Ab epitope mapping and the sequence alignment of PD-1 from different species. Fig. S4 shows the PD-1-PDL-1-mediated suppression in phospho-signaling following stimulation of exhausted T cells and the relief of this suppression mediated by anti-PD-1 Abs. Table S1 shows the x-ray data statistics for the hPD-1-NBO1a Fab complex.

## Acknowledgments

We are grateful to N. Grandchamp, P. Pochon, X. Bron, M. Graff, A. Crétignier, R. Mamin, and C. André for technical assistance. We are also grateful to D. Hacker at the Ecole Polytechnique Fédérale de Lausanne for the production and purification of the nonblocking anti-PD-1 Abs used in this study.

W. Weissenhorn acknowledges support from the Institut Universitaire de France, the platforms of the Grenoble Instruct-ERIC Center (Integrated Structural Biology Grenoble; UMS 3518 CNRS-CEA-UJF-EMBL) supported by the French Infrastructure for Integrated Structural Biology Initiative (ANR-10-INSB-05-02) and Grenoble Alliance for Integrated Structural Cell Biology (ANR-10-LABX-49-01) within the Grenoble Partnership for Structural Biology, the European Synchrotron Research Facility and European Molecular Biology Laboratory Joint Structural Biology Group for access and support at the ESRF beam lines, and J. Marquez (European Molecular Biology Laboratory) from the crystallization platform.

G. Pantaleo and C. Fenwick are cofounders of MabQuest SA, which owns the patent rights to the novel Abs described in this report (WO 2016/020856 A2, US patent number 9,982,052 B2 and WO 2017/125815A2). The remaining authors declare no competing financial interests.

Author contributions: V. Joo performed the signaling studies; C. Pellaton, T. Decaillon, and A. Noto performed the CFSE proliferation and cytokine assays; and A. Farina, L. Esteves-Leuenerger, and N. Rajah performed the remaining experiments. J.-L. Loredó-Varela and W. Weissenhorn designed and performed the crystallography and structural modeling studies. M. Suffiotti, K. Ohmiti, and R. Gottardo performed statistical analyses. G. Pantaleo and C. Fenwick conceived the study, designed the experiments, and wrote the manuscript.

Submitted: 19 December 2018

Revised: 20 March 2019

Accepted: 1 May 2019

## References

Adams, P.D., P.V. Afonine, G. Bunkóczi, V.B. Chen, I.W. Davis, N. Echols, J.J. Headd, L.W. Hung, G.J. Kapral, R.W. Grosse-Kunstleve, et al. 2010. PHENIX: a comprehensive Python-based system for macromolecular structure solution. *Acta Crystallogr. D Biol. Crystallogr.* 66:213–221. <https://doi.org/10.1107/S0907444909052925>

Ay, J., T. Keitel, G. Küttner, H. Wessner, C. Scholz, M. Hahn, and W. Höhne. 2000. Crystal structure of a phage library-derived single-chain Fv fragment complexed with turkey egg-white lysozyme at 2.0 Å resolution. *J. Mol. Biol.* 301:239–246. <https://doi.org/10.1006/jmbi.2000.3971>

Baitsch, L., P. Baumgaertner, E. Devèvre, S.K. Raghav, A. Legat, L. Barba, S. Wiekowski, H. Bouzourene, B. Deplancke, P. Romero, et al. 2011. Exhaustion of tumor-specific CD8<sup>+</sup> T cells in metastases from melanoma patients. *J. Clin. Invest.* 121:2350–2360. <https://doi.org/10.1172/JCI46102>

Barber, D.L., E.J. Wherry, D. Masopust, B. Zhu, J.P. Allison, A.H. Sharpe, G.J. Freeman, and R. Ahmed. 2006. Restoring function in exhausted CD8 T cells during chronic viral infection. *Nature.* 439:682–687. <https://doi.org/10.1038/nature04444>

Callahan, M.K., M.A. Postow, and J.D. Wolchok. 2016. Targeting T Cell Co-receptors for Cancer Therapy. *Immunity.* 44:1069–1078. <https://doi.org/10.1016/j.immuni.2016.04.023>

Carbognin, L., S. Pilotto, M. Milella, V. Vaccaro, M. Brunelli, A. Calì, F. Cuppone, I. Sperduti, D. Giannarelli, M. Chilosi, et al. 2015. Differential Activity of Nivolumab, Pembrolizumab and MPDL3280A according to

the Tumor Expression of Programmed Death-Ligand-1 (PD-L1): Sensitivity Analysis of Trials in Melanoma, Lung and Genitourinary Cancers. *PLoS One.* 10:e0130142. <https://doi.org/10.1371/journal.pone.0130142>

Chemnitz, J.M., R.V. Parry, K.E. Nichols, C.H. June, and J.L. Riley. 2004. SHP-1 and SHP-2 associate with immunoreceptor tyrosine-based switch motif of programmed death 1 upon primary human T cell stimulation, but only receptor ligation prevents T cell activation. *J. Immunol.* 173: 945–954. <https://doi.org/10.4049/jimmunol.173.2.945>

Chen, S., L.F. Lee, T.S. Fisher, B. Jessen, M. Elliott, W. Evering, K. Logronio, G.H. Tu, K. Tsaparikos, X. Li, et al. 2015. Combination of 4-1BB agonist and PD-1 antagonist promotes antitumor effector/memory CD8 T cells in a poorly immunogenic tumor model. *Cancer Immunol. Res.* 3:149–160. <https://doi.org/10.1158/2326-6066.CIR-14-0118>

Day, C.L., D.E. Kaufmann, P. Kiepiela, J.A. Brown, E.S. Moodley, S. Reddy, E.W. Mackey, J.D. Miller, A.J. Leslie, C. DePierres, et al. 2006. PD-1 expression on HIV-specific T cells is associated with T-cell exhaustion and disease progression. *Nature.* 443:350–354. <https://doi.org/10.1038/nature05115>

Emsley, P., and K. Cowtan. 2004. Coot: model-building tools for molecular graphics. *Acta Crystallogr. D Biol. Crystallogr.* 60:2126–2132. <https://doi.org/10.1107/S0907444904019158>

Galecki, A., and T. Burzykowski. 2013. *Linear Mixed-Effects Models Using R: A Step-by-Step Approach.* Springer, New York. 542 pp. <https://doi.org/10.1007/978-1-4614-3900-4>

Gallegos, A., J.R. Gasdaska, C.W. Taylor, G.D. Paine-Murrieta, D. Goodman, P.Y. Gasdaska, M. Berggren, M.M. Briehl, and G. Powis. 1996. Transfection with human thioredoxin increases cell proliferation and a dominant-negative mutant thioredoxin reverses the transformed phenotype of human breast cancer cells. *Cancer Res.* 56:5765–5770.

Gandini, S., D. Massi, and M. Mandalà. 2016. PD-L1 expression in cancer patients receiving anti PD-1/PD-L1 antibodies: A systematic review and meta-analysis. *Crit. Rev. Oncol. Hematol.* 100:88–98. <https://doi.org/10.1016/j.critrevonc.2016.02.001>

Hamid, O., C. Robert, A. Daud, F.S. Hodi, W.J. Hwu, R. Keefe, J.D. Wolchok, P. Hersey, R.W. Joseph, J.S. Weber, et al. 2013. Safety and tumor responses with lambrolizumab (anti-PD-1) in melanoma. *N. Engl. J. Med.* 369:134–144. <https://doi.org/10.1056/NEJMoa1305133>

Huang, A., D. Peng, H. Guo, Y. Ben, X. Zuo, F. Wu, X. Yang, F. Teng, Z. Li, X. Qian, and F.X. Qin. 2017. A human programmed death-ligand 1-expressing mouse tumor model for evaluating the therapeutic efficacy of anti-human PD-L1 antibodies. *Sci. Rep.* 7:42687. <https://doi.org/10.1038/srep42687>

Huang, H., N.B. Suslov, N.S. Li, S.A. Shelke, M.E. Evans, Y. Koldobskaya, P.A. Rice, and J.A. Piccirilli. 2014. A G-quadruplex-containing RNA activates fluorescence in a GFP-like fluorophore. *Nat. Chem. Biol.* 10:686–691. <https://doi.org/10.1038/nchembio.1561>

Hui, E., J. Cheung, J. Zhu, X. Su, M.J. Taylor, H.A. Wallweber, D.K. Sasmal, J. Huang, J.M. Kim, I. Mellman, and R.D. Vale. 2017. T cell costimulatory receptor CD28 is a primary target for PD-1-mediated inhibition. *Science.* 355:1428–1433. <https://doi.org/10.1126/science.aaf1292>

Kabsch, W. 2010. Xds. *Acta Crystallogr. D Biol. Crystallogr.* 66:125–132. <https://doi.org/10.1107/S0907444909047337>

Kamphorst, A.O., A. Wieland, T. Nasti, S. Yang, R. Zhang, D.L. Barber, B.T. Konieczny, C.Z. Daugherty, L. Koenig, K. Yu, et al. 2017. Rescue of exhausted CD8 T cells by PD-1-targeted therapies is CD28-dependent. *Science.* 355:1423–1427. <https://doi.org/10.1126/science.aaf0683>

Kokolus, K.M., Y. Zhang, J.M. Sivik, C. Schmeck, J. Zhu, E.A. Repasky, J.J. Drabick, and T.D. Schell. 2017. Beta blocker use correlates with better overall survival in metastatic melanoma patients and improves the efficacy of immunotherapies in mice. *Oncotarget.* 7:e1405205. <https://doi.org/10.1080/2162402X.2017.1405205>

Krissinel, E., and K. Henrick. 2007. Inference of macromolecular assemblies from crystalline state. *J. Mol. Biol.* 372:774–797. <https://doi.org/10.1016/j.jmb.2007.05.022>

Kuzu, O.F., F.D. Nguyen, M.A. Noory, and A. Sharma. 2015. Current State of Animal (Mouse) Modeling in Melanoma Research. *Cancer Growth Metastasis.* 8(Suppl 1):81–94.

Larkin, J., V. Chiarion-Sileni, R. Gonzalez, J.J. Grob, C.L. Cowey, C.D. Lao, D. Schadendorf, R. Dummer, M. Smylie, P. Rutkowski, et al. 2015. Combined Nivolumab and Ipilimumab or Monotherapy in Untreated Melanoma. *N. Engl. J. Med.* 373:23–34. <https://doi.org/10.1056/NEJMoa1504030>

Lázár-Molnár, E., Q. Yan, E. Cao, U. Ramagopal, S.G. Nathenson, and S.C. Almo. 2008. Crystal structure of the complex between programmed death-1 (PD-1) and its ligand PD-L2. *Proc. Natl. Acad. Sci. USA.* 105: 10483–10488. <https://doi.org/10.1073/pnas.0804453105>

- Lee, J.Y., H.T. Lee, W. Shin, J. Chae, J. Choi, S.H. Kim, H. Lim, T. Won Heo, K.Y. Park, Y.J. Lee, et al. 2016. Structural basis of checkpoint blockade by monoclonal antibodies in cancer immunotherapy. *Nat. Commun.* 7: 13354. <https://doi.org/10.1038/ncomms13354>
- Lin, D.Y., Y. Tanaka, M. Iwasaki, A.G. Gittis, H.P. Su, B. Mikami, T. Okazaki, T. Honjo, N. Minato, and D.N. Garboczi. 2008. The PD-1/PD-L1 complex resembles the antigen-binding Fv domains of antibodies and T cell receptors. *Proc. Natl. Acad. Sci. USA.* 105:3011-3016. <https://doi.org/10.1073/pnas.0712278105>
- Lute, K.D., K.F. May Jr., P. Lu, H. Zhang, E. Kocak, B. Mosinger, C. Wolford, G. Phillips, M.A. Caligiuri, P. Zheng, and Y. Liu. 2005. Human CTLA4 knock-in mice unravel the quantitative link between tumor immunity and autoimmunity induced by anti-CTLA-4 antibodies. *Blood.* 106:3127-3133. <https://doi.org/10.1182/blood-2005-06-2298>
- Mandonnet, E., J.Y. Delattre, M.L. Tanguy, K.R. Swanson, A.F. Carpentier, H. Duffau, P. Cornu, R. Van Effenterre, E.C. Alvord Jr., and L. Capelle. 2003. Continuous growth of mean tumor diameter in a subset of grade II gliomas. *Ann. Neurol.* 53:524-528. <https://doi.org/10.1002/ana.10528>
- Matthews, J.N., D.G. Altman, M.J. Campbell, and P. Royston. 1990. Analysis of serial measurements in medical research. *BMJ.* 300:230-235. <https://doi.org/10.1136/bmj.300.6719.230>
- McCoy, A.J., R.W. Grosse-Kunstleve, P.D. Adams, M.D. Winn, L.C. Storoni, and R.J. Read. 2007. Phaser crystallographic software. *J. Appl. Cryst.* 40: 658-674. <https://doi.org/10.1107/S0021889807021206>
- McNicholas, S., E. Potterton, K.S. Wilson, and M.E. Noble. 2011. Presenting your structures: the CCP4mg molecular-graphics software. *Acta Crystallogr. D Biol. Crystallogr.* 67:386-394. <https://doi.org/10.1107/S0907444911007281>
- Mellman, I., G. Coukos, and G. Dranoff. 2011. Cancer immunotherapy comes of age. *Nature.* 480:480-489. <https://doi.org/10.1038/nature10673>
- Murshudov, G.N., P. Skubák, A.A. Lebedev, N.S. Pannu, R.A. Steiner, R.A. Nicholls, M.D. Winn, F. Long, and A.A. Vagin. 2011. REFMAC5 for the refinement of macromolecular crystal structures. *Acta Crystallogr. D Biol. Crystallogr.* 67:355-367. <https://doi.org/10.1107/S0907444911001314>
- Pantaleo, G., and C. Fenwick. 2016. Immunological reagents. MabQuest SA patent application WO/2016/020856 A2, filed August 5, 2015, and published February 11, 2016.
- Parry, R.V., J.M. Chemnitz, K.A. Frauwirth, A.R. Lanfranco, I. Braunstein, S.V. Kobayashi, P.S. Linsley, C.B. Thompson, and J.L. Riley. 2005. CTLA-4 and PD-1 receptors inhibit T-cell activation by distinct mechanisms. *Mol. Cell. Biol.* 25:9543-9553. <https://doi.org/10.1128/MCB.25.21.9543-9553.2005>
- Patsoukis, N., J. Brown, V. Petkova, F. Liu, L. Li, and V.A. Boussiotis. 2012. Selective effects of PD-1 on Akt and Ras pathways regulate molecular components of the cell cycle and inhibit T cell proliferation. *Sci. Signal.* 5:ra46. <https://doi.org/10.1126/scisignal.2002796>
- Patsoukis, N., L. Li, D. Sari, V. Petkova, and V.A. Boussiotis. 2013. PD-1 increases PTEN phosphatase activity while decreasing PTEN protein stability by inhibiting casein kinase 2. *Mol. Cell. Biol.* 33:3091-3098. <https://doi.org/10.1128/MCB.00319-13>
- Pauken, K.E., and E.J. Wherry. 2015. Overcoming T cell exhaustion in infection and cancer. *Trends Immunol.* 36:265-276. <https://doi.org/10.1016/j.it.2015.02.008>
- Perreau, M., and E.J. Kremer. 2005. Frequency, proliferation, and activation of human memory T cells induced by a nonhuman adenovirus. *J. Virol.* 79:14595-14605. <https://doi.org/10.1128/JVI.79.23.14595-14605.2005>
- Read, R.J., and A.J. McCoy. 2011. Using SAD data in Phaser. *Acta Crystallogr. D Biol. Crystallogr.* 67:338-344. <https://doi.org/10.1107/S0907444910051371>
- Rizvi, N.A., J. Mazières, D. Planchar, T.E. Stinchcombe, G.K. Dy, S.J. Antonia, L. Horn, H. Lena, E. Minenza, B. Mennequier, et al. 2015. Activity and safety of nivolumab, an anti-PD-1 immune checkpoint inhibitor, for patients with advanced, refractory squamous non-small-cell lung cancer (CheckMate 063): a phase 2, single-arm trial. *Lancet Oncol.* 16: 257-265. [https://doi.org/10.1016/S1470-2045\(15\)70054-9](https://doi.org/10.1016/S1470-2045(15)70054-9)
- Sharma, P., and J.P. Allison. 2015. The future of immune checkpoint therapy. *Science.* 348:56-61. <https://doi.org/10.1126/science.aaa8172>
- Sheppard, K.A., L.J. Fitz, J.M. Lee, C. Benander, J.A. George, J. Wooters, Y. Qiu, J.M. Jussif, L.L. Carter, C.R. Wood, and D. Chaudhary. 2004. PD-1 inhibits T-cell receptor induced phosphorylation of the ZAP70/CD3zeta signalosome and downstream signaling to PKCtheta. *FEBS Lett.* 574: 37-41. <https://doi.org/10.1016/j.febslet.2004.07.083>
- Stanfield, L., and D. Eilat. 2014. Crystal structure determination of anti-DNA Fab A52. *Proteins.* 82:1674-1678. <https://doi.org/10.1002/prot.24514>
- Topalian, S.L., F.S. Hodi, J.R. Brahmer, S.N. Gettinger, D.C. Smith, D.F. McDermott, J.D. Powderly, R.D. Carvajal, J.A. Sosman, M.B. Atkins, et al. 2012. Safety, activity, and immune correlates of anti-PD-1 antibody in cancer. *N. Engl. J. Med.* 366:2443-2454. <https://doi.org/10.1056/NEJMoal200690>
- Trautmann, L., L. Janbazian, N. Chomont, E.A. Said, S. Gimmig, B. Bessette, M.R. Boulassel, E. Delwart, H. Sepulveda, R.S. Balderas, et al. 2006. Upregulation of PD-1 expression on HIV-specific CD8+ T cells leads to reversible immune dysfunction. *Nat. Med.* 12:1198-1202. <https://doi.org/10.1038/nm1482>
- Tumeh, P.C., C.L. Harview, J.H. Yearley, I.P. Shintaku, E.J. Taylor, L. Robert, B. Chmielowski, M. Spasic, G. Henry, V. Ciobanu, et al. 2014. PD-1 blockade induces responses by inhibiting adaptive immune resistance. *Nature.* 515:568-571. <https://doi.org/10.1038/nature13954>
- Vajpayee, M., S. Kaushik, V. Sreenivas, N. Wig, and P. Seth. 2005. CDC staging based on absolute CD4 count and CD4 percentage in an HIV-1-infected Indian population: treatment implications. *Clin. Exp. Immunol.* 141:485-490. <https://doi.org/10.1111/j.1365-2249.2005.02857.x>
- Wherry, E.J., and M. Kurachi. 2015. Molecular and cellular insights into T cell exhaustion. *Nat. Rev. Immunol.* 15:486-499. <https://doi.org/10.1038/nri3862>
- Winn, M.D., C.C. Ballard, K.D. Cowtan, E.J. Dodson, P. Emsley, P.R. Evans, R.M. Keegan, E.B. Krissinel, A.G. Leslie, A. McCoy, et al. 2011. Overview of the CCP4 suite and current developments. *Acta Crystallogr. D Biol. Crystallogr.* 67:235-242. <https://doi.org/10.1107/S0907444910045749>
- Woods, D.M., A.L. Sodré, A. Villagra, A. Sarnaik, E.M. Sotomayor, and J. Weber. 2015. HDAC Inhibition Upregulates PD-1 Ligands in Melanoma and Augments Immunotherapy with PD-1 Blockade. *Cancer Immunol. Res.* 3:1375-1385. <https://doi.org/10.1158/2326-6066.CIR-15-0077-T>
- Yokosuka, T., M. Takamatsu, W. Kobayashi-Imanishi, A. Hashimoto-Tane, M. Azuma, and T. Saito. 2012. Programmed cell death 1 forms negative costimulatory microclusters that directly inhibit T cell receptor signaling by recruiting phosphatase SHP2. *J. Exp. Med.* 209:1201-1217. <https://doi.org/10.1084/jem.20112741>
- Zak, K.M., R. Kite, S. Przetocka, P. Golik, K. Guzik, B. Musielak, A. Dömling, G. Dubin, and T.A. Holak. 2015. Structure of the Complex of Human Programmed Death 1, PD-1, and Its Ligand PD-L1. *Structure.* 23: 2341-2348. <https://doi.org/10.1016/j.str.2015.09.010>
- Zamarin, D., J.M. Ricca, S. Sadekova, A. Oseledchik, Y. Yu, W.M. Blumenschein, J. Wong, M. Gigoux, T. Merghoub, and J.D. Wolchok. 2018. PD-L1 in tumor microenvironment mediates resistance to oncolytic immunotherapy. *J. Clin. Invest.* 128:5184. <https://doi.org/10.1172/JCI125039>
- Zhang, J.Y., Z. Zhang, X. Wang, J.L. Fu, J. Yao, Y. Jiao, L. Chen, H. Zhang, J. Wei, L. Jin, et al. 2007. PD-1 up-regulation is correlated with HIV-specific memory CD8+ T-cell exhaustion in typical progressors but not in long-term nonprogressors. *Blood.* 109:4671-4678. <https://doi.org/10.1182/blood-2006-09-044826>

## Supplemental material

Fenwick et al., <https://doi.org/10.1084/jem.20182359>

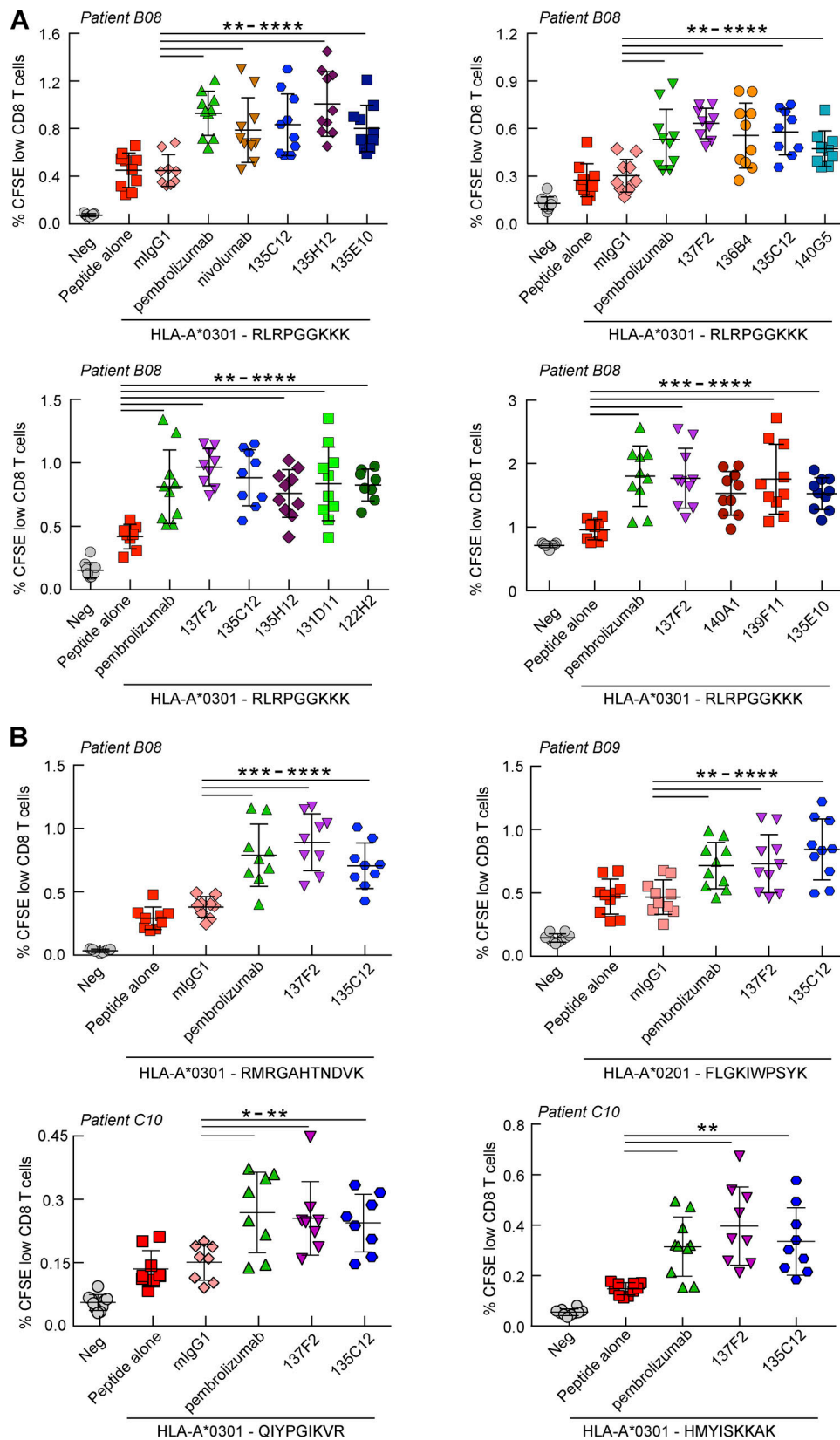
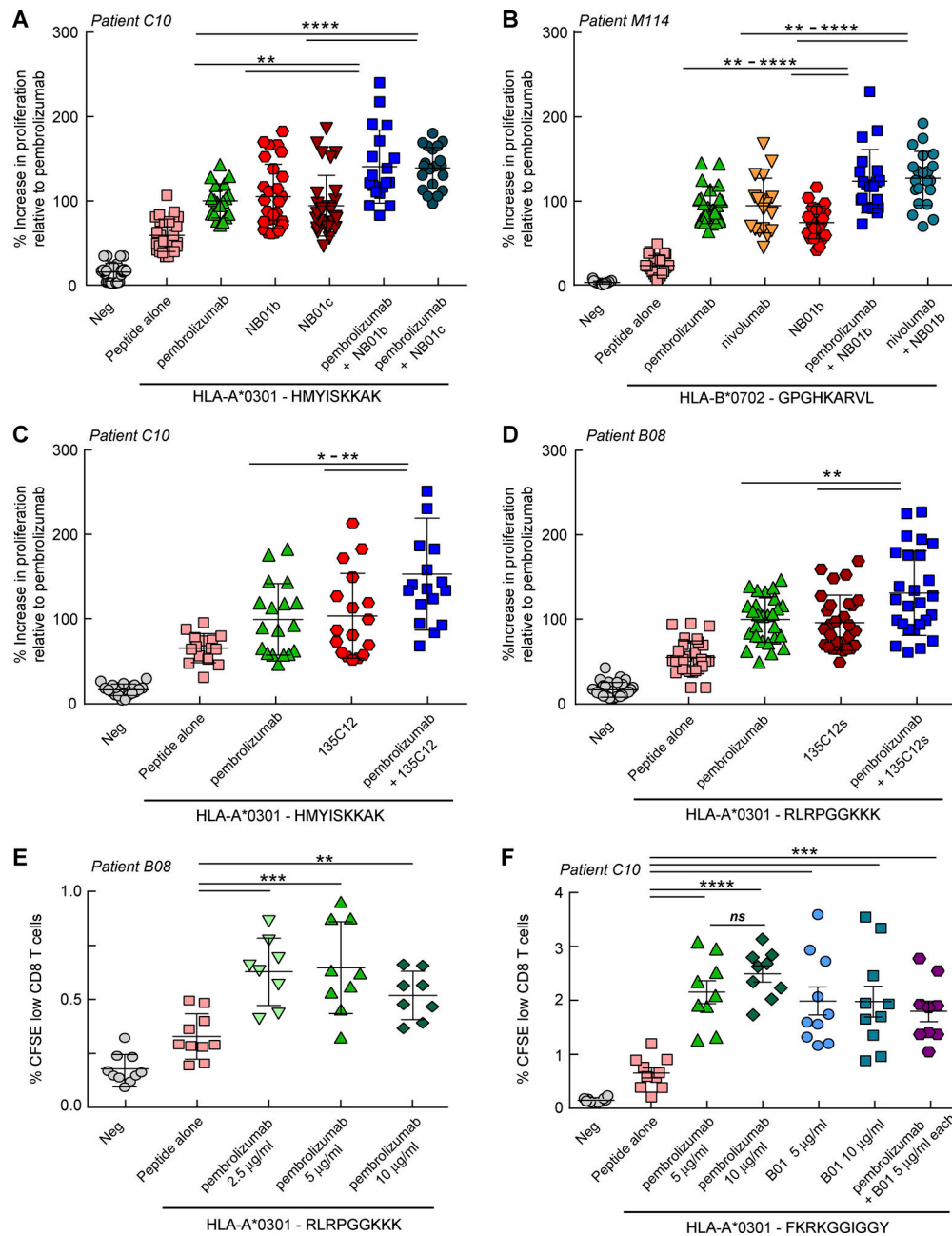


Figure S1. **Enhancement of proliferation of Ag-specific exhausted CD8 T cells by a panel of prioritized anti-PD-1 Abs.** (A) Effects of the prioritized set of anti-PD-1 Abs on the recovery of the proliferation of HIV-specific CD8 T cells. Blood mononuclear cells from an HIV-positive donor were labeled with CFSE and stimulated with the specific HIV-derived peptide in the presence or absence of an anti-PD-1 Ab for 6 d. (B) Select Abs were further analyzed using different HIV-derived peptides and in two different patients. Untreated samples (Neg) were used as a negative control in each experiment. Graphs show the mean  $\pm$  SD. \*\*,  $P < 0.0029$ ; \*\*\*,  $P < 0.0006$ ; \*\*\*\*,  $P < 0.0001$  (unpaired  $t$  test with Welch's correction).



**Figure S2. Blocking and nonblocking anti-PD-1 Abs combinations synergize in recovering the proliferation of exhausted Ag-specific CD8 T cells.** (A–D) Enhanced Ag-specific proliferation of CD8 T cells is observed in the in vitro CFSE functional exhaustion assay upon treatment with combinations of a blocking anti-PD-1 Ab (pembrolizumab or nivolumab) and a nonblocking anti-PD-1 Ab (NB01b or NB01c Abs in A, NB01b Ab in B, 135C15 mouse Ab in C, and a 135C12 mouse sibling Ab in D). The data shown are an average of two independent experiments and show a statistically significant increase in CD8 T cell proliferation. (E) Effect of different concentrations of anti-PD-1 Abs in the in vitro functional recovery CFSE assay shows maximum enhancement of CD8 T cell proliferation induced by pembrolizumab at 5 µg/ml, with no significant improvement at higher doses. (F) Lack of evidence of synergy using combinations comprising two blocking anti-PD-1 Abs (pembrolizumab + B01) used at 5 µg/ml each. ANOVA performed between the individual Abs and Ab combinations confirmed a statistical difference with the Ab combination therapy. Untreated samples (Neg) were used as a negative control in each experiment. Graphs show the mean ± SD. ns, not significant; \*, P < 0.02; \*\*, P < 0.0086; \*\*\*, P < 0.0006; \*\*\*\*, P < 0.0001 (unpaired *t* test with Welch’s correction).

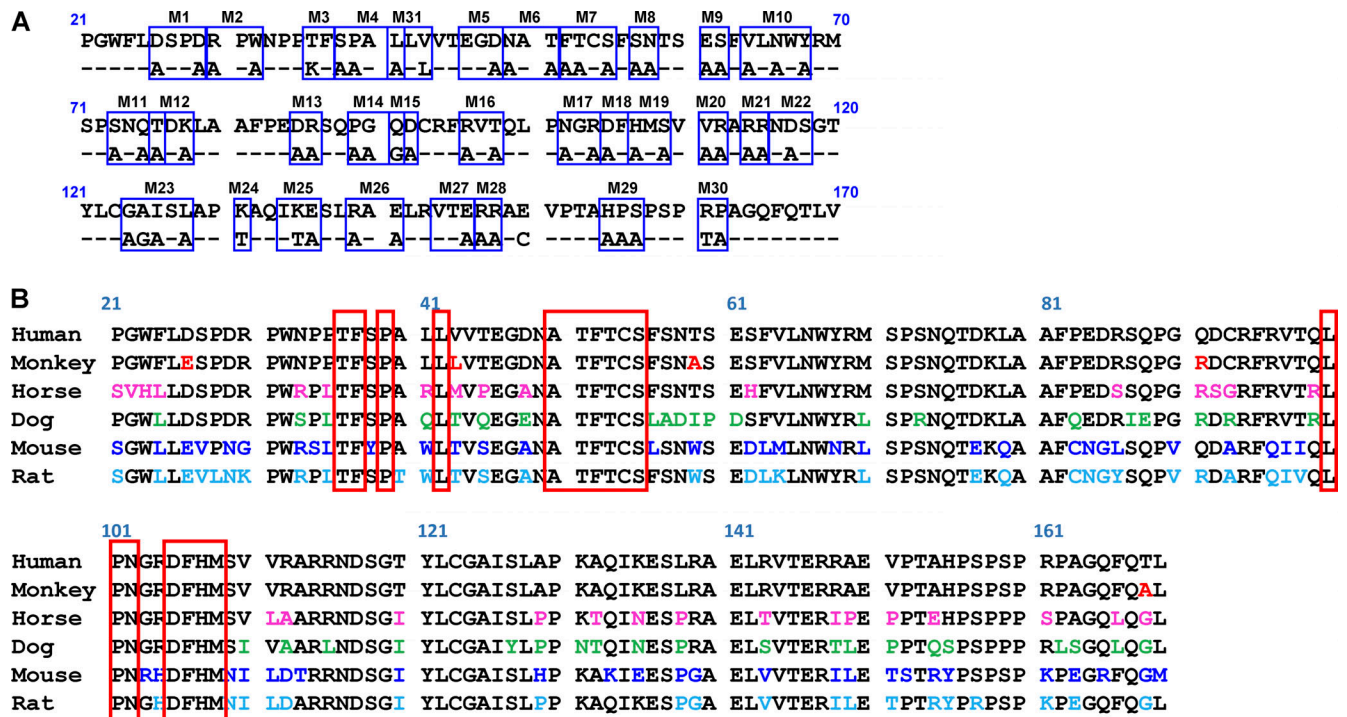


Figure S3. PD-1 sequence map of mutations used for Ab epitope mapping and sequence alignment of PD-1 from different species. (A) Site-directed mutagenesis studies performed with human PD-1 constructs with discrete amino acid substitutions at solvent-accessible residues of the ectodomain that were designed to map the binding of anti-PD-1 Abs to PD-1 expressed at the surface of transiently transfected HeLa cells. The M32 mutation was generated with substitutions L41A/V43T/S137A/L138A/R139T after observing a small reduction in binding of the 135C12 Ab to PD-1 expressed from the M26 and M31 vectors. (B) Amino acid sequence alignment of the ectodomains for human, monkey, dog, horse, mouse, and rat PD-1 proteins. The different species are 96.6% (monkey), 72.5% (dog), 79.2% (horse), 61.7% (mouse), and 66.4% (rat) identical compared with human PD-1. Residues outlined in red boxes come together at the surface of PD-1 to form the P1 conserved patch that partially overlaps with the binding epitopes for 135C12/NB01 and 136B4 Abs. These Abs were demonstrated to bind monkey PD-1, but no specific binding could be detected with cell-surface mouse PD-1, indicating that residues outside the P1 patch are also important for high-affinity binding.

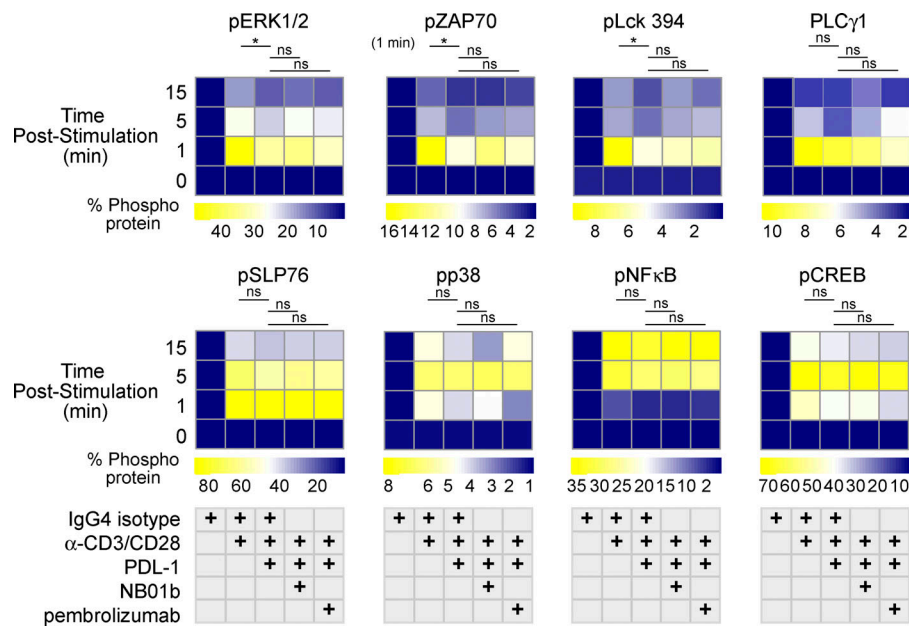


Figure S4. **PD-1-PDL-1-mediated suppression in phosphosignaling following stimulation of exhausted T cells.** Heatmap of mean phosphorylation levels in CD45RA<sup>-</sup> memory T cells treated with (1) IgG4 isotype control Ab, (2) IgG4 control + anti-CD3/CD28 Abs, (3) anti-CD3/CD28 Abs + PDL-1 Fc fusion protein, (4) anti-CD3/CD28 Abs + PDL-1 Fc fusion protein + NB01b, and (5) anti-CD3/CD28 Abs + PDL-1 Fc fusion protein + pembrolizumab. Significant suppression of T cell signaling mediated through PDL-1 was observed for AKT pT308, AKT pS473, PDK1 pS421, and ERK1/2 pT202/pY204 at the 5- to 15-min time points. ZAP70 pY319 and Src pY418/Lck pY394 showed significant PDL-1-mediated suppression only at the 1-min time point after stimulation. Additional phosphoproteins at different time points showed trends toward PDL-1 mediated suppression or anti-PD-1-mediated relief of exhaustion. However, these failed to meet statistical significance in our studies ( $n = 4-8$  experiments for the different phosphoproteins). False discovery rate-corrected Student's  $t$  tests were used to evaluate the statistical difference between the treatment conditions. ns, not significant; \*,  $P < 0.05$  for the indicated comparisons.

Table S1. X-ray data statistics for the hPD-1-NB01a Fab complex

<b>hPD-1-Fab A35774 complex</b>	
X-ray source	Beamline ID29, ESRF (Grenoble, France)
Detector	Pilatus 6M (Dectris)
Wavelength (Å)	0.97625
Space group	$P 1 2_1 2$
Cell dimensions (Å)	$A = 64.5, b = 63, c = 68.3$ $\alpha, \gamma = 90, \beta = 106^\circ$
Resolution range (Å)	65.49–2.20 (2.27–2.20)
Number of unique reflections	26,237 (2,621)
$R_{\text{merge}}$ (%)	6.96 (52.0)
$R_{\text{meas}}$ (%)	8.54 (64.5)
Average $I/\sigma(I)$	10.77 (2.16)
Completeness (%)	97.59 (98.28)
Multiplicity	2.9 (2.7)
CC (1/2)	0.997 (0.711)
Wilson B-factor (truncate; Å <sup>2</sup> )	33.88
Solvent content (%)	40.39
Number of reflections used in refinement	26,236 (2,621)
Number of reflections used for $R_{\text{free}}$	1,265 (143)
$R_{\text{work}}$ (%)	21.48 (28.57)
$R_{\text{free}}$ (%)	26.97 (37.04)
Rms bond length (Å)	0.002
Rms bond angle (°)	0.49
Ramachandran favored (%)	96.86
Ramachandran allowed (%)	2.73
Ramachandran outliers (%)	0.42
Clash score	2.97

CC, Pearson's correlation coefficient; Rms, root mean square.



## INVITED REVIEW

# T-cell exhaustion in HIV infection

Craig Fenwick<sup>1</sup> | Victor Joo<sup>1</sup> | Patricia Jacquier<sup>1</sup> | Alessandra Noto<sup>1</sup> |  
Riddhima Banga<sup>1</sup> | Matthieu Perreau<sup>1</sup> | Giuseppe Pantaleo<sup>1,2</sup> 

<sup>1</sup>Service of Immunology and Allergy,  
Department of Medicine, Lausanne  
University Hospital, University of Lausanne,  
Lausanne, Switzerland

<sup>2</sup>Swiss Vaccine Research Institute, Lausanne  
University Hospital, University of Lausanne,  
Lausanne, Switzerland

**Correspondence**

Giuseppe Pantaleo, Swiss Vaccine Research  
Institute, Lausanne University Hospital,  
University of Lausanne, Lausanne,  
Switzerland.  
Email: giuseppe.pantaleo@chuv.ch

**Funding information**

the Swiss Vaccine Research Institute,  
Grant/Award Number: N/A; the Swiss  
National Fund, Grant/Award Number:  
310030\_179246

**Abstract**

The T-cell response is central in the adaptive immune-mediated elimination of pathogen-infected and/or cancer cells. This activated T-cell response can inflict an overwhelming degree of damage to the targeted cells, which in most instances leads to the control and elimination of foreign invaders. However, in conditions of chronic infection, persistent exposure of T cells to high levels of antigen results in a severe T-cell dysfunctional state called exhaustion. T-cell exhaustion leads to a suboptimal immune-mediated control of multiple viral infections including the human immunodeficiency virus (HIV). In this review, we will discuss the role of T-cell exhaustion in HIV disease progression, the long-term defect of T-cell function even in aviremic patients on antiretroviral therapy (ART), the role of exhaustion-specific markers in maintaining a reservoir of latently infected cells, and exploiting these markers in HIV cure strategies.

**KEYWORDS**

chronic viral infection, HIV, immune checkpoint inhibitors, PD-1, T-cell exhaustion

## 1 | GENERAL INTRODUCTION ON T-CELL EXHAUSTION

The T-cell activation paradigm proceeds in a highly organized process involving three signals consisting of antigen recognition, receptor costimulation, and a termination signal that are required for the tight regulation of a strong functional and proliferative response.

Signal one in T-cell activation represents the specific recognition through the T-cell receptor (TCR) of their cognate antigen presented by professional antigen-presenting cells (APCs) including dendritic cells, macrophages, and B cells.

Signal two is the costimulatory signal where receptors on the T cells bind to their counterpart ligands. CD28 is the primary costimulatory receptor for T cells that acts through interaction with its ligands, CD80 and CD86 expressed on APCs. Costimulation is essential for T-cell activation since signal one TCR/antigen recognition in the absence of signal two drives the cell toward an anergic

and/or tolerogenic state.<sup>1</sup> Additional costimulatory receptors that can enhance T-cell activation include CD27, OX40 (CD134), ICOS (CD278), CD40L (CD154), CD226 that bind to CD70, OX40L (CD252), B7-H2 (CD275), CD40, and CD155/CD112, respectively, on APCs.<sup>2</sup> The concentration of costimulatory and ligand molecules can vary significantly such that either no positive signal is sent or a paired interaction provides a strong supporting signal two to the T cells. Soluble pro-inflammatory cytokines including IL-12 and type I interferons contribute to a fully activated T-cell response.

Signal three arises in the days following T-cell activation, the effector phase of the immune response, and eventually the elimination of the pathogen. Signal three is responsible for terminating the immune response. Inhibitory receptors, also called immune checkpoint inhibitors (ICIs), exert their influence on T-cell activation at this stage where under normal conditions, ICIs including programmed cell death receptor 1 (PD-1), cytotoxic T lymphocyte antigen-4 (CTLA-4), LAG3 (lymphocyte activation gene protein), and TIM3 (T-cell immunoglobulin domain and mucin domain-containing protein 3) are transiently

This article is part of a series of reviews covering Tolerance and Exhaustion in Peripheral T and B cells appearing in Volume 292 of *Immunological Reviews*.

This is an open access article under the terms of the Creative Commons Attribution License, which permits use, distribution and reproduction in any medium, provided the original work is properly cited.

© 2019 The Authors. *Immunological Reviews* published by John Wiley & Sons Ltd

upregulated on the surface of effector T cells within hours to days following T-cell activation. Here, their purpose is to attenuate T-cell activation and limit immune function at the end stages of an acute infection when a pathogen is controlled. Upon clearance of antigen, the expression of these ICIs on memory T cells declines to normal levels over time. Termination of the T-cell response is an essential self-limiting mechanisms to help preserve self-tolerance. However, in the case of chronic infection or cancer when the immune response is incapable of clearing the foreign antigen and there persistent chronic stimulation, T cells can enter a dysfunctional state called exhaustion.

T-cell exhaustion is a progressive condition with increasing loss in effector function coinciding with increased expression levels and assortment of ICIs. PD-1 is recognized as the master inhibitory regulator of T-cell function but with increased degrees of exhaustion comes elevated levels of additional ICIs including CTLA-4, TIM3, LAG3, T-cell immunoreceptor with Ig and ITIM domains (TIGIT), 2B4 (CD244), and CD160<sup>3,4</sup> (Figure 1). T-cell exhaustion mediated through PD-1 relies on interaction with its cognate ligands, PDL-1 and PD-L2, which regulate the delicate balance between immune defense and the protection of healthy tissue. Immune cells, non-immune endothelial, and epithelial cells constitutively express PDL-1, while PDL-2 expression is limited to APCs. The expression of PDL-1 is further upregulated after activation, which modulates the immune responses against self and foreign antigens.<sup>5</sup> In a likewise fashion, the interaction of additional ICIs with their respective ligands exert a further level of control and suppression of T-cell function.

## 2 | FUNCTIONAL PROFILE

In exhausted CD8 T cells, the increased expression of ICIs leads to a hierarchical loss of function that begins with reduced IL-2 secretion, cytokine polyfunctionality, and diminished proliferative

potential. Functional defects progress to the loss in cytotoxic capacity and TNF- $\alpha$  secretion with highly exhausted cells having reduced ability to produce IFN- $\gamma$ .<sup>6-8</sup> Although T-cell exhaustion was first identified in CD8 T cells, it is now accepted that CD4 T cells are also subject to exhaustion leading to reduced production of IL-2, IFN- $\gamma$ , and TNF- $\alpha$ <sup>9-11</sup> along with reduced CD4 T-cell help.<sup>12</sup> In addition to persistent antigen and pathogen burden, the loss or reduction of CD4 T-cell help is an important factor that contributes to the initial establishment of exhaustion.<sup>13-15</sup> The precise nature of optimal CD4 T-cell help needed to antagonize exhaustion is unclear, but is likely to involve the production of IL-2 and IL-21 cytokines that support CD8 T-cell response both directly and indirectly through activation of APCs.<sup>16</sup>

Aside from a blunted immune response against infected or cancerous cells, exhausted T cells have a poor or varied response to homeostatic cytokines including IL-7 and IL-15 responsible for the maintenance of memory T cells. In the case of complete clearance of a viral pathogen or in adoptive transfer studies to antigen-free mice, exhausted T cells are poorly maintained through self-renewal.<sup>17-19</sup> Instead, persistence of exhausted T cells occurs through continual antigen signals that promotes proliferation.<sup>20</sup> Exhausted T cells can persist *in vivo* for years but in the final stages of exhaustion with high antigen stimulation, there is a loss of the virus or tumor-specific cells through apoptosis.<sup>7,21</sup> Further characteristics of T-cell exhaustion include altered transcription factor expression, metabolic profile and epigenetic modifications that are distinct from other memory T-cell subsets.

## 3 | TRANSCRIPTIONAL PROFILE

The transcriptional profile of exhausted CD4 and CD8 T cells are significantly different from all memory T-cell subsets. Although several transcriptional factors are correlated with exhausted T

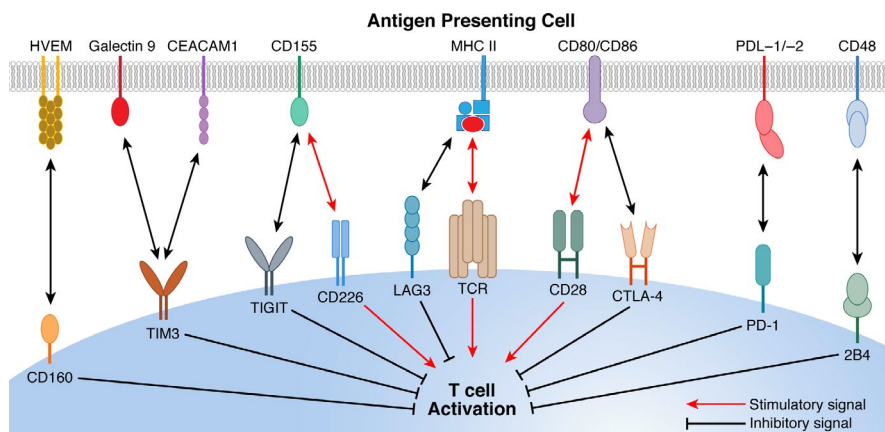


**FIGURE 1** T-cell immune checkpoint inhibitors and related ligands. TCR interaction with the antigenic peptide-MHC complex displayed by professional APCs delivers the primary signal for T-cell activation. The CD28 co-receptor and other costimulatory receptors enhance the T-cell stimulatory signal following interaction with their corresponding ligands. Immune checkpoint inhibitors including PD-1, CTLA-4, LAG3, TIGIT, TIM3, CD160, and 2B4 act to suppress T-cell signal following interaction with their related ligands expressed on APCs

cells including NFAT, Batf, IRF-4, T-bet, Eomes, and Blimp-1, no master regulator of exhaustion has been identified. NFAT activation during chronic infection along with a corresponding low nuclear translocation of AP-1 induces strong transcriptional activation of ICIs including PD-1, LAG3, and Tim3.<sup>22-25</sup> Signaling through the PD-1 receptor induces the upregulation of the Batf transcription factor, which in turn inhibits AP-1 activation and contributes to the sustained high levels of PD-1. Indeed, exhausted CD8 T cells from chronically infected HIV donors have elevated levels of Batf with higher levels observed in patients that experience disease progression compared to those that spontaneously controlled their HIV viral loads.<sup>24</sup> In the chronic lymphocytic choriomeningitis virus (LCMV) mouse infection model, IRF-4 contributes to T-cell exhaustion in consort with Batf and NFAT and reduction of IRF-4 expression restores the functional properties of exhausted antigen-specific T cells.<sup>26</sup> T-bet and Eomes transcription factors are individually important for the development of KLRG-1+ terminal effector CD8 T cells in response to inflammation and the maintenance of memory cells, respectively. In contrast, both are essential for the development of exhaustion as demonstrated in studies involving the genetic deletion of either<sup>20</sup> and both are upregulated in exhausted T cells with different viral infections.<sup>27</sup> Although necessary for exhaustion, high levels of the T-bet directly repress the transcription of the PD-1 gene. It is therefore interesting that in combined expression with Eomes, the T-bet<sup>high</sup> Eomes<sup>dim</sup> population represent an intermediate exhausted subset with progenitor capacity and a sustained virus-specific CD8 T-cell response during chronic infection.<sup>28,29</sup> In HIV-infected donors, exhausted T cells with a skewed balance toward T-bet<sup>dim</sup> Eomes<sup>high</sup> expression profile represent a highly functionally exhausted state with elevated levels of multiple ICIs including PD-1, CD160, and 2B4 on CD8 T cells.<sup>30-32</sup> Blimp-1 is a primary transcription factor for the differentiation of germinal center B cells; however, it is also upregulated in exhausted T cells and correlates with the protein expression levels of ICIs. Similar to Batf, Blimp-1 is upregulated in progressor patients with chronic HIV infection compared to non-progressors that control HIV viral loads.<sup>33</sup> Blimp-1 expression in CD4 T cells mediates the production of IL-10, which can further contribute to the dysfunctional state of exhausted T cells during chronic viral infection.<sup>34</sup> Exhausted T cells may coexpression pairs of transcription factors including Blimp-1 and Eomes, however, expression is not uniform where combinations of different factors may coexist. Therefore, along with the phenotypic and functional profiles, exhausted T cells consist of a heterogeneous population with varied expression of transcription factors.<sup>12,22,35</sup> This diversity of exhausted T-cell populations is exemplified in a recent study using high dimensional mass cytometry to analyze cells from chronic HIV-infected donors and in human tumors. Using phenotypic, functional, transcription factor, and ICI coexpression patterns, nine distinct exhausted CD8 T-clustered cell populations were identified.<sup>36</sup>

## 4 | METABOLIC ABNORMALITIES AND EXHAUSTION

The metabolic profile of T cells shifts from the use of the oxidative phosphorylation pathway in naive cells to glycolysis in the acute phase of an infection when activated effector cells have increased bioenergetics needs. Once the infection is cleared, memory cells revert to a quiescent state that uses oxidative phosphorylation and gains the additional metabolic ability for fatty acid oxidation.<sup>37</sup> With chronic antigen stimulation and the onset of exhaustion, the suppression of the glycolysis pathway ensues with reduced cellular glucose uptake and signs of a dysregulated mitochondrial function.<sup>38</sup> The utilization of endogenous fatty acids by exhausted cells may dictate the available energy reserves under conditions of ICIs engagement.<sup>39</sup> Metabolic pathways implicated in this defective state include transcriptions control through Foxo1<sup>40</sup> and PGC1 $\alpha$ .<sup>41</sup>

## 5 | EPIGENETICS AND EXHAUSTION

Epigenetic modifications associated with T-cell exhaustion begins within the first 2-3 weeks of chronic LCMV infection. This programming is irreversible, even in adoptively transferred studies with uninfected antigen-free mice where T cells maintain their exhausted transcriptional and functional profile.<sup>12,27,42</sup> The epigenetic landscape of exhaustion has been studied by comparing CD8 T cells during acute and chronic phases of LCMV infection. Changes consisted in large reorganizations of chromatin-accessible regions resulting in altered access to transcriptional start sites. These modifications were associated with the induction of multiple genes including Pdc1 (PD-1), Havcr2 (Tim3), and Batf which are known to be upregulated in exhausted CD8 T cells. The epigenetic modifications in Pdc1 include histone acetylation in the promoter and proximal enhancer region followed by full demethylation in these regions that is maintained in exhausted cells and allows for consistent high PD-1 expression. These epigenetic changes are also present in several chronic viral infections including HIV, CMV, and EBV.<sup>43</sup> Indeed, the vast majority of this epigenetic program linked to exhaustion in mice (approximately 80%) was also successfully mapped to tetramer positive CD8 T cells of treatment naive chronically infected HIV donors.<sup>44-46</sup> As such, epigenetic modifications play a key role in maintaining T cells in an exhausted state.

## 6 | T-CELL EXHAUSTION IN HIV INFECTION (CAUSES OF EXHAUSTION, PHENOTYPIC MARKERS OF EXHAUSTION, AND FUNCTIONAL EXHAUSTION)

T-cell exhaustion was first described in mouse models with chronic LCMV infection where antigen-specific CD8 T cells progressively lost their effector functions and developed a reduced capacity to kill virally

infected cells.<sup>47-50</sup> Subsequent to these studies, it became clear that the same principles of T-cell exhaustion occurred in human chronic viral infections including HIV, HCV, HBV, and HTLV-1 as well as cancer.

Chronic HIV infection occurs in most patients in the presence of persistent high levels of virus replication and is associated with a loss of immune control of virus replication. Virus-specific CD8 T cells partially suppress HIV viral replication in the initial stages of infection. In a similar manner, SIV-infected macaque studies showed that CD8 T-cell depletion leads to a dramatic increase in viral load.<sup>51</sup> However, with persistent high levels of viral antigen, HIV-specific T cells become exhausted and lose their capacity to kill efficiently infected cells. In addition to high levels of viral antigen, the strong pro-inflammatory immune activation during HIV infection and a compromised T-cell homeostasis during HIV infection contribute to the development of T-cell exhaustion.<sup>52,53</sup>

In HIV-1 infection, PD-1 expression on virus-specific T cells is the primary marker of exhaustion that correlates with disease progression. Pivotal studies showed that PD-1 expression correlated with impairment of CD8 T cells functionality, viral load, and reduced the CD4 T-cell counts.<sup>54-56</sup> Importantly, cytomegalovirus-specific CD8 T cells from the same HIV-infected donors did not upregulate PD-1 and preserved the functional capacity to produce high levels of cytokines. This demonstrated that the T-cell defects were HIV-specific and driven primarily by the high level of antigen that induced exhaustion. Longitudinal studies show that following ART initiation, PD-1 expression levels gradually decrease on HIV-specific CD8 T cells. Long-term non-progressors (LTNPs) or viremic controllers were also evaluated and show lower levels of PD-1 expression on HIV-specific T cells that exhibited a stronger effector functions as compared to progressors<sup>54,55</sup> (Figure 2). Aside from PD-1, other ICIs including LAG3, Tim3, TIGIT, 2B4, and CD160 expressed independently or combined lead to more

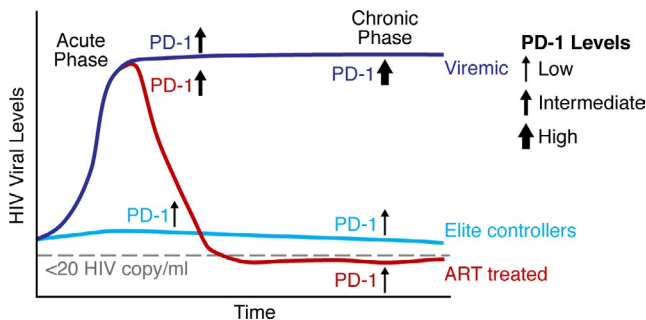


**FIGURE 2** HIV Infection and progression of exhaustion. During the acute phase of HIV infection, the majority of individuals experience a dramatic increase in HIV viral load and increased levels of the PD-1 receptor on HIV-specific T cells. In contrast, elite controllers maintain low viral load levels and consequently, T cells express low levels of PD-1. Untreated patients with high viral load progress to the chronic phase of HIV infection where persistent elevated levels of HIV antigen result in T-cell exhaustion with high expression levels of PD-1. ART in most patients significantly inhibits viral replication, resulting in decreased plasma viral load to levels below the limit of detection with standard assays. With low levels of viral antigen present, PD-1 expression decreases to lower levels on HIV-specific T cells

pronounced stages of CD8 T-cell exhaustion.<sup>54,57-62</sup> Coexpression of PD-1 with TIGIT was shown to correlate with disease progression in both HIV-infected patients and SIV infection model.<sup>58</sup> PD-1 and LAG3 expression either alone or in combination with CD38 expression also correlates with the with plasma viral load of patients and was predictive of the time to disease progression.<sup>63</sup> Similarly, simultaneous expression of PD-1, CD160, 2B4, and LAG3 on CD8 T-cell populations correlated directly with HIV load and inversely with the multiplicity of functional outputs exhibited by HIV-specific CD8 T cells<sup>64</sup> (Figure 3).

The progressive loss of CD8 T-cell function starts with an initial loss of proliferative capacity, cytotoxic potential, and a restricted IL-2 production. In more pronounced stages of exhaustion associated with chronic exposure of T cells to viral antigen, T cells eventually lose the ability to produce IFN- $\gamma$ .<sup>55,56,65,66</sup> HIV-specific CD8 T cells with elevated levels of PD-1 also show greater susceptible to apoptosis that was attributed to lower levels of the pro-survival Bcl-2 and higher levels of CD95/Fas surface receptor compared to the PD-1 low T cells.<sup>67</sup>

The focus of T-cell exhaustion is often on the loss of CD8 T cells function that is primarily responsible for the killing infected cells. However, CD4 helper T cells also exhibit functional defects during HIV infection. Exhausted CD4 T cells exhibit a reduced HIV-specific proliferative capacity and a loss in polyfunctional cytokine response that centers on reduced IL-2 production.<sup>68,69</sup> Exhausted virus-specific CD4 T cells also express PD-1 with elevated levels correlating with disease progression, viral loads and reduced CD4 T-cell count.<sup>70</sup> As such, PD-1 is a common regulator of exhaustion on HIV-specific CD4 and CD8 T cells. In contrast, the CTLA-4 ICI is more selectively upregulated on exhausted CD4 T cells that correlates with disease progression and T-cell dysfunction.<sup>71</sup> Conversely, the ICIs 2B4 and CD160 that are characteristically upregulated on exhausted CD8 T cells are virtually absent from exhausted CD4 T cells.<sup>72</sup> As with CD8 T cells, expression of multiple ICIs including PD-1, CTLA-4, and TIM3 is associated with a more pronounced state of functional CD4 T-cell exhaustion.<sup>73</sup> A characteristic feature of CD4 and CD8 exhausted T cells is both experience at least partial restoration of antigen-specific proliferative and functional activity following antibody-mediated ICI blockade therapy.

Aside from increased levels of ICIs during HIV infection, an activated T-cell phenotype with upregulated levels of CD38 on CD8 and CD4 T cells is a well-established predictive marker for disease progression.<sup>74</sup> Additional activation markers upregulated during HIV infection include CD38/HLA-DR coexpression on CD8 T cells and signs of ongoing replication as determined by Ki-67+ T cells.<sup>75</sup> T cells also exhibit impaired T-cell maturation characterized by reduced expression of CD28 and high levels of CD27 costimulatory molecules, suggesting a decreased effector phenotype.<sup>76</sup> Decreased levels of CD28 on HIV-specific CD8 T cells are associated with shorter telomere lengths and reduced proliferation.<sup>77</sup> HIV-specific CD8 T cells with elevated levels of CD27 also have reduced Granzyme A and perforin cytotoxic activity compared to CD27 low effector T cells.<sup>78</sup> Moreover, HIV-specific memory CD8 T cells were also found to have a preterminally differentiated phenotype (CD45RA-CCR7-), when compared to CMV-specific cells that instead expressed a terminally differentiated (CD45RA + CCR7-) phenotype.<sup>79,80</sup>

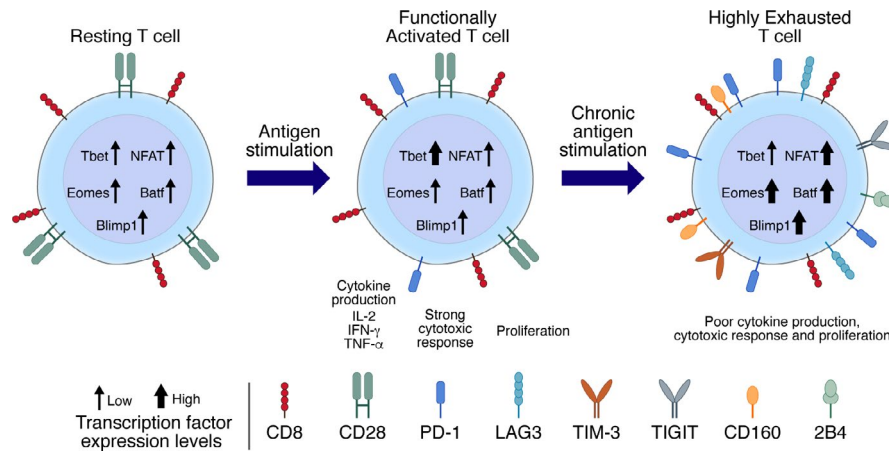


**FIGURE 3** Phenotype, transcriptional, and functional profile of T cells progressing to exhaustion. Antigen-specific stimulation of resting T cells leads to a functionally active T-cell response with increased cell surface PD-1, upregulated expression of the T-bet transcription factor and a strong functional and proliferative response. Chronic stimulation with high levels of antigen drive T cells into an exhausted state characterized by high levels of PD-1, an increased expression of additional immune checkpoint inhibitors and a pronounced T-cell dysfunction. Compared to functionally active T cells, highly exhausted T cells have elevated expression of transcription factors including NFAT, Batf, Eomes, and Blimp-1 with decreased levels of T-bet

Cytokines including IL-10 are also implicated in T-cell exhaustion during HIV infection. IL-10 production is part of the body's response to chronic inflammation established primarily through strong upregulation of the type I and II IFN-related genes and pathways. Tregs accumulate at the sites of chronic HIV infection and play a direct role in the promotion of T-cell exhaustion through production of IL-10 that inhibits T-cell proliferation.<sup>81</sup> Aside from Tregs, multiple cell types contribute to IL-10 production and patients with elevated plasma levels of IL-10 correlate with rapid disease progression and impaired CD4 T-cell help. In vitro blockade of IL-10 increases proliferation of HIV-specific CD4 and CD8 T cells and increases production of cytokines by CD4 T cells.<sup>82,83</sup>

Overall, HIV-specific T-cell exhaustion established in the early stages of infection represents an almost insurmountable barrier to the immune mediate control of viral load and the elimination of HIV-infected cells. Individuals who can spontaneously control HIV infection are rare, representing  $\leq 1\%$  of those infected.<sup>84</sup> However, a recent longitudinal study provides evidence that T-cell exhaustion plays an important role in the loss of viral control by these rare HIV controllers. These studies showed that just prior to increases in patient viremia, PD-1 levels increased on HIV-specific CD8 T cells and these cells exhibited reduced in vitro capacity to kill HIV-infected cells.<sup>85</sup> As such, a delicate balance may exist between T-cell-mediated control of viral infection and the progressive development of T-cell exhaustion.

## 7 | T-CELL EXHAUSTION IN OTHER VIRAL INFECTIONS

Pathogens have evolved through natural selection to evade immune-mediated elimination by exploiting the IC pathways needed by the host to maintain peripheral tolerance and limits immunopathology

under physiologic conditions. A key advantage in the discovering T-cell exhaustion using the LCMV mouse infection model was the different viral laboratory strains and/or different viral inoculum that induce either an acute infection that could be resolved or a persistent chronic infection.<sup>47-49</sup> Although CD8 T-cell dysfunction was known to be an essential feature of exhaustion, the identification of PD-1 as a key player during chronic infection was revealed much later through gene expression analysis. These studies showed that in the early stage of infection, PD-1 was upregulated to similar levels in mice infected with either Armstrong (acute) or clone 13 (chronic) LCMV viruses. Clearance of Armstrong strain lead to a rapid downregulation of PD-1 on virus-specific CD8 T cells. However, in chronic clone 13 strain LCMV infection, virus-specific CD8 T cells showed sustained increase PD-1 levels that progressively lost their functionality. In this model, transient depletion of CD4 T cells has no effect on an acute viral strain that can be resolved within 2 weeks. However, in studies using a chronic LCMV variants that requires >3 months to be contained and cleared by the LCMV-specific CD8 T-cell response, even transient depletion of CD4 T cells at the time of infection resulted in a complete loss of CD8 T-cell response to control the virus.<sup>14</sup> These studies provide support for the concept that loss of CD4 T-cell help can enhance conditions that lead to CD8 T-cell exhaustion. An important concept validated in the LCMV model was that antibody-mediated blockade of the PD-1/PDL-1 interaction reversed signature featured of T-cell exhaustion that allowed for proliferation and increased functionality of LCMV-specific T cells that lead to the killing of infected cells and decrease viral load.

Human cases of viral hepatitis have common features with LCMV infection where virus is either cleared by the immune system or leads to chronic infection in 10% and 70% of HBV- and HCV-infected patients, respectively. The important role of virus-specific CD8 T cells was demonstrated in non-human primate models for

HBV and HCV infection where depletion of CD8 cells lead to a prolonged viremia that only declined when CD8 T cells returned.<sup>86,87</sup> The two primary mechanism for chronic hepatitis infection in patients is viral mutation that leads to escape from antiviral CD8 T cells and through exhaustion where CD8 T cells lose their effector function. A strong and early CD4 T-cell helper response in HCV infection is also associated with viral clearance in patients. In contrast, development of HCV-specific CD4 T cells with limited proliferative potential at an early stage following infection resulted in the evolution of a chronic infection.<sup>88</sup> Studies performed with blood mononuclear cells from chronically infected HBV patients showed that blockade of the PD-1 pathway resulted in enhanced proliferation and functionality of HBV-specific CD8+ T cells.<sup>10,89</sup> Furthermore, a HBV-related chronic hepadnaviral infection model in woodchucks showed that PD-1 blockade in combination with an antiviral agent and therapeutic DNA vaccination restored virus-specific CD8+ T cells functionality and enhanced a continual immune-mediated viral control.<sup>90</sup> PD-1 blockade alone had a moderate therapeutic result in patients with chronic HCV infection where 20% of those treated showed a significant drop in viral load.<sup>91</sup> However, this result may be due to the nature of exhaustion associated with HCV since *in vitro* studies showed that hepatic PD-1 + CTLA-4 + virus-specific CD8 + T cells where only functionally restored with a combination of CTLA-4 and PD-1 blockade and not with either therapy administered alone.<sup>92</sup>

Human T-cell lymphotropic/leukemia virus type 1 (HTLV-1) causes adult T-cell leukemia/lymphoma and in both asymptomatic carriers and ATL patients there is an inverse correlation between HTLV proviral load and the functionality of CD8 T cells in response to viral antigens. Decreased functionality correlated directly with PD-1 levels expressed on CD8 T cells and blockade through PDL-1 significantly increased anti-HTLV functionality. Of note, CD8 T-cell functionality and levels of HTLV-1 provirus did not correlate with expression levels of TIM3, LAG3, or CTLA-4, indicating that different chronic viral infections or the extent of exhaustion may favor the upregulation of different ICI subsets.<sup>93,94</sup>

## 8 | MAJOR SIGNALING PATHWAYS INVOLVED IN T-CELL EXHAUSTION

T-cell activation takes place in a highly organized process where the antigenic peptide-MHC complex on APCs binds to its cognate T-cell TCR complex forming the core of the cell-cell interaction. This primary contact sets into motion the reorganization of cell surface and cytosolic molecules leading to the formation of the immunological synapse. It is during this contact with the APC that ICIs exert their inhibitory effect to suppress signaling events needed for a fully activated T-cell response.

Following immunological synapse formation, Lck phosphorylation of TCR-associated CD3  $\zeta$ -chains initiates the intracellular signaling cascades with ZAP-70 propagating the TCR signal through phosphorylation of downstream intermediaries including

PLC- $\gamma$ 1.<sup>95,96</sup> T-cell costimulation through CD28 is needed for robust, functional T-cell response and acts through phosphatidylinositol 3-kinase (PI3K) to activate the PI3K/AKT/mTOR signaling network. Both the TCR and CD28 costimulatory pathways converge to up-regulate the activation of AP1, NFAT, and NF $\kappa$ B, which induce the transcription of T-cell immune response genes such as IL-2, IRF-4, and pro-survival factors.<sup>97</sup> The strength, affinity, and duration of the initial TCR-peptide-MHC complex as well as the presence of costimulatory receptors dictate the level of response from the different signaling cascades and degree of their contributions on transcription factor activation.

ICIs exert their regulatory effect on T cells through a variety of mechanism. Several receptors including PD-1 have intracellular domains containing immunotyrosine inhibitory motif (ITIM) and/or immunotyrosine switch motif (ITSM). These ITIM or ITSM motifs can recruit SHP tyrosine phosphatase proteins and other adapter into the vicinity of the TCR in order to disrupt positive signaling events. ICIs that suppress T-cell activation through the ITIM/ITSM mechanism includes PD-1, 2B4, LAIR-1, and KLRG-1.<sup>98</sup> A second mechanism of T-cell regulation through inhibitors receptors is by direct competition with costimulatory receptors. CTLA-4 is the best studies example that can bind tightly to the CD80 and CD86 on APCs. In so doing, CTLA-4 outcompetes CD28 for interaction with its natural ligands and increases the T-cell activation threshold, especially for antigens that do not effectively induce T-cell activation.<sup>99</sup> ICIs including LAG3 and TIM3 have varied intracellular domains distinct from the classical ITIM/ITSM motifs and that recruit a different subset of molecules that are suppressive of T-cell signaling. Finally, negative regulation can occur via receptors including TIGIT and BTLA that operate through a combination of different mechanism. TIGIT not only possess an intracellular ITIM motif on its cytoplasmic tail but also acts through a receptor competition mechanism in binding the CD155 and CD112 ligands on APCs that can activate T cells through interaction with CD226.<sup>98</sup>

PD-1-mediated inhibition of T-cell signaling is the best-studied ICI pathway involved in T-cell exhaustion. During T-cell activation, the PD-1 receptor migrates into T-cell/APC contact region where it forms microclusters upon binding with PDL-1. This recruitment brings the SHP2 and SHP1 phosphatases into membrane proximal region of the TCR and costimulatory receptors, inducing dephosphorylation of TCR-linked signaling proteins CD3 $\zeta$ , ZAP-70, PLC- $\gamma$ 1,<sup>95,96</sup> and the CD28 pathway involving PI3K and the associated downstream cascade through the AKT pathway. The PD-1/SHP2 complex attenuates phosphorylation events associated with PKC $\theta$ , PI3K/AKT/mTOR, and Ras/MAPK/Erk signaling pathways needed for optimal T-cell activation, proliferation, survival, and an altered cellular metabolism.<sup>100,101</sup> The dynamics of PD-1 with CD28 and intracellular partners has been observed in fluorescence microscopy imaging studies where PD-1 exists in microclusters on the cell surface and is recruited along with SHP2 phosphatase into the immunological synapse to suppress phosphorylation events during TCR activation.<sup>3,95,96,102-104</sup> One caveat with many of these mechanistic studies is that PD-1 expression on T cells was achieved through

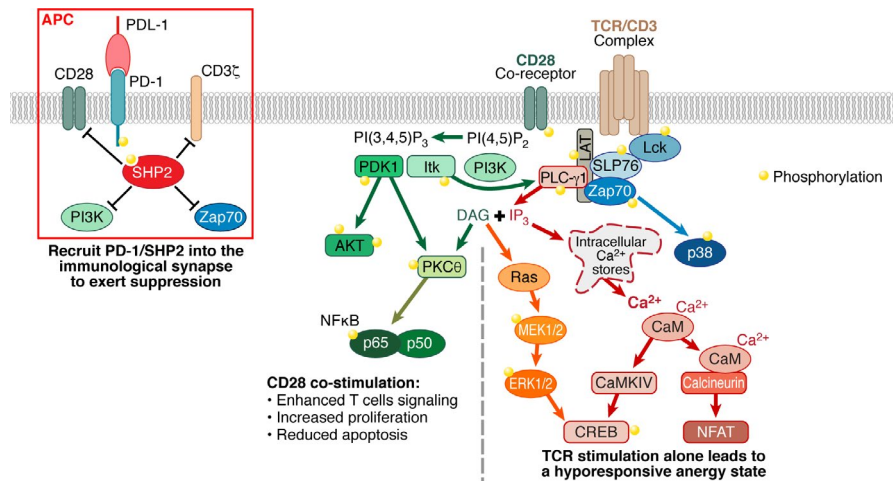


**FIGURE 4** Signaling in T-cell activation and PD-1-mediated suppression. T-cell activation through the TCR/CD3 complex leads to the phosphorylation of proximal signaling molecules that trigger downstream activation of NFAT, CREB, and p38 pathways. In the absence of a costimulatory signaling through CD28, TCR activation of T cells leads to a hyporesponsive, anergic state. Signaling through the CD28 costimulatory receptor enhances activation of the PI3K/AKT/NFκB pathways that support T-cell proliferation and reduce apoptosis. Interaction of PD-1 with PDL-1 during T-cell activation recruits the PD-1/SHP2 tyrosine phosphatase complex into the vicinity of TCR/CD3 and the CD28 co-receptor. This recruitment results in the dephosphorylation of membrane proximal PI3K, ZAP-70 and the intracellular domains of CD28 and the CD3ζ chain, which suppresses T-cell activation. In PD-1 high exhausted T cells from chronically infected HIV donors, the ligation of PD-1 with PDL-1 results in reduced phosphorylation of TCR proximal Lck and Zap-70 and downstream Erk1/2 in the Ras-MEK1/2-Erk1/2 pathway. PD-1 suppression of T-cell activation also results in reduced calcium mobilization that is upstream of CREB and NFAT transcription factors. In the CD28 costimulatory receptor pathway, ligation of PD-1 with PDL-1 significantly inhibits the PI3K/AKT/NFκB pathway with reduced phosphorylation of PDK1 and AKT

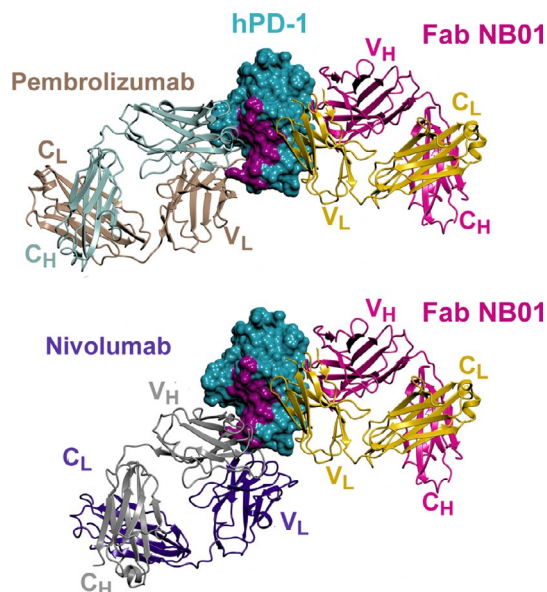


**FIGURE 5** Antagonistic antibodies binding the PD-1 receptor. The structure of human PD-1 (hPD-1) in complex with the anti-PD-1 NB01 Fab was solved by molecular replacement using crystals that diffracted to 2.2 Å resolution (6HIG). Molecular modeling by  $\alpha$  superpositioning of hPD-1 coordinates with the pembrolizumab (PDB 5GGS) and the nivolumab (PDB 5GGR) confirms that NB01 Fab binding to PD-1 does not interfere with the binding of either pembrolizumab or nivolumab anti-PD-1 Abs. The hPDL-1-binding surface (PDB 4ZQK) on hPD-1 is colored in purple and is distinct from the binding epitope of the NB01 Fab that is non-blocking of the PD-1/PDL-1 interaction

prolonged in vitro T-cell stimulation as opposed to exhausted T cells produced in vivo in response to chronic infection.

Our own laboratory recently reported a direct evaluation of signaling in truly exhausted T cells with elevated levels of PD-1 from a chronically infected HIV donor.<sup>105</sup> T-cell activation in concert with PD-1 ligation by PDL-1 suppressed signaling event in both the TCR and CD28 pathways. TCR proximal phosphorylation of the Lck and ZAP-70 was inhibited along with the downstream Ras-MEK1/2 pathway monitored through Erk1/2 phosphorylation. Calcium flux experiments using exhausted T cells also showed a reduced degree of calcium mobilization in stimulations performed in the presence of PDL-1, which leads to reduced activation of the NFAT pathway.<sup>106</sup> The suppression of the CD28 signaling pathway resulted in significantly reduced phosphorylation of PDK1 and its direct target, AKT, phosphorylated at position T308. Formation of the full catalytically activation AKT, phosphorylated at S473 by mTORC2, was also inhibited in the exhausted T cells (Figure 4).

An important validation of the signaling pathways involved in PD-1/PDL-1-mediated T-cell exhaustion is to monitor the restoration of specific phosphoprotein levels following anti-PD-1 therapy. In classical anti-PD-1 antibody therapy, relief of T-cell exhaustion is achieved through PD-1/PDL-1 blockade. However, we recently reported the discovery and validation of a novel class of antagonistic anti-PD-1 antibody that are non-blocking of the PD-1/PDL-1 interaction. Biochemical and structural studies demonstrated that these antibodies bound to the opposite face of the PD-1 protein relative to the PD-1/PDL-1 interaction site. The region on PD-1 targeted by these non-blocking antibodies is highly conserved across six different species and may potentially represent

a binding site for a yet to be identified alternate PD-1 ligand or a region important for transmitting the negative regulatory effect of PD-1. Structural modeling and competitive binding studies with cell surface PD-1 also showed that the non-blocking anti-PD-1 antibody NB01 could bind PD-1 concomitantly with either pembrolizumab or nivolumab blocking anti-PD-1 antibodies (Figure 5). Consistent with blocking and non-blocking antibodies both exerting distinct immune-enhancing functional activity through PD-1, treatment with combinations of the two antibody classes resulted in synergistic functional recovery of proliferation and IFN- $\gamma$  production from exhausted HIV-specific CD8 T cells. In signaling studies performed in the presence of PD-1/PDL-1 suppression, both blocking and non-blocking anti-PD-1 antibodies partially restored signaling phosphorylation of PDK1 and AKT at positions T308 and S473 in the CD28 pathway. These results are consistent with two recent studies showing that anti-PD-1-mediated tumor suppressive activity is primarily dependent of the CD28 costimulatory receptor.<sup>103,104</sup> Both classes of anti-PD-1 antibodies also restored calcium mobilization that is downstream of the TCR activation pathway (Figure 4).

Aside from the signaling relationship between PD-1 and the CD28 pathway, immunoprecipitation studies performed with the pembrolizumab blocking anti-PD-1 antibody further demonstrated that in stimulated T cells, PD-1 exists in a complex that includes CD28, SHP2, PI3K, and phosphorylated Lck Src protein. Importantly, our antagonistic non-blocking anti-PD-1 antibody pulled down PD-1 in complex with SHP2 and phosphorylated Lck Src, but showed significantly reduced interaction with CD28 and associated PI3K. This indicates that elevated levels of PD-1 on a T cell may suppress T-cell activation by two mechanism. One through PDL-1-mediated recruitment of PD-1 into the immunological synapse and other through a PD-1 cis-complex with the CD28 costimulatory receptor. The later colocalization would bring CD28-associated intracellular kinases essential for T-cell costimulation into contact with PD-1-associated SHP2 phosphatase, resulting in a direct inhibition of the CD28 costimulatory signaling (Figure 6).

The coexpression of additional ICIs with PD-1 in exhausted HIV-specific T cells reflects an increased level of T-cell dysfunction that is linked to the suppression of T-cell signaling. These ICs include TIM3, TIGIT, and Lag3 that acting on distinct or overlapping points of the signaling cascade relative to PD-1. TIM3 suppresses T-cell activation through Lck, Fyn, and PI3K<sup>107,108</sup> TIGIT recruits SHIP1 into the signaling complex which blocks further signal transduction to PI3K, MAPK pathways, and NF $\kappa$ B<sup>109</sup> and LAG3 is structurally similar to the CD4 co-receptor and acts through a poorly defined mechanism.<sup>110</sup> With their combined inhibitory effect, it is not surprising that T cells with elevated levels of these ICIs are almost completely functionally defective and incapable of mounting an effective immune response.

## 9 | RECOVERY OF T-CELL FUNCTION: EFFECT OF ART

Upon initiating ART, the majority of patient have a dramatic reduction of viral load and HIV-1 productively infected cells in both the

periphery and lymph nodes.<sup>111</sup> However, despite a spectacular efficacy in reducing morbidity and mortality associate with HIV infection, these drugs only inhibit viral replication and cannot cure those infected. ART maintains the level of plasma HIV-1 RNA below the limit of detection for most treated patients. However, long-lived latently infected memory CD4 T cells persist and the potential for residual virus replication prevent the eradication of infected cells.<sup>112</sup> Even after decades of viral suppression, interruption of ART in patients invariably leads to a rapid viral rebound. In this regard, the continued immune dysfunction, while on ART is evident by the inability of the virus-specific immune response to delay significantly the reemergence of the HIV virus. The major causes of this immune dysfunction in HIV are T-cell exhaustion that prevents a functional control of the virus and necessitates life-long ART in most infected patients to suppress viremia and prevent disease progression.

Patient under fully suppressive ART with undetectable HIV-1 plasma viral loads gradual experience a downregulation of immune ICI expression on T cells, although frequencies remain higher compared to HIV-uninfected individuals. A similar trend is observed CD38 + HLA-DR + T cells, which represent an increased immune activation state.<sup>113,114</sup> The functionality of HIV-specific T cells improves with ART treatment with both CD4 and CD8 T cells producing increased levels of IL-2 following stimulation.<sup>115,116</sup> However, PD-1, TIM3 and LAG3 expression on the T cells of ART-treated patients was shown to be associated with the time to viral rebound in studies following standardized treatment interruptions.<sup>117</sup> This demonstrates that the extent of T-cell exhaustion contributes an underlying immune dysfunction that is unable to control even the low levels of virus produced from the latent HIV reservoir in the absence of ART. Our own unpublished results confirm a persistent functional exhaustion of HIV-specific CD8 T cells in long-term suppressive ART patients where PD-1 blockade significantly restores IFN- $\gamma$  production by twofold. Similarly, combined blockade studies targeting TIGIT and PDL-1 restored the proliferative capacity of virus-specific CD8 T cells with enhanced proliferation compared to either single blockade.<sup>58</sup>

Early initiation of ART is clearly beneficial to patients on multiple levels. Early adoption of ART in the acute phase of viral infection correlates with a lower burden of latent HIV-1 reservoir and reduced systemic inflammation.<sup>118-122</sup> Since the development of T-cell exhaustion is a progressive condition with hierarchical loss of functionality, early ART initiation represents the best opportunity to preserve a patient's HIV-specific response before more pronounced and effectively irreversible T-cell dysfunction is established.

## 10 | INFLUENCE ON ICIS IN PERSISTENCE OF HIV

Multiple observational studies have demonstrated a clear association between expression of ICIs and the HIV reservoir. Amongst these, a pivotal study indicated that central memory CD4 T cells expressing PD-1 were enriched in HIV-infected cells, thus providing the first evidence for ICI expression on HIV-infected cells.<sup>123</sup> However, the first demonstration

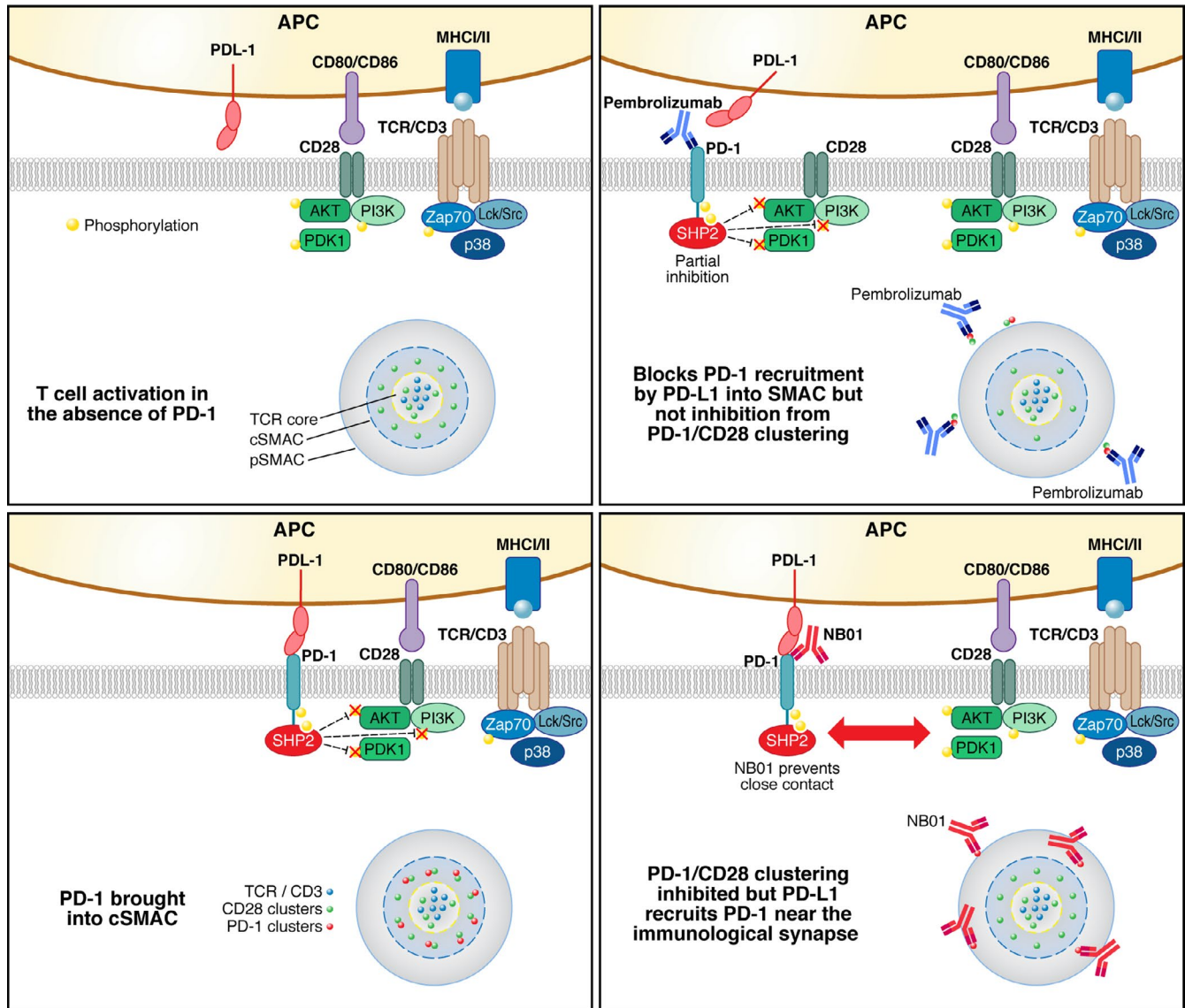


**FIGURE 6** Anti-PD-1 antibody-mediated restoration of exhausted T cells. (A) In the standard activation model of T cells expressing low levels of PD-1, the immunological synapse forms with the TCR/CD3 complex at the core, surrounded by the CD28 costimulatory receptor within the cSMAC. This distribution forms a close complex of signaling molecules that enhances the T-cell activation cascade. (B) In PD-1 high T cells, PDL-1 binding to PD-1 recruits the PD-1/SHP2 complex into the cSMAC that effectively suppresses signaling through the SHP2 phosphatase-mediated dephosphorylation of TCR/CD3 and CD28 proximal signaling molecules. (C) Use of blocking anti-PD-1 antibodies such as pembrolizumab partially restores T-cell signaling through limiting PD-1/PDL-1-mediated recruitment of the PD-1/SHP2 complex into the cSMAC. The exclusion of SHP2 from the cSMAC reduces dephosphorylation of signaling molecules including ZAP-70, Lck, PI3K, and AKT. However, our studies show that in activated T cells, pembrolizumab binding to PD-1 pulls down a complex that includes SHP2, CD28, and PI3K following T-cell activation. As such, PD-1 may partially suppress T-cell activation by recruiting CD28 away from the cSMAC and suppressing CD28 costimulation through the SHP2 phosphatase. (D) Our newly discovered anti-PD-1 antibody NB01 is non-blocking of the PD-1/PDL-1 interaction and has equivalent antagonistic activity compared to pembrolizumab in restoring T-cell signaling and antigen-specific functional and proliferative activity to exhausted HIV-specific T cells. Based on immunoprecipitation studies, our proposal is that non-blocking anti-PD-1 antibodies act through inhibiting close contact of the PD-1/SHP2 complex with CD28 and associated signaling molecules following T-cell activation. As such, CD28 is free to migrate into the cSMAC and enhance T-cell activation

that PD-1 expressing CD4 T cells might also be the source of replication competent virus was provided with the isolation and analysis of PD-1<sup>+</sup> and PD-1<sup>hi</sup>/Tfh cells from subjects with non-progressive infection and low viremia.<sup>124</sup> Since then, many studies have shown a significant correlation between the frequency of PD-1<sup>+</sup> CD4 T cells with HIV persistence during ART in blood<sup>125,126</sup> and in tissues.<sup>127</sup> However, the direct

evidence of a clear relationship between HIV reservoir and PD-1 expression came from isolated memory CD4 T cells from blood and lymph node of HIV-infected aviremic ART-treated individuals. These studies demonstrated that inducible replication competent HIV was found to be highly enriched in lymph node PD-1<sup>+</sup> CD4 T cells, containing the Tfh cell population.<sup>128</sup> Recently, a further enrichment in HIV infection

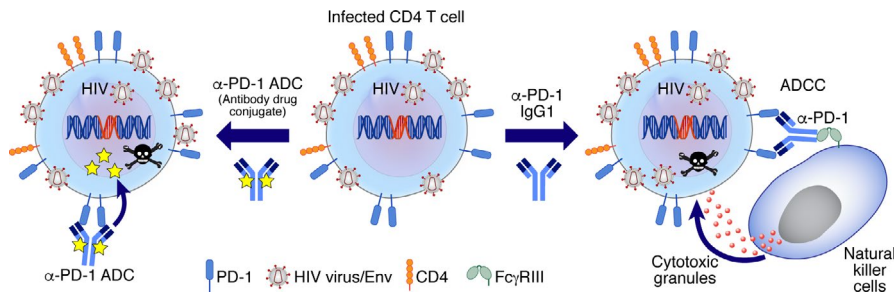


**FIGURE 7** Targeted killing of PD-1-positive HIV-infected cells. PD-1 expressing CD4 T cells represent the primary compartment of HIV-infected cells that produce replication competent virus. Targeted killing of these PD-1 positive cells represents a novel therapeutic strategy that can deplete the HIV reservoir of infected cells. Antibody drug conjugates (ADC) use a toxin-conjugated antibody that binds to the cell surface PD-1 receptor. Internalization of PD-1 results in ADC degradation within the lysosome, resulting in toxin release that specifically kills the PD-1 expressing cell. An alternate strategy for the targeted killing of HIV infected PD-1 positive cells is through antibody-dependent cellular cytotoxicity (ADCC) with an IgG1 anti-PD-1 antibody. The Fc portion of the antibody binds to the Fc $\gamma$ RIII receptors expressed on effector cells including natural killer (NK) cells. NK cells release cytotoxic granules that kill the PD-1-positive HIV-infected CD4 T cell

was shown in cells that express multiple ICIs simultaneously including PD-1, TIGIT, and LAG3, suggesting that these inhibitory receptors not only suppress T-cell activation but consequently suppress HIV transcription,<sup>129</sup> and therefore favor HIV latency.<sup>130</sup> These observations have prompted the investigation of whether ICI signaling through inhibition of T-cell activation facilitate the establishment of latent HIV infection. Indeed, Evans *et al* recently demonstrated that PD-1 blockade prior to in vitro HIV infection decreased the frequency of latently HIV-infected cells in their in vitro model of HIV latency, highlighting the potential of ICIs blockade to disrupt latency.<sup>130</sup> In addition, we recently observed that PD-1/PDL-1 interactions strongly inhibited TCR-mediated reactivation of HIV transcription and viral production from lymph nodes memory CD4 T cells. Furthermore, PD-1 blockade with anti-PD-1 monoclonal antibody treatment reactivated HIV replication from primary latently infected cells in vitro.<sup>131</sup> These illuminating results revealing the association between HIV persistence and ICIs expression are now being further explored in in vivo studies in individuals with HIV and cancer. Several case report studies tested the potential benefit of using ICI blockers, that is, anti-PD-1 or anti-CTLA-4 monoclonal antibodies to (a) potentially reverse HIV latency in CD4 T cells, thereby allowing the expression of HIV proteins on the cell surface and to (b) reinvigorate HIV-specific CD8 T cells from their exhausted state to potentiate the elimination of reactivated HIV-infected cells. While several reports highlighted a potential reactivation of HIV reservoir markers,<sup>132-134</sup> only one study reported a subsequent decrease in HIV reservoir size.<sup>132</sup> Taken together, these revelations highlighted the enrichment of HIV replication competent virus within ICIs expressing CD4 T cells. Further investigation is needed to determine if targeting these T cells and relieving exhaustion could break latency and eliminate the HIV reservoir.

## 11 | EXPLOITING PD-1 TARGETING TO PURGE THE HIV RESERVOIR

Immunotherapy through PD-1 blockade represents a major breakthrough that has provided a significant clinical benefit to patients

for the treatment of different cancers.<sup>135-137</sup> In vitro studies using the cells of HIV-infected patients have established a clear proof of principle benefit in using anti-PD-1 or PDL-1 antibodies to relieve exhaustion and enhance HIV-antigen-specific functionality and proliferation. Our own in vitro studies show that the combination of classical blocking anti-PD-1 antibodies with novel antagonistic anti-PD-1 antibodies that are non-blocking of the PD-1/PDL-1 interaction synergize to relieve functional exhaustion of HIV-specific CD8 T cells and represent an exciting option for HIV immunotherapy.<sup>105</sup> In vivo PD-1 blockade studies with SIV-infected macaques demonstrated a rapid expansion and functional quality of virus-specific CD8 T cells in both the blood and gut tissue. PD-1 blockade reduction of plasma viral load and impressively prolonged the survival of SIV-infected macaques.<sup>138</sup> Anti-PD-1 therapy combined with ART vs ART alone in SIV-infected monkeys also had a more rapid suppression of viral loads and delayed rebound after a standardized treatment interruption.<sup>139</sup> Despite the success of these studies and others at boosting the immune-mediated antiviral activity, SIV-infected monkeys were not able to maintain immunological control of the SIV virus. As such, relieving T-cell-mediated exhaustion through anti-PD-1 blockade is unlikely to be successful as a monotherapy. Although results are preliminary for several clinical studies employing PD-1 blockade, the patients tested thus far have only shown a modest response at best.<sup>132-134</sup> This indicates that immunotherapy targeting several ICIs in combination with other strategies to reactivate the virus from latently infected cells may be needed to purge the HIV reservoir.

The HIV virus has developed a considerable stealth in evading detection from a patient's immunological response. Antibody-mediated immunotherapy targeting ICIs can address T-cell functional exhaustion. However, a limitation is the lack of access of HIV-specific cytotoxic CD8 T cells to privileged anatomic compartments including lymphoid organs where persistent viremia and/or residual virus replication may occur in memory CD4 T cells.<sup>140,141</sup> Approaches for the targeted killing of infected cells would provide an orthogonal method of eliminating the highly heterogeneous latent population of infected cells. Passive immunization using broadly neutralizing antibodies (bNabs) against the HIV-1 Envelope protein may contribute to the killing of infected cells through

antibody-mediated effector function. However, a recent clinical study was unable to show a benefit in reducing HIV-1 persistence in ART suppressed patients with a combined bNab therapy.<sup>142</sup> A strategy currently under evaluation by our group exploits the fact that PD-1 + CD4 T cells from blood and lymph nodes represent the major cell reservoir for replication competent and infectious HIV in chronic and in long-term antiretroviral-treated subjects. An anti-PD-1 antibody drug conjugate (ADC) was developed with a PNU toxin and in vitro studies show specific induction of apoptosis and cell death in PD-1 positive cells. Anti-PD-1 ADC treatment of CD4 T cells from chronically infected HIV-1 donors significantly reduced viral production relative to a control anti-PD-1 antibody. This therapy was also effective in aviremic ART donors, purging the majority of cells from that were capable of producing infectious virus (Figure 7).<sup>131</sup> Although these data are very encouraging, a primary consideration with all of therapeutic approaches to eliminate the HIV reservoir will be safety. Considerable strides have led to the development of highly potent ART that effectively suppressed viral loads in most patients for decades with limited adverse events and liabilities. As such, the bar will be set high to demonstrate a clear medical need for the use of curative strategies that present any dangers to the long-term health of patients.

## ACKNOWLEDGMENTS

We thank A. Farina and C. Pellaton for their contributions to this manuscript. The Swiss Vaccine Research Institute and the Swiss National Fund (310030\_179246) provided funding during the preparation of this manuscript.

## CONFLICT OF INTEREST

All authors declare no conflict of interest with this review.

## ORCID

Giuseppe Pantaleo  <https://orcid.org/0000-0003-3651-2721>

## REFERENCES

- Schwartz RH. T cell anergy. *Annu Rev Immunol.* 2003;21:305-334.
- Chen L, Flies DB. Molecular mechanisms of T cell co-stimulation and co-inhibition. *Nat Rev Immunol.* 2013;13(4):227-242. <https://doi.org/10.1038/nri3405>.
- Wherry EJ, Kurachi M. Molecular and cellular insights into T cell exhaustion. *Nat Rev Immunol.* 2015;15(8):486-499. <https://doi.org/10.1038/nri3862>.
- Attanasio J, Wherry EJ. Costimulatory and Coinhibitory Receptor Pathways in Infectious Disease. *Immunity.* 2016;44(5):1052-1068. <https://doi.org/10.1016/j.immuni.2016.04.022>.
- Keir ME, Liang SC, Guleria I, et al. Tissue expression of PD-L1 mediates peripheral T cell tolerance. *J Exp Med.* 2006;203(4):883-895. <https://doi.org/10.1084/jem.20051776>.
- Fuller MJ, Zajac AJ. Ablation of CD8 and CD4 T cell responses by high viral loads. *J Immunol.* 2003;170(1):477-486.
- Wherry EJ, Blattman JN, Murali-Krishna K, van der Most R, Ahmed R. Viral persistence alters CD8 T-cell immunodominance and tissue distribution and results in distinct stages of functional impairment. *J Virol.* 2003;77(8):4911-4927.
- Welsh RM. Assessing CD8 T cell number and dysfunction in the presence of antigen. *J Exp Med.* 2001;193(5):F19-F22. <https://doi.org/10.1084/jem.193.5.F19>.
- Antoine P, Olislagers V, Huygens A, et al. Functional exhaustion of CD4+ T lymphocytes during primary cytomegalovirus infection. *J Immunol.* 2012;189(5):2665-2672.
- Wherry EJ. T cell exhaustion. *Nat Immunol.* 2011;12(6):492-499.
- Kaufmann DE, Walker BD. PD-1 and CTLA-4 inhibitory cosignaling pathways in HIV infection and the potential for therapeutic intervention. *J Immunol.* 2009;182(10):5891-5897. <https://doi.org/10.4049/jimmunol.0803771>.
- Crawford A, Angelosanto JM, Kao C, et al. Molecular and transcriptional basis of CD4(+) T cell dysfunction during chronic infection. *Immunity.* 2014;40(2):289-302. <https://doi.org/10.1016/j.immuni.2014.01.005>.
- Zajac AJ, Blattman JN, Murali-Krishna K, et al. Viral immune evasion due to persistence of activated T cells without effector function. *J Exp Med.* 1998;188(12):2205-2213.
- Matloubian M, Concepcion RJ, Ahmed R. CD4+ T cells are required to sustain CD8+ cytotoxic T-cell responses during chronic viral infection. *J Virol.* 1994;68(12):8056-8063.
- Aubert RD, Kamphorst AO, Sarkar S, et al. Antigen-specific CD4 T-cell help rescues exhausted CD8 T cells during chronic viral infection. *Proc Natl Acad Sci USA.* 2011;108(52):21182-21187. <https://doi.org/10.1073/pnas.1118450109>.
- Zhang S, Zhang H, Zhao J. The role of CD4 T cell help for CD8 CTL activation. *Biochem Biophys Res Commun.* 2009;384(4):405-408. <https://doi.org/10.1016/j.bbrc.2009.04.134>.
- Shin H, Blackburn SD, Blattman JN, Wherry EJ. Viral antigen and extensive division maintain virus-specific CD8 T cells during chronic infection. *J Exp Med.* 2007;204(4):941-949. <https://doi.org/10.1084/jem.20061937>.
- Utzschneider DT, Legat A, Fuertes Marraco SA, et al. T cells maintain an exhausted phenotype after antigen withdrawal and population reexpansion. *Nat Immunol.* 2013;14(6):603-610. <https://doi.org/10.1038/ni.2606>.
- Wherry EJ, Barber DL, Kaech SM, Blattman JN, Ahmed R. Antigen-independent memory CD8 T cells do not develop during chronic viral infection. *Proc Natl Acad Sci USA.* 2004;101(45):16004-16009. <https://doi.org/10.1073/pnas.0407192101>.
- Paley MA, Kroy DC, Odorizzi PM, et al. Progenitor and terminal subsets of CD8+ T cells cooperate to contain chronic viral infection. *Science.* 2012;338(6111):1220-1225. <https://doi.org/10.1126/science.1229620>.
- Fuller MJ, Khanolkar A, Tebo AE, Zajac AJ. Maintenance, loss, and resurgence of T cell responses during acute, protracted, and chronic viral infections. *J Immunol.* 2004;172(7):4204-4214.
- Wherry EJ, Ha SJ, Kaech SM, et al. Molecular signature of CD8+ T cell exhaustion during chronic viral infection. *Immunity.* 2007;27(4):670-684. <https://doi.org/10.1016/j.immuni.2007.09.006>.
- Martinez GJ, Pereira RM, Aijo T, et al. The Transcription factor NFAT promotes exhaustion of activated CD8 + T cells. *Immunity.* 2015;42(2):265-278. <https://doi.org/10.1016/j.immuni.2015.01.006>.
- Quigley M, Pereyra F, Nilsson B, et al. Transcriptional analysis of HIV-specific CD8+ T cells shows that PD-1 inhibits T cell function by upregulating BATF. *Nat Med.* 2010;16(10):1147-1151. <https://doi.org/10.1038/nm.2232>.
- Oestreich KJ, Yoon H, Ahmed R, Boss JM. NFATc1 regulates PD-1 expression upon T cell activation. *J Immunol.* 2008;181(7):4832-4839.
- Man K, Gabriel SS, Liao Y, et al. Transcription Factor IRF4 Promotes CD8+ T Cell Exhaustion and Limits the Development of Memory-like

- T Cells during Chronic Infection. *Immunity*. 2017;47(6):1129-1141. e5. <https://doi.org/10.1016/j.immuni.2017.11.021>.
27. Doering TA, Crawford A, Angelosanto JM, Paley MA, Ziegler CG, Wherry EJ. Network analysis reveals centrally connected genes and pathways involved in CD8+ T cell exhaustion versus memory. *Immunity*. 2012;37(6):1130-1144. <https://doi.org/10.1016/j.immuni.2012.08.021>.
  28. Im SJ, Hashimoto M, Gerner MY, et al. Defining CD8+ T cells that provide the proliferative burst after PD-1 therapy. *Nature*. 2016;537(7620):417-421. <https://doi.org/10.1038/nature19330>.
  29. Utzschneider DT, Charmoy M, Chennupati V, et al. T cell factor 1-expressing memory-like CD8+ T cells sustain the immune response to chronic viral infections. *Immunity*. 2016;45(2):415-427. <https://doi.org/10.1016/j.immuni.2016.07.021>.
  30. Odorizzi PM, Pauken KE, Paley MA, Sharpe A, Wherry EJ. Genetic absence of PD-1 promotes accumulation of terminally differentiated exhausted CD8+ T cells. *J Exp Med*. 2015;212(7):1125-1137. <https://doi.org/10.1084/jem.20142237>.
  31. Huang AC, Postow MA, Orlowski RJ, et al. T-cell invigoration to tumour burden ratio associated with anti-PD-1 response. *Nature*. 2017;545(7652):60-65. <https://doi.org/10.1038/nature22079>
  32. Buggert M, Tauriainen J, Yamamoto T, et al. T-bet and eomes are differentially linked to the exhausted phenotype of CD8+ T cells in HIV infection. *PLoS Pathog*. 2014;10(7):e1004251.
  33. de Masson A, Kirilovsky A, Zoorob R, et al. Blimp-1 overexpression is associated with low HIV-1 reservoir and transcription levels in central memory CD4+ T cells from elite controllers. *AIDS*. 2014;28(11):1567-1577. <https://doi.org/10.1097/QAD.000000000000295>.
  34. Parish IA, Marshall HD, Staron MM, et al. Chronic viral infection promotes sustained Th1-derived immunoregulatory IL-10 via BLIMP-1. *J Clin Invest*. 2014;124(8):3455-3468. <https://doi.org/10.1172/JCI66108>.
  35. Shin H, Blackburn SD, Intlekofer AM, et al. A role for the transcriptional repressor blimp-1 in CD8+ T Cell Exhaustion during chronic viral infection. *Immunity*. 2009;31(2):309-320. <https://doi.org/10.1016/j.immuni.2009.06.019>.
  36. Bengsch B, Ohtani T, Khan O, et al. Epigenomic-guided mass cytometry profiling reveals disease-specific features of exhausted CD8 T cells. *Immunity*. 2018;48(5):1029-1045.e5.
  37. O'Sullivan D, Pearce EL. Targeting T cell metabolism for therapy. *Trends Immunol*. 2015;36(2):71-80. <https://doi.org/10.1016/j.it.2014.12.004>.
  38. Bengsch B, Johnson AL, Kurachi M, et al. Bioenergetic insufficiencies due to metabolic alterations regulated by the inhibitory receptor PD-1 are an early driver of CD8 + T cell exhaustion. *Immunity*. 2016;45(2):358-373. <https://doi.org/10.1016/j.immuni.2016.07.008>.
  39. Patsoukis N, Bardhan K, Chatterjee P, et al. PD-1 alters T-cell metabolic reprogramming by inhibiting glycolysis and promoting lipolysis and fatty acid oxidation. *Nat Commun*. 2015;6(1): <https://doi.org/10.1038/ncomms7692>.
  40. Staron MM, Gray SM, Marshall HD, et al. The transcription factor FoxO1 sustains expression of the inhibitory receptor PD-1 and survival of antiviral CD8+ T cells during chronic infection. *Immunity*. 2014;41(5):802-814. <https://doi.org/10.1016/j.immuni.2014.10.013>.
  41. Scharping NE, Menk AV, Moreci RS, et al. The tumor microenvironment represses T cell mitochondrial biogenesis to drive intratumoral T cell metabolic insufficiency and dysfunction. *Immunity*. 2016;45(2):374-388. <https://doi.org/10.1016/j.immuni.2016.07.009>.
  42. Philip M, Fairchild L, Sun L, et al. Chromatin states define tumour-specific T cell dysfunction and reprogramming. *Nature*. 2017;545(7655):452-456. <https://doi.org/10.1038/nature22367>.
  43. Youngblood B, Noto A, Porichis F, et al. Cutting edge: prolonged exposure to HIV reinforces a poised epigenetic program for PD-1 expression in virus-specific CD8 T cells. *J Immunol*. 2013;191(2):540-544. <https://doi.org/10.4049/jimmunol.1203161>.
  44. Sen DR, Kaminski J, Barnitz RA, et al. The epigenetic landscape of T cell exhaustion. *Science*. 2016;354(6316):1165-1169. <https://doi.org/10.1126/science.aae0491>.
  45. Austin JW, Lu P, Majumder P, Ahmed R, Boss JM. STAT3, STAT4, NFATc1, and CTCF Regulate PD-1 through Multiple Novel Regulatory Regions in Murine T Cells. *J Immunol*. 2014;192(10):4876-4886. <https://doi.org/10.4049/jimmunol.1302750>.
  46. Scott-Browne JP, Lopez-Moyado IF, Trifari S, et al. Dynamic Changes in Chromatin Accessibility Occur in CD8 + T Cells Responding to Viral Infection. *Immunity*. 2016;45(6):1327-1340. <https://doi.org/10.1016/j.immuni.2016.10.028>.
  47. Ahmed R, Salmi A, Butler LD, Chiller JM, Oldstone MB. Selection of genetic variants of lymphocytic choriomeningitis virus in spleens of persistently infected mice. Role in suppression of cytotoxic T lymphocyte response and viral persistence. *J Exp Med*. 1984;160(2):521-540.
  48. Zinkernagel RM. Lymphocytic choriomeningitis virus and immunology. *Curr Top Microbiol Immunol*. 2002;263:1-5.
  49. Gallimore A, Glithero A, Godkin A, et al. Induction and exhaustion of lymphocytic choriomeningitis virus-specific cytotoxic T lymphocytes visualized using soluble tetrameric major histocompatibility complex class I-peptide complexes. *J Exp Med*. 1998;187(9):1383-1393.
  50. Barber DL, Wherry EJ, Masopust D, et al. Restoring function in exhausted CD8 T cells during chronic viral infection. *Nature*. 2006;439(7077):682-687. <https://doi.org/10.1038/nature04444>.
  51. Jin X, Bauer DE, Tuttleton SE, et al. Dramatic rise in plasma viremia after CD8(+) T cell depletion in simian immunodeficiency virus-infected macaques. *J Exp Med*. 1999;189(6):991-998.
  52. Papagno L, Spina CA, Marchant A, et al. Immune activation and CD8+ T-cell differentiation towards senescence in HIV-1 infection. *PLoS Biol*. 2004;2(2):e20-<https://doi.org/10.1371/journal.pbio.0020020>.
  53. Douek DC, Brenchley JM, Betts MR, et al. HIV preferentially infects HIV-specific CD4+ T cells. *Nature*. 2002;417(6884):95-98. <https://doi.org/10.1038/417095a>.
  54. Day CL, Kaufmann DE, Kiepiela P, et al. PD-1 expression on HIV-specific T cells is associated with T-cell exhaustion and disease progression. *Nature*. 2006;443(7109):350-354. <https://doi.org/10.1038/nature05115>.
  55. Trautmann L, Janbazian L, Chomont N, et al. Upregulation of PD-1 expression on HIV-specific CD8+ T cells leads to reversible immune dysfunction. *Nat Med*. 2006;12(10):1198-1202. <https://doi.org/10.1038/nm1482>.
  56. Petrovas C, Casazza JP, Brenchley JM, et al. PD-1 is a regulator of virus-specific CD8+ T cell survival in HIV infection. *J Exp Med*. 2006;203(10):2281-2292. <https://doi.org/10.1084/jem.20061496>.
  57. Blackburn SD, Shin H, Haining WN, et al. Coregulation of CD8+ T cell exhaustion by multiple inhibitory receptors during chronic viral infection. *Nat Immunol*. 2009;10(1):29-37. <https://doi.org/10.1038/ni.1679>.
  58. Chew GM, Fujita T, Webb GM, et al. TIGIT Marks Exhausted T Cells, Correlates with Disease Progression, and Serves as a Target for Immune Restoration in HIV and SIV Infection. *PLoS Pathog*. 2016;12(1):e1005349. <https://doi.org/10.1371/journal.ppat.1005349>.
  59. Pombo C, Wherry EJ, Gostick E, Price DA, Betts MR. Elevated expression of CD160 and 2B4 defines a cytolytic HIV-specific CD8+

- T-cell population in elite controllers. *J Infect Dis.* 2015;212(9):1376-1386. <https://doi.org/10.1093/infdis/jiv226>.
60. Jones RB, Ndhlovu LC, Barbour JD, et al. Tim-3 expression defines a novel population of dysfunctional T cells with highly elevated frequencies in progressive HIV-1 infection. *J Exp Med.* 2008;205(12):2763-2779. <https://doi.org/10.1084/jem.20081398>.
  61. Peretz Y, He Z, Shi Y, et al. CD160 and PD-1 Co-expression on HIV-specific CD8 T cells defines a subset with advanced dysfunction. *PLoS Pathog.* 2012;8(8):e1002840. <https://doi.org/10.1371/journal.ppat.1002840>.
  62. Jin HT, Anderson AC, Tan WG, et al. Cooperation of Tim-3 and PD-1 in CD8 T-cell exhaustion during chronic viral infection. *Proc Natl Acad Sci USA.* 2010;107(33):14733-14738. <https://doi.org/10.1073/pnas.1009731107>.
  63. Hoffmann M, Pantazis N, Martin GE, et al. Exhaustion of activated CD8 T cells predicts disease progression in primary HIV-1 infection. *PLoS Pathog.* 2016;12(7):e1005661. <https://doi.org/10.1371/journal.ppat.1005661>.
  64. Yamamoto T, Price DA, Casazza JP, et al. Surface expression patterns of negative regulatory molecules identify determinants of virus-specific CD8+ T-cell exhaustion in HIV infection. *Blood.* 2011;117(18):4805-4815. <https://doi.org/10.1182/blood-2010-11-317297>.
  65. Appay V, Nixon DF, Donahoe SM, et al. HIV-specific CD8(+) T cells produce antiviral cytokines but are impaired in cytolytic function. *J Exp Med.* 2000;192(1):63-75. <https://doi.org/10.1084/jem.192.1.63>.
  66. Kostense S, Vandenberghe K, Joling J, et al. Persistent numbers of tetramer+ CD8(+) T cells, but loss of interferon-gamma+ HIV-specific T cells during progression to AIDS. *Blood.* 2002;99(7):2505-2511.
  67. Petrovas C, Mueller YM, Dimitriou ID, et al. Increased mitochondrial mass characterizes the survival defect of HIV-specific CD8+ T cells. *Blood.* 2007;109(6):2505-2513. <https://doi.org/10.1182/blood-2006-05-021626>
  68. Younes SA, Yassine-Diab B, Dumont AR, et al. HIV-1 viremia prevents the establishment of interleukin 2-producing HIV-specific memory CD4+ T cells endowed with proliferative capacity. *J Exp Med.* 2003;198(12):1909-1922. <https://doi.org/10.1084/jem.20031598>.
  69. Palmer BE, Boritz E, Wilson CC. Effects of sustained HIV-1 plasma viremia on HIV-1 Gag-specific CD4+ T cell maturation and function. *J Immunol.* 2004;172(5):3337-3347. <https://doi.org/10.4049/jimmunol.172.5.3337>.
  70. D'Souza M, Fontenot AP, Mack DG, et al. Programmed death 1 expression on HIV-specific CD4+ T cells is driven by viral replication and associated with T cell dysfunction. *J Immunol.* 2007;179(3):1979-1987. <https://doi.org/10.4049/jimmunol.179.3.1979>.
  71. Kaufmann DE, Kavanagh DG, Pereyra F, et al. Upregulation of CTLA-4 by HIV-specific CD4+ T cells correlates with disease progression and defines a reversible immune dysfunction. *Nat Immunol.* 2007;8(11):1246-1254. <https://doi.org/10.1038/ni1515>.
  72. Porichis F, Kwon DS, Zupkosky J, et al. Responsiveness of HIV-specific CD4 T cells to PD-1 blockade. *Blood.* 2011;118(4):965-974. <https://doi.org/10.1182/blood-2010-12-328070>.
  73. Kassu A, Marcus RA, D'Souza MB, et al. Regulation of virus-specific CD4+ T cell function by multiple costimulatory receptors during chronic HIV infection. *J Immunol.* 2010;185(5):3007-3018. <https://doi.org/10.4049/jimmunol.1000156>.
  74. Giorgi JV, Hultin LE, McKeating JA, et al. Shorter survival in advanced human immunodeficiency virus type 1 infection is more closely associated with T lymphocyte activation than with plasma virus burden or virus chemokine coreceptor usage. *J Infect Dis.* 1999;179(4):859-870. <https://doi.org/10.1086/314660>.
  75. Zaunders JJ, Cunningham PH, Kelleher AD, et al. Potent antiretroviral therapy of primary human immunodeficiency virus type 1 (HIV-1) infection: partial normalization of T lymphocyte subsets and limited reduction of HIV-1 DNA despite clearance of plasma viremia. *The J Infect Dis.* 1999;180(2):320-329. <https://doi.org/10.1086/314880>.
  76. Appay V, Dunbar PR, Callan M, et al. Memory CD8+ T cells vary in differentiation phenotype in different persistent virus infections. *Nat Med.* 2002;8(4):379-385. <https://doi.org/10.1038/nm0402-379>.
  77. Speiser DE, Migliaccio M, Pittet MJ, et al. Human CD8(+) T cells expressing HLA-DR and CD28 show telomerase activity and are distinct from cytolytic effector T cells. *Eur J Immunol.* 2001;31(2):459-466.
  78. van Baarle D, Kostense S, Hovenkamp E, et al. Lack of Epstein-Barr virus- and HIV-specific CD27- CD8+ T cells is associated with progression to viral disease in HIV-infection. *AIDS.* 2002;16(15):2001-2011.
  79. Champagne P, Ogg GS, King AS, et al. Skewed maturation of memory HIV-specific CD8 T lymphocytes. *Nature.* 2001;410(6824):106-111. <https://doi.org/10.1038/35065118>.
  80. Ellefsen K, Harari A, Champagne P, Bart PA, Sekaly RP, Pantaleo G. Distribution and functional analysis of memory antiviral CD8 T cell responses in HIV-1 and cytomegalovirus infections. *Eur J Immunol.* 2002;32(12):3756-3764.
  81. Veiga-Parga T, Sehrawat S, Rouse BT. Role of regulatory T cells during virus infection. *Immunol Rev.* 2013;255(1):182-196. <https://doi.org/10.1111/imr.12085>.
  82. Stylianou E, Aukrust P, Kvale D, Muller F, Froland SS. IL-10 in HIV infection: increasing serum IL-10 levels with disease progression-down-regulatory effect of potent anti-retroviral therapy. *Clin Exp Immunol.* 1999;116(1):115-120.
  83. Brockman MA, Kwon DS, Tighe DP, et al. IL-10 is up-regulated in multiple cell types during viremic HIV infection and reversibly inhibits virus-specific T cells. *Blood.* 2009;114(2):346-356. <https://doi.org/10.1182/blood-2008-12-191296>.
  84. Deeks SG, Walker BD. Human immunodeficiency virus controllers: mechanisms of durable virus control in the absence of antiretroviral therapy. *Immunity.* 2007;27(3):406-416. <https://doi.org/10.1016/j.immuni.2007.08.010>.
  85. Rosas-Umbert M, Llano A, Bellido R, et al. Mechanisms of abrupt loss of virus control in a cohort of previous HIV controllers. *J Virol.* 2019;93(4): <https://doi.org/10.1128/JVI.01436-18>.
  86. Shoukry NH, Grakoui A, Houghton M, et al. Memory CD8+ T cells are required for protection from persistent hepatitis C virus infection. *J Exp Med.* 2003;197(12):1645-1655. <https://doi.org/10.1084/jem.20030239>.
  87. Thimme R, Wieland S, Steiger C, et al. CD8(+) T cells mediate viral clearance and disease pathogenesis during acute hepatitis B virus infection. *J Virol.* 2003;77(1):68-76.
  88. Schulze Zur Wiesch J, Ciuffreda D, Lewis-Ximenez L, et al. Broadly directed virus-specific CD4+ T cell responses are primed during acute hepatitis C infection, but rapidly disappear from human blood with viral persistence. *J Exp Med.* 2012;209(1):61-75. <https://doi.org/10.1084/jem.20100388>.
  89. Fiscaro P, Valdatta C, Massari M, et al. Antiviral intrahepatic T-cell responses can be restored by blocking programmed death-1 pathway in chronic hepatitis B. *Gastroenterology.* 2010;138(2):682-693. <https://doi.org/10.1053/j.gastro.2009.09.052>.
  90. Liu J, Zhang E, Ma Z, et al. Enhancing virus-specific immunity in vivo by combining therapeutic vaccination and PD-L1 blockade in chronic hepatitis B infection. *PLoS Pathog.* 2014;10(1):e1003856-<https://doi.org/10.1371/journal.ppat.1003856>.
  91. Gardiner D, Lalezari J, Lawitz E, et al. A randomized, double-blind, placebo-controlled assessment of BMS-936558,

- a fully human monoclonal antibody to programmed death-1 (PD-1), in patients with chronic hepatitis C virus infection. *PLoS ONE*. 2013;8(5):e63818. <https://doi.org/10.1371/journal.pone.0063818>.
92. Fuller MJ, Callendret B, Zhu B, et al. Immunotherapy of chronic hepatitis C virus infection with antibodies against programmed cell death-1 (PD-1). *Proc Natl Acad Sci USA*. 2013;110(37):15001-15006. <https://doi.org/10.1073/pnas.1312772110>.
  93. Masaki A, Ishida T, Suzuki S, et al. Human T-cell lymphotropic/leukemia virus type 1 (HTLV-1) Tax-specific T-cell exhaustion in HTLV-1-infected individuals. *Cancer Sci*. 2018;109(8):2383-2390. <https://doi.org/10.1111/cas.13654>.
  94. Kozako T, Yoshimitsu M, Akimoto M, et al. Programmed death-1 (PD-1)/PD-1 ligand pathway-mediated immune responses against human T-lymphotropic virus type 1 (HTLV-1) in HTLV-1-associated myelopathy/tropical spastic paraparesis and carriers with autoimmune disorders. *Hum Immunol*. 2011;72(11):1001-1006. <https://doi.org/10.1016/j.humimm.2011.07.308>.
  95. Yokosuka T, Takamatsu M, Kobayashi-Imanishi W, Hashimoto-Tane A, Azuma M, Saito T. Programmed cell death 1 forms negative costimulatory microclusters that directly inhibit T cell receptor signaling by recruiting phosphatase SHP2. *J Exp Med*. 2012;209(6):1201-1217. <https://doi.org/10.1084/jem.20112741>.
  96. Sheppard KA, Fitz LJ, Lee JM, et al. PD-1 inhibits T-cell receptor induced phosphorylation of the ZAP70/CD3zeta signalosome and downstream signaling to PKC $\theta$ . *FEBS Lett*. 2004;574(1-3):37-41.
  97. Conley JM, Gallagher MP, Berg LJT. Cells and gene regulation: the switching on and turning up of genes after T cell receptor stimulation in CD8 T cells. *Front Immunol*. 2016;7: <https://doi.org/10.3389/fimmu.2016.00076>.
  98. McLane LM, Abdel-Hakeem MS, Wherry EJ. CD8 T cell exhaustion during chronic viral infection and cancer. *Ann Rev Immunol*. 2019;37(1):457-495. <https://doi.org/10.1146/annurev-immunol-041015-055318>.
  99. Egen JG, Kuhns MS, Allison JP. CTLA-4: new insights into its biological function and use in tumor immunotherapy. *Nat Immunol*. 2002;3(7):611-618. <https://doi.org/10.1038/ni0702-611>.
  100. Parry RV, Chemnitz JM, Frauwirth KA, et al. CTLA-4 and PD-1 Receptors Inhibit T-Cell Activation by Distinct Mechanisms. *Mol Cell Biol*. 2005;25(21):9543-9553. <https://doi.org/10.1128/MCB.25.21.9543-9553.2005>.
  101. Patsoukis N, Brown J, Petkova V, Liu F, Li L, Boussiotis VA. Selective Effects of PD-1 on Akt and Ras pathways regulate molecular components of the cell cycle and inhibit T cell proliferation. *Sci Signal*. 2012;5(230):ra46-ra46. <https://doi.org/10.1126/scisignal.2002796>.
  102. Chemnitz JM, Parry RV, Nichols KE, June CH, Riley JL. SHP-1 and SHP-2 associate with immunoreceptor tyrosine-based switch motif of programmed death 1 upon primary human T cell stimulation, but only receptor ligation prevents T cell activation. *J Immunol*. 2004;173(2):945-954.
  103. Hui E, Cheung J, Zhu J, et al. T cell costimulatory receptor CD28 is a primary target for PD-1-mediated inhibition. *Science*. 2017;355(6332):1428-1433. <https://doi.org/10.1126/science.aaf1292>.
  104. Kamphorst AO, Wieland A, Nasti T, et al. Rescue of exhausted CD8 T cells by PD-1-targeted therapies is CD28-dependent. *Science*. 2017;355(6332):1423-1427. <https://doi.org/10.1126/science.aaf0683>.
  105. Fenwick C, Loreda-Varela JL, Joo V, et al. Tumor suppression of novel anti-PD-1 antibodies mediated through CD28 costimulatory pathway. *J Exp Med*. 2019;216(7):1525-1541. <https://doi.org/10.1084/jem.20182359>.
  106. Trebak M, Kinet JP. Calcium signalling in T cells. *Nat Rev Immunol*. 2019;19(3):154-169. <https://doi.org/10.1038/s41577-018-0110-7>.
  107. Anderson AC, Joller N, Kuchroo VK. Calcium signalling in T cells. *Nat Rev Immunol*. 2019;19(3):154-169. <https://doi.org/10.1038/s41577-018-0110-7>.
  108. Rangachari M, Zhu C, Sakuishi K, et al. Bat3 promotes T cell responses and autoimmunity by repressing Tim-3-mediated cell death and exhaustion. *Nat Med*. 2012;18(9):1394-1400. <https://doi.org/10.1038/nm.2871>.
  109. He W, Zhang H, Han F, et al. CD155/TIGIT signaling regulates CD8(+) T-cell metabolism and promotes tumor progression in human gastric cancer. *Cancer Res*. 2017;77(22):6375-6388. <https://doi.org/10.1158/0008-5472.CAN-17-0381>.
  110. Maruhashi T, Okazaki IM, Sugiura D, et al. LAG-3 inhibits the activation of CD4+ T cells that recognize stable pMHCII through its conformation-dependent recognition of pMHCII. *Nat Immunol*. 2018;19(12):1415-1426. <https://doi.org/10.1038/s41590-018-0217-9>.
  111. Li Q, Schacker T, Carlis J, Beilman G, Nguyen P, Haase AT. Functional genomic analysis of the response of HIV-1-infected lymphatic tissue to antiretroviral therapy. *J Infect Dis*. 2004;189(4):572-582. <https://doi.org/10.1086/381396>.
  112. Eisele E, Siliciano RF. Redefining the viral reservoirs that prevent hiv-1 eradication. *Immunity*. 2012;37(3):377-388. <https://doi.org/10.1016/j.immuni.2012.08.010>.
  113. Pallikkuth S, Fischl MA, Pahwa S. Combination antiretroviral therapy with raltegravir leads to rapid immunologic reconstitution in treatment-naive patients with chronic HIV infection. *J Infect Dis*. 2013;208(10):1613-1623. <https://doi.org/10.1093/infdis/jit387>.
  114. Serrano-Villar S, Sainz T, Lee SA, et al. HIV-Infected Individuals with low CD4/CD8 ratio despite effective antiretroviral therapy exhibit altered T cell subsets, heightened CD8+ T Cell activation, and increased risk of non-AIDS morbidity and mortality. *PLoS Pathog*. 2014;10(5):e1004078. <https://doi.org/10.1371/journal.ppat.1004078>.
  115. Harari A, Petitpierre S, Valleliau F, Pantaleo G. Skewed representation of functionally distinct populations of virus-specific CD4 T cells in HIV-1-infected subjects with progressive disease: changes after antiretroviral therapy. *Blood*. 2004;103(3):966-972. <https://doi.org/10.1182/blood-2003-04-1203>.
  116. Rehr M, Cahenzli J, Haas A, et al. Emergence of polyfunctional CD8+ T cells after prolonged suppression of human immunodeficiency virus replication by antiretroviral therapy. *J Virol*. 2008;82(7):3391-3404. <https://doi.org/10.1128/JVI.02383-07>.
  117. Hurst J, Hoffmann M, Pace M, et al. Immunological biomarkers predict HIV-1 viral rebound after treatment interruption. *Nat Commun*. 2015;6(1): <https://doi.org/10.1038/ncomms9495>.
  118. Jain V, Hartogensis W, Bacchetti P, et al. Antiretroviral therapy initiated within 6 months of hiv infection is associated with lower T-cell activation and smaller hiv reservoir size. *J Infect Dis*. 2013;208(8):1202-1211. <https://doi.org/10.1093/infdis/jit311>.
  119. Laanani M, Ghosn J, Essat A, et al. Impact of the timing of initiation of antiretroviral therapy during primary HIV-1 infection on the decay of cell-associated HIV-DNA. *Clin Infect Dis*. 2015;60(11):1715-1721. <https://doi.org/10.1093/cid/civ171>.
  120. Archin NM, Vaidya NK, Kuruc JD, et al. Immediate antiviral therapy appears to restrict resting CD4+ cell HIV-1 infection without accelerating the decay of latent infection. *Proc Natl Acad Sci USA*. 2012;109(24):9523-9528. <https://doi.org/10.1073/pnas.1120248109>.
  121. Sereti I, Krebs SJ, Phanuphak N, et al. Persistent, albeit reduced, chronic inflammation in persons starting antiretroviral therapy in acute HIV infection. *Clin Infect Dis*. 2017;64(2):124-131. <https://doi.org/10.1093/cid/ciw683>.

122. Rajasuriar R, Wright E, Lewin SR. Impact of antiretroviral therapy (ART) timing on chronic immune activation/inflammation and end-organ damage. *Curr Opin HIV AIDS*. 2015;10(1):35-42. <https://doi.org/10.1097/COH.0000000000000118>.
123. Chomont N, El-Far M, Ancuta P, et al. HIV reservoir size and persistence are driven by T cell survival and homeostatic proliferation. *Nat Med*. 2009;15(8):893-900. <https://doi.org/10.1038/nm.1972>.
124. Perreau M, Savoye AL, De Crignis E, et al. Follicular helper T cells serve as the major CD4 T cell compartment for HIV-1 infection, replication, and production. *J Exp Med*. 2013;210(1):143-156. <https://doi.org/10.1084/jem.20121932>.
125. Hatano H, Scherzer R, Wu Y, et al. A randomized controlled trial assessing the effects of raltegravir intensification on endothelial function in treated hiv infection. *J Acquir Immune Defic Syndr*. 2012;61(3):317-325. <https://doi.org/10.1097/QAI.0b013e31826e7d0f>.
126. Cockerham LR, Jain V, Sinclair E, et al. Programmed death-1 expression on CD4+ and CD8+ T cells in treated and untreated HIV disease. *AIDS*. 2014;28(12):1749-1758. <https://doi.org/10.1097/QAD.0000000000000314>.
127. Khoury G, Fromentin R, Solomon A, et al. Human immunodeficiency virus persistence and T-cell activation in blood, rectal, and lymph node tissue in human immunodeficiency virus-infected individuals receiving suppressive antiretroviral therapy. *J Infect Dis*. 2017;215(6):911-919. <https://doi.org/10.1093/infdis/jix039>.
128. Banga R, Procopio FA, Noto A, et al. PD-1+ and follicular helper T cells are responsible for persistent HIV-1 transcription in treated aviremic individuals. *Nat Med*. 2016;22(7):754-761. <https://doi.org/10.1038/nm.4113>.
129. Fromentin R, Bakeman W, Lawani MB, et al. CD4+ T Cells Expressing PD-1, TIGIT and LAG-3 Contribute to HIV persistence during ART. *PLoS Pathog*. 2016;12(7):e1005761. <https://doi.org/10.1371/journal.ppat.1005761>.
130. Evans VA, van der Sluis RM, Solomon A, et al. Programmed cell death-1 contributes to the establishment and maintenance of HIV-1 latency. *AIDS*. 2018;32(11):1491-1497. <https://doi.org/10.1097/QAD.0000000000001849>.
131. Banga R, Rebecchini C, Procopio FA, et al. Lymph node migratory dendritic cells modulate HIV-1 transcription through PD-1 engagement. *PLoS Pathog*. 2019;15(7):e1007918. <https://doi.org/10.1371/journal.ppat.1007918>.
132. Guihot A, Marcelin AG, Massiani MA, et al. Drastic decrease of the HIV reservoir in a patient treated with nivolumab for lung cancer. *Ann Oncol*. 2018;29(2):517-518. <https://doi.org/10.1093/annonc/mdx696>.
133. Le Garff G, Samri A, Lambert-Niclot S, et al. Transient HIV-specific T cells increase and inflammation in an HIV-infected patient treated with nivolumab. *AIDS*. 2017;31(7):1048-1051. <https://doi.org/10.1097/QAD.0000000000001429>.
134. Wightman F, Solomon A, Kumar SS, et al. Effect of ipilimumab on the HIV reservoir in an HIV-infected individual with metastatic melanoma. *AIDS*. 2015;29(4):504-506. <https://doi.org/10.1097/QAD.0000000000000562>.
135. Mellman I, Coukos G, Dranoff G. Cancer immunotherapy comes of age. *Nature*. 2011;480(7378):480-489. <https://doi.org/10.1038/nature10673>.
136. Sharma P, Allison JP. The future of immune checkpoint therapy. *Science*. 2015;348(6230):56-61. <https://doi.org/10.1126/science.aaa8172>.
137. Callahan MK, Postow MA, Wolchok JD. Targeting T cell co-receptors for cancer therapy. *Immunity*. 2016;44(5):1069-1078. <https://doi.org/10.1016/j.immuni.2016.04.023>.
138. Velu V, Titanji K, Zhu B, et al. Enhancing SIV-specific immunity in vivo by PD-1 blockade. *Nature*. 2009;458(7235):206-210. <https://doi.org/10.1038/nature07662>.
139. Mylvaganam GH, Chea LS, Tharp GK, et al. Combination anti-PD-1 and antiretroviral therapy provides therapeutic benefit against SIV. *JCI Insight*. 2018;3(18): <https://doi.org/10.1172/jci.insight.122940>.
140. Connick E, Mattila T, Folkvord JM, et al. CTL fail to accumulate at sites of HIV-1 replication in lymphoid tissue. *J Immunol*. 2007;178(11):6975-6983.
141. Fukazawa Y, Lum R, Okoye AA, et al. B cell follicle sanctuary permits persistent productive simian immunodeficiency virus infection in elite controllers. *Nat Med*. 2015;21(2):132-139. <https://doi.org/10.1038/nm.3781>.
142. Riddler SA, Zheng L, Durand CM, et al. Randomized clinical trial to assess the impact of the broadly neutralizing HIV-1 monoclonal antibody VRC01 on HIV-1 persistence in individuals on effective ART. *Open Forum Infect Dis*. 2018;5(10): <https://doi.org/10.1093/ofid/ofy242>.

**How to cite this article:** Fenwick C, Joo V, Jacquier P, et al. T-cell exhaustion in HIV infection. *Immunol Rev*. 2019;292:149-163. <https://doi.org/10.1111/imr.12823>

# **An Alternative Fc-mediated Mechanism of Regulating PD-1 Expression in Anti-PD-1 Therapy (manuscript in preparation)**

## **Abstract**

Therapeutic monoclonal antibodies (mAb) targeting the immune checkpoint inhibitor programmed cell death protein 1 (PD-1) have achieved considerable clinical success in anti-cancer therapy through relieving T cell exhaustion. Blockade of PD-1 interaction with its ligands PD-L1 and PD-L2 is an important determinant in potentiating the antigen specific activation of exhausted T cells. However, here we show that anti-PD-1 Abs act through an alternative antagonistic mechanism leading to the downregulation of PD-1 expression on memory CD4<sup>+</sup> and CD8<sup>+</sup> T cells. PD-1 receptor downregulation and internalization occur through distinct processes whereby the presence of CD14<sup>+</sup> monocytes are necessary for the mAb mediated PD-1 downregulation on T cells but not for PD-1 antibody internalization. Furthermore, we show that CD64 or Fc gamma receptor 1 on monocytes acts as the primary determinant for this T cell extrinsic process. Our studies show a novel route for reducing cell surface level of PD-1 that may represent an unrecognized element in relieving T exhaustion that can influence the efficacy of anti-PD-1 Ab and restore T cell functionality in cancer immunotherapy.

## **Introduction**

In recent years, anti-PD-1 monoclonal antibodies have become a conventional line of immunotherapy in the successful treatment of numerous advanced cancer malignancies. Antibodies targeting the PD1–PDL1 interaction have now been approved as first-line/ second-line therapies for melanoma, lymphomas, lung cancers, bladder cancer, gastroesophageal cancer, head and neck squamous cell cancer, renal cell cancer, and liver cancer [1]. Despite the promising success in initial treatment responses, a large proportion of patients are either unresponsive or partially responsive and can acquire primary and/or secondary resistance to PD-1 therapy while only a fraction achieve complete responses from PD-1 therapy [2]. Immune suppression within the tumor microenvironment, the phenotype of local immune cell populations, the degree of T cell infiltration, and levels of tumor inflammation are all contributing elements that can affect the efficacy of anti-PD-1 therapy [3]. Therefore, more work is needed to better understand the key T cell intrinsic and extrinsic components that promote a beneficial clinical response to anti-PD-1 therapy.

The primary inhibitory mechanism of PD-1 is contingent on its recruitment of SHP2 and the following SHP2 mediated dephosphorylation of an activated TCR and CD28 receptor. Specifically, anti-PD-1 antibodies have been shown to impart a restorative effect mainly through the CD28 costimulatory pathway and its downstream mediators in a number of studies [4-7]. Furthermore, countless studies have also shown that anti-PD-1 therapies increase cytokine production and proliferative capacities in memory T cells, described as rescue or reinvigoration from T cell exhaustion [5, 6, 8, 9].

Despite these significant advances in elucidating the mechanism of action of anti-PD-1 therapy on restoring functional T cell responses, the trajectory of bound PD-1 antibody-receptor complex and its effect on surface expression of PD-1 in memory T cells has yet to be fully understood. A number of studies have sought to address the spatial localization and transport of PD-1 receptor itself. The paper by Meng, X. et al [10] reported that upregulated PD-1 was internalized, K48-ubiquitinated, and degraded by the proteasome after activation with PHA in a Jurkat cell line. In the paper by Bricogne, C. et al [11], surface PD-1 was shown to be shed in ectosomes and regulated by TMEM16F ion channels in the presence of ionomycin treatment on PD-1-GFP expressing Jurkats. In addition, an early study [12] showed that 3-day OVA peptide stimulated OT-II cells were shown to have the PD-1 receptor localized in endosomal compartments proximal to Golgi matrix proteins and were coexpressed with the trans-Golgi network while absent from recycling endosomes or lysosomes. While a clear agreement on the internalization or transport route of the PD-1 receptor has not been reached, another question

remains if bound PD-1 antibodies affect internalization of PD-1 receptor within the same transport pathways and furthermore, if any potential Fc-dependent mechanisms occur on bound PD-1 antibodies.

The IgG4 subclass in commercially approved PD-1 antibodies such as pembrolizumab (Keytruda®) and nivolumab (Opdivo®) is known to have minimal Fc $\gamma$  receptor (Fc $\gamma$ R) binding which abrogates antibody-mediated interactions such as antibody-dependent cell-mediated cytotoxicity (ADCC) and antibody-dependent cell-mediated phagocytosis (ADCP) in comparison to the more clinically predominant IgG1 subclass of typical monoclonal antibody therapies. In addition, the C1q binding site is disrupted in the IgG4 C<sub>H</sub>2 domain BC and FG loops, resulting in the inhibition of complement dependent cytotoxicity (CDC) [13]. These intrinsic, non-activating characteristics of IgG4 antibodies are currently being utilized or investigated for the blocking/ neutralization of antigens without engagement of host Fc effector functions [14-16]. However, it has been well established that IgG4 antibodies are not completely safeguarded from Fc $\gamma$ R binding and will bind under high avidity or aggregation conditions with high affinity to Fc $\gamma$ RI (CD64) and to a lesser degree, Fc $\gamma$ RIIA (CD32a), Fc $\gamma$ RIIB (CD32b), and Fc $\gamma$ RIIIA (CD16a) [17]. Specifically, the high affinity Fc receptor CD64 was previously believed to be constitutively saturated with monomeric antibodies from the serum, thereby outcompeting binding with monoclonal antibody therapies. However, it is now known that IgG4 antibodies that are complexed or opsonized can bind CD64 with a binding affinity on the same order of magnitude as IgG1 and IgG3 antibodies [18]. Moreover, inside-out-signaling has been shown for CD64, whereby activation by local cytokines/ chemokines induces ITAM phosphorylation on the  $\gamma$ -chain, Fc $\gamma$ R clustering, cytoskeletal rearrangement, and conformational changes which amplifies the IgG4 binding avidity [19, 20].

Recent studies have implicated the engagement of several, different Fc $\gamma$ Rs with mouse and human anti-PD-1 antibodies as a means of tumor resistance, emphasizing the role that anti-PD-1 Fc-FcR crosslinking interactions may have for therapeutic outcomes [21-23]. Furthermore, a non-blocking antibody to PD-1 was able to promote T cell proliferation, cytokine production, and tumor clearance [6], indicating that other antagonistic interactions are involved beyond the blockade of ligand binding site and that further investigation is warranted on these alternative mechanisms.

Here, using primary T cells, we investigated two pharmacologic mechanisms inherent to monoclonal antibody studies: antibody internalization as well as the surface downregulation of its target PD-1 receptor. We utilized commercial blocking anti-PD-1-IgG4 antibodies pembrolizumab and nivolumab as well as NB01, a novel non-blocking antagonistic anti-PD-1-IgG4 antibody that binds on the opposite face of the PD-1-PD-L1 interaction site. We sought to investigate whether PD-1 antibodies functioned differently based on their binding site and whether the combination of blocking and non-blocking PD-1 antibodies produced an additive effect. Furthermore, we investigated whether the different PD-1 antibodies were capable of downregulating surface PD-1 levels and the mechanisms that were involved. Our results confirm that anti-PD-1 therapies are internalized in PD-1<sup>+</sup> memory T cells at a fixed rate but the downregulation of surface PD-1 receptor is dependent on the presence of CD14<sup>+</sup> HLA-DR<sup>+</sup> monocytes. In addition, the frequency of monocytes in PBMCs proved to be a reliable indicator for the effect of PD-1 downregulation and antibody-Fc $\gamma$ R interactions were mediated primarily through CD64.

## Results

### **Surface PD-1 downregulation observed in exhausted memory T cells from HIV infected donors when treated with anti-PD-1 antibodies**

In our preliminary observations, PBMCs isolated from chronically infected HIV<sup>+</sup> donors were treated with various anti-PD-1-IgG4 antibodies (pembrolizumab, NB01, or pembrolizumab + NB01) in order to evaluate any intrinsic immunomodulatory effects on exhausted memory CD4 and CD8 T cells. Due to the physiologically high expression of the PD-1 receptor on memory T cells in chronically infected donors, we were able to assess the changes in surface PD-1 levels when samples were treated with antibodies over a period of days (Figure 1A, B). We observed that PD-1 expression was gradually reduced from steady state when treated with all three antibody conditions, the greatest effect seen with

the combination therapy. Combination therapy with pembrolizumab and NB01 significantly reduced surface PD-1 levels after 6 hours of incubation while all three antibody conditions were significantly decreased by the 24-hour time point in comparison to the IgG4 control.

Furthermore, PD-1 surface expression steadily dropped for the following days before plateauing to approximately 18% surface expression on both memory CD4 and CD8 for the combination therapy, representing over a 71% decrease from baseline (Figure 1C). Separately, pembrolizumab reached to 61% decrease in PD-1 expression and NB01 was seen as a 50% decrease compared to the IgG4 control by 72 hours. While anti-PD-1 antibodies were effective in reducing the overall expression of PD-1, a complete abrogation of PD-1 expression did not occur. Furthermore, total memory CD4 and CD8 T cells frequencies as well as the proportion of live CD3<sup>+</sup> cells remained steady across antibody conditions, confirming that the depletion of PD-1 expressing T cells was not a factor for PD-1 receptor downregulation (Supplemental). The addition of anti-PD-L1 in parallel with pembrolizumab or IgG4 control had no impact on the downregulation of PD-1 expression, which validated that the blockade of PD-1-PD-L1 interaction was not a contributing factor in the decline of PD-1 surface expression on memory T cells (Supplemental).

### **Surface PD-1 downregulation kinetics occurs at a slower rate than PD-1 antibody internalization and requires the presence of effector cells within the PBMC composition**

In order to determine if antibody induced surface PD-1 downregulation was related to the internalization of antibody-receptor complex, we used pHrodo fluorophores conjugated to antibodies to quantify the total amount of endocytosed anti-PD-1 antibodies. The pHrodo compound acts as a pH indicator, remaining undetectable with low background at neutral pH and increasing in fluorescence as acidity in its immediate environment increases. pHrodo conjugation was performed on pembrolizumab, NB01, nivolumab, and IgG4 isotype control antibodies and the conjugated antibodies performed similarly to their respective unconjugated antibody formats in terms of PD-1 downregulation (data not shown).

We measured surface PD-1 downregulation and PD-1 antibody internalization simultaneously by flow cytometry, looking at earlier time-points due to the fact that endocytotic events are typically rapidly induced and occur within minutes to hours. We also compared two cell type compositions, total PBMCs and purified T cells, to see if either the downregulation and/or internalization was T cell intrinsic or required the help of bystander effector cells. Kinetic rates of PD-1 antibody internalization and surface PD-1 downregulation were measured by linear regression analysis.

Within the first hour, the PD-1 antibodies did not show major increases in the total amount of internalized antibody compared to the IgG4 control (Figure 2B). However, from 3-6 hours, all three PD-1 antibodies were significantly internalized in memory CD4 and CD8 and a clear divergence was shown between the PD-1 antibodies, with NB01 having the highest total amount internalized followed by pembrolizumab and nivolumab. The rate of internalization per hour for each antibody condition in total PBMC conditions: NB01 3.4% and 8.0%, pembrolizumab 2.3% and 4.8%, and nivolumab 1.6% and 4.5% for memory CD4 and CD8, respectively (Figure 2D). Isolation of T cells also showed a small, significant increase in the rate of internalization for memory CD8. However, the total PBMC and purified T cell compositions did not show any significant differences in the total amount of internalized PD-1 antibody, which verified that memory CD4 and CD8 were internalizing bound anti-PD-1 antibody, independent of the presence of other cell populations.

In contrast, surface PD-1 downregulation showed that pembrolizumab and nivolumab had a greater effect in reducing surface PD-1 levels while NB01 was less effective than the two. The rate of surface PD-1 downregulation per hour for each antibody condition in total PBMC conditions: NB01 -1.4% and -3.9%, pembrolizumab -2.1% and -4.9%, nivolumab -2.2% and -4.8% for memory CD4 and CD8, respectively (Figure 2D). Furthermore, the total PBMC condition was able to downregulate surface PD-1 as seen before but purified T cells were severely obstructed in downregulating PD-1 for all three anti-PD-1 antibodies, indicating that an effector population was necessary for the downregulation effect and was removed upon the isolation of CD3<sup>+</sup> T cells.

Finally, we visually inspected the quantity of internalized antibody-vesicles in CD3<sup>+</sup> T cells by confocal microscopy after 6 hours (Figure 2F). The increased antibody internalization for NB01 antibody that was previously observed by flow cytometry was shown as more vesicles per PD-1<sup>+</sup> CD3<sup>+</sup> T cells compared to pembrolizumab.

### **Inhibition of dynamin and actin mobilization prevents both surface PD-1 downregulation and PD-1 antibody internalization in memory T cells while dasatinib selectively impairs monocyte FcγR cross-linking of T cell bound PD-1 antibodies**

We next sought to determine the pathways involved in surface PD-1 downregulation and used a diverse panel of chemical inhibitors targeting endocytosis, actin mobilization, protein degradation, and transport pathways (Figure 3a). Inhibition of dynamin mediated endocytosis (dyngo4a) as well as actin mobility (cytochalasin D, CK666, rhosin) and lysosomal activity (bafilomycin A) were all shown to prevent antibody induced surface PD-1 downregulation. Protein synthesis inhibitor cycloheximide was also shown to inhibit PD-1 downregulation, which can be attributed to pleiotropic effects on cytoskeletal rearrangement. Proteasomal degradation, which was inhibited by MG132, has recently been described as the physiological route for PD-1 receptor turnover [10]. In our experiments, we observed that the inhibition of proteasome had an insignificant impact on anti-PD-1 mediated downregulation. This indicated that the homeostatic PD-1 receptor turnover in the absence of antibody and PD-1 receptor downregulation in the presence of bound antibodies were controlled by distinct processes.

Broad MMP inhibition with EDTA, exosome secretion inhibition with GW4869, mTOR inhibition with rapamycin, and protein transport inhibition with monensin or brefeldin A had a non-significant or no effect on surface PD-1 downregulation. Finally, we found that SFK inhibitors dasatinib and PPI as well as 3-MA, an autophagy inhibitor, were able to prevent PD-1 downregulation on memory T cells.

We further investigated six of these inhibitory compounds (rhosin, dyngo4a, CK666, 3-MA, dasatinib) that were able to significantly inhibit surface PD-1 downregulation to validate their effects on PD-1 downregulation and PD-1 antibody internalization in tandem. Here, we observed that rhosin, dyngo4a, and CK666 were able to effectively prevent both PD-1 antibody internalization and PD-1 downregulation in the memory T cell populations (Figure 3b). On the other hand, dasatinib and 3-MA inhibited surface downregulation of PD-1 but had no inhibitory effect on the internalization of PD-1 antibody and rather slightly increased the total amount of internalized PD-1 antibody in T cells compared to the no inhibitor control.

We selected dasatinib for further investigation on different PBMC subsets (memory CD4, memory CD8, B cells, NK cells, monocytes, and dendritic cells) in a pulse-chase experiment using pHrodo-conjugated PD-1 antibodies preloaded onto T cells and the supernatant replaced with their respective unlabeled antibodies. The cross-linking of immune complexes and FcR produces endocytic/phagocytic responses that require the recruitment of Src kinases and activation of Syk in myeloid and granulocytic cells. [24-26] Dasatinib, which was initially designed as a kinase inhibitor against Bcr-Abl for myeloid leukemia and gastrointestinal stromal tumors, is known to have a wide range of targets within Src family kinases (SFK) and inhibits FcR function [27-29].

In untreated PBMC, the amount of internalized PD-1 antibodies was found to be the highest in the monocyte population (HLA-DR<sup>+</sup> CD14<sup>+</sup> CD11b<sup>+</sup>), indicating that this was likely the main effector population responsible for the removal of PD-1 antibody bound on memory T cells (Figure 3D). We also found that B cells (CD19<sup>+</sup>) and to a small degree, dendritic cells (Lin<sup>-</sup> CD14<sup>-</sup> HLA-DR<sup>+</sup>) were also involved in the adsorption and internalization of T cell bound PD-1 antibody. With the dasatinib treatment, only monocyte mediated PD-1 antibody transfer and internalization was drastically reduced and represented the highest proportional loss, signifying that the increased levels of PD-1 surface expression on memory T cells under dasatinib were due to the inhibition of monocytic activity in antibody uptake and likely to be the main effector population.

### **Antibody mediated PD-1 downregulation requires the presence of monocytes and is mediated by the binding of PD-1 antibody Fc domain with Fc receptor CD64**

Given that the PBMC subsets that uptake PD-1 antibodies have high expression of Fc receptors, we next asked if the interaction of surface PD-1 downregulation was contingent on availability of Fc receptors for binding the Fc domain of the PD-1 antibodies. We found that Fc $\gamma$ R blockade in the presence of PD-1 antibodies had no impact on the internalization of PD-1 antibodies in memory T cells (Figure 4A). On the other hand, Fc $\gamma$ R blockade had a drastic effect on the downregulation of surface PD-1 for all three antibody conditions, demonstrating that the activity of Fc $\gamma$ R interaction is necessary to observe PD-1 downregulation on memory T cells.

Next, we performed the PD-1 downregulation experiment over days using total PBMC, purified T cells, and purified T cells reconstituted with their autologous CD3<sup>-</sup> or CD14<sup>+</sup> fractions at a 5:1 ratio. Purified T cells did not have a significant reduction in surface PD-1 expression compared to its IgG4 control throughout the time course; however, reconstitution of autologous populations brought downregulation kinetics to similar levels as the PBMC control, verifying that effector PBMC subsets in CD3<sup>-</sup> or CD14<sup>+</sup> fractions were necessary for PD-1 surface downregulation (Figure 4C).

We also checked in ten HIV<sup>+</sup> donors for the percent downregulation of surface PD-1 under anti-PD-1 treatment compared against the relative frequencies of different PBMC subsets. While some correlations were observed in dendritic cells ( $r = 0.467$ ,  $p = \text{n.s.}$ ) and B cells ( $r = -0.532$ ,  $p = \text{n.s.}$ ), only the frequencies of monocytes were significantly correlated with surface PD-1 downregulation ( $r = 0.777$ ,  $p < 0.01$ ) after 24 hours (Figure 4D).

We used transfected 293T cells expressing CD32, CD64, CD32 + CD64, or empty vector control and cocultured with primary T cells to distinguish the Fc receptor responsible for PD-1 downregulation. We observed that both CD32 and CD64 strongly reduced PD-1 levels on memory T cells; however, CD64 alone had a more pronounced effect on PD-1 levels which were significantly lower than the CD32 alone (Figure 4E). The co-transfection of CD32 and CD64 did not augment the downregulation effect in comparison to CD64 alone, indicating that CD64 alone represented the bulk of this interaction. We also checked for CD16a activity using a stable transfected Jurkat cell line but this Fc receptor did not have any impact on PD-1 downregulation (Supplemental). Lastly, we verified whether ADCP was a factor in the downregulation of PD-1 in memory T cells by using autologous monocytes and differentiated macrophages. None of the anti-PD-1 antibodies increased the proportion of phagocytosed T cells compared to the IgG4 control (Supplemental).

### **FcR-mediated anti-PD-1 downregulation enhances CD8 proliferation under antigen-specific stimulation**

We next addressed the functionality of PD-1 downregulation under antigen-specific conditions. F(ab')<sub>2</sub> variants of pembrolizumab and NB01 were generated to make antibodies that retained antigen binding sites but lacked Fc effector binding. In a six day stimulation experiment using pooled Gag peptides, significantly higher proliferation was observed for all standard antibody conditions in memory CD8 compared to their respective F(ab')<sub>2</sub> variants (Figure 5B). All 3 full antibody conditions as well as combination of pembrolizumab F(ab')<sub>2</sub> + NB01 F(ab')<sub>2</sub> were significantly increased in proliferation compared to the peptide + IgG4 control while pembrolizumab F(ab')<sub>2</sub> nor NB01 F(ab')<sub>2</sub> was not significantly increased. Furthermore, PD-1 expression was significantly decreased when using the standard format of the PD-1 antibodies compared to their their respective F(ab')<sub>2</sub> variants. Of note, the PD-1 F(ab')<sub>2</sub> antibodies individually and in combination were able to significantly reduce PD-1 expression compared to the control but to a much lesser degree than the full antibodies. The lower total availability of PD-1 receptor during antigenic stimulation is likely to drive the increased proliferative capacities of exhausted PD-1<sup>+</sup> CD8 T cells. Given that the anti-PD-1 F(ab')<sub>2</sub> antibodies were unable to efficiently reduce PD-1 expression, their impact on antigen-specific CD8 proliferation was shown to be reduced compared to their respective full antibodies.

## Discussion

In this study, we have shown that PD-1 antibody internalization and PD-1 surface downregulation occur as distinct processes. To our knowledge, this is the first reported study showing primary human T cells engaging in the active internalization of anti-PD-1 antibodies. We also showed that the standard IgG4 format of anti-PD-1 antibodies is necessary to engage Fc receptors on monocytes and that the downregulation of PD-1 has a distinct effect in restoring T cell functionality, regardless of receptor blockade.

The internalization of anti-PD-1 antibodies in memory T cells was shown to be more rapidly induced and occurred regardless of the composition of its surrounding cells in a T cell intrinsic process. While antibody internalization could possibly be attributed to inherent surface PD-1 turnover, we did not observe any increases in surface PD-1 expression with MG132 inhibition of the proteasome compared to the no inhibitor control, indicating that proteasomal receptor degradation was not a factor in regulating PD-1 surface expression. This was in contrast with a previous report that showed PD-1 surface expression increasing when the proteasomal degradation pathway was blocked [10]. However, the regulation of activation induced PD-1 expression under stimulation conditions compared to the PD-1 exhaustion profile acquired *in vivo* in the course of chronic viral infection that we used in this study may explain this disparity. Furthermore, when memory T cells were treated with bafilomycin A, we saw an increase in surface PD-1 expression, which indicated that anti-PD-1 antibody binding directed the lysosomal degradation of the PD-1 receptor.

The downregulation of total surface PD-1 expression in memory T cells occurred more slowly, reaching its peak at 24-48 hours and required the presence of Fc receptor expressing cells. Monocytes were shown to be the cell subset with the highest impact for the PD-1 downregulation effect within the PBMC composition and increased monocyte frequencies positively correlated with the degree of surface PD-1 downregulation. Numerous studies have shown that with monoclonal antibody therapies targeted against CD4, CD20, CD25, CD38, HER2, CTLA-4, PD-1, and PD-L1, Fc $\gamma$ R-expressing effector cells such as monocytes, macrophages, and granulocytes imparted a significant effect onto target cells by the crosslinking of the Fc domain of target antibody bound to its antigen and an Fc $\gamma$ R *in trans* [23, 30-36]. Above all, the effects of anti-CD20 antibodies on downregulating surface CD20 expression has been heavily investigated over the past decade. The recent paper by Dahal, L. et al showed that the internalization and the downregulation of anti-CD20 antibodies occurred as separate processes whereby the downregulation of anti-CD20 on opsonized B cells occurred as a byproduct of phagocytotic events by macrophages in conditions where phagocytic capacity was inhibited due to bead uptake and saturation [37]. Moreover, the authors found that obinutuzmab, a type II anti-CD20 antibody with low internalization capacity, had increased receptor downregulation in primary CLL samples mediated by monocyte-derived macrophages. The culmination of these reports show that antibody mediated receptor downregulation represents an underappreciated but consistently observed effect that has the potential to dictate the outcomes in mAb therapies.

In our work, we have clearly shown that the availability of Fc $\gamma$ R binding was critical in observing PD-1 downregulation as shown by the Fc $\gamma$ R blockade experiments. Additionally, the transfection studies revealed that the Fc $\gamma$ R CD64 was primarily responsible for producing this effect. CD64 expression is mainly expressed on monocytes/macrophages and monocyte-derived DCs while inducible in neutrophils, eosinophils, and mast cells and therefore, the likely mediators of this interaction by homeostatic abundance would be the monocytic population [38]. In the work by Kreig, C, et al., higher frequencies of CD14<sup>+</sup> CD16<sup>-</sup> HLA-DR<sup>+</sup> CD64<sup>+</sup> monocytes were shown to be a positive indicator for anti-tumor responses in anti-PD-1 therapy measured by progression-free survival and overall survival in responders compared to non-responders in stage IV melanoma [39]. While the authors did not conclude on the mechanism that drove this finding, we believe that antibody induced PD-1 downregulation linked with higher monocytic frequencies may play a role in this observation.

We also showed that CD32a was capable of inducing downregulation but the effects were significantly lower in comparison to CD64. CD32a has been previously implicated in other studies to mediate downregulation of anti-CD20 bound surface receptors, in particular, by neutrophils which constitutively express high levels of CD32a and CD16b [40, 41]. Within physiological conditions, neutrophils are likely to play a role in downregulating surface receptors bound by antibodies as well.

There are reports that show that PD-1 antibodies are affected by Fc-Fc $\gamma$ R interactions and other groups have evaluated detrimental effects in the functional activity of PD-1 antibodies when engaging Fc receptors on macrophages within the tumor microenvironment. Lo Russo et. al. showed that Fc-FcR interactions with nivolumab aided in tumor progression in SCID mice with patient-derived xenografts from NSLC hyperprogressive patients [21]. Furthermore, Arlauckas and colleagues showed reduced treatment efficacy with anti-PD-1 transfer and uptake by macrophages in C57BL6/J mice with MC38 murine adenocarcinoma [22]. In both studies, while the specific Fc receptors involved were not clearly explicated, experiments with Fc receptor blockade or F(ab)<sub>2</sub> antibodies showed tumor size reduction in their *in vivo* model. This stood in contrast with our results which showed a significantly increased functional recovery of memory CD8 T cells when using the complete mAb format over its respective F(ab')<sub>2</sub> variant. A possible explanation for this discrepancy would be the population of macrophages that make up the tumor microenvironment in an *in vivo* model. The phenotype of tumor-associated macrophages (TAM) in the tumor milieu is governed by the presence of cytokines and growth factors that regulate differential expression levels of CD64 as well as M1/M2 polarization. Increasing levels of inflammatory IFN $\gamma$  or anti-inflammatory IL-10 have both been shown to drive CD64 expression on tissue macrophages, which indicates that both anti- and pro-tumorigenic responses can produce effector myeloid cells capable of downregulating PD-1 expression on T cells [38]. Nonetheless, a higher M1-/M2-like ratio has been shown for various cancer types to be a predictor for better prognosis [42-44]. A limitation of our study was the use of an *ex vivo* system with monocytes as the primary mediator of this interaction and thereby losing the effect of tumor polarized macrophages and the cytokine composition of the tumor microenvironment. However, the use of human anti-PD-1 antibodies with human primary cells in our study represents a simpler yet relevant model to reveal the possible human Fc-FcR interactions in PD-1 therapy that can be further investigated. We have shown that with antigen-specific stimulation of memory CD8, Fc $\gamma$ R engagement and subsequent downregulation of PD-1 is superior for driving proliferation than PD-1 binding alone.

Throughout our experiments, we found dasatinib to be an effective inhibitor of monocyte mediated PD-1 downregulation. This is due to the impairment of Fc $\gamma$ R crosslinking functionality regulated by the inhibition of associated SFK and the ensuing prevention of ITAM phosphorylation on Fc $\gamma$ R cytoplasmic tail [28]. We also found that dasatinib did not affect dynamin-mediated endocytosis as T cell internalization of PD-1 antibodies remained unperturbed. The use of dasatinib is currently being investigated in combination with anti-PD-1 therapy in a phase I clinical trial for the targeted repression of DDR2 with immune checkpoint inhibition in advanced non-small lung cancer [45]. As the presence of immunosuppressive macrophages is generally associated with poor prognosis and tumor progression, the loss of an anti-PD-1 downregulation mechanism and its effector cells may be inconsequential in comparison to chemotherapeutic targeting of DDR2, which was shown to sensitize cancer cells to anti-PD-1 therapy and increased CD8<sup>+</sup> infiltration. However, the role of macrophages within the tumor microenvironment remains contentious and the depletion of existing anti-tumor macrophages may be detrimental to controlling tumor burden. A more conciliatory approach would be the reprogramming TAMs to a more proinflammatory phenotype such as the use of CD40 agonists, anti-MACRO or PI3K $\gamma$  antagonists in parallel with anti-PD-1 therapy which would be able to increase anti-tumor effects of tissue resident macrophages while increasing CD64 expression and mediating PD-1 downregulation [46, 47].

The results presented in this report show the relevance of an alternative, FcR mediated mechanism by which PD-1 antibodies can downregulate the expression of PD-1 on memory T cells, regardless of a ligand blocking interaction. While all PD-1 antibodies tested were able to effectively internalize in memory T cells, the downregulation of the PD-1 receptor itself was reliant on CD64 expressing monocytes, leading to implications for the prediction of efficacy in anti-PD-1 therapy. Thus, our

findings emphasize the necessity of understanding the interactions of PD-1 mAb therapy within a complete immunological setting and further investigations are needed to distinguish the influence of CD64, other potential FcRs, and the immune cell subsets that express them for PD-1 therapy in clinical settings.

## **Materials and Methods**

### **Study samples and cell lines**

Twelve HIV+ viremic donors were used throughout in this study. PBMCs were maintained in complete RPMI (Invitrogen) supplemented with 10% heat-inactivated fetal bovine serum (FBS, Biowest), 100 U/ml penicillin (BioConcept), and 100 µg/ml streptomycin (BioConcept). 293T cells were maintained in DMEM (Invitrogen) supplemented with 10% (v/v) FBS, 100 U/ml penicillin (BioConcept), and 100 µg/ml streptomycin (BioConcept). Cells were kept at 37°C, 5% CO<sup>2</sup> for the following experiments.

### **Antibodies and reagents**

The following antibodies were used in this study: anti-CD3 (OKT3), anti-CD4 (RPA-T4), anti-CD8 (RPA-T8), anti-CD45RA (HI100), anti-CD14 (61D3), anti-HLA-DR (G46-6), anti-CD11b, anti-CD56 (HCD56), anti-CD19 (HIB19), anti-CD16 (3G8), anti-CD32 (FUN-2), anti-CD64 (10.1), anti-PD-L1 (29E.2A3). Anti-PD-1 antibodies pembrolizumab (Merck), nivolumab (Bristol-Myers Squibb), and NB01 were used for experimental conditions and for the primary staining of PD-1 with their respective antibody condition. Anti-human IgG Fc secondary antibodies conjugated with Alexa Fluor 594 (Biolegend) or APC (Biolegend) were used for the detection of surface PD-1 expression. Preclinical grade IgG4 isotype control (Bingo Bio) was as a negative control for all anti-PD-1 experiments.

### **pH-sensitive dye conjugation**

200 µg of anti-PD-1 antibody or IgG4 isotype control was concentrated with Amicon® Ultra-0.5 50 kDA spin filter (Millipore) at 12'000 g for 10 minutes. 100 µL of 4 mM TCEP solution (Thermo) was added to the spin column, mixed by pipetting, and incubated for 30 min at 37°C before washing two times in PBS and resuspension with PBS at 100uL. 10 mM pHrodo™ Red or pHrodo™ Green maleimide (Thermo) solution was freshly prepared with DMSO and a 10 molar ratio excess of pHrodo maleimide was added to the antibody and incubated for 2 hours at 37°C. After conjugation, antibody-pHrodo mixture was washed four times in PBS and resuspended in 200 µL of PBS followed by filter sterilization with Ultrafree-MC Centrifugal Filter 0.22 µm (Merck). Protein concentration and degree of labeling were measured as described in the manufacturer's protocol. (Thermo)

### **Surface PD-1 downregulation /antibody internalization assay**

PBMCs from selected donors were thawed and rested overnight at 37°C. PBMCs were then treated with 5 µg/mL with different anti-PD-1 antibodies with or without pHrodo conjugation and 5 µg/mL of IgG4 isotype control in complete RPMI for hours to days depending on the length of the experiment. Cells were washed at each time point and stained again with the combination of blocking and non-blocking anti-PD-1 antibodies to quantify total surface PD-1 before proceeding to extracellular staining for memory T cells. Internalized PD-1 antibody was measured as fluorescence intensity from pHrodo Red or Green. All flow cytometry measurements were obtained on BD Fortessa.

T cell isolation was performed with EasySep™ Human T Cell Isolation Kit, CD3- fraction was isolated from the supernatant after magnetic attachment using the EasySep™ Human CD3 Positive Selection Kit II, and the CD14+ fraction was isolated using EasySep™ Human Monocyte Enrichment Kit without CD16 Depletion kit.

### **Inhibitors**

Chemical compounds selected for inhibiting protein endocytosis, transport, and degradation pathways were used at the following concentrations: EDTA (100 µM), cycloheximide (5 µg/mL), cytochalasin D (100 nM), monensin (2 µM), brefeldin A (10ug/mL), rapamycin (1 µM), PP1 (20 µM), dasatinib (1 µM), MG132 (250 nM), CK666 (150 µM), rhosin (200 µM), dyngo4a (60 µM), bafilomycin A (500 nM), 3-methyladenine (5mM), GW4869 (5 µM). Inhibitors were titrated for the highest usable

concentration with minimal cytotoxicity in complete RPMI within a 24-hour incubation period for experiments. PBMCs were pretreated with each inhibitor for 1 hour at 37°C before the addition of anti-PD-1 antibodies at 5 µg/mL and the continuation of internalization / downregulation experiments for 24 hours with subsequent surface staining followed by flow cytometry.

### **Confocal microscopy**

PBMCs were incubated with pHrodo-PD-1 or pHrodo-IgG4 antibodies for six hours at 37°C. PBMCs were then stained with anti-CD3-APC for 20 minutes in PBS/ 2% FBS solution. Cells were washed, resuspended in Live Cell Imaging Solution (Thermo) and transferred to 8-well glass bottom Lab-Tek™ II Chamber Slides (Nunc) coated with poly-L-lysine, then adhered for 30 minutes at 37°C before taken for microscopy imaging. Confocal images were taken on a Zeiss LSM 880 Airyscan and image analysis was done with ImageJ.

### **Pulse-chase experiment with pHrodo-conjugated antibodies**

PBMCs were incubated with 5 µg/mL anti-PD-1-pHrodo antibodies for 30 minutes at 4°C in the presence of Human Trustain FcX block (Biolegend). Cells were washed twice and resuspended in complete RPMI containing 5 µg/mL of their respective unlabeled antibodies and incubated for 24 hours with or without dasatinib treatment at 1 µM. Surface panel for different PBMC subset compositions were used and internalized pHrodo-antibody was detected within the subsets by flow cytometry.

### **Fc receptor blockade**

PBMCs were set up for PD-1 downregulation and internalization assay as before but in the presence of 50µg/mL of human IgG4 (Sigma) and 50µg/mL of anti-CD32 / CD64 (Biolegend) for unspecific and specific blocking of the Fc receptors. PBMCs were incubated with FcR blocking antibodies for 1 hour at 37°C before the addition of pHrodo-PD-1 antibodies at 5 µg/mL and the continuation of the internalization / downregulation experiments for 24 hours and subsequent surface staining followed by flow cytometry.

### **293T transfection of CD32 and CD64**

Low passage HEK293T cells were seeded into 6-well plates and kept overnight at 37°C for attachment. Plasmids for CD32a and CD64 (Sino Biological) were incorporated into Fugene HD transfection reagent (Promega), resuspended in OptiMEM (Invitrogen) and added onto confluent cells for 6 hours. Cells were washed and resupplied with complete DMEM and kept in the incubator for 24 hours before detachment and seeding into flat-bottom 96 wells. Purified primary T cells were isolated as previously described above and added at a 1:2 ratio (293T: T cells) and cocultured for 48 hours before extracellular staining and FACS analysis.

### **F(ab')<sub>2</sub> preparation**

PD-1 antibodies were cleaved using a modified IdeS protease FabRICATOR (Genovis) into F(ab')<sub>2</sub> and Fc fragments at 1 unit per µg of antibody for 30 minutes at 37°C and buffer exchange was done using 50 kDa Amicon® spin filters (Merck). Free Fc fragments were removed using Pierce™ protein A columns (Thermo) and purity was assessed by SDS-PAGE/ Coomassie blue.

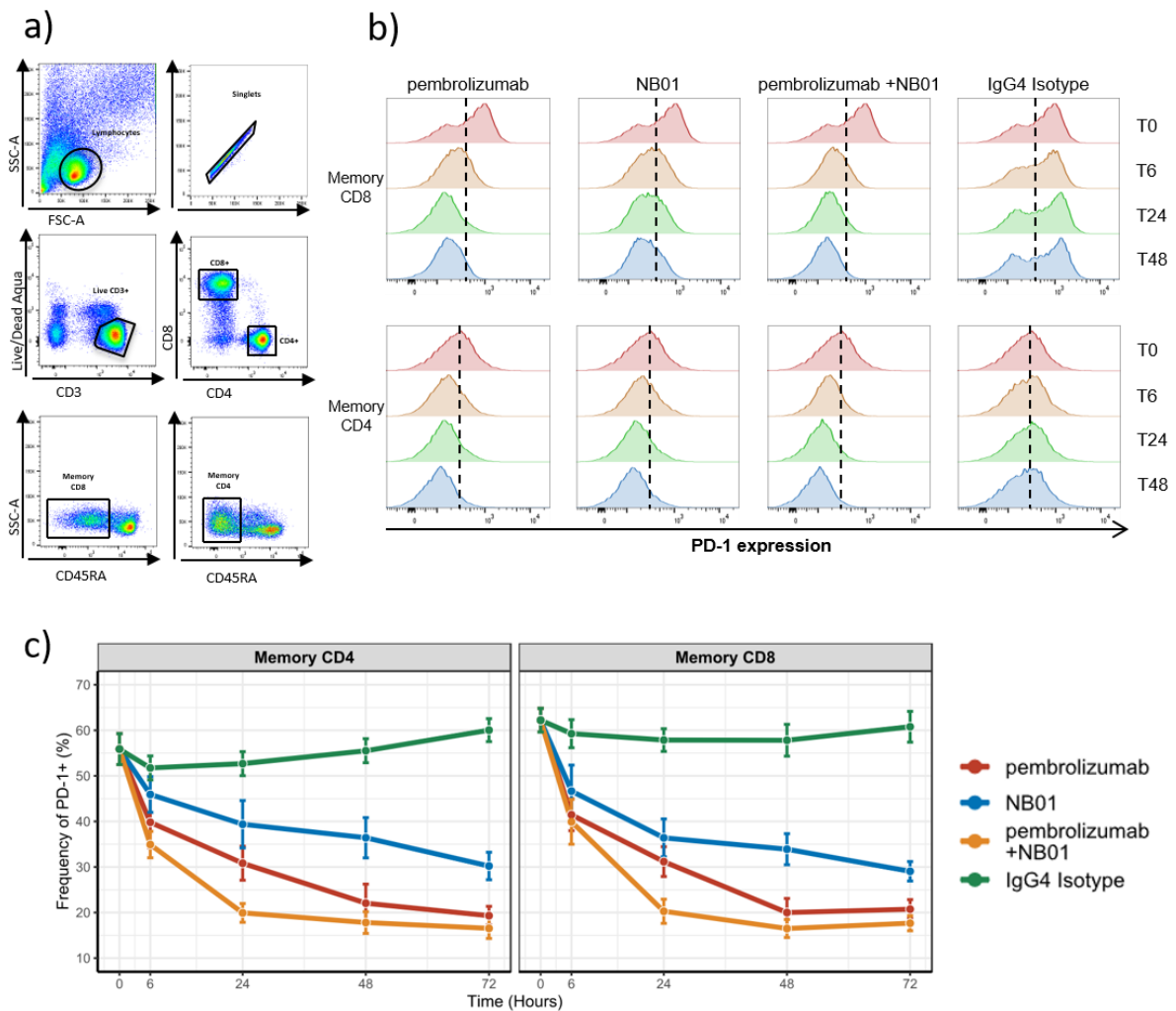
### **Macrophage polarization and ADCP assay**

Primary monocytes from healthy donors were enriched and plated into 6-well plates at 1 million cells per mL. For M1 polarization, GM-CSF was added at 50 ng/mL and for M2 polarization, M-CSF was added at 50 ng/mL for 3 days before washing and supplementing for an additional 3 days. Afterwards, M1- and M2-polarized macrophages were further activated for an additional 2 days. M1 macrophage activation was induced by GM-CSF (50 ng/mL), IFN-γ (20 ng/mL), and LPS (20 ng/mL) while M2 macrophage activation was induced by M-CSF (50 ng/mL) and IL-4 (50 ng/mL). Autologous primary T cells were isolated and stained with CFSE/ CTFR before co-culture with differentiated macrophages at 5:1 ratio. Anti-PD-1 antibodies were added at 5 µg/mL and ADCP was measured in CD11b<sup>+</sup> CD14<sup>+</sup> macrophages 24 hours later by flow cytometry.

### **Statistical Analyses**

Statistical significance was obtained either using a two-tailed, unpaired parametric t-test analysis with Welch's corrections for comparison of frequencies or by one-way analysis of variance (ANOVA) for multiple group comparisons with Bonferroni's correction when necessary. Linear regression was used to calculate slope kinetics and Pearson's correlation test was used for correlation coefficients.

**Figure 1**



**PD-1 antibody mediated downregulation of surface PD-1 receptors on memory T cells from chronic HIV donors. (A)** Gating strategy for memory CD4 and CD8 T cells. **(B)** Representative histogram profiles of PD-1 expression on memory T cells over days when treated with 5ug/mL of PD-1 antibodies pembrolizumab, NB01, or the combination of pembrolizumab and NB01. **(C)** Kinetics of surface PD-1 downregulation over 72 hours with same antibody conditions as (B) in 5 different donors.

**Figure 2**

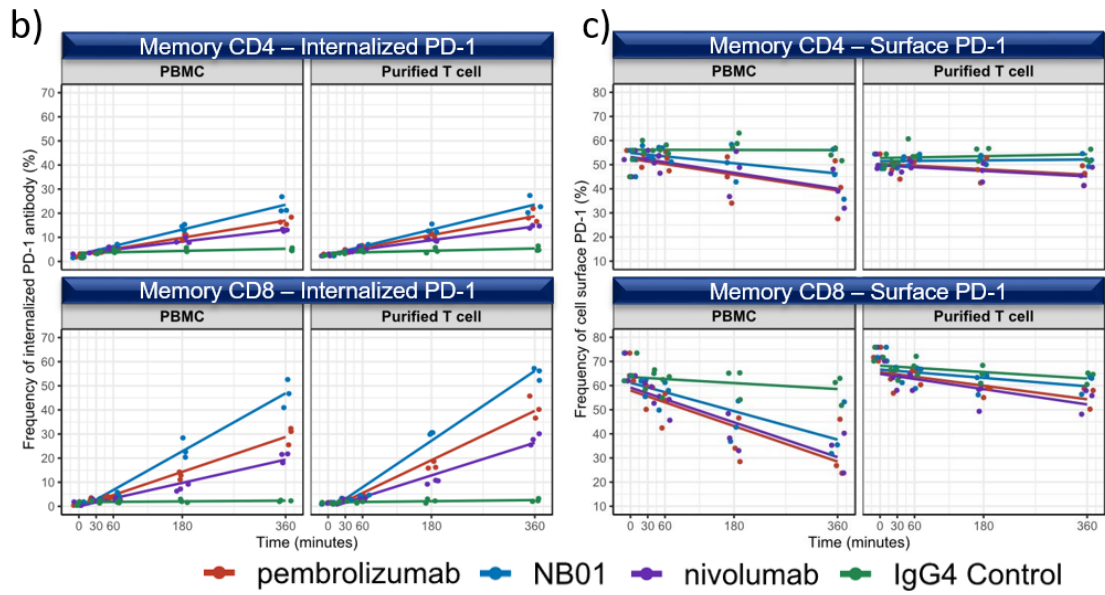
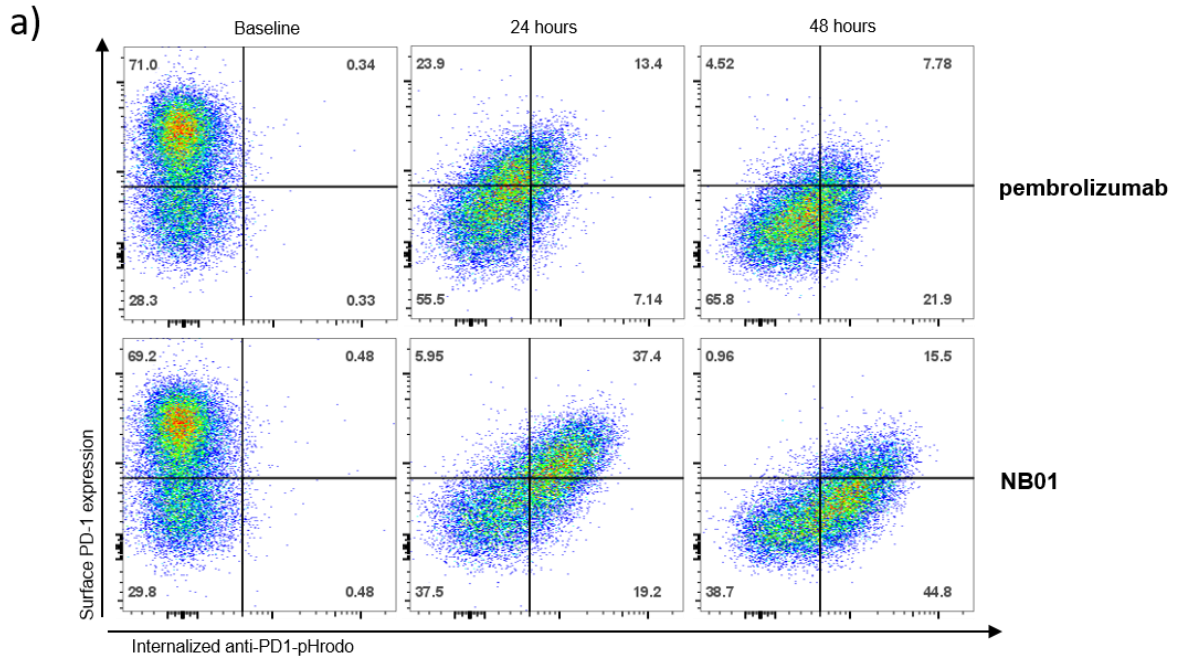
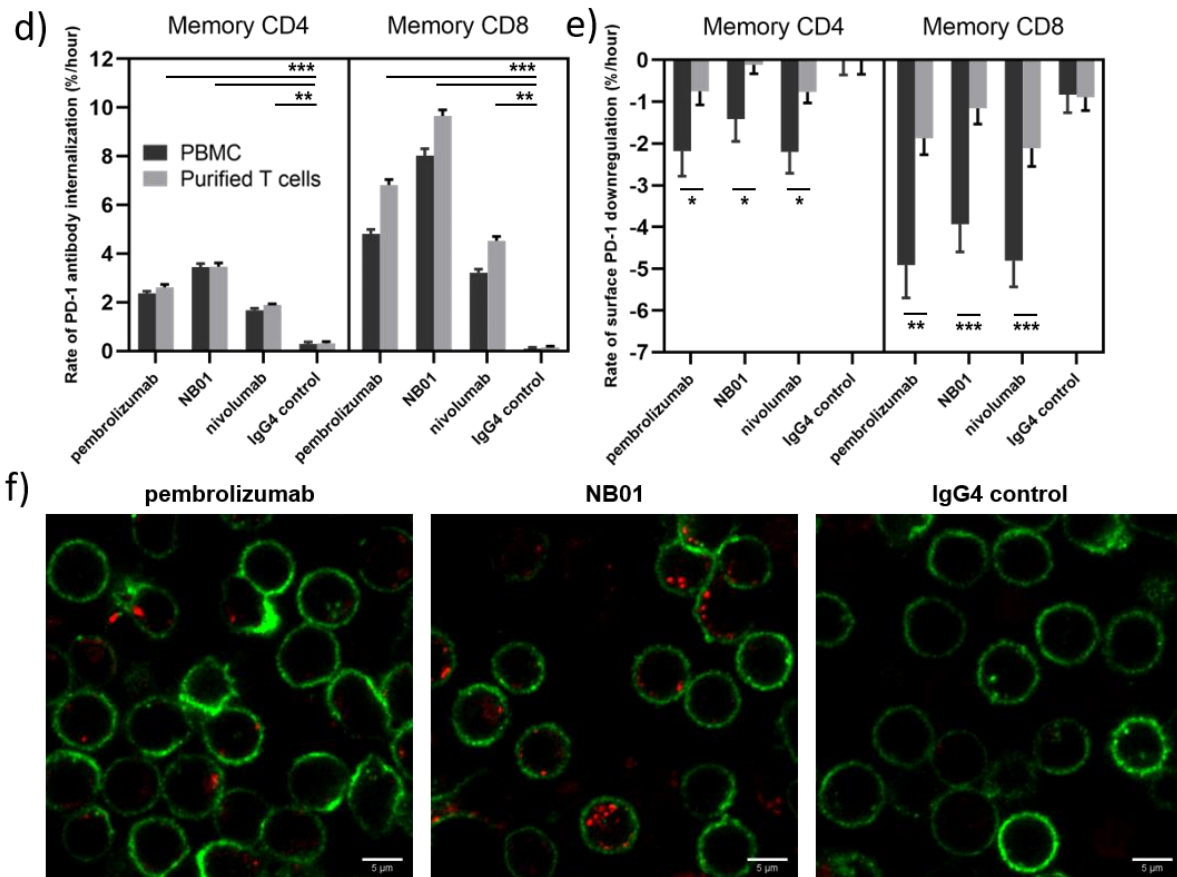


**Figure 2 cont.**



**Internalization of PD-1 antibodies and the downregulation of PD-1 surface receptor induced by anti-PD-1 antibodies occur at different rates and surface PD-1 downregulation is contingent on the presence of effector cells. (A)** PD1 surface expression vs internalized anti-PD-1 antibody measured over 24 and 48 hours in memory CD8. Early time-points (0, 30, 60, 180, and 360 minutes) measured for **(B)** internalized PD-1 antibody and **(C)** PD-1 downregulation in memory T cells with PBMC or purified T cell compositions using pembrolizumab, nivolumab, NB01, or IgG4. (n=3, linear regression model) **(D)** Kinetic rate of antibody internalization and **(E)** rate of surface receptor downregulation. **(F)** Live cell imaging of T cells incubated for 24 hours with pHrodo conjugated pembrolizumab, NB01, or IgG4 (red) costained with CD3 (green) for T lymphocyte detection

**Figure 3**

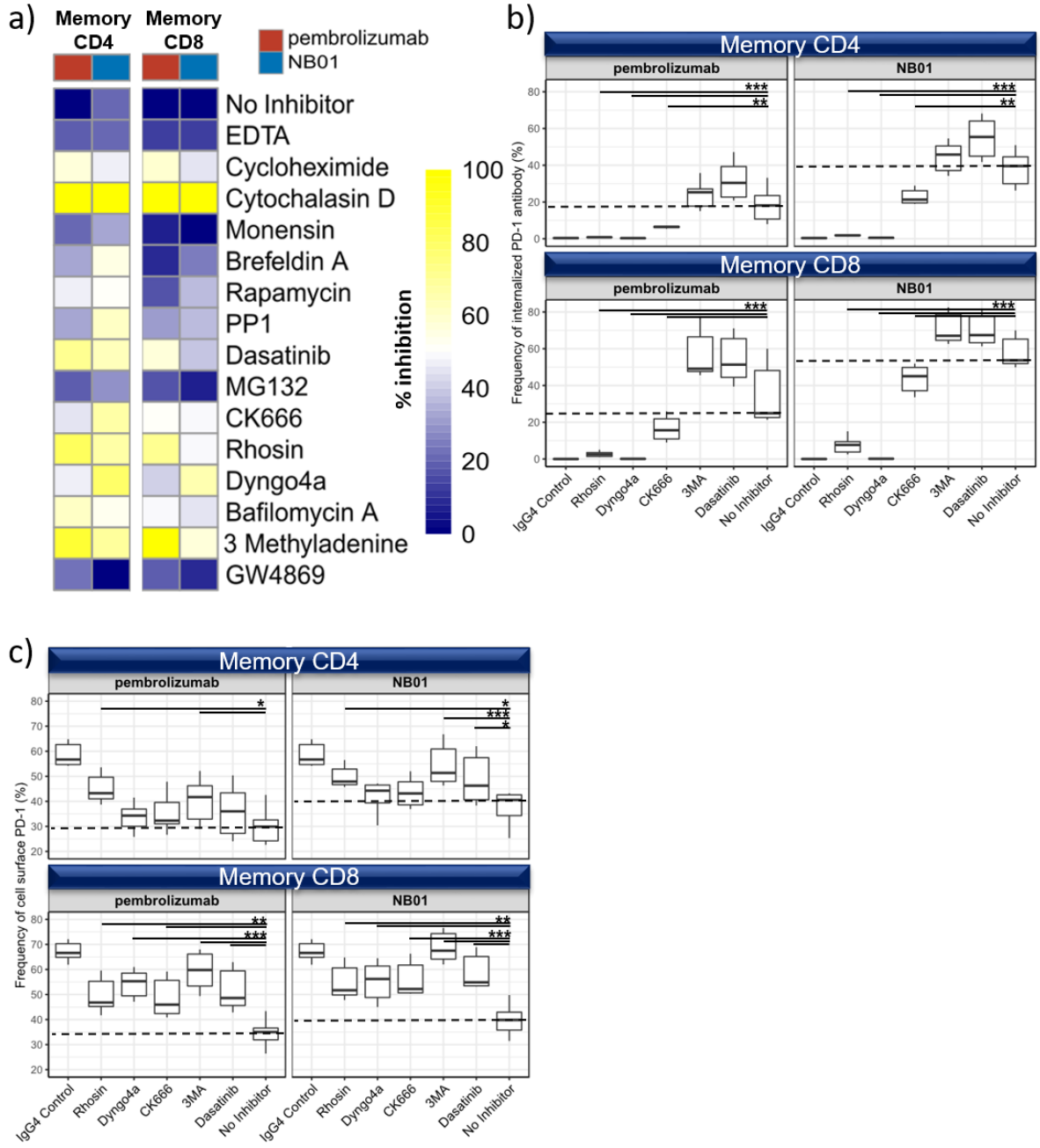
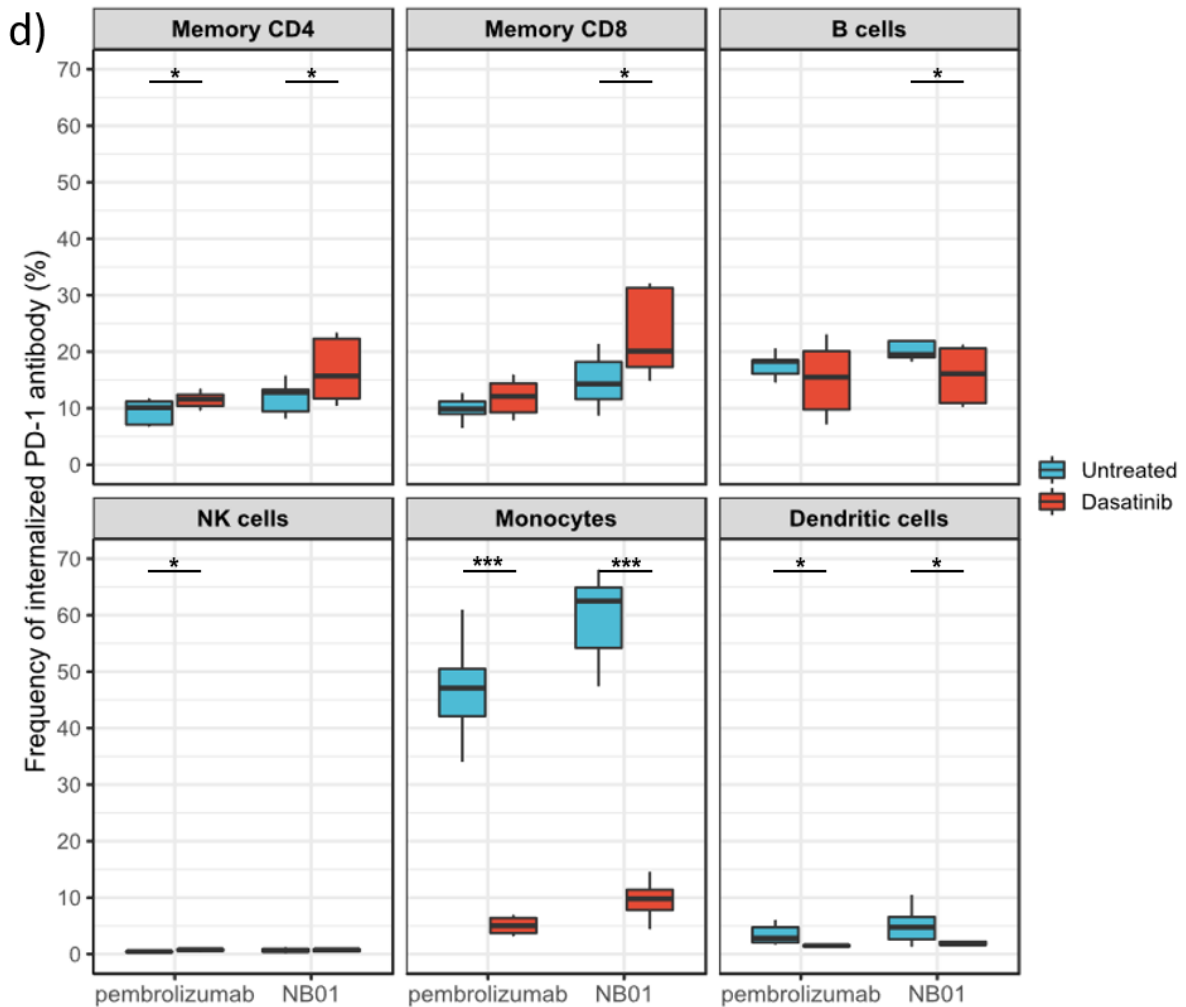


**Figure 3 cont.**



**Selective inhibition of dynamin/actin-mediated processes disrupts PD-1 antibody internalization on T cells and dasatinib prevents monocyte FcγR cross-linking necessary for PD-1 downregulation. (A)** Heatmap of surface PD-1 expression after 24 hours of anti-PD-1 incubation with a panel of 15 inhibitors targeting protein internalization, transport, and degradation pathways in memory T cells within total PBMCs. **(B)** Selected inhibitors used to measure the inhibition of surface PD-1 downregulation in memory T cells. **(C)** Selected inhibitors used to measure the inhibition of PD-1 antibody internalization in memory T cells. **(D)** Pulse chase experiment with anti-PD-1-pHrodo bound to T cells in the presence of Fc block, removed from supernatant, and reconstituted with unlabeled PD-1 antibodies and incubated for 24 hours in the presence or absence of dasatinib. (n=3, unpaired *t* test with Welch's correction)

**Figure 4**

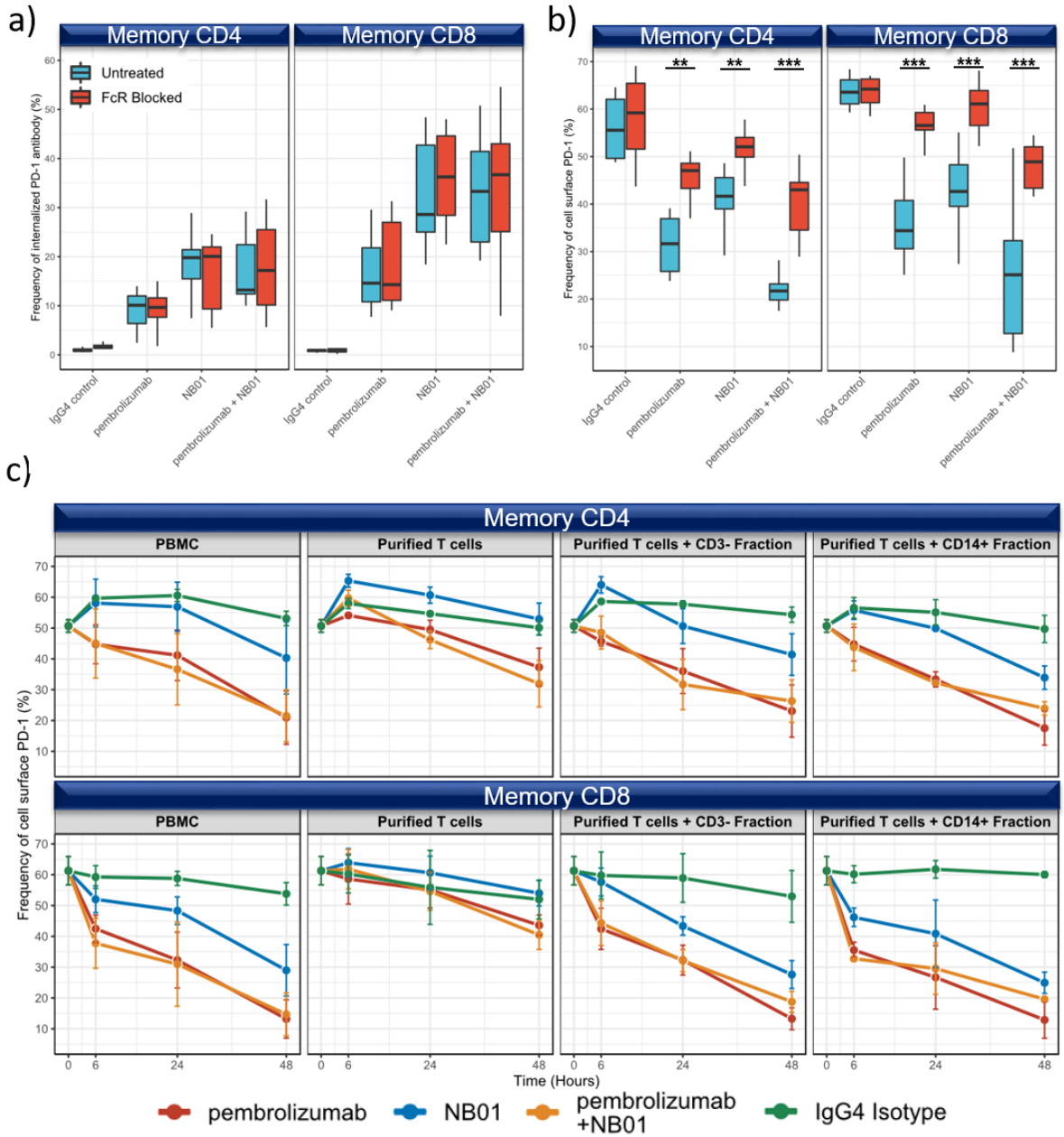
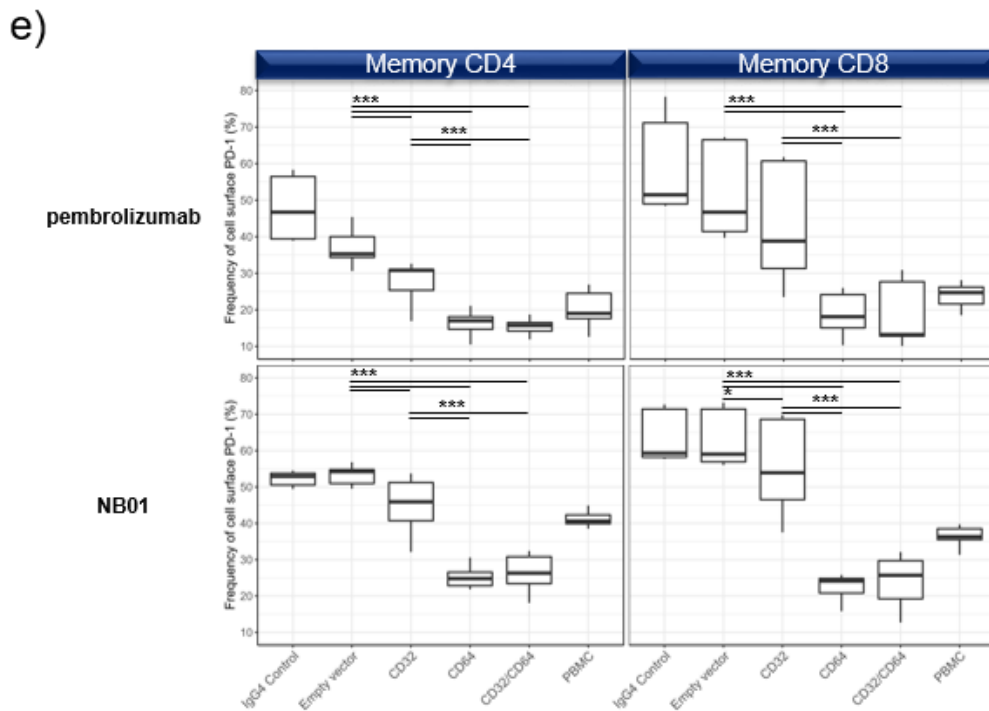
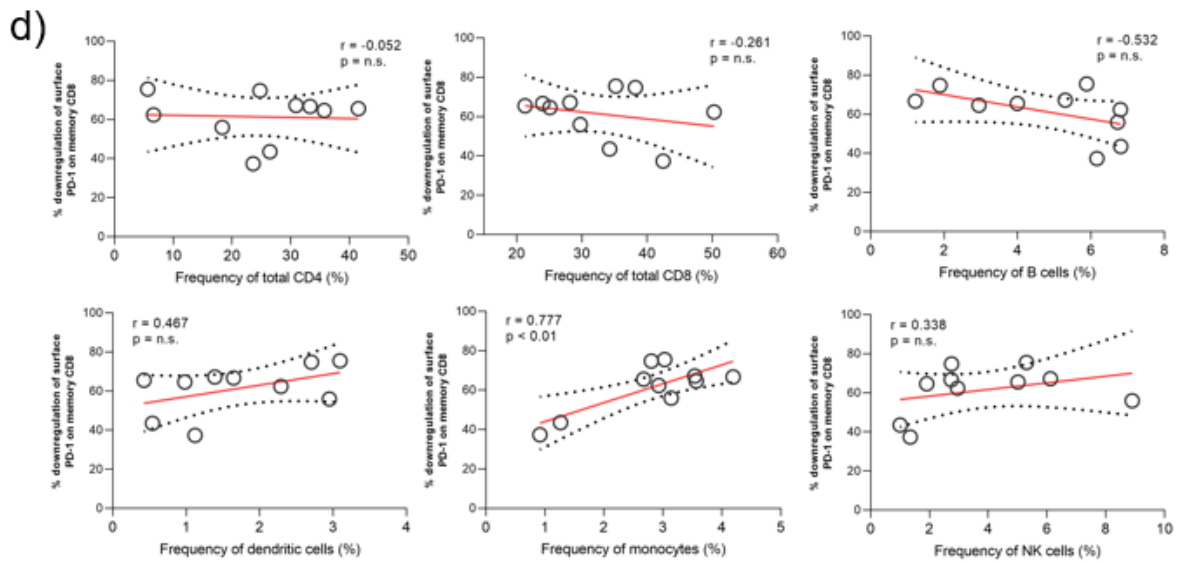


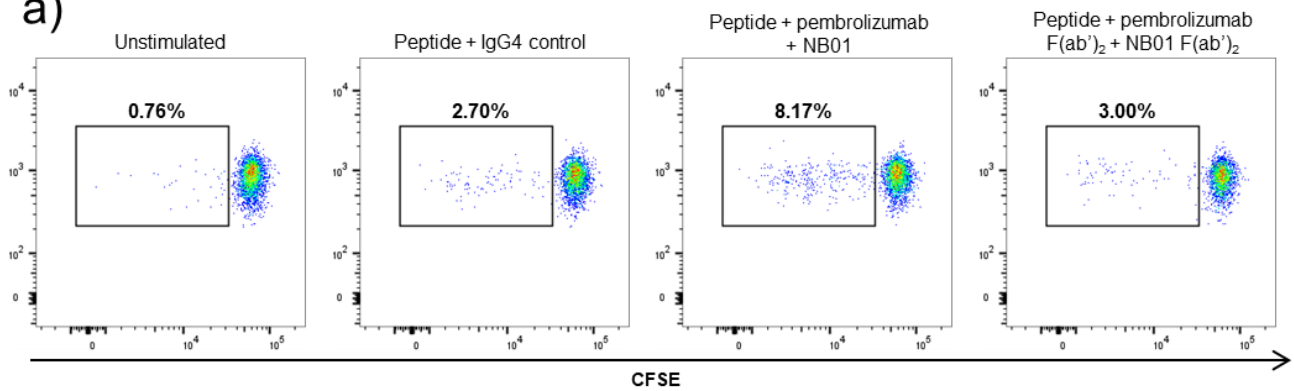
**Figure 4 cont.**



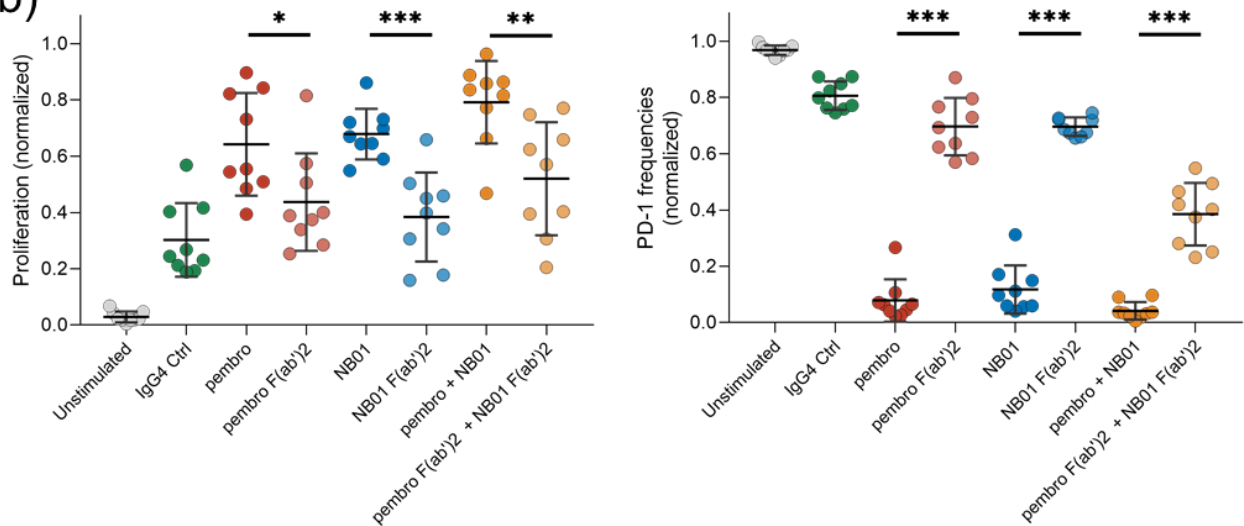
**Surface PD-1 downregulation by anti-PD-1 antibodies is mediated primarily through the crosslinking of bound PD-1 antibody Fc region with CD64. (A, B)** Fc receptor blockade with 50ug/mL of human IgG and anti-CD32/CD64 was measured for internalized PD-1 antibody (A) and surface PD-1 expression (B) after 24 hours of incubation. (n=4) (C) Antibody mediated downregulation kinetics measured in PBMC, purified T cells, and purified T cells reconstituted with autologous CD3- or CD14+ fraction (5:1 ratio) (n=3, one-way ANOVA). (D) Pearson's correlation on chronic HIV infected donors for the % decrease of surface PD-1 induced by combined pembrolizumab and NB01 antibodies relative to PBMC subset compositions after 24 hours (n=10) (E) 293T transfection of empty vector, CD32, CD64, CD32 and CD64 and cocultured with purified T cells in the presence of pembrolizumab, NB01, or IgG4 control (n=3, unpaired *t* test with Welch's correction).

## Figure 5

a)

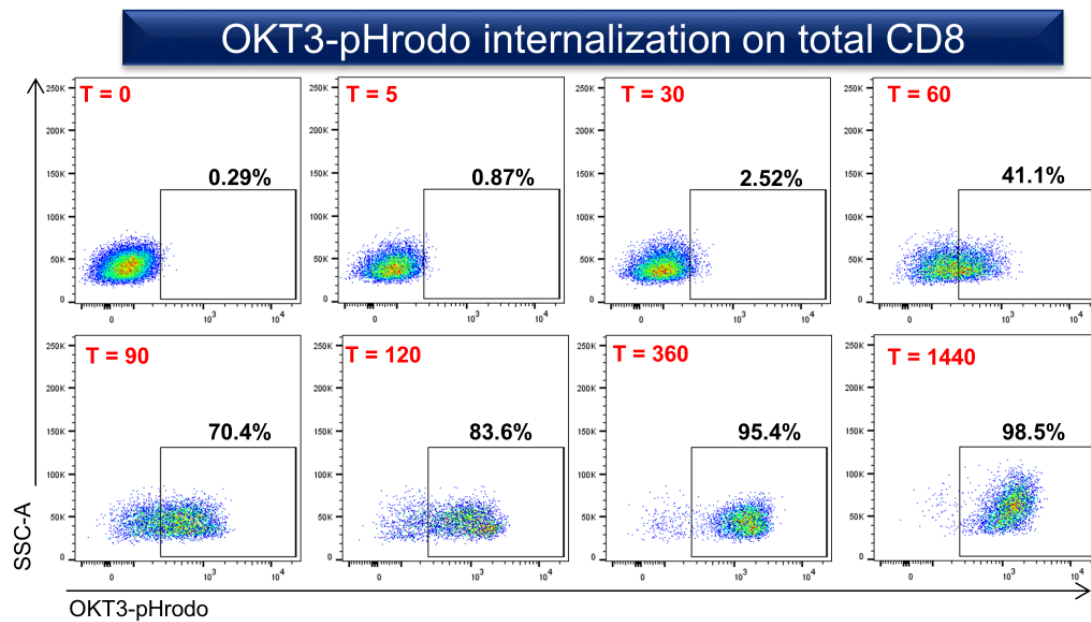


b)



**Standard anti-PD-1 antibodies boost antigen-specific T cell proliferation compared to their F(ab')<sub>2</sub> variants. (A)** Frequencies of proliferating CFSE<sup>lo</sup> memory CD8 T cells in different antibody conditions stimulated with pooled Gag PTE peptides for 6 days. **(B)** Frequency of proliferation and PD-1 MFI in memory CD8 with different antibody conditions. (n = 9, data normalized to each donor, unpaired *t* test with Welch's correction)

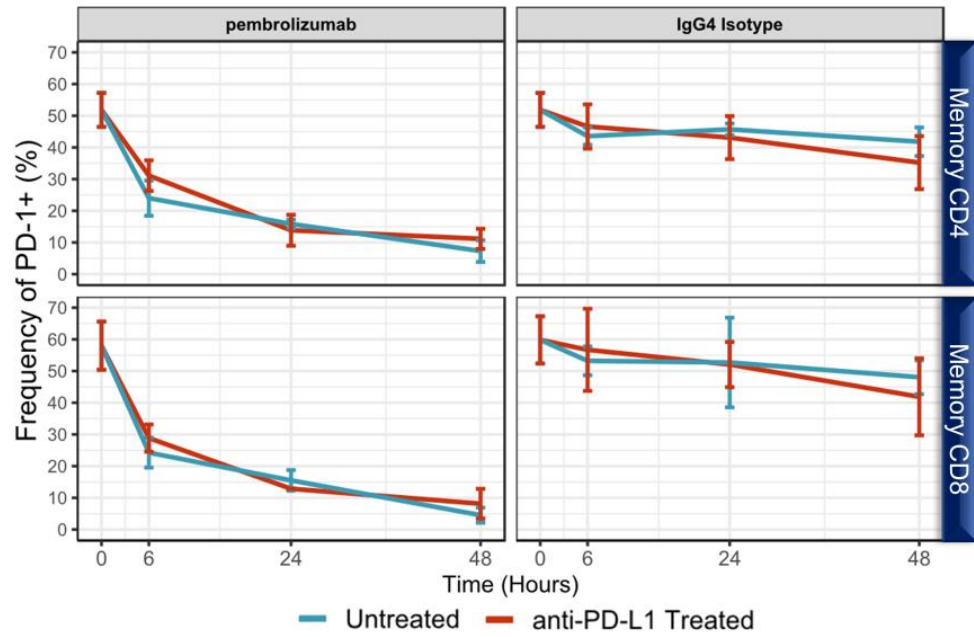
## Supplemental Figures



### Validation of pHrodo sensitivity using OKT3-pHrodo for CD3 internalization

Total CD8s were incubated with anti-CD3 (5ug/mL) for 0, 5, 30, 60, 90, 120, 360, and 1440 minutes.

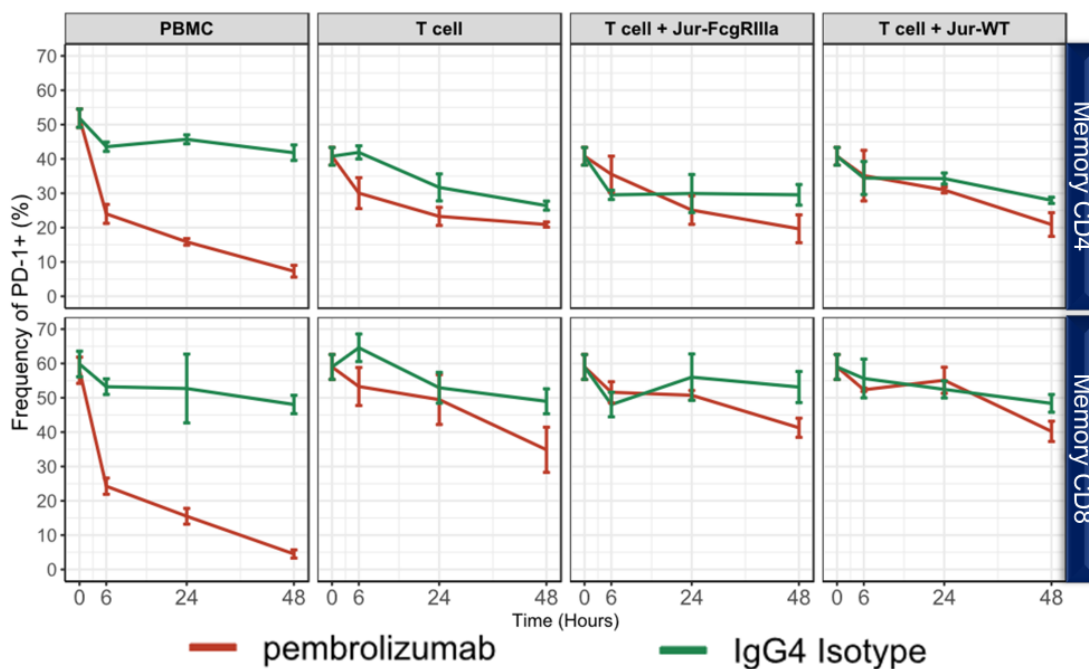
## Supplemental Figures



### Effect of anti-PDL1 combined with anti-PD-1 on PD-1 downregulation.

Total PBMCs were incubated with pembrolizumab or IgG4 (5ug/mL) with or without anti-PD-L1 (5ug/mL) for 0, 6, 24, and 48 hours.

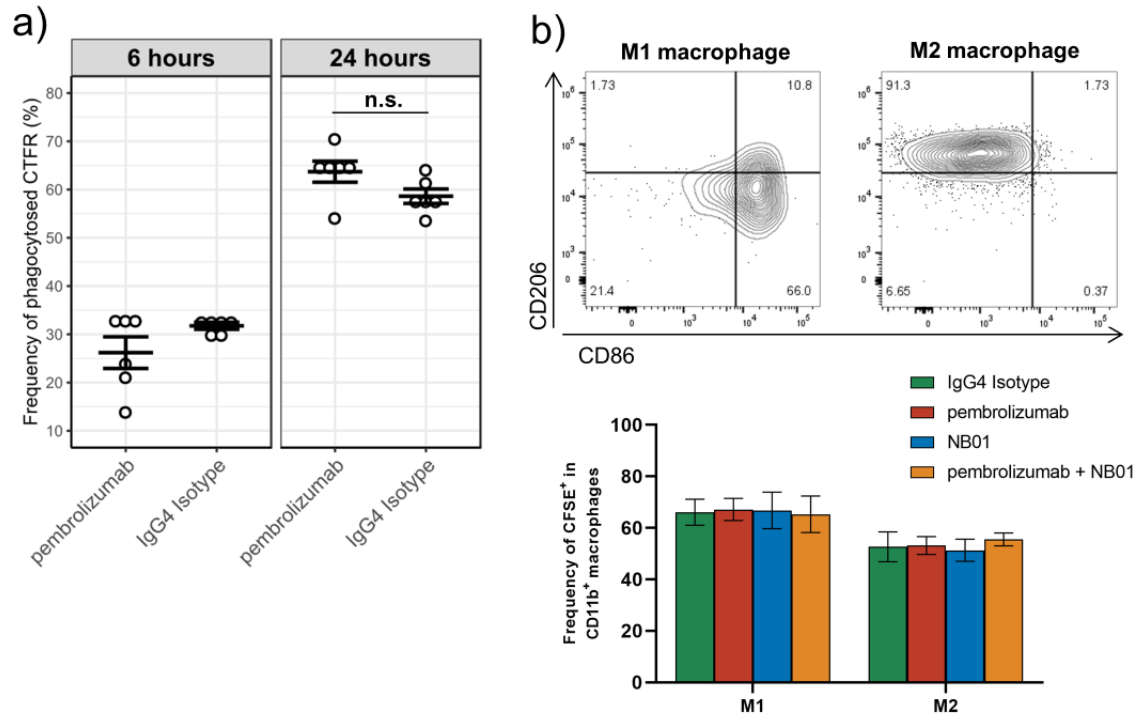
## Supplemental Figures



### Effect of CD16a on PD-1 downregulation.

Total PBMCs, purified T cells or purified T cells cocultured with WT Jurkats or Jurkats overexpressing CD16a (5:1 ratio) were measured for PD-1 downregulation in the presence of pembrolizumab or IgG4 control.

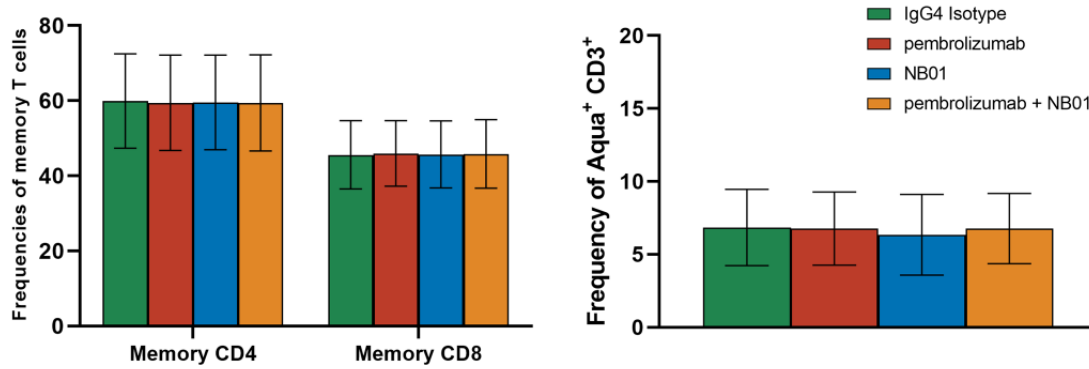
## Supplemental Figures



### ADCP activity in monocytes and differentiated macrophages with PD-1 antibody treatment.

(A) Phagocytic capacity measured in monocytes using purified T cells labeled with CTFR and cocultured with autologous monocytes incubated with pembrolizumab or IgG4 control for 24 hours. (B) Phagocytic capacity was measured in activated, M1- /M2-differentiated macrophages from healthy donors cocultured for 24 hours with autologous purified T cells labeled with CFSE.

## Supplemental Figures



### Total cell events and ADCC activity after anti-PD-1 treatment for 24 hours.

Frequencies of viable memory CD4 and CD8 within total CD4 and CD8 respectively were measured after 24 hours with different antibody treatments. Frequencies of dead T cells within total T cells indicating ADCC (CD3+ Aqua+) were measured after 24 hours with different antibody treatments. (n = 16)

## References

1. Havel, J.J., D. Chowell, and T.A. Chan, *The evolving landscape of biomarkers for checkpoint inhibitor immunotherapy*. Nat Rev Cancer, 2019. **19**(3): p. 133-150.
2. Nowicki, T.S., S. Hu-Lieskovan, and A. Ribas, *Mechanisms of Resistance to PD-1 and PD-L1 Blockade*. Cancer J, 2018. **24**(1): p. 47-53.
3. Darvin, P., et al., *Immune checkpoint inhibitors: recent progress and potential biomarkers*. Exp Mol Med, 2018. **50**(12): p. 165.
4. Hui, E., et al., *T cell costimulatory receptor CD28 is a primary target for PD-1-mediated inhibition*. Science, 2017. **355**(6332): p. 1428-1433.
5. Kamphorst, A.O., et al., *Rescue of exhausted CD8 T cells by PD-1-targeted therapies is CD28-dependent*. Science, 2017. **355**(6332): p. 1423-1427.
6. Fenwick, C., et al., *Tumor suppression of novel anti-PD-1 antibodies mediated through CD28 costimulatory pathway*. J Exp Med, 2019. **216**(7): p. 1525-1541.
7. Yokosuka, T., et al., *Programmed cell death 1 forms negative costimulatory microclusters that directly inhibit T cell receptor signaling by recruiting phosphatase SHP2*. J Exp Med, 2012. **209**(6): p. 1201-17.
8. Barber, D.L., et al., *Restoring function in exhausted CD8 T cells during chronic viral infection*. Nature, 2006. **439**(7077): p. 682-7.
9. Wang, C., et al., *In vitro characterization of the anti-PD-1 antibody nivolumab, BMS-936558, and in vivo toxicology in non-human primates*. Cancer Immunol Res, 2014. **2**(9): p. 846-56.
10. Meng, X., et al., *FBXO38 mediates PD-1 ubiquitination and regulates anti-tumour immunity of T cells*. Nature, 2018. **564**(7734): p. 130-135.
11. Bricogne, C., et al., *TMEM16F activation by Ca(2+) triggers plasma membrane expansion and directs PD-1 trafficking*. Sci Rep, 2019. **9**(1): p. 619.
12. Pentcheva-Hoang, T., et al., *Programmed death-1 concentration at the immunological synapse is determined by ligand affinity and availability*. Proc Natl Acad Sci U S A, 2007. **104**(45): p. 17765-70.
13. Davies, A.M., et al., *Structural determinants of unique properties of human IgG4-Fc*. J Mol Biol, 2014. **426**(3): p. 630-44.
14. Topalian, S.L., C.G. Drake, and D.M. Pardoll, *Targeting the PD-1/B7-H1(PD-L1) pathway to activate anti-tumor immunity*. Curr Opin Immunol, 2012. **24**(2): p. 207-12.
15. Cuesta-Mateos, C., et al., *Monoclonal Antibody Therapies for Hematological Malignancies: Not Just Lineage-Specific Targets*. Front Immunol, 2017. **8**: p. 1936.
16. Corraliza-Gorjon, I., et al., *New Strategies Using Antibody Combinations to Increase Cancer Treatment Effectiveness*. Front Immunol, 2017. **8**: p. 1804.
17. Bruhns, P., et al., *Specificity and affinity of human Fcγ receptors and their polymorphic variants for human IgG subclasses*. Blood, 2009. **113**(16): p. 3716-25.
18. Mancardi, D.A., et al., *The high-affinity human IgG receptor FcγRI (CD64) promotes IgG-mediated inflammation, anaphylaxis, and antitumor immunotherapy*. Blood, 2013. **121**(9): p. 1563-73.
19. Brandsma, A.M., et al., *Fc receptor inside-out signaling and possible impact on antibody therapy*. Immunol Rev, 2015. **268**(1): p. 74-87.
20. van der Poel, C.E., et al., *Cytokine-induced immune complex binding to the high-affinity IgG receptor, FcγRI, in the presence of monomeric IgG*. Blood, 2010. **116**(24): p. 5327-33.
21. Lo Russo, G., et al., *Antibody-Fc/FcR Interaction on Macrophages as a Mechanism for Hyperprogressive Disease in Non-small Cell Lung Cancer Subsequent to PD-1/PD-L1 Blockade*. Clin Cancer Res, 2019. **25**(3): p. 989-999.
22. Arlauckas, S.P., et al., *In vivo imaging reveals a tumor-associated macrophage-mediated resistance pathway in anti-PD-1 therapy*. Sci Transl Med, 2017. **9**(389).
23. Dahan, R., et al., *FcγRs Modulate the Anti-tumor Activity of Antibodies Targeting the PD-1/PD-L1 Axis*. Cancer Cell, 2015. **28**(3): p. 285-95.

24. Hallal-Calleros, C., et al., *Syk and Lyn phosphorylation induced by FcγRI and FcγRII crosslinking is determined by the differentiation state of U-937 monocytic cells.* Immunol Lett, 2005. **99**(2): p. 169-79.
25. Huang, Z. Y., et al., *Differential kinase requirements in human and mouse Fc-gamma receptor phagocytosis and endocytosis.* J Leukoc Biol, 2006. **80**(6): p. 1553-62.
26. Park, M., et al., *Leukocyte immunoglobulin-like receptor B4 regulates key signalling molecules involved in FcγRI-mediated clathrin-dependent endocytosis and phagocytosis.* Sci Rep, 2016. **6**: p. 35085.
27. Schade, A.E., et al., *Dasatinib, a small-molecule protein tyrosine kinase inhibitor, inhibits T-cell activation and proliferation.* Blood, 2008. **111**(3): p. 1366-77.
28. Greuber, E.K. and A.M. Pendergast, *Abl family kinases regulate FcγR-mediated phagocytosis in murine macrophages.* J Immunol, 2012. **189**(11): p. 5382-92.
29. Futosi, K., et al., *Dasatinib inhibits proinflammatory functions of mature human neutrophils.* Blood, 2012. **119**(21): p. 4981-91.
30. Beum, P.V., et al., *Binding of rituximab, trastuzumab, cetuximab, or mAb T101 to cancer cells promotes trogocytosis mediated by THP-1 cells and monocytes.* J Immunol, 2008. **181**(11): p. 8120-32.
31. Beum, P.V., et al., *Loss of CD20 and bound CD20 antibody from opsonized B cells occurs more rapidly because of trogocytosis mediated by Fc receptor-expressing effector cells than direct internalization by the B cells.* J Immunol, 2011. **187**(6): p. 3438-47.
32. Zhang, Y., et al., *Daclizumab reduces CD25 levels on T cells through monocyte-mediated trogocytosis.* Mult Scler, 2014. **20**(2): p. 156-64.
33. Vogel, S., et al., *Antibody induced CD4 down-modulation of T cells is site-specifically mediated by CD64(+) cells.* Sci Rep, 2015. **5**: p. 18308.
34. Nakashima, M., et al., *Trogocytosis of ligand-receptor complex and its intracellular transport in CD30 signalling.* Biol Cell, 2018. **110**(5): p. 109-124.
35. Krejcik, J., et al., *Monocytes and Granulocytes Reduce CD38 Expression Levels on Myeloma Cells in Patients Treated with Daratumumab.* Clin Cancer Res, 2017. **23**(24): p. 7498-7511.
36. Simpson, T.R., et al., *Fc-dependent depletion of tumor-infiltrating regulatory T cells co-defines the efficacy of anti-CTLA-4 therapy against melanoma.* J Exp Med, 2013. **210**(9): p. 1695-710.
37. Dahal, L.N., et al., *Shaving Is an Epiphenomenon of Type I and II Anti-CD20-Mediated Phagocytosis, whereas Antigenic Modulation Limits Type I Monoclonal Antibody Efficacy.* J Immunol, 2018. **201**(4): p. 1211-1221.
38. Swisher, J.F. and G.M. Feldman, *The many faces of FcγRI: implications for therapeutic antibody function.* Immunol Rev, 2015. **268**(1): p. 160-74.
39. Krieg, C., et al., *High-dimensional single-cell analysis predicts response to anti-PD-1 immunotherapy.* Nat Med, 2018. **24**(2): p. 144-153.
40. Roghanian, A., et al., *Antagonistic human FcγRIIB (CD32B) antibodies have anti-tumor activity and overcome resistance to antibody therapy in vivo.* Cancer Cell, 2015. **27**(4): p. 473-88.
41. Valgardsdottir, R., et al., *Human neutrophils mediate trogocytosis rather than phagocytosis of CLL B cells opsonized with anti-CD20 antibodies.* Blood, 2017. **129**(19): p. 2636-2644.
42. De Henau, O., et al., *Overcoming resistance to checkpoint blockade therapy by targeting PI3Kγ in myeloid cells.* Nature, 2016. **539**(7629): p. 443-447.
43. Cao, W., et al., *Macrophage subtype predicts lymph node metastasis in oesophageal adenocarcinoma and promotes cancer cell invasion in vitro.* Br J Cancer, 2015. **113**(5): p. 738-46.
44. Maccio, A., et al., *Role of M1-polarized tumor-associated macrophages in the prognosis of advanced ovarian cancer patients.* Sci Rep, 2020. **10**(1): p. 6096.
45. Tu, M.M., et al., *Targeting DDR2 enhances tumor response to anti-PD-1 immunotherapy.* Sci Adv, 2019. **5**(2): p. eaav2437.
46. DeNardo, D.G. and B. Ruffell, *Macrophages as regulators of tumour immunity and immunotherapy.* Nat Rev Immunol, 2019. **19**(6): p. 369-382.

47. Cassetta, L. and J.W. Pollard, *Targeting macrophages: therapeutic approaches in cancer*. Nat Rev Drug Discov, 2018. **17**(12): p. 887-904.

## ABSTRACT

---

**Background.** Seasonal influenza continues to be a global health burden and effective vaccination requires the interactions of B cells and T follicular helper cells (Tfh). The age-associated decline of immune responses in influenza vaccination results in a decrease of serological titers, memory B cells, and Tfh which prevents protective responses against seasonal influenza.

**Hypothesis.** Lower influenza vaccination responses in elderly individuals can be compensated by higher doses of vaccination

**Objectives.** To characterize the antigen-specific memory B cells and circulating Tfh subsets in different age groups and to assess whether a double dose (DD) vaccination is more effective in elderly individuals than a single dose (SD) vaccination.

**Experimental strategy.** 1) We took PBMCs and sera from a cohort of 164 vaccinated individuals at baseline, 1 week, 2 weeks, 4 weeks, and 24 weeks which were stratified by age and measured antibody titers by HAI assay and the phenotype of antigen-specific memory B cells using A/H1N1/2009 tetramers as well as circulating Tfh subsets by flow cytometry.

**Results.** We demonstrated that all age groups were capable of significantly increasing their antibody responses by 2 weeks and reached near 100% seroprotection by week 4. We also found that induced H1N1-specific memory B cells in the 25-45Y group were significantly higher in frequencies relative to both the 66Y+ SD and DD groups but absolute counts were only higher than the 66Y+ SD group. We found that for the induced CXCR3<sup>+</sup> cTfh, the 25-45Y group was significantly higher in frequencies and counts to the 66Y+SD group. However, the 25-45Y group was not significantly higher than the 46-65Y and 66Y+ DD groups. Furthermore, the 66Y+ DD group was similar in frequencies to and greater than in counts to the 46-65Y group level for induced CXCR3<sup>+</sup> cTfh.

**Conclusions.** All age groups are able to produce seroprotective titers to influenza vaccination across all 3 strains, demonstrating that influenza vaccinations are effective regardless of age. We also saw a trend for a higher response in the 66Y+ DD with increases to similar levels of antigen-specific memory B cell counts and CXCR3<sup>+</sup> cTfh with similar frequencies and greater counts to the 46-65Y group. This data shows that increasing the dosage for elderly individuals shows potential in increasing both memory B cell and Tfh responses from an increased immunogenicity.

## ABSTRACT (en Français)

---

**Contexte:** La grippe saisonnière continue de représenter un fardeau pour la santé mondiale et une vaccination efficace nécessite les interactions des cellules B et des cellules T auxiliaires folliculaires (Tfh). Le déclin des réponses immunitaires associé à l'âge dans la vaccination antigrippale entraîne une diminution des titres sérologiques, des cellules B mémoire et de la Tfh, ce qui empêche les réponses protectrices contre la grippe saisonnière.

**Hypothèse:** Des réponses vaccinales plus faibles chez les personnes âgées peuvent être compensées par des doses plus élevées de vaccination.

**Objectifs:** Caractériser les lymphocytes B mémoires spécifiques de l'antigène et les sous-ensembles de Tfh circulants dans différents groupes d'âge et évaluer si une vaccination à double dose (DD) est plus efficace chez les personnes âgées qu'une vaccination à dose unique (SD).

**Stratégie expérimentale:** 1) Nous avons prélevé des PBMC et des sérums d'une cohorte de 164 individus vaccinés au départ, 1 semaine, 2 semaines, 4 semaines et 24 semaines qui ont été stratifiés en fonction de l'âge et des titres d'anticorps mesurés par test HAI et le phénotype de la mémoire B spécifique de l'antigène cellules utilisant des tétramères A / H1N1 / 2009 ainsi que des sous-ensembles de Tfh circulants par cytométrie en flux.

**Résultats:** Nous avons démontré que tous les groupes d'âge étaient capables d'augmenter significativement leurs réponses anticorps de 2 semaines et atteignaient près de 100% de séroprotection à la semaine 4. Nous avons également constaté que les cellules B mémoire induites spécifiques au H1N1 dans le groupe 25-45Y étaient significativement plus élevées dans les fréquences contre les deux groupes 66Y+ SD et DD, mais les nombres étaient seulement plus élevés que le groupe 66Y+ SD. Nous avons constaté que pour le CXCR3<sup>+</sup> cTfh induit, le groupe 25-45Y était significativement plus élevé en fréquences et en nombres que le groupe 66Y+ SD. Cependant, le groupe 25-45 ans n'était pas significativement plus élevé que les groupes 46-65 ans et 66Y+ DD. En outre, le groupe 66Y+ DD présentait des fréquences similaires et supérieures à celles du groupe 46-65Y pour le CXCR3<sup>+</sup> cTfh induit.

**Conclusion:** Tous les groupes d'âge sont capables de produire des titres séroprotecteurs à la vaccination antigrippale pour les 3 souches, ce qui démontre que les vaccinations antigrippales sont efficaces quel que soit l'âge. Nous avons également observé une tendance à une réponse plus élevée dans le 66Y + DD avec des augmentations à des niveaux similaires de numération des cellules B mémoire spécifiques de l'antigène et CXCR3 + cTfh avec des fréquences similaires et des comptes plus élevés pour le groupe 46-65Y. Ces données montrent que

l'augmentation de la posologie pour les personnes âgées montre un potentiel d'augmentation des réponses des lymphocytes B mémoire et Tfh à partir d'une immunogénicité accrue.

## LIST OF ABBREVIATIONS

---

1. **IAV**: influenza A
2. **IBV**: influenza A
3. **ICV**: influenza A
4. **IDV**: influenza A
5. **HA**: hemagglutinin
6. **NA**: neuraminidase
7. **NP**: nucleoprotein
8. **M1**: matrix protein
9. **PB1**: polymerase basic 1
10. **vNRP**: viral ribonucleoprotein
11. **HAI**: hemagglutination inhibition
12. **ASC**: antibody secreting cells
13. **Tfh**: T follicular helper cell

## LIST OF FIGURES

---

**FIGURE 1:** Influenza A virion and associated proteins

**FIGURE 2:** Influenza virus replication cycle

**FIGURE 3:** Effectiveness of seasonal influenza vaccines from 2009 to 2019

## CHAPTER 5: INTRODUCTION

---

This topic for my PhD thesis was a secondary, side project but could not be merged with the main topic of PD-1 antibodies. Thus, I have created an addendum mini-thesis to integrate with the main thesis. We will begin with an introduction covering influenza biology and the current state of influenza vaccinations.

### 5.1 Influenza classification and epidemiology

Influenza viruses are negative-sense, single-stranded, enveloped RNA viruses and members of the Orthomyxoviridae family. Influenza viruses are categorized in four distinct genera – A (IAV), B (IBV), C (ICV), and D (IDV) [1]. For IAV, the hemagglutinin (HA) and neuraminidase (NA) subtype is designated after the viral isolate [1]. Based on viral surface antigens, there are 18 HA (H1-18) and 11 NA (N1-11) subtypes of IAV and two known circulating lineages for IBV, Victoria and Yamagata [2].

According to WHO estimates, the annual epidemics of seasonal influenza reach an estimated 1 billion infections with 3-5 million cases of severe illness and about 10% of those severe cases resulting in mortality [3]. Various pre-existing medical conditions can increase the incidence of severe influenza infections such as asthma, HIV, cancer, and with one of the most important risk factors being age [4]. The very young (less than 1 year of age) and the elderly (greater than 65 years of age) individuals represent the most vulnerable populations [4, 5]. Severe disease incidences and/or mortalities in patients with influenza are due to either viral-induced pneumonia or secondary bacterial infections as a complication [6]. Viral pneumonia is caused by high viral replication due to a migration of infection to the lower respiratory tract, followed by a strong proinflammatory response.

IAV and IBV represent the dominant genera of circulating influenza viruses and vaccination strategies are actively developed against them. IAV infects humans and widely circulates in birds and numerous other animals while IBV is known to only infect only humans [7]. ICV infections are rare and do not contain the potential for antigenic drift while IDV infects only cattle and swine; therefore, vaccinations against these influenza genera are not a major public health concern. The severity of seasonal influenza depends on various conditions such as the virulence of the viral strain and the levels of cross-reactivity and pre-existing immunity [8, 9].

## 5.2 Influenza viral proteins

Between IAV and IBV, their encoded viral proteins have shared and similar functions. PB1, PB2, and PA are responsible for RNA synthesis and replication in infected cells (**Fig. 1**)[10]. The viral glycoprotein hemagglutinin (HA) is responsible for binding to sialic acid and viral entry; it contains a head and stalk domain[11]. The function of neuraminidase (NA) is release of viruses from binding non-functional receptors and in aiding viral spread [1]. Nucleoprotein (NP) binds to the RNA genome[10]. Matrix protein (M1) regulates the scaffold that provides the virion structure and M1 together with nuclear export protein (NEP) regulates the movement of viral RNA[10]. Membrane protein (M2/BM2) acts as proton ion channel required for entry and exit[10]. Nonstructural protein (NS1) and accessory proteins PB1 and F2 serve as virulence factor that prevent antiviral responses[1].

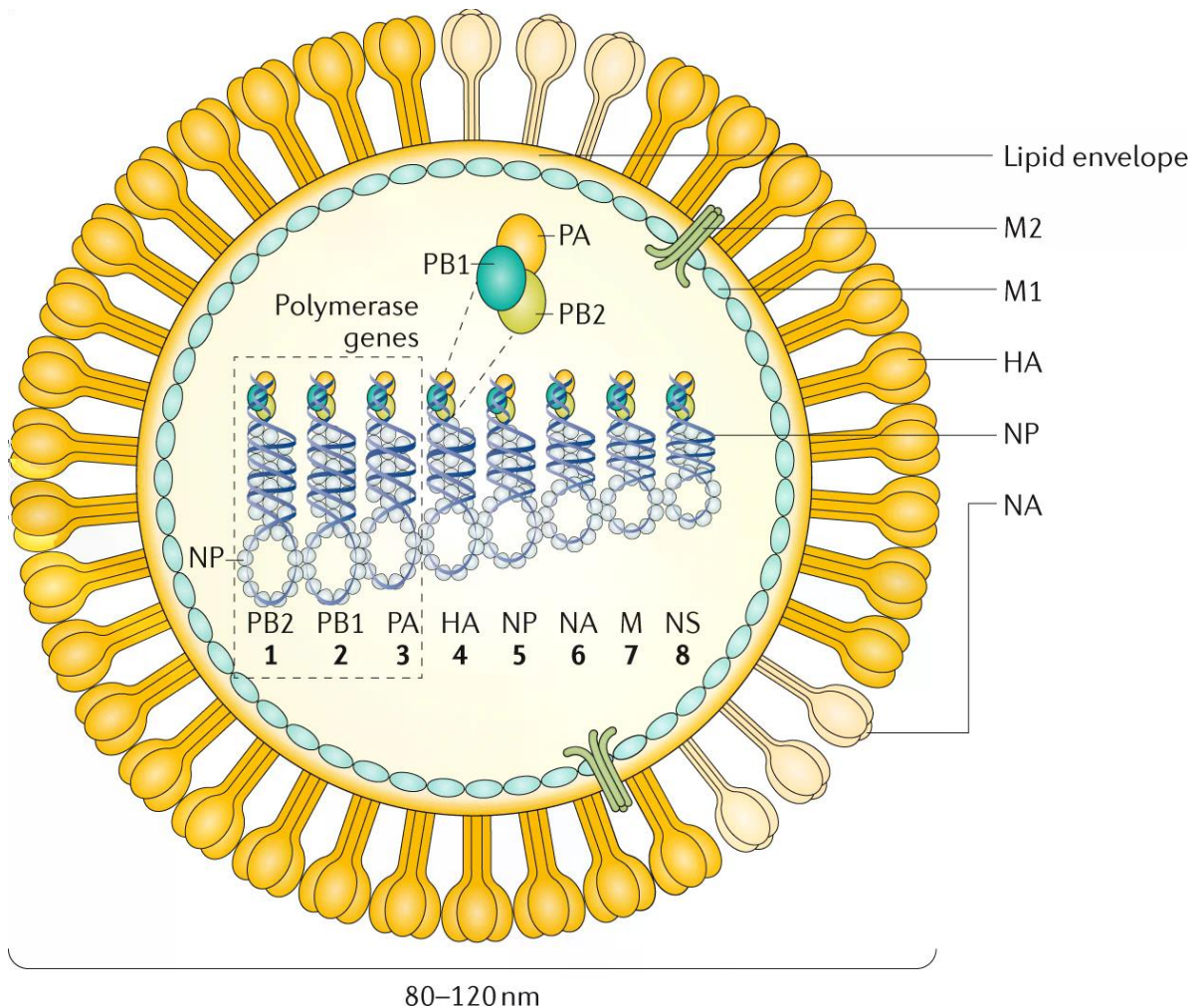
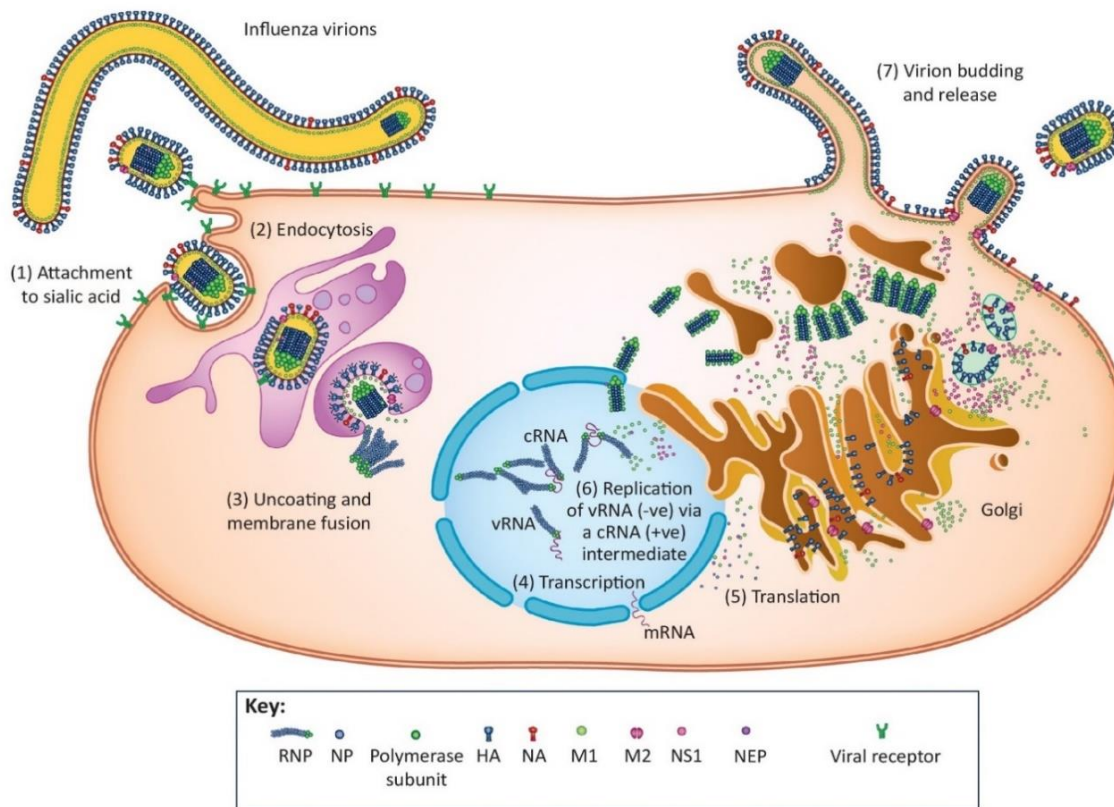


**Figure 1.** Influenza A virion and associated proteins. From Krammer F, et al. *Nat Rev Dis Primers*. 2018 Jun 28;4(1):3.

### 5.3 Influenza Life Cycle and Pathogenesis

Human influenza viruses are transmitted through aerosol droplets and targets the epithelial cell lining of the upper respiratory tract for infection and replication while extending to the lower respiratory tract in severe cases[12]. For IAV and IBV, HA proteins on the viral surface preferentially bind sialic acid on epithelial cells and internalize (**Fig. 2**)[13, 14]. Once the internalized viral particle is trafficked inside the cell, the acidification of the endosome causes a conformational change in the virus that creates a fusion of the viral envelope with the endosome[15]. This fusion causes the release of viral ribonucleoproteins (vRNP) into the cytoplasm and the released vRNPs are imported into the nucleus[16].



Trends in Microbiology

**Figure 2.** Influenza virus replication cycle. From Hutchinson EC. Influenza Virus. Trends Microbiol. 2018 Sep;26(9):809-810.

Transcription and replication of viral mRNA is processed by viral polymerase complexes attached to vRNPs[17]. Newly generated mRNAs are exported into the endoplasmic reticulum for translation into viral proteins [1]. From this point, newly synthesized viral polymerases and viral NP translocate back into the nucleus to boost the rate of RNA synthesis while membrane-bound

proteins such as HA, and NA are moved to the plasma membrane[18, 19]. M1 and NEP move to nucleus, bind the vRNPs to mediate their export to the cytoplasm at the late stages of infection and incorporate the vRNPs into the budding virions which take on the host membrane containing viral glycoproteins[20]. The end result is viral-induced apoptosis[21].

#### 5.4 Influenza Vaccines

The annual influenza vaccine is composed of two strains of IAV virus (H1N1 and H3N2) and one or two strains of the IBV as a trivalent or quadrivalent vaccines, respectively. Currently approved vaccines contain inactivated (split viruses or subunit influenza antigens) or live attenuated influenza viruses[17]. Every year, the influenza vaccine is reformulated and prepared six months in advance with strain forecasting implemented through the WHO Global Influenza Surveillance and Response System[18]. The reason for this is due to constant antigenic drift of IAV and to lesser extent, IBV.

Antigenic drift is the accumulation of amino acid substitutions in HA and NA surface proteins that generate novel immunological strains and provide selective advantages in circumventing the host antibody response[19]. For IAV, mutations are commonly occurring given the lack of proofreading mechanisms on the viral RNA polymerase and these error rates are estimated to be approximately  $1-8 \times 10^{-3}$  substitutions per site per year[20]. Selective pressure from immune mice infected with influenza was shown to drive single point mutations in the HA gene that increased receptor binding avidity while naïve mice infected with influenza had increased selective pressure for decreased receptor binding avidity[21]. When a substitution allows for immunological evasion and confer a fitness advantage, the mutated influenza strain can outcompete and replace the circulating strain[19]. Antigenic shift, which occurs only in IAV, is the gene reassortment with a novel HA, NA, or both gene segments from the avian reservoirs into the circulating human influenza, generating an immunologically unknown strain; this is the case for pandemic influenza[19].

Seasonal influenza vaccines have a narrow window of coverage and are strain-specific; these circulating strains are constantly evolving despite the extensive surveillance and predictions. Vaccine efficacy and effectiveness can vary dramatically from year to year, depending on how well the vaccine strain matches the circulating strain (**Fig. 3**). For example, in 2018-2019 season, the overall interim estimate showed a vaccine effectiveness of 43% against influenza A/H3N2 in

all age groups combined while in the 2014-2015 seasons, vaccine effectiveness was shown to be 23% due to high levels of antigenic drift in the influenza A/H3N2 viruses[22, 23]. Furthermore, vaccine effectiveness contrasts significantly with age: children aged 6 months–17 years had 61% vaccine effectiveness against all influenza virus types while adults  $\geq 50$  years showed 24% in the 2018-2019 season[22].

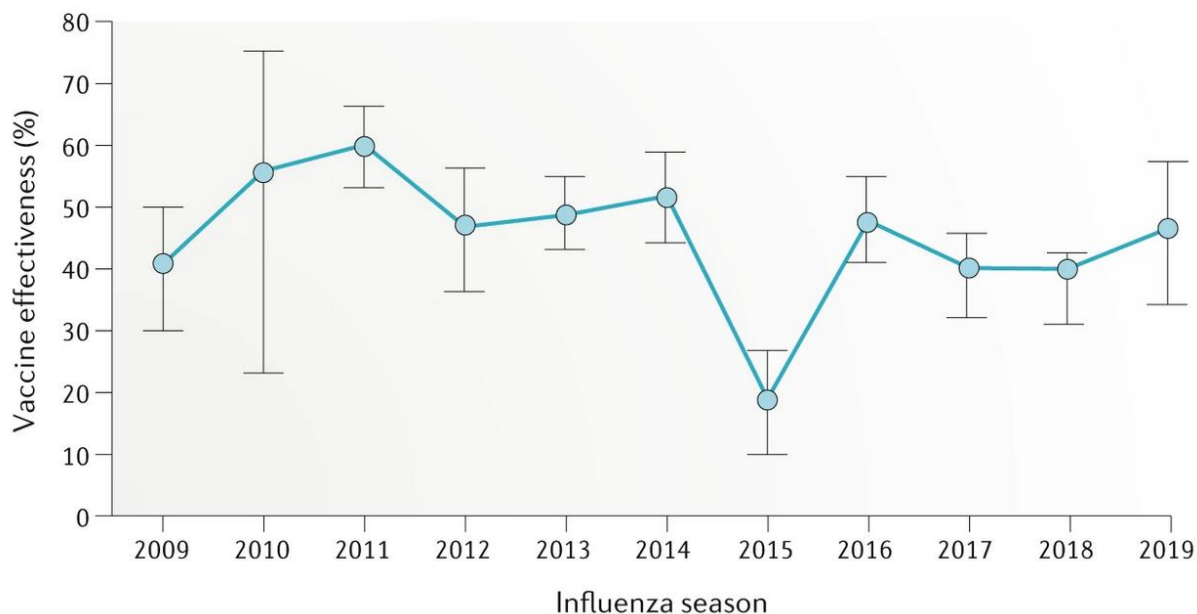


**Figure 3.** Effectiveness of seasonal influenza vaccines from 2009 to 2019 using data from “CDC: Past Seasons Vaccine Effectiveness Estimates”. From Wei CJ, et al. *Nat Rev Drug Discov.* 2020 Apr;19(4):239-252.

Despite such varied responses over the years, annual vaccination for influenza remains the most efficient and cost-effective strategy for public health. Currently, there is ongoing research to create universal influenza vaccines that produce broadly neutralizing antibodies against conserved epitopes of the hemagglutinin stalk domain. These antibodies have been found to be cross-reactive and inhibit the viral membrane fusion by locking HA in its prefusion form[24]. However, these antibodies have been found to be less potent neutralizers than the standard HA head antibodies, necessitating further research[25].

### 5.5 Immune correlates of protection

Vaccination responses are typically assessed by antibody titers generated from the vaccination. The hemagglutination inhibition assay (HAI) represents the gold standard for assessing protection from influenza. It is the primary method for quantitatively measuring antibody

titers for influenza virus and used for vaccine efficacy/effectiveness studies and epidemiological studies[26]. The assay directly measures the intrinsic binding of viral HA to bind sialic acid present on the surface of red blood cells. Patient sera containing HA antibodies will block viral attachment and prevent agglutination. The current standard for seroprotection is estimated as an HAI titer of 40 or above, regarded as a 50% or greater reduction in the likelihood for contracting influenza[27]. Another metric, seroconversion, is defined as the number of patients with  $\geq 4$ -fold increase in HAI titers[28]. While these assays are informative and cost-effective, there are limitations such as protocol standardization and reproducibility from different laboratories[26]. In a recent paper by Ng, S. et al., the authors found that HA stalk antibodies could be used instead of full-length HA antibodies to determine protection rates in natural influenza infections, which cannot be accurately measured with the standard HAI assay[29].

There is active research in identifying additional cellular immune correlates of protection for influenza vaccinations[30]. Given that the HAI titers are a result of the B cell response to vaccination, numerous studies have examined the presence of antibody-secreting cells (ASC) post-vaccination[31-33]. Antigen-specific B cells are readily detectable from 1-2 weeks post-vaccination and their increased numbers have been positively correlated with antibody titers[32]. However, given that B cell responses for influenza are dominated by recall responses in adults, it is critical to make the distinction between *de novo* ASCs and broadly cross-reactive memory B cells[34]. T cell responses have also been investigated; in particular, heterosubtypic responses (immunity generated by a given IAV subtype that protects against challenge with other IAV subtypes) have been observed in both CD4<sup>+</sup> and CD8<sup>+</sup> T cells[35-37]. Cross-reactive T cells target epitopes in highly conserved regions of influenza proteins positioned in the cytoplasm such as PB1, M1, and NP. In a recent paper by Koutsakos, M et al., the authors found a conserved CD8 epitope, PB1<sub>413</sub>, which was cross-reactive against IAV, IBV, and ICV measured as IFN $\gamma$  production in response to infected autologous PBMCs[37].

In recent years, there has been great interest in the role of T follicular helper cells (Tfh) in influenza vaccine responses[38-40]. Tfh cells are a specialized subset of antigen-experienced CD4<sup>+</sup> that express Bcl-6 and play an essential role in the formation and maintenance of germinal centers by directly providing co-stimulation via CD40 which interacts with CD40L on B cells and producing IL-21 and IL-4 to drive B cell proliferation[41]. In turn, the germinal B cells undergo isotype class-switching and somatic hypermutation, which generates antibody isotypes with better

effector functions and greater affinity, respectively. Circulating Tfh (cTfh) which are found in the peripheral blood, serves as a surrogate population as activated Tfh that have egressed from the lymph nodes[42, 43]. It has been found in a number of studies on influenza vaccinations that the frequencies of cTfh in the blood positively correlate with antibody responses and HA-specific B cells[40]. Furthermore, it has been shown that the expression of CXCR3<sup>+</sup> cTfh, which are designated as Th1-like, are correlated with vaccine responses but not CXCR3<sup>-</sup> cTfh[44]. These studies show the potential for cTfh to serve as a metric for influenza vaccination responses.

## **5.6 Influenza vaccination in the elderly**

In an aged immune system, diminished vaccine responses lead to increased susceptibility and more severe incidences of influenza. All aspects of the adaptive immunity are affected in elderly individuals for influenza vaccinations. Influenza-specific antibody titers are found to be significantly lower in elderly individuals compared with young adults and B cells have more restricted repertoire diversity and fewer somatic hypermutation events due to significantly lower expression of activation-induced cytidine deaminase, which is critically involved in class switch recombination and somatic hypermutation[45-47]. Blimp-1 expression and IgG secretion was also found to be significantly reduced, indicating that plasma cell differentiation was impaired[48].

Furthermore, cTfh in vaccinated elderly individuals was shown to be lower in frequencies, produce less IL-21, decrease B cell help in the form of lower IgG production, and have a greater expression of ICOS compared to young adults[39]. These defects in Tfh functionality directly contribute to reduced B cell responses. CD8<sup>+</sup> impairment in elderly individuals for influenza vaccination is presented as the increased expression of T-bet and senescence-associated markers CD57 and KLRG1 as well as reduced frequencies of influenza-specific CD8<sup>+</sup> [49, 50]. Remarkably, elderly individuals show a reduced diversity of clonotypes but retain dominant T cell repertoires with enhanced cross-reactivity[51].

Despite these reduced immunologic capacities, elderly individuals are still capable of producing a protective antibody titers and influenza vaccinations significantly reduce the risk of hospitalizations in individuals aged 65 and older[52, 53]. Therefore, taking into consideration the reduced responses of an aged immune system would allow for the design of more effective and/or more immunogenic vaccine strategies that can compensate for these deficiencies and enable immunological protection in elderly individuals.

## CHAPTER VI: RESULTS

---

### **Paper I: Age-associated decline in influenza vaccination (manuscript in preparation)**

In this study, we measured vaccination responses at baseline, 1 week, 2 weeks, 4 weeks, and 24 weeks in individuals stratified into groups by age: 25-45Y, 46-65Y, 66Y+ SD (single dose), and 66Y+DD (double dose). We evaluated HAI titers for each of the 3 strains in the 2014-2015 vaccine schedule composed of: H1N1-A/CA/2009, H3N2-A/TX/2012, and Influenza B-MA/2012. All age groups had maintained high levels of seroprotective titers at baseline; however, all age groups were shown to be significantly increased in their geometric mean titers at 2 weeks post-vaccination compared to baseline.

We measured CA/2009-specific IgG<sup>+</sup> memory B cells between age groups; the 25-45Y group was shown to be significantly higher than all other age groups. Furthermore, all age groups were shown to be significantly higher than baseline at the 2-week timepoint. For induced CA/2009-specific memory B cell frequencies, the 66Y+ SD and DD groups were both significantly lower in frequencies ( $p < 0.05$ ) compared to the 25-45Y group. However, in terms of induced absolute counts, the 66Y+ DD group was increased to levels similar to the 46-65Y age group while the 66Y+ SD was the only age group significantly lower than the 25-45Y ( $p < 0.01$ ). A positive correlation was observed for CA/2009-specific memory B cells and CA/2009 antibody titers at 2 weeks ( $R = 0.47$ ,  $p < 0.001$ ) and 4 weeks ( $R = 0.41$ ,  $p < 0.001$ ). No significant changes were observed in plasma cell frequencies and counts except for the 25-45Y group at 1 week compared to baseline. We next measured the frequencies and counts of CXCR3<sup>+</sup> and CXCR3<sup>-</sup> cTfh populations in the vaccinated age groups. Frequencies and counts in peak CXCR3<sup>+</sup> cTfh at 1 week were significantly higher than baseline for all age groups except for frequencies in the 46-65Y group. For induced CXCR3<sup>+</sup> cTfh, only the 66Y+ SD group was significantly lower than the 25-45Y group. ( $p < 0.05$ ) The 66Y+ DD group showed comparable or greater levels to the frequencies and counts of the 45-65Y group, respectively. As for the CXCR3<sup>-</sup> cTfh, only the 66Y+ SD group showed significant increases at the peak expression at 2 weeks. Furthermore, no differences in the induced CXCR3<sup>-</sup> cTfh were observed among all age groups. These results show that there are age related deficiencies in memory B cells and CXCR3<sup>+</sup> cTfh from vaccine responses in the elderly but higher doses could possibly circumvent these immunological impairments.

**Contribution:** I contributed to experimental implementation of antigen-specific B cell response, generated and analyzed the cumulative data and written the original draft of the manuscript.

## Chapter VII: DISCUSSION

---

We conducted a randomized study to evaluate the immunogenicity for influenza vaccinations in different age groups and found some age-related differences in B cell and T cell responses. Primarily, we observed lasting immunity to all 3 strains of influenza from the vaccine schedule even with age-associated disparities. Prior exposure to influenza and/or previous influenza vaccinations is responsible for the relatively high initial seroprotection rates observed at baseline. Moreover, all age groups produced vaccination responses approaching 100% seroprotection by week 2 that persisted throughout the remainder of the study. The responses to H3N2 strain (TX 2012) were the most pronounced, showing the highest increase in titers for all age groups. It should be noted that the actual H3N2 strain in 2014 experienced significant antigenic drift from the predicted strain, leading to a vaccine mismatch and an overall reduction in vaccine effectiveness [54]. However, this created a unique situation in which the vaccine responses to the TX/2012 antigen were likely to be formed *de novo* and not influenced by cross-reactivity to current or prior H3N2 exposure. For the TX/2012 strain antigen, higher numbers of elderly donors with double dose had seroconverted against 1 or more strains compared to the single dose group by week 4.

The detection of strain-specific memory B cells shows that all age groups are capable of developing or inducing memory responses to influenza vaccination. In elderly individuals, double dose of influenza vaccine was shown to elevate influenza-specific memory B cells counts and CXCR3<sup>+</sup> cTfh frequencies/ counts compared to the single dose; these increases were not found to be statistically significant but established response levels to the same as or higher than the 46-65Y group. Several studies have concluded that higher doses of influenza vaccinations for elderly individuals generated stronger protective responses [55-57]. In North America, there are options for elderly individuals to receive either a high dose vaccination at 60 ug per influenza strain with the quadrivalent Fluzone HD or adjuvanted FLUAD containing MF59. Our studies only included a double dose – 30 ug per strain – for the elderly group, which could account for why a less pronounced effect was observed. While previous studies have broadly defined different age groups as either young or old, we present here data that stratifies the older age group into 46-65 and 66+ groups in order to better represent the age-associated decline in vaccine responses and to underscore potential strategies to circumvent it. We were able to measure all relevant timepoints for both the early and sustained vaccine responses for the different age groups; this showed that

influenza vaccination was effective even at 6 months post-vaccination in providing continuous seroprotection to all age groups despite the contraction of memory B cell and cTfh populations and mediated by long-lived plasma cells.

In future work, analyzing the immunoglobulin repertoire between young and elderly donors could help clarify any beneficial or differential responses with higher or more immunogenic doses of influenza vaccination. In the study by Henry, C. et al., influenza vaccinations in elderly individuals produced less *de novo* somatic hypermutation which resulted in elderly individuals not being able to effectively adjust to newer strains and a reduction in neutralization capacity to highly potent or drifting epitopes against HA[46]. We would like to test if different formulations or higher concentrations of influenza vaccinations could potentially increase immunoglobulin gene somatic hypermutation events. Furthermore, given that elderly individuals generate antibodies preferentially targeting more conserved NA, NP, or other non-HA proteins, we would like to observe if any increases in relevant HA epitopes may occur with different vaccine formulations.

On the other hand, we did not observe significant increases in plasma cell levels post-vaccination in age groups over 45 years old. In a report by Kim, JH et al., plasma cells were found to be increased at day 7 using the HD influenza vaccination in elderly individuals (65Y+) compared to the SD while no changes were observed in memory B cell populations [58]. In contrast, our data showed that while plasma cells were induced, no significant differences were shown between the SD or DD groups and higher counts of antigen-specific memory B cells were found in the DD group. This difference in results could be attributed to the higher concentration of influenza antigen in the HD vaccine leading to a more efficient acute response. We also did not observe changes in total memory B cell frequencies; only the antigen-specific memory B cell responses were effectively induced. In our work, the extent of immune aging with decreased plasma cell frequencies and counts was observed but interestingly, the age-associated loss of plasma cells did not significantly alter the seroprotection nor seroconversion rates. Even with the overall lower memory B cells frequencies and counts for the older age groups, memory B cells were still effectively induced or recalled and significantly correlated with the increase of antibody titers, indicating that the memory B cells were responsible for generating effective, long-term influenza responses rather than transient increases in plasma cells. The induction of plasma cells may be

more applicable to individuals under 45Y of age with reduced prior exposure to influenza antigens [46].

In a previous study by Herati, R. et al., elderly individuals were shown have 35% fewer cTfh and expressed more ICOS compared to young adults [39]. Given that baseline levels of CXCR3<sup>+</sup> cTfh were markedly reduced in elderly individuals of this study, our data is in agreement for observing a similar effect in the age groups above 66Y. Strictly between the 25-45Y and 46-65Y groups, we found that while both age groups retained similar baseline levels of CXCR3<sup>+</sup> cTfh, the magnitude of CXCR3<sup>+</sup> Tfh abundance post-vaccination was markedly reduced in the 46-65Y age group, confirming an age-related decline in CXCR3<sup>+</sup> cTfh proliferation. Regardless of the age of donors, we found that the peak frequencies of CXCR3<sup>+</sup> Tfh at week 1 was positively correlated with CA/2009-specific memory B cell responses at weeks 1, 2, and 4 for all donors combined. One potential limitation was the fact that we only measured CA/2009-specific memory B cell responses and more information about the reactivity to other 2 strains may have revealed more robust measures for correlates of protection.

We did not observe a correlation between CXCR3<sup>-</sup> cTfh and memory B cell responses for all time points. The 46-65Y group had lower CXCR3<sup>-</sup> cTfh at baseline compared to the younger group, but was still capable of producing CXCR3<sup>-</sup> cTfh similarly in magnitude to the 25-45Y group after vaccination. Neither the single and double dose group for 66Y+ generated CXCR3<sup>-</sup> cTfh sufficiently. In the work by Koutsakos M. et al, no changes were observed in CXCR3<sup>-</sup> CCR6<sup>+/-</sup> cTfh across all timepoints after inactivated influenza vaccination [59]. We observed a trend in the increase of CXCR3<sup>-</sup> cTfh at 2 weeks post vaccination but also did not observe significant increases. The possibility that we did not include markers for CCR6 to delineate cTfh2 and cTfh17 subsets may explain for this lack of difference. In further work, we would like to characterize the circulating cTfh populations more thoroughly (for the subsets cTfh1, cTfh2, and cTfh17) as well as vaccine-specific stimulation of cytokine production and B cell help in terms of IgG production in co-culture from different cTfh subsets. Gene expression profiling of these different subsets of cTfh before and after vaccination with young or elderly individuals could also help us understand the individual contributions of each cTfh subset and their transcriptional changes post-vaccination to better define the deficiencies from an aged immune response. Furthermore, we would also like

to compare the relationship between cTfh and germinal center Tfh during influenza vaccination. Although normally difficult to obtain, recent progress with fine needle aspirates of the lymph node has allowed for a way to collect cells from the germinal center with a minimally invasive technique [60, 61]. The longitudinal analysis of Tfh from different anatomical compartments may yield more information on the contributions of GC Tfh and cTfh on influenza vaccine responses.

It is being debated at the moment whether the CXCR3<sup>+</sup> (cTfh1) and/or CXCR3<sup>-</sup> (cTfh2/17) subsets are positively correlated with antibody responses. Different cTfh subsets have been indicated for the positive correlation of vaccine responses in other diseases such as HPV [62], yellow fever [63] for CXCR3<sup>+</sup> cTfh and malaria [64], Ebola [65] for CXCR3<sup>-</sup> cTfh. Furthermore, acute infections produce distinct cTfh subset profiles that emerge as better mediators for neutralizing responses. For example, responders to SARS-CoV-2 produce both CXCR3<sup>+</sup> cTfh1 and CCR6<sup>+</sup> CXCR3<sup>-</sup> cTfh17 – this combination generating the most neutralizing antibodies [66] and the emergence of CXCR3<sup>+</sup> cTfh1 are positively correlated with neutralizing responses in HCV [67] and HIV [68] infections.

These results outline the importance of CXCR3<sup>+</sup> cTfh in parallel with memory B cells for immune responses to influenza vaccination, in agreement with other published reports. Furthermore, we validate the fact that influenza vaccine responses also adhere to elderly individuals in consideration of CXCR3<sup>+</sup> cTfh. Understanding the underlying immunological responses that mediate long-term immunity in both young and elderly individuals remains crucial to designing improved vaccines. Given that Tfh are intimately involved with memory B cell responses, vaccines that are capable of inducing Tfh proliferation and maintenance are likely to be more effective.

## Chapter VIII: REFERENCES

---

1. Krammer, F., et al., *Influenza*. Nat Rev Dis Primers, 2018. **4**(1): p. 3.
2. Mathew, N.R. and D. Angeletti, *Recombinant Influenza Vaccines: Saviors to Overcome Immunodominance*. Front Immunol, 2019. **10**: p. 2997.
3. Sherman, A.C., et al., *The Future of Flu: A Review of the Human Challenge Model and Systems Biology for Advancement of Influenza Vaccinology*. Front Cell Infect Microbiol, 2019. **9**: p. 107.
4. Martinez, A., et al., *Risk factors associated with severe outcomes in adult hospitalized patients according to influenza type and subtype*. PLoS One, 2019. **14**(1): p. e0210353.
5. Shi, T., et al., *Mortality risk factors in children with severe influenza virus infection admitted to the pediatric intensive care unit*. Medicine (Baltimore), 2019. **98**(35): p. e16861.
6. David, L.M., et al., *Premature Mortality Due to PM2.5 Over India: Effect of Atmospheric Transport and Anthropogenic Emissions*. Geohealth, 2019. **3**(1): p. 2-10.
7. Ducatez, M.F., R.G. Webster, and R.J. Webby, *Animal influenza epidemiology*. Vaccine, 2008. **26 Suppl 4**: p. D67-9.
8. Tscherne, D.M. and A. Garcia-Sastre, *Virulence determinants of pandemic influenza viruses*. J Clin Invest, 2011. **121**(1): p. 6-13.
9. Abreu, R.B., et al., *Preexisting subtype immunodominance shapes memory B cell recall response to influenza vaccination*. JCI Insight, 2020. **5**(1).
10. Bouvier, N.M. and P. Palese, *The biology of influenza viruses*. Vaccine, 2008. **26 Suppl 4**: p. D49-53.
11. Couceiro, J.N., J.C. Paulson, and L.G. Baum, *Influenza virus strains selectively recognize sialyloligosaccharides on human respiratory epithelium; the role of the host cell in selection of hemagglutinin receptor specificity*. Virus Res, 1993. **29**(2): p. 155-65.
12. Kuiken, T. and J.K. Taubenberger, *Pathology of human influenza revisited*. Vaccine, 2008. **26 Suppl 4**: p. D59-66.
13. Gamblin, S.J. and J.J. Skehel, *Influenza hemagglutinin and neuraminidase membrane glycoproteins*. J Biol Chem, 2010. **285**(37): p. 28403-9.
14. Weis, W., et al., *Structure of the influenza virus haemagglutinin complexed with its receptor, sialic acid*. Nature, 1988. **333**(6172): p. 426-31.
15. Bullough, P.A., et al., *Structure of influenza haemagglutinin at the pH of membrane fusion*. Nature, 1994. **371**(6492): p. 37-43.
16. Stegmann, T., *Membrane fusion mechanisms: the influenza hemagglutinin paradigm and its implications for intracellular fusion*. Traffic, 2000. **1**(8): p. 598-604.
17. Mameli, C., et al., *Influenza Vaccination: Effectiveness, Indications, and Limits in the Pediatric Population*. Front Pediatr, 2019. **7**: p. 317.
18. Perofsky, A.C. and M.I. Nelson, *The challenges of vaccine strain selection*. Elife, 2020. **9**.
19. Treanor, J., *Influenza vaccine--outmaneuvering antigenic shift and drift*. N Engl J Med, 2004. **350**(3): p. 218-20.
20. Chen, R. and E.C. Holmes, *Avian influenza virus exhibits rapid evolutionary dynamics*. Mol Biol Evol, 2006. **23**(12): p. 2336-41.
21. Hensley, S.E., et al., *Hemagglutinin receptor binding avidity drives influenza A virus antigenic drift*. Science, 2009. **326**(5953): p. 734-6.

22. Doyle, J.D., et al., *Interim Estimates of 2018-19 Seasonal Influenza Vaccine Effectiveness - United States, February 2019*. MMWR Morb Mortal Wkly Rep, 2019. **68**(6): p. 135-139.
23. Flannery, B., et al., *Early estimates of seasonal influenza vaccine effectiveness - United States, January 2015*. MMWR Morb Mortal Wkly Rep, 2015. **64**(1): p. 10-5.
24. Ekiert, D.C., et al., *Antibody recognition of a highly conserved influenza virus epitope*. Science, 2009. **324**(5924): p. 246-51.
25. Wei, C.J., et al., *Next-generation influenza vaccines: opportunities and challenges*. Nat Rev Drug Discov, 2020. **19**(4): p. 239-252.
26. Zacour, M., et al., *Standardization of Hemagglutination Inhibition Assay for Influenza Serology Allows for High Reproducibility between Laboratories*. Clin Vaccine Immunol, 2016. **23**(3): p. 236-42.
27. Trombetta, C.M. and E. Montomoli, *Influenza immunology evaluation and correlates of protection: a focus on vaccines*. Expert Rev Vaccines, 2016. **15**(8): p. 967-76.
28. Manuel, O., et al., *Humoral response to the influenza A H1N1/09 monovalent AS03-adjuvanted vaccine in immunocompromised patients*. Clin Infect Dis, 2011. **52**(2): p. 248-56.
29. Ng, S., et al., *Novel correlates of protection against pandemic H1N1 influenza A virus infection*. Nat Med, 2019. **25**(6): p. 962-967.
30. Erbeding, E.J., et al., *A Universal Influenza Vaccine: The Strategic Plan for the National Institute of Allergy and Infectious Diseases*. J Infect Dis, 2018. **218**(3): p. 347-354.
31. Cox, R.J., et al., *An early humoral immune response in peripheral blood following parenteral inactivated influenza vaccination*. Vaccine, 1994. **12**(11): p. 993-9.
32. Halliley, J.L., et al., *Peak frequencies of circulating human influenza-specific antibody secreting cells correlate with serum antibody response after immunization*. Vaccine, 2010. **28**(20): p. 3582-7.
33. Ellebedy, A.H., et al., *Defining antigen-specific plasmablast and memory B cell subsets in human blood after viral infection or vaccination*. Nat Immunol, 2016. **17**(10): p. 1226-34.
34. Li, G.M., et al., *Pandemic H1N1 influenza vaccine induces a recall response in humans that favors broadly cross-reactive memory B cells*. Proc Natl Acad Sci U S A, 2012. **109**(23): p. 9047-52.
35. Wilkinson, T.M., et al., *Preexisting influenza-specific CD4+ T cells correlate with disease protection against influenza challenge in humans*. Nat Med, 2012. **18**(2): p. 274-80.
36. Kreijtz, J.H., et al., *Cross-recognition of avian H5N1 influenza virus by human cytotoxic T-lymphocyte populations directed to human influenza A virus*. J Virol, 2008. **82**(11): p. 5161-6.
37. Koutsakos, M., et al., *Human CD8(+) T cell cross-reactivity across influenza A, B and C viruses*. Nat Immunol, 2019. **20**(5): p. 613-625.
38. Bentebibel, S.E., et al., *ICOS(+)PD-1(+)CXCR3(+) T follicular helper cells contribute to the generation of high-avidity antibodies following influenza vaccination*. Sci Rep, 2016. **6**: p. 26494.
39. Herati, R.S., et al., *Circulating CXCR5+PD-1+ response predicts influenza vaccine antibody responses in young adults but not elderly adults*. J Immunol, 2014. **193**(7): p. 3528-37.
40. Ueno, H., *Tfh cell response in influenza vaccines in humans: what is visible and what is invisible*. Curr Opin Immunol, 2019. **59**: p. 9-14.

41. Crotty, S., *T follicular helper cell differentiation, function, and roles in disease*. Immunity, 2014. **41**(4): p. 529-42.
42. Herati, R.S., et al., *Successive annual influenza vaccination induces a recurrent oligoclonotypic memory response in circulating T follicular helper cells*. Sci Immunol, 2017. **2**(8).
43. Vella, L.A., et al., *T follicular helper cells in human efferent lymph retain lymphoid characteristics*. J Clin Invest, 2019. **129**(8): p. 3185-3200.
44. Bentebibel, S.E., et al., *Induction of ICOS+CXCR3+CXCR5+ TH cells correlates with antibody responses to influenza vaccination*. Sci Transl Med, 2013. **5**(176): p. 176ra32.
45. Goodwin, K., C. Viboud, and L. Simonsen, *Antibody response to influenza vaccination in the elderly: a quantitative review*. Vaccine, 2006. **24**(8): p. 1159-69.
46. Henry, C., et al., *Influenza Virus Vaccination Elicits Poorly Adapted B Cell Responses in Elderly Individuals*. Cell Host Microbe, 2019. **25**(3): p. 357-366 e6.
47. Frasca, D., et al., *Intrinsic defects in B cell response to seasonal influenza vaccination in elderly humans*. Vaccine, 2010. **28**(51): p. 8077-84.
48. Frasca, D., et al., *The generation of memory B cells is maintained, but the antibody response is not, in the elderly after repeated influenza immunizations*. Vaccine, 2016. **34**(25): p. 2834-40.
49. Wagar, L.E., et al., *Influenza-specific T cells from older people are enriched in the late effector subset and their presence inversely correlates with vaccine response*. PLoS One, 2011. **6**(8): p. e23698.
50. Dolfi, D.V., et al., *Increased T-bet is associated with senescence of influenza virus-specific CD8 T cells in aged humans*. J Leukoc Biol, 2013. **93**(6): p. 825-36.
51. Gil, A., et al., *Narrowing of human influenza A virus-specific T cell receptor alpha and beta repertoires with increasing age*. J Virol, 2015. **89**(8): p. 4102-16.
52. Nunez, I.A., et al., *Impact of age and pre-existing influenza immune responses in humans receiving split inactivated influenza vaccine on the induction of the breadth of antibodies to influenza A strains*. PLoS One, 2017. **12**(11): p. e0185666.
53. Rondy, M., et al., *Effectiveness of influenza vaccines in preventing severe influenza illness among adults: A systematic review and meta-analysis of test-negative design case-control studies*. J Infect, 2017. **75**(5): p. 381-394.
54. Chambers, B.S., et al., *Identification of Hemagglutinin Residues Responsible for H3N2 Antigenic Drift during the 2014-2015 Influenza Season*. Cell Rep, 2015. **12**(1): p. 1-6.
55. DiazGranados, C.A., et al., *Efficacy and immunogenicity of high-dose influenza vaccine in older adults by age, comorbidities, and frailty*. Vaccine, 2015. **33**(36): p. 4565-71.
56. Lee, J.K.H., et al., *Efficacy and effectiveness of high-dose versus standard-dose influenza vaccination for older adults: a systematic review and meta-analysis*. Expert Rev Vaccines, 2018. **17**(5): p. 435-443.
57. Pilkinton, M.A., et al., *Greater activation of peripheral T follicular helper cells following high dose influenza vaccine in older adults forecasts seroconversion*. Vaccine, 2017. **35**(2): p. 329-336.
58. Kim, J.H., et al., *High-dose influenza vaccine favors acute plasmablast responses rather than long-term cellular responses*. Vaccine, 2016. **34**(38): p. 4594-4601.
59. Koutsakos, M., et al., *Circulating TFH cells, serological memory, and tissue compartmentalization shape human influenza-specific B cell immunity*. Sci Transl Med, 2018. **10**(428).

60. Havenar-Daughton, C., et al., *Direct Probing of Germinal Center Responses Reveals Immunological Features and Bottlenecks for Neutralizing Antibody Responses to HIV Env Trimer*. Cell Rep, 2016. **17**(9): p. 2195-2209.
61. Crotty, S., *T Follicular Helper Cell Biology: A Decade of Discovery and Diseases*. Immunity, 2019. **50**(5): p. 1132-1148.
62. Matsui, K., et al., *Circulating CXCR5(+)/CD4(+) T Follicular-Like Helper Cell and Memory B Cell Responses to Human Papillomavirus Vaccines*. PLoS One, 2015. **10**(9): p. e0137195.
63. Huber, J.E., et al., *Dynamic changes in circulating T follicular helper cell composition predict neutralising antibody responses after yellow fever vaccination*. Clin Transl Immunology, 2020. **9**(5): p. e1129.
64. Bowyer, G., et al., *CXCR3(+) T Follicular Helper Cells Induced by Co-Administration of RTS,S/AS01B and Viral-Vectored Vaccines Are Associated With Reduced Immunogenicity and Efficacy Against Malaria*. Front Immunol, 2018. **9**: p. 1660.
65. Farooq, F., et al., *Circulating follicular T helper cells and cytokine profile in humans following vaccination with the rVSV-ZEBOV Ebola vaccine*. Sci Rep, 2016. **6**: p. 27944.
66. Juno, J.A., et al., *Humoral and circulating follicular helper T cell responses in recovered patients with COVID-19*. Nat Med, 2020. **26**(9): p. 1428-1434.
67. Zhang, J., et al., *Circulating CXCR3(+) Tfh cells positively correlate with neutralizing antibody responses in HCV-infected patients*. Sci Rep, 2019. **9**(1): p. 10090.
68. Baiyegunhi, O., et al., *Frequencies of Circulating Th1-Biased T Follicular Helper Cells in Acute HIV-1 Infection Correlate with the Development of HIV-Specific Antibody Responses and Lower Set Point Viral Load*. J Virol, 2018. **92**(15).

# **Circulating CXCR3<sup>+</sup> Tfh and Antigen-specific B cells Expand in Elderly individuals During Influenza Vaccination (Manuscript in preparation)**

Victor Joo, Alessandra Noto, Matthieu Perreau, Craig Fenwick, and Giuseppe Pantaleo

## **Abstract**

Influenza infections continue to represent a significant public health threat and successful vaccination requires the coordination of B cells and T follicular helper cells (Tfh) to generate neutralizing antibody titers. Age-associated immunological alterations are reported to reduce vaccine effectiveness distinguished by the reduction in serological titers, plasma cells, memory B cells, and Tfh in elderly individuals. Here, we measured longitudinal responses from 2014/2015 influenza vaccination schedule with individuals grouped in different age ranges between 25-66Y+. We find that young and elderly individuals were capable of producing protective responses to influenza vaccination and that all age groups were able to sustain high levels of protective antibody titers. Moreover, all age groups were able to generate influenza-specific memory B cells and CXCR3<sup>+</sup> cTfh cells in response to the vaccination but decreased in magnitude as age increased. Although an overall age-associated decline was seen in total memory B cells and CXCR3<sup>+</sup> cTfh compartments during peak expression, higher doses of influenza vaccination were able to partially compensate this loss in individuals over 66 years of age. Given the lower vaccination responses in elderly individuals, targeted strategies are warranted to improve vaccine effectiveness in an aged immune system.

## **Introduction**

Seasonal vaccination is presently the most effective strategy for the prevention of circulating influenza strains. Current influenza vaccines are composed of inactivated, live-attenuated, or recombinant vaccines containing 3 or 4 strains (H1N1, H3N2, and influenza B lineages) projected separately in advance by antigenic prevalence for the northern and southern hemispheres and recommended for healthy individuals aged from 6 months and older.

In a meta-analysis review, pooled influenza vaccine effectiveness between 2004 to 2015 was shown to reach 67% for H1N1 (95% CI: 28–85), 61% for H1N1 pdm09 (95% CI: 57–65), 33% for H3N2 (95% CI: 26–39), and 54% for influenza B (95% CI: 46–61) [1]. While vaccine effectiveness varied considerably across different strains, influenza vaccines were overall capable of producing moderately protective responses. Despite the progress and the comprehensive surveillance made with influenza vaccinations over the decades, seasonal influenza remains as a global health burden. The evolution of circulating strains is attributed to antigenic drift – mutations in the surface hemagglutinin (HA) and neuraminidase (NA) antigens, requiring different compositions of vaccines annually. Furthermore, antigenic shift – the reassortment of different animal strains leading to the formation of a novel influenza A strain, is responsible for creating potential pandemic scenarios such as the 2009 H1N1 epidemic [2].

Seasonal influenza vaccines are designed to elicit HA head-specific neutralizing antibody responses and provide protection by the generation or boosting of high affinity antibodies against hemagglutinin [3]. The principal immune correlate of protection is traditionally assessed by the quantification of antibody titers that indicate whether the vaccinated individual has generated strain-specific, neutralizing antibodies which in turn reflects the successful generation of activated B cells, plasma cells, and memory B cells [4].

Among healthy adults, influenza vaccines have been shown to provide protection while among the elderly, influenza vaccines are less effective but can still reduce overall disease severity and incidence of complications [5]. The consequences for this reduced vaccine efficacy in the B cells of older individuals

are reduced plasma cell generation, reduced antibody titers, and antibody affinity as well as lower memory B-cell recall responses [6]. Furthermore, T cell expansion and functionality is decreased in older individuals which directly impacts the T-cell dependent B cell response [7].

Numerous reports have shown that follicular helper T cells (Tfh) play a critical role in the generation of antibody responses from vaccinations [8-10]. Tfh belong to a specialized subset of CD4 T cells that reside in the germinal center (GC) and express Bcl-6, CD-40L, ICOS, PD-1, and CXCR5. They are responsible for the induction of a high affinity antibody response for influenza vaccination through the germinal center reactions and via production of IL-4 and IL-21, which supports GC B cell survival and differentiation. Studies have shown that the abundancies of circulating Tfh cells (cTfh) can act as an indicator for responsiveness to influenza vaccination [11, 12]. These cTfh are shown to have considerable phenotypic and functional overlap with lymphoid Tfh such as the expression of CXCR5 and PD-1 and antigen-specific B cell help, respectively. The cTfh do not express the canonical Tfh transcription factor Bcl6 and can be further defined into cTfh1 (CXCR3<sup>+</sup>), cTfh2 (CXCR3<sup>-</sup> CCR6<sup>-</sup>), cTfh17 (CXCR3<sup>-</sup> CCR6<sup>+</sup>) subsets with their own transcriptional and cytokine profiles. More specifically, influenza vaccinations have been shown to induce a Th1-like CXCR3<sup>+</sup> cTfh responses in numerous studies and responsible for the generation of plasma cell and memory B cell responses [12].

In this study, we compared longitudinal influenza vaccine responses during the 2014/2015 season with 3 groups of age ranges (25-45Y, 46-65Y, 66Y+) stratified for the vaccinated donors. Furthermore, we also compared the effects of single dose (SD) or double dose (DD) of influenza vaccine in donors above the age of 65. We measured protective antibody induction by HAI titers, the antigen-specific memory B cell response, and the prevalence of CXCR3<sup>+</sup> and CXCR3<sup>-</sup> cTfh subpopulations. We found age-associated decreases in vaccine responses in terms of antigen-specific memory B cells and both cTfh populations. Despite the increases in antibody titers being induced for all age groups, B cell and cTfh responses were significantly reduced in 66Y+ age group compared to the 25-45Y and 46-65Y age group. However, we observed that double dose of vaccine in 66Y+ group trended towards increased seroconversion rates, influenza-specific memory B cells, and CXCR3<sup>+</sup> cTfh compared to the single dose 66Y+ group. Overall, age-related vaccine responses were reflective on the availability and response of cTfh and antigen-specific memory B cells and increasing the dosage of influenza vaccination was associated with a more robust vaccine response for elderly individuals.

## Results

### Antibody generation and seroprotection rates of different age groups

We measured the HAI titers of different age groups of donors for time points 0, 2, 4 and 24 weeks to establish the trend of vaccine-induced antibody production. The antibody induction to the 3 different strains CA/2009, TX/2012, and MA/2012 that comprised the vaccination schedule were individually assessed and titer counts were plotted (Fig. 1A). All age groups were significantly increased in their antibody responses for all 3 strains by 2 weeks and remained significantly elevated until the completion of the study at 6 months when compared to their baseline titers. (CA: p<0.05, TX: p<0.05, and MA: p<0.01)

We next evaluated the different age groups for seroprotection, which was assessed as HAI titer counts above 40. A large percentage of donors with previously established seroprotection was present at baseline to varying degrees between the 3 different strains [25-45Y: 70-80%, 46-65Y: 50-80%, 66Y+ SD: 50-90%, 66Y+ DD: 60-90%]. (Fig. 1B) This can be attributed to prior exposure to influenza infections and/or influenza vaccinations, which drove these pre-existing baseline titers. All age groups achieved near 100% seroprotection by the 24-week time point (Table S1).

Seroconversion was also measured for the different age groups. Seroconversion was represented as a 4-fold increases or higher in baseline HAI titer counts. Seroconversion against CA/2009 was maintained at similar

levels across all age groups for both weeks 2 and 4 (Fig. 1B). Age-associated decline in seroconversion rates against TX/2012 and MA/2012 was observed for weeks 2 and 4 with the exception of the 66Y+ DD group, which showed a sharp increase at week 4 to TX/2012 strain in comparison to the 66Y+ SD group. When comparing concurrent seroconversions against 1 or more strains, an overall age-related decline was observed with the exception of the 66Y+ DD group which was boosted by reactivity against TX/2012. (Fig. 1C) These results validate the numerous previous studies on age-associated decline to vaccine responses and address two key points: While immune responses decline in aged individuals, a higher dose of influenza vaccine can boost humoral responses in elderly individuals and, regardless of the magnitude of HAI titer responses, seroprotection was similarly observed across all age groups after vaccination.

### **Antigen-specific memory B cell responses to influenza vaccination in different age groups**

Given the lower initial seroprotection rates at baseline across all age groups for CA/2009 compared to TX/2012 and MA/2012, we used CA/2009 tetramers to study the overall influenza-specific B cell response by flow cytometry (Fig. 2A). IgG class-switched memory B cells were gated as CD19<sup>+</sup> CD21<sup>+</sup> CD27<sup>+</sup> IgD<sup>-</sup> IgM<sup>-</sup> IgG<sup>+</sup> and plasma cells were gated as CD19<sup>+</sup> CD20<sup>-</sup> CD27<sup>+</sup> CD38<sup>++</sup> (Fig. S2).

All age groups were able to show significant increased frequencies and total counts at weeks 2 and 4 compared to time 0 and had significantly reduced levels by week 24 (Fig. 2B). The 25-45Y age group had a significantly higher response in both frequencies and counts compared to other age groups for weeks 1, 2, and 4. In terms of absolute counts, 25-45Y age group generated the highest number of CA/2009<sup>+</sup> IgG<sup>+</sup> memory B cells compared to older groups ( $p < 0.01$ ), followed by similar levels between the 46-65Y and 66Y+ DD group with the 66Y+ SD group having the lowest amount of total CA/2009<sup>+</sup> B cells. Both the 46-65Y and 66Y+ DD group showed a similar trend in increases of total counts at week 1 and 2 but were not significantly higher than the 66Y+ SD group.

We further looked at the vaccine-induced responses by measuring the difference between peak expression levels and baseline levels and comparing the  $\Delta$  change in frequencies and counts across all age groups. (Fig. 2C) We observed that the 25-45Y age group induced significantly higher antigen-specific memory B cells in frequencies compared both the SD and DD 66Y+ group ( $p < 0.05$ ) but in absolute counts, only against the SD group ( $p < 0.01$ ). The total counts of antigen-specific memory B cells induced in the 66Y+ DD group were elevated to similar levels as the 46-65Y group.

Pooled frequencies of CA/2009 specific memory B cells from all age groups combined were shown to positively correlate with antibody titers (Fig. 2F). CA/2009 titers from 2 weeks and 4 weeks were significantly correlated with IgG<sup>+</sup> CA/2009<sup>+</sup> memory B cells from 2 weeks ( $r = 0.47$ ,  $p < 0.001$ ) and 4 weeks ( $r = 0.41$ ,  $p < 0.001$ ), which verified that the elevation of antibody titers was associated with the increase of CA/2009-specific memory B cells.

Net increases in plasma cells frequencies were observed between weeks 1 and 2 for all age groups but did not correlate with antibody titers. Only the 25-45Y group showed significant increases in plasma cells for both frequencies and total counts at week 1 ( $p < 0.05$ ) but the other age groups were not significantly increased. (Fig. 2E) This underscores the age-related deficiencies in plasmablast generation and that the abundance of plasma cells may not serve as a reliable indicator for vaccine response in older individuals. Finally, total naïve, unswitched, switched memory, and double negative B cell populations did not change significantly over the course of the study and remained similar to each individual donor's baseline frequencies while only flu-specific IgG<sup>+</sup> memory B cells increased. (Fig. S1)

### **cTfh responses to influenza vaccination in different age groups**

Given the role of Tfh in enhancing B cell mediated vaccine responses, we next assessed the abundance of cTfh (gated as CD3<sup>+</sup> CD4<sup>+</sup> CD45RA<sup>-</sup> PD-1<sup>+</sup> CXCR5<sup>+</sup>) during influenza vaccination and compared between the CXCR3<sup>+</sup> and CXCR3<sup>-</sup> Tfh subsets (Fig. 3a). Baseline frequencies and absolute counts of CXCR3<sup>+</sup> cTfh

were found to be the highest in the 25-45Y group with similar levels with the 46-65Y group. We observed dramatic decreases in basal levels of CXCR3<sup>+</sup> Tfh in both groups of 66Y+ (Fig. 3b).

We found that CXCR3<sup>+</sup> cTfh were consistently elevated for all donor groups in both frequencies and total counts in response to influenza vaccination compared to their baseline. In particular, peak increases were observed at 1 week for the CXCR3<sup>+</sup> cTfh for 25-45Y, 66Y+ SD, and 66Y+ DD groups and remained elevated by week 2. All age groups were significantly increased at week 1 and week 2 compared to baseline for both frequencies and total counts ( $p < 0.01$ ). The 25-45Y age group was significantly higher than all other age groups ( $p < 0.05$ ). While the 66Y+ DD group was not significantly higher than the SD group, we found that the 45-65Y group was significantly higher than the 66Y+ SD group ( $p < 0.05$ ) but not the DD group, indicating a trend for the 66Y+ DD group in generating CXCR3<sup>+</sup> cTfh levels to comparable levels as the 46-65Y group.

We again measured the vaccine induced responses for the  $\Delta$  change in frequencies and counts compared across all age groups of CXCR3<sup>+</sup> cTfh. (Fig. 3C) Here, we observed that 25-45Y group produced significantly higher levels of CXCR3<sup>+</sup> cTfh to only the 66Y+ SD group for both frequencies and absolute counts ( $p < 0.05$ ). As seen previously with the antigen-specific memory B cells counts, the 66Y+ DD produced CXCR3<sup>+</sup> cTfh to similar frequencies and higher absolute counts as the 46-65Y group, indicating that the double dose was able to induce CXCR3<sup>+</sup> cTfh to levels than the single dose alone in elderly individuals.

Peak increases for CXCR3<sup>-</sup> cTfh were observed at week 2, which paralleled with peak increases in memory B cell responses. The 25-45Y group was significantly higher in CXCR3<sup>-</sup> cTfh in total counts ( $p < 0.01$ ) but not in frequencies compared to all other age groups at week 2 (Fig. 3D). CXCR3<sup>-</sup> cTfh frequencies or absolute counts were not significantly induced from baseline levels between all age groups. (Fig. 3E)

CXCR3<sup>+</sup> cTfh were shown to be predictive indicator of vaccine responses with antigen-specific memory B cells as shown by correlative analysis. Significant correlations were found in peak CXCR3<sup>+</sup> cTfh induction at week 1 compared to CA/2009-specific B cells at week 1 ( $r = 0.36$ ,  $p < 0.01$ ), week 2 ( $r = 0.47$ ,  $p < 0.001$ ), and week 4 ( $r = 0.41$ ,  $p < 0.001$ ) (Fig. 4A). No significant correlations were found between CXCR3<sup>-</sup> cTfh and CA/2009-specific memory B cells despite showing peak expression within the same duration. Finally, across all age groups combined, significant age-related decline in frequencies was shown for CA/2009<sup>+</sup> IgG<sup>+</sup> memory B cells ( $r = -0.54$ ,  $p < 0.001$ ), CXCR3<sup>+</sup> cTfh ( $r = -0.52$ ,  $p < 0.001$ ), and CXCR3<sup>-</sup> cTfh ( $r = -0.4$ ,  $p < 0.05$ ) (Fig. 4b).

## Discussion

We conducted a randomized controlled study to evaluate the immunogenicity for influenza vaccinations in different age groups and found some age-related differences in B cell and T cell responses. Primarily, we observed lasting immunity to all 3 strains of influenza from the vaccine schedule even with age-associated disparities. Prior exposure to influenza and/or previous influenza vaccinations is responsible for the relatively high initial seroprotection rates observed at baseline. Moreover, all age groups produced vaccination responses approaching 100% seroprotection by week 2 that persisted throughout the remainder of the study. The responses to H3N2 strain (TX 2012) was the most pronounced, showing the highest increase in titers for all age groups. It should be noted that the H3N2 strain in 2014 experienced significant antigenic drift from the predicted strain, leading to a vaccine mismatch and an overall reduction in vaccine effectiveness [13]. However, this created a unique situation in which the vaccine responses to the TX/2012 antigen were likely to be formed *de novo* and not influenced by cross-reactivity to current or prior H3N2 exposure. For the TX/2012 strain antigen, higher numbers of elderly donors with double dose had seroconverted against 1 or more strains compared to the single dose group by week 4.

The detection of strain-specific memory B cells shows that all age groups are capable of developing or inducing memory responses to influenza vaccination. In elderly individuals, double dose of influenza vaccine was shown to elevate influenza-specific memory B cells counts and CXCR3<sup>+</sup> cTfh frequencies/counts compared to the single dose; these increases were not found to be statistically significant but established response levels to the same as or higher than the 46-65Y group. Several studies have concluded that higher doses of influenza vaccinations for elderly individuals generated stronger protective responses [14-16]. In North America, there are options for elderly individuals to receive either a high dose vaccination at 60 ug per influenza strain with the quadrivalent Fluzone HD or adjuvanted FLUAD containing MF59. Our studies only included a double dose – 30 ug per strain – for the elderly group, which could account for why a less pronounced effect was observed. While previous studies have broadly defined different age groups as either young or old, we present here data that stratifies the older age group into 46-65 and 66+ groups as well as dosage in 66Y+ individuals in order to better represent the age-associated decline in vaccine responses and to underscore potential strategies to circumvent it.

We were able to measure all relevant timepoints for both the early and sustained vaccine responses for the different age groups; this showed that influenza vaccination was effective even at 6 months post-vaccination in providing continuous seroprotection to all age groups despite the contraction of memory B cell and cTfh populations and mediated by long-lived plasma cells in the bone marrow.

On the other hand, we did not observe significant increases in plasma cell levels post-vaccination in age groups over 45 years old. In a study by Kim, JH et. al., plasma cells were found to be increased at day 7 using the HD influenza vaccination in elderly individuals (65Y+) compared to the SD while no changes were observed in memory B cell populations [17]. In contrast, our data showed that while plasma cells were induced, no significant differences were shown between the SD or DD groups while higher counts of antigen-specific memory B cells were found in the DD group. This difference in results could be attributed to the higher concentration of influenza antigen in the HD vaccine leading to a more efficient acute response. We also did not observe changes in frequencies of total memory B cell compartment; only the antigen-specific memory B cell responses were effectively induced. In our work, the extent of immune aging with decreased plasma cell frequencies and counts was observed but interestingly, the age-associated loss of plasma cells did not significantly alter the seroprotection nor seroconversion rates. Even with the overall lower memory B cells frequencies and counts for the older age groups, memory B cells were still effectively induced or recalled and significantly correlated with the increase of antibody titers, indicating that the memory B cells were responsible for generating effective, long-term influenza responses rather than transient increases in plasma cells. The induction of plasma cells may be more applicable to individuals under 45Y of age with reduced prior exposure to influenza antigens [18].

A previous study showed that elderly individuals have 35% fewer cTfh and expressed more ICOS compared to young adults [19]. Given that baseline levels of CXCR3<sup>+</sup> cTfh were markedly reduced in elderly individuals of this study, our data is in agreement for observing a similar effect in the age groups above 66Y. Strictly between the 25-45Y and 46-65Y groups, we found that while both age groups retained similar baseline levels of CXCR3<sup>+</sup> cTfh, the magnitude of CXCR3<sup>+</sup> Tfh abundance post-vaccination was noticeably reduced in the 46-65Y age group, confirming an age-related decline in CXCR3<sup>+</sup> cTfh proliferation. Regardless of the age of donors, we found that the peak frequencies of CXCR3<sup>+</sup> Tfh at week 1 was positively correlated with CA/2009-specific memory B cell responses at weeks 1, 2, and 4 for all donors combined. One potential limitation was the fact that we only measured CA/2009-specific memory B cell responses and more information about the reactivity to other 2 strains may have revealed more robust measures for correlates of protection.

We did not observe a correlation between CXCR3<sup>-</sup> cTfh and memory B cell responses for all time points. The 46-65Y group had lower CXCR3<sup>-</sup> cTfh at baseline compared to the younger group, but was still capable of producing CXCR3<sup>-</sup> cTfh similarly in magnitude to the 25-45Y group after vaccination. Neither the single

and double dose group for 66Y+ generated CXCR3<sup>-</sup> cTfh sufficiently. In the work by Koutsakos M. et al, no changes were observed in CXCR3<sup>-</sup> CCR6<sup>+/-</sup> cTfh across all timepoints after inactivated influenza vaccination [20]. We observed a trend in the increase of CXCR3<sup>-</sup> cTfh at 2 weeks post vaccination but also did not observe significant increases. The possibility that we did not include markers for CCR6 to delineate cTfh2 and cTfh17 subsets may explain for this lack of difference and further research is necessary to define cTfh17 responses in vaccination strategies.

It is currently under consideration whether the CXCR3<sup>+</sup> (cTfh1) and/or CXCR3<sup>-</sup> (cTfh2/17) subsets are positively correlated with antibody responses. Different cTfh subsets have been indicated for the positive correlation of vaccine responses in other diseases such as HPV [21], yellow fever [22] for CXCR3<sup>+</sup> cTfh and malaria [23], Ebola [24] for CXCR3<sup>-</sup> cTfh. Furthermore, acute infections produce distinct cTfh subset profiles that may emerge as better mediators for neutralizing responses. For example, responders to SARS-CoV-2 produce both CXCR3<sup>+</sup> cTfh1 and CCR6<sup>+</sup> CXCR3<sup>-</sup> cTfh17 – this combination generating the most neutralizing antibodies [25] and the emergence of CXCR3<sup>+</sup> cTfh1 are positively correlated with neutralizing responses in HCV [26] and HIV [27] infections.

These observations outline the importance of CXCR3<sup>+</sup> cTfh in parallel with memory B cells for immune responses to influenza vaccination, in agreement with other published reports. Furthermore, we validate the fact that influenza vaccine responses also adhere to elderly individuals in consideration of CXCR3<sup>+</sup> cTfh. Understanding the underlying immunological responses that mediate long-term immunity in both young and elderly individuals remains crucial to designing improved vaccines. Given that Tfh are intimately involved with memory B cell responses, vaccines that are capable of inducing Tfh proliferation and maintenance are likely be more effective.

## **Materials and methods**

### **Study participants and design**

Study participants were recruited by the investigator and provided written informed consent. The study protocol was approved by local Ethics Committee and Swiss regulatory authorities, CER-VD and Swissmedic and registered at Clinicaltrials.gov with the identifier NCT02746783. This study was a single centre, parallel, open-label, randomized trial performed at the University Hospital of Lausanne, Switzerland.

### **Vaccination procedures**

The vaccine used in this study was the 2014–2015 season Mutagrip® (Sanofi Pasteur, France), a trivalent inactivated split-virion composed of 15µg of HA antigen each for the influenza strains A/California/7/2009 (H1N1)-like virus, influenza A/Texas/50/2012 (H3N2)-like virus, and influenza B/Massachusetts/2/2012 (Yamagata lineage). Donors allocated to the SD group received one intramuscular injection (15 µg of HA antigen per strain) in the deltoid muscle of the non-dominant arm and patients allocated to the DD group received two simultaneous intramuscular injections (one on the deltoid of each arm, for a total of 30 µg of HA antigen per strain) of the same influenza vaccine. Serum samples were collected at baseline before vaccination and 2, 4, and 24 weeks after vaccination and frozen at -80 °C for further batch measurement of influenza titers. Blood samples were collected at baseline before vaccination and 1, 2, 4, and 24 weeks after vaccination.

### **HAI titers**

Antibody titers against each viral strain were determined by hemagglutination inhibition assay (HAI) as previously described. [20193791] Sera and influenza antiserum were incubated with 10% chicken red blood cells at room temperature for 30 min and centrifuged at 10,000g for 10 min at 4 C. Supernatants were then collected and incubated with neuraminidase at 10 mU/mL overnight at 37°C. Sera was then incubated at 56°C for 1 h to inhibit neuraminidase activity. Twofold dilutions of sera and influenza antiserum were preincubated with each viral strain at 4 UHA per 50ml for 1 hour and incubated with chicken red blood cells at 0.5% for 45 minutes at room temperature. The inverse of the highest dilution of each serum sample that gave a 100% inhibition of hemagglutination was reported as the HAI titer. HAI titers below the limit of detection (<10) were arbitrarily assigned as 10. All samples were analyzed in triplicates.

### **Antigen-specific B cell Tetramers**

California and New Caledonia A/H1N1 HA plasmids containing inserts for the extracellular domain of HA fused at the C-terminus to the foldon domain of trimeric T4 fibrin, a biotinylatable AviTag sequence GLNDIFEAQKIEWHE, and a hexahistidine affinity tag were kindly gifted by Richard Koup. [24501410] Tetramers were produced by the Protein Production and Structure Core Facility (PTPSP) at EPFL.

### **Flow cytometry**

Antibodies used in this study were CD3-BV510 (UCHT1), CD19-APC-Cy7 (SJ25C1), CD38-V450 (HB7), IgG-BV605 (G18-145), IgD-PE-CF594 (IA6-2), CD21-PE-Cy7 (B-ly4), CD27-APC (M-T271), CD24-PerCP-Cy5.5 (ML5), CD20-Alexa Fluor 700 (2H7) and purchased from BD Biosciences. IgM-FITC (MHM-88) and Live/Dead Aqua were purchased from Biolegend and Thermo Scientific, respectively. For the cTfh panel, the antibodies used were CD3-PE (UCHT1), CD4-APC-H7 (RPA-T4 ), CXCR5-Alexa Fluor 647 (RF8B2), CXCR3-Pacific Blue (1C6), PD-1-PE-Cy7(EH12.1), ICOS-PerCP (DX29), CD45RO-FITC (UCHL1). Total PBMCs for all timepoints for each donor (3 donors each batch) were thawed at the same time and PBMCs were counted to 5 million PBMCs per test. For tetramer staining, total PBMCs were washed in PBS and incubated with 5µg/mL of H1N1 tetramer-AviTag for 30 minutes at 37 C in PBS. Afterwards, PBMCs were washed again in PBS and surface staining with antibody cocktails for B cell phenotype including streptavidin-PE (1:500) for tetramer detection. Cells were washed and fixed in 2% formaldehyde before running on the flow cytometer.

## References

1. Belongia, E.A., et al., *Variable influenza vaccine effectiveness by subtype: a systematic review and meta-analysis of test-negative design studies*. *Lancet Infect Dis*, 2016. **16**(8): p. 942-51.
2. Neumann, G., T. Noda, and Y. Kawaoka, *Emergence and pandemic potential of swine-origin H1N1 influenza virus*. *Nature*, 2009. **459**(7249): p. 931-9.
3. Nachbagauer, R. and F. Krammer, *Universal influenza virus vaccines and therapeutic antibodies*. *Clin Microbiol Infect*, 2017. **23**(4): p. 222-228.
4. Ohmit, S.E., et al., *Influenza hemagglutination-inhibition antibody titer as a correlate of vaccine-induced protection*. *J Infect Dis*, 2011. **204**(12): p. 1879-85.
5. Arriola, C., et al., *Influenza Vaccination Modifies Disease Severity Among Community-dwelling Adults Hospitalized With Influenza*. *Clin Infect Dis*, 2017. **65**(8): p. 1289-1297.
6. Gustafson, C.E., et al., *Influence of immune aging on vaccine responses*. *J Allergy Clin Immunol*, 2020. **145**(5): p. 1309-1321.
7. Crooke, S.N., et al., *Immunosenescence and human vaccine immune responses*. *Immun Ageing*, 2019. **16**: p. 25.
8. Koutsakos, M., T.H.O. Nguyen, and K. Kedzierska, *With a Little Help from T Follicular Helper Friends: Humoral Immunity to Influenza Vaccination*. *J Immunol*, 2019. **202**(2): p. 360-367.
9. Crotty, S., *T Follicular Helper Cell Biology: A Decade of Discovery and Diseases*. *Immunity*, 2019. **50**(5): p. 1132-1148.
10. Ueno, H., *Tfh cell response in influenza vaccines in humans: what is visible and what is invisible*. *Curr Opin Immunol*, 2019. **59**: p. 9-14.
11. Bentebibel, S.E., et al., *Induction of ICOS+CXCR3+CXCR5+ TH cells correlates with antibody responses to influenza vaccination*. *Sci Transl Med*, 2013. **5**(176): p. 176ra32.
12. Bentebibel, S.E., et al., *ICOS(+)PD-1(+)CXCR3(+) T follicular helper cells contribute to the generation of high-avidity antibodies following influenza vaccination*. *Sci Rep*, 2016. **6**: p. 26494.
13. Chambers, B.S., et al., *Identification of Hemagglutinin Residues Responsible for H3N2 Antigenic Drift during the 2014-2015 Influenza Season*. *Cell Rep*, 2015. **12**(1): p. 1-6.
14. DiazGranados, C.A., et al., *Efficacy and immunogenicity of high-dose influenza vaccine in older adults by age, comorbidities, and frailty*. *Vaccine*, 2015. **33**(36): p. 4565-71.
15. Lee, J.K.H., et al., *Efficacy and effectiveness of high-dose versus standard-dose influenza vaccination for older adults: a systematic review and meta-analysis*. *Expert Rev Vaccines*, 2018. **17**(5): p. 435-443.
16. Pilkinton, M.A., et al., *Greater activation of peripheral T follicular helper cells following high dose influenza vaccine in older adults forecasts seroconversion*. *Vaccine*, 2017. **35**(2): p. 329-336.
17. Kim, J.H., et al., *High-dose influenza vaccine favors acute plasmablast responses rather than long-term cellular responses*. *Vaccine*, 2016. **34**(38): p. 4594-4601.
18. Henry, C., et al., *Influenza Virus Vaccination Elicits Poorly Adapted B Cell Responses in Elderly Individuals*. *Cell Host Microbe*, 2019. **25**(3): p. 357-366 e6.
19. Herati, R.S., et al., *Circulating CXCR5+PD-1+ response predicts influenza vaccine antibody responses in young adults but not elderly adults*. *J Immunol*, 2014. **193**(7): p. 3528-37.
20. Koutsakos, M., et al., *Circulating TFH cells, serological memory, and tissue compartmentalization shape human influenza-specific B cell immunity*. *Sci Transl Med*, 2018. **10**(428).
21. Matsui, K., et al., *Circulating CXCR5(+)CD4(+) T Follicular-Like Helper Cell and Memory B Cell Responses to Human Papillomavirus Vaccines*. *PLoS One*, 2015. **10**(9): p. e0137195.
22. Huber, J.E., et al., *Dynamic changes in circulating T follicular helper cell composition predict neutralising antibody responses after yellow fever vaccination*. *Clin Transl Immunology*, 2020. **9**(5): p. e1129.
23. Bowyer, G., et al., *CXCR3(+) T Follicular Helper Cells Induced by Co-Administration of RTS,S/AS01B and Viral-Vectored Vaccines Are Associated With Reduced Immunogenicity and Efficacy Against Malaria*. *Front Immunol*, 2018. **9**: p. 1660.

24. Farooq, F., et al., *Circulating follicular T helper cells and cytokine profile in humans following vaccination with the rVSV-ZEBOV Ebola vaccine*. *Sci Rep*, 2016. **6**: p. 27944.
25. Juno, J.A., et al., *Humoral and circulating follicular helper T cell responses in recovered patients with COVID-19*. *Nat Med*, 2020. **26**(9): p. 1428-1434.
26. Zhang, J., et al., *Circulating CXCR3(+) Tfh cells positively correlate with neutralizing antibody responses in HCV-infected patients*. *Sci Rep*, 2019. **9**(1): p. 10090.
27. Baiyegunhi, O., et al., *Frequencies of Circulating Th1-Biased T Follicular Helper Cells in Acute HIV-1 Infection Correlate with the Development of HIV-Specific Antibody Responses and Lower Set Point Viral Load*. *J Virol*, 2018. **92**(15).

Figure 1.

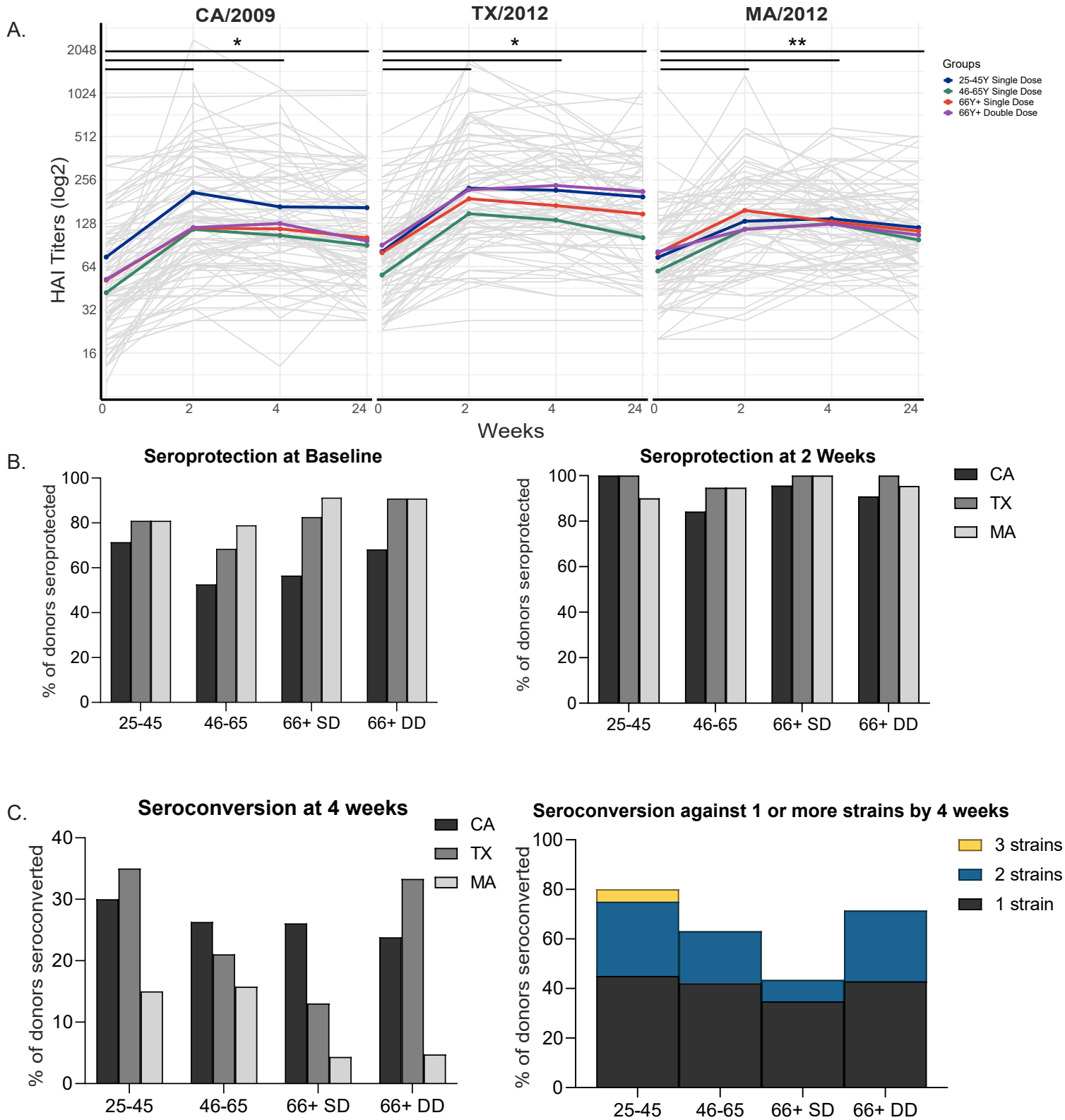


Figure 1. Vaccine immunogenicity measured by HIA titer responses  
HIA titers were measured for all donors at baseline, 2 weeks, 4 weeks and 24 weeks post vaccination. (A) Geometric mean of vaccine responses for each group. (B) Seroprotection at baseline and at 2 weeks post-vaccination. (C) Seroconversion rates were measured at 4 weeks for different age groups and seroconversion against 1 or more strains were measured within age groups

Figure 2.

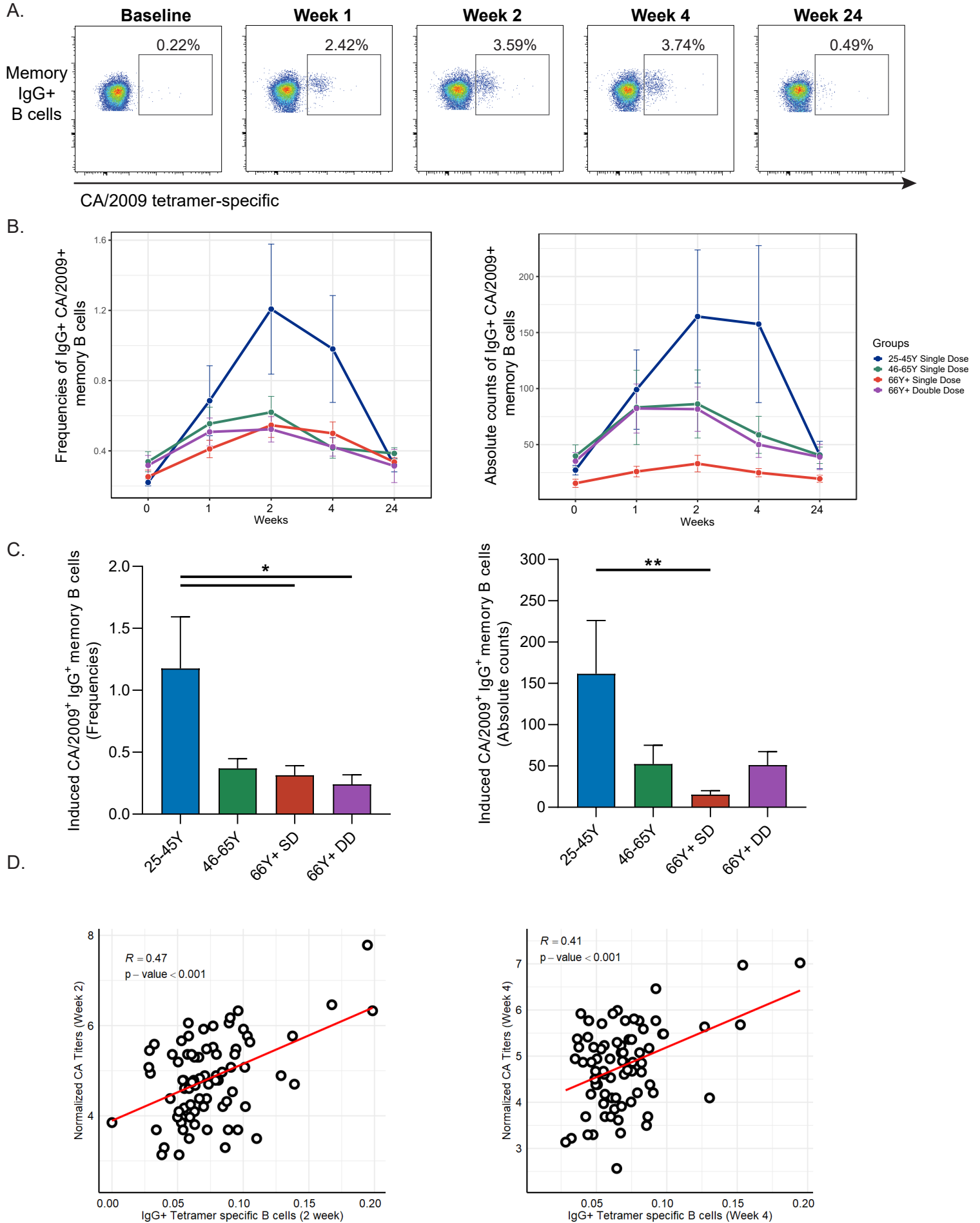


Figure 2 cont.

E.

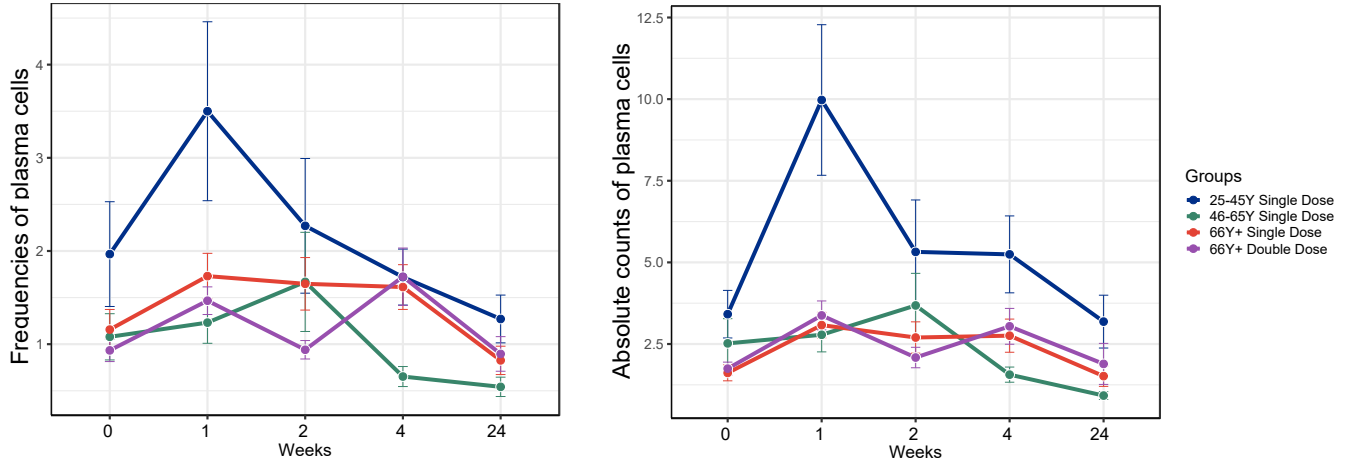


Figure 2. Antigen-specific memory IgG+ B cell response

(A) Memory B cell response to CA/2009 tetramer shown over time on a representative donor. (B) Mean frequencies and absolute counts shown for each age group over time. (C) Induced frequencies and absolute counts of CA/2009+ IgG+ memory B cells from baseline to peak expression (2 weeks) measured across all age groups. (D) Pearson's correlations of CA/2009-specific IgG+ memory B cell frequencies (arcsinh-transformed) at week 2 and 4 with CA titer values (log-transformed) from week 2 and week 4, respectively. (E) Mean frequencies and absolute counts of plasma cells (CD19+ CD27+ CD38++ IgG+) shown for all age groups and time points.

Figure 3.

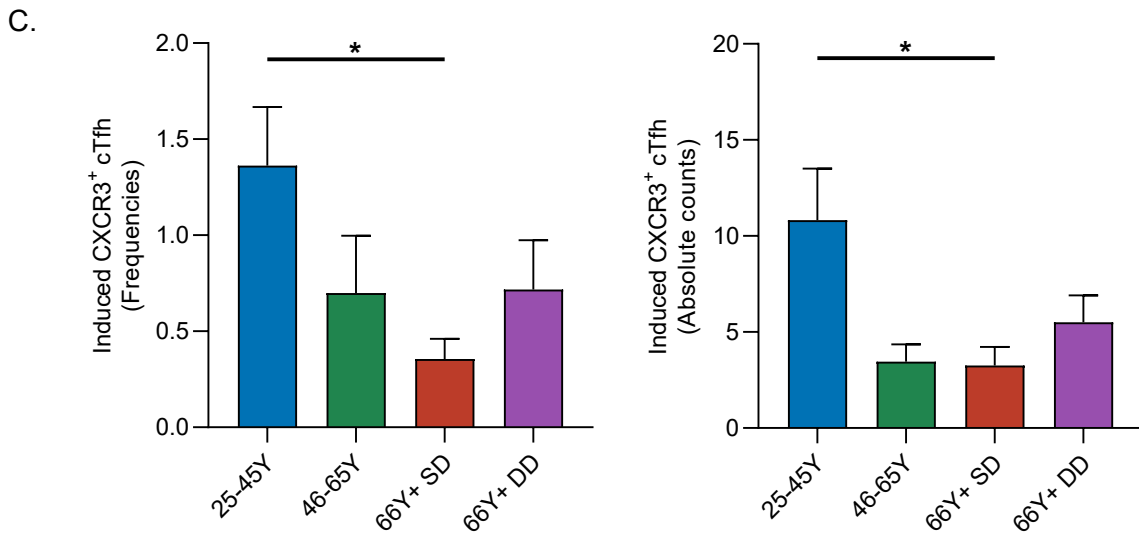
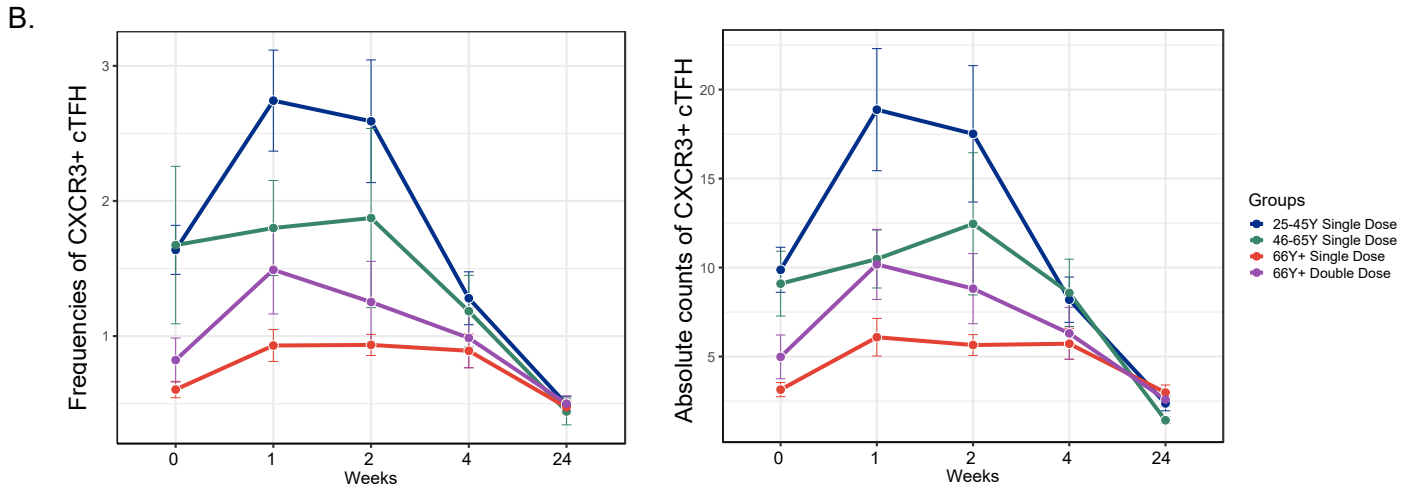
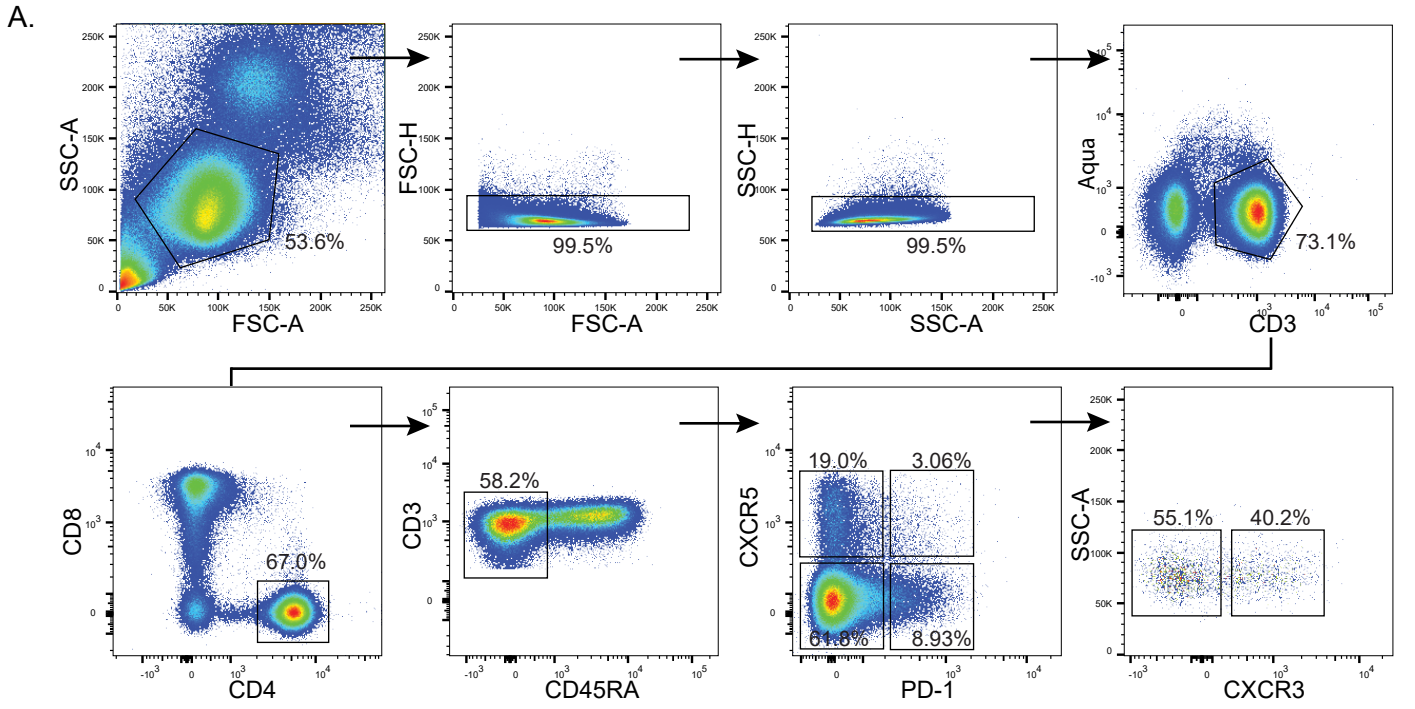


Figure 3 cont.

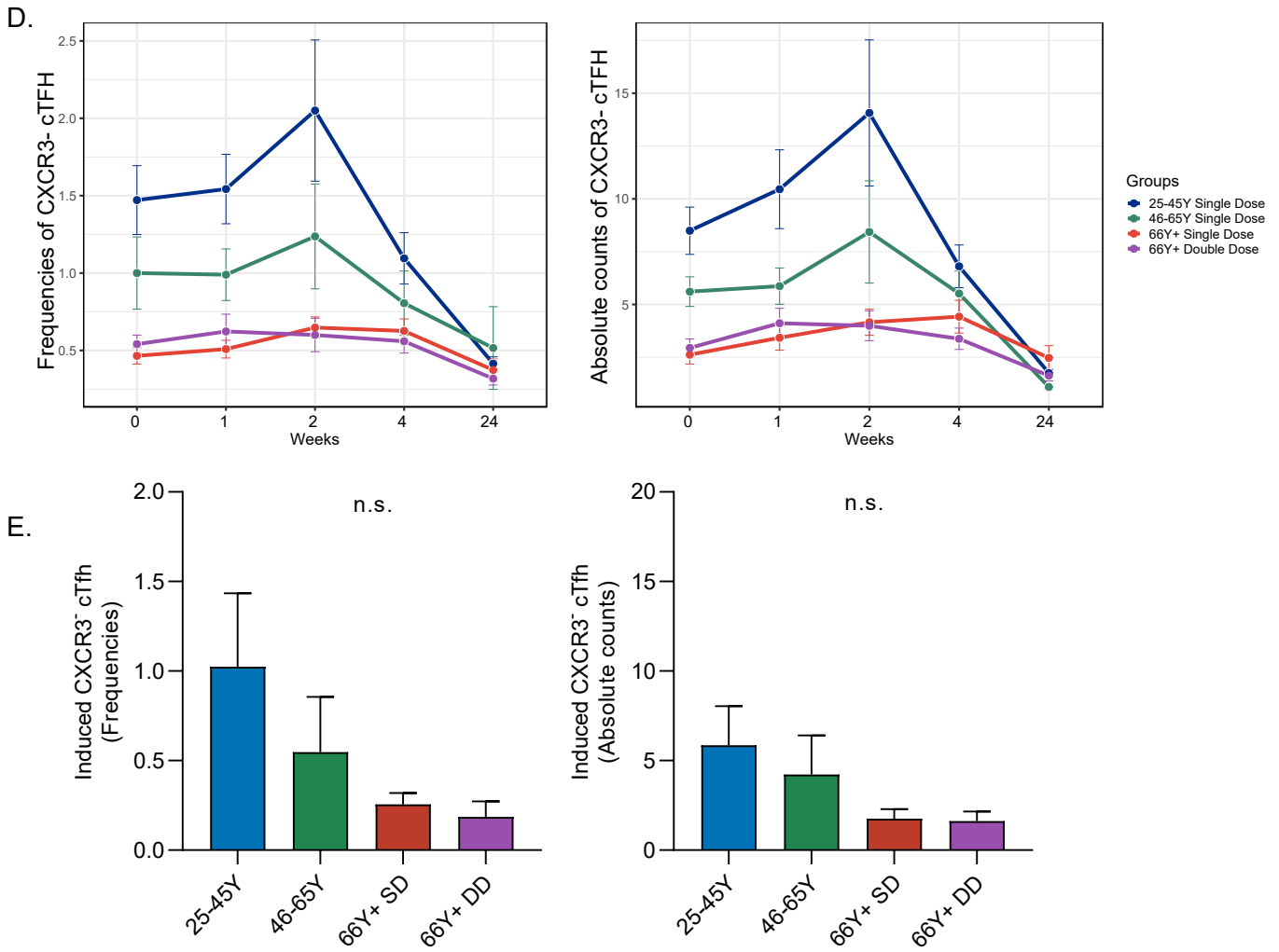
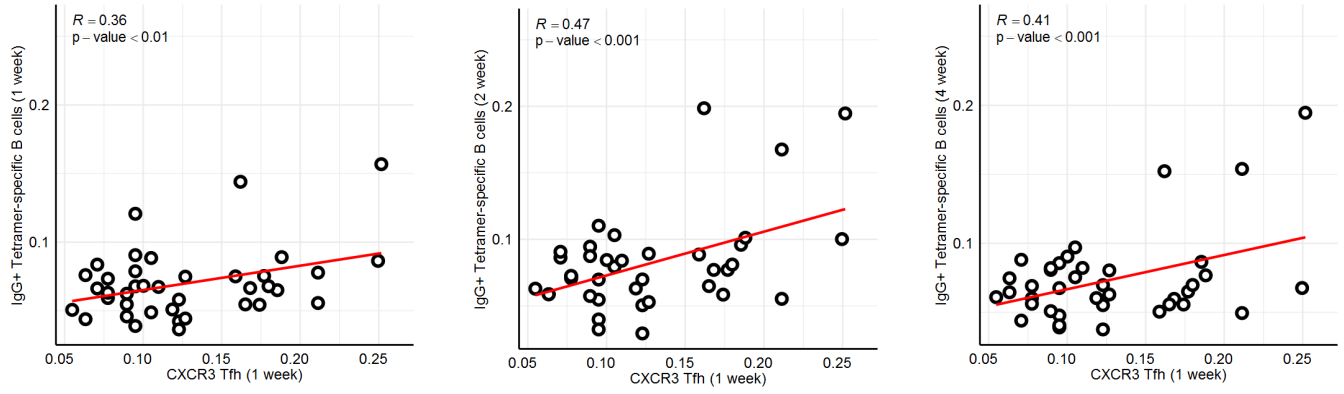


Figure 3. cTFH response in different age groups with influenza vaccination

(A) Gating strategy for cTFH phenotype (CD3<sup>+</sup> CD4<sup>+</sup> CD45RA<sup>-</sup> PD-1<sup>+</sup> CXCR5<sup>+</sup>) from blood. (B) Mean frequencies and absolute counts for CXCR3<sup>+</sup> cTfh for all age groups and time points. (C) Induced frequencies and absolute counts of CXCR3<sup>+</sup> cTfh from baseline to peak expression (1 week) measured across all age groups. (D) Mean frequencies and absolute counts of CXCR3<sup>+</sup> cTfh for all age groups and time points. (E) Induced frequencies and absolute counts of CXCR3<sup>+</sup> cTfh from baseline to peak expression (2 weeks) measured across all age groups.

Figure 4.

A.



B.

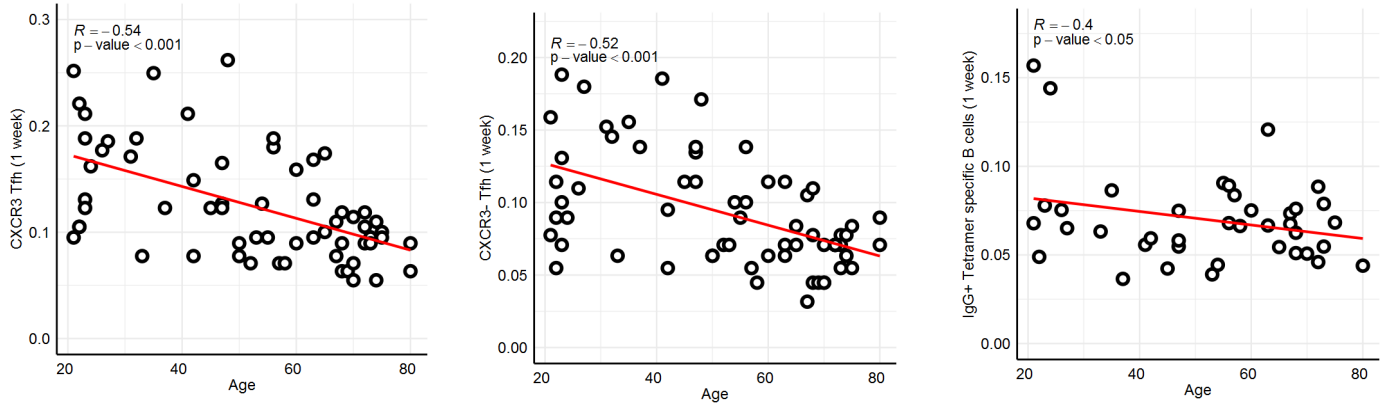


Figure 4. Correlative responses for antigen-specific B cells, cTfh, and age (A) Pearson's correlation on antigen-specific memory B cell frequencies over 1, 2, 4 weeks measured against CXCR3+ cTfh frequencies (arcsinh-transformed). (B) Pearson's correlation of cTFH and tetramer+ B cell frequencies with age.

TABLE S1: Longitudinal seroprotection rates measured by HIA quantification

	Influenza strain		
	CA/2009	TX/2012	MA/2012
<b>Baseline</b>			
25 – 45	15 (71.4)	17 (80.9)	17 (80.9)
46 – 65	10 (52.6)	13 (68.4)	15 (78.9)
66 + <i>SD</i>	13 (56.5)	19 (82.6)	21 (91.3)
66 + <i>DD</i>	15 (68.2)	20 (90.9)	20 (90.9)
<b>2 Weeks</b>			
25 – 45	20 (100)	20 (100)	18 (90.0)
46 – 65	16 (84.2)	18 (94.7)	18 (94.7)
66 + <i>SD</i>	22 (95.6)	23 (100)	23 (100)
66 + <i>DD</i>	20 (90.9)	22 (100)	21 (95.4)
<b>4 Weeks</b>			
25 – 45	19 (95.0)	20 (100)	19 (95)
46 – 65	16 (84.2)	18 (94.7)	19 (100)
66 + <i>SD</i>	22 (95.6)	23 (100)	23 (100)
66 + <i>DD</i>	20 (95.2)	21 (100)	21 (100)
<b>6 Months</b>			
25 – 45	19 (95.0)	20 (100)	19 (95)
46 – 65	17 (89.5)	18 (94.7)	18 (94.7)
66 + <i>SD</i>	20 (86.9)	23 (100)	23 (100)
66 + <i>DD</i>	20 (90.9)	22 (100)	22 (100)

Seroprotection is designated as  $\geq 40$  HIA titer values

Table S1. Seroprotection rates of different age groups at each time point to the 3 influenza strains. Antibody titers were measured by HIA quantification and rates of seroprotection were determined by titer values 40 or above.

Supplemental Figure 1.

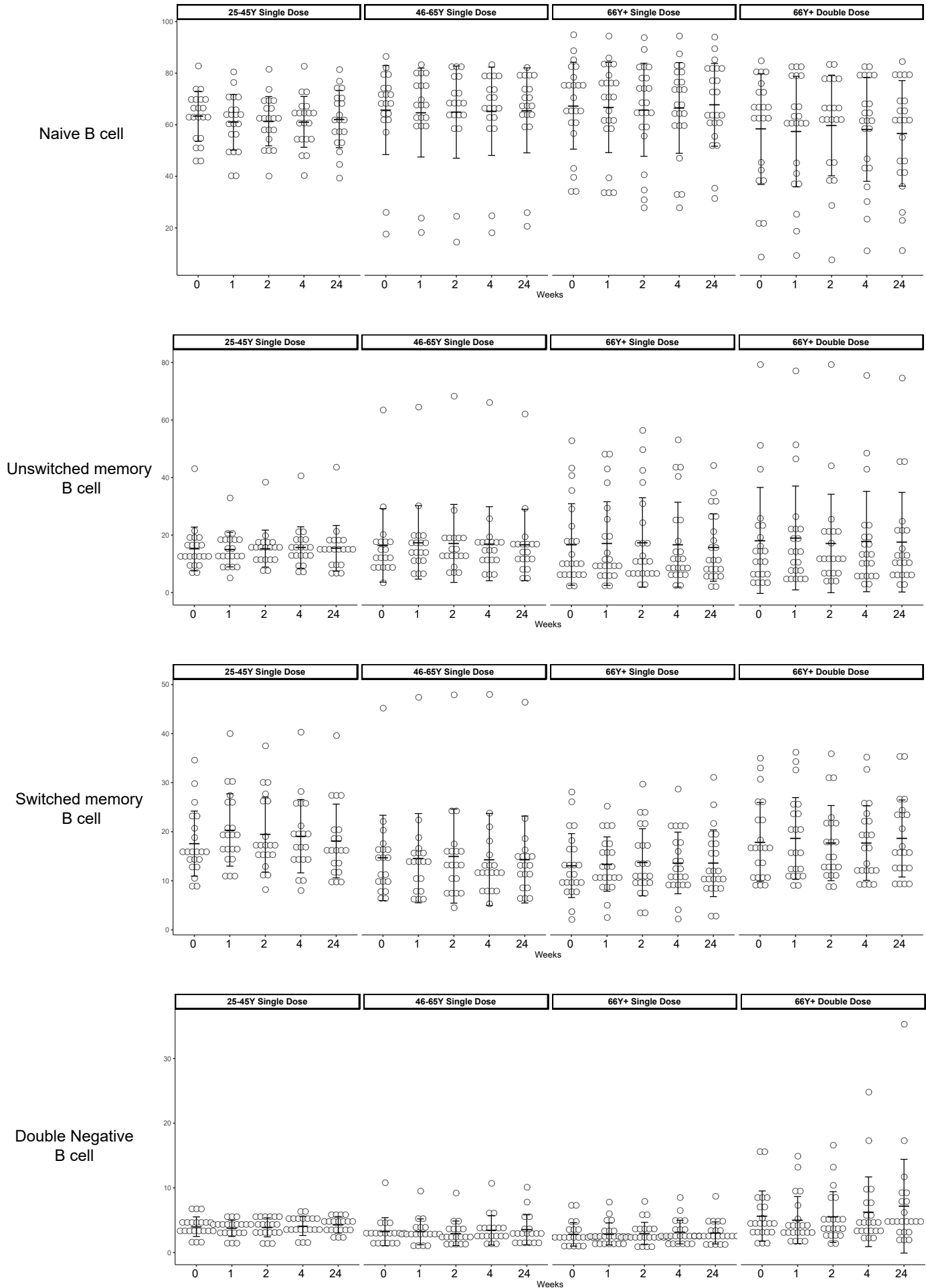


Figure S1. Frequencies of B cell populations with different age groups for baseline, 1, 2, 4, and 24 weeks post-vaccination. Naive (CD27-, IgD+), unswitched memory (CD27+, IgD+), switched memory (CD27+, IgD-), and double negative (CD27-, IgD-) B cell frequencies plotted for each donor; mean and standard error bar for each group and timepoint is overlaid.

Supplemental Figure 2.

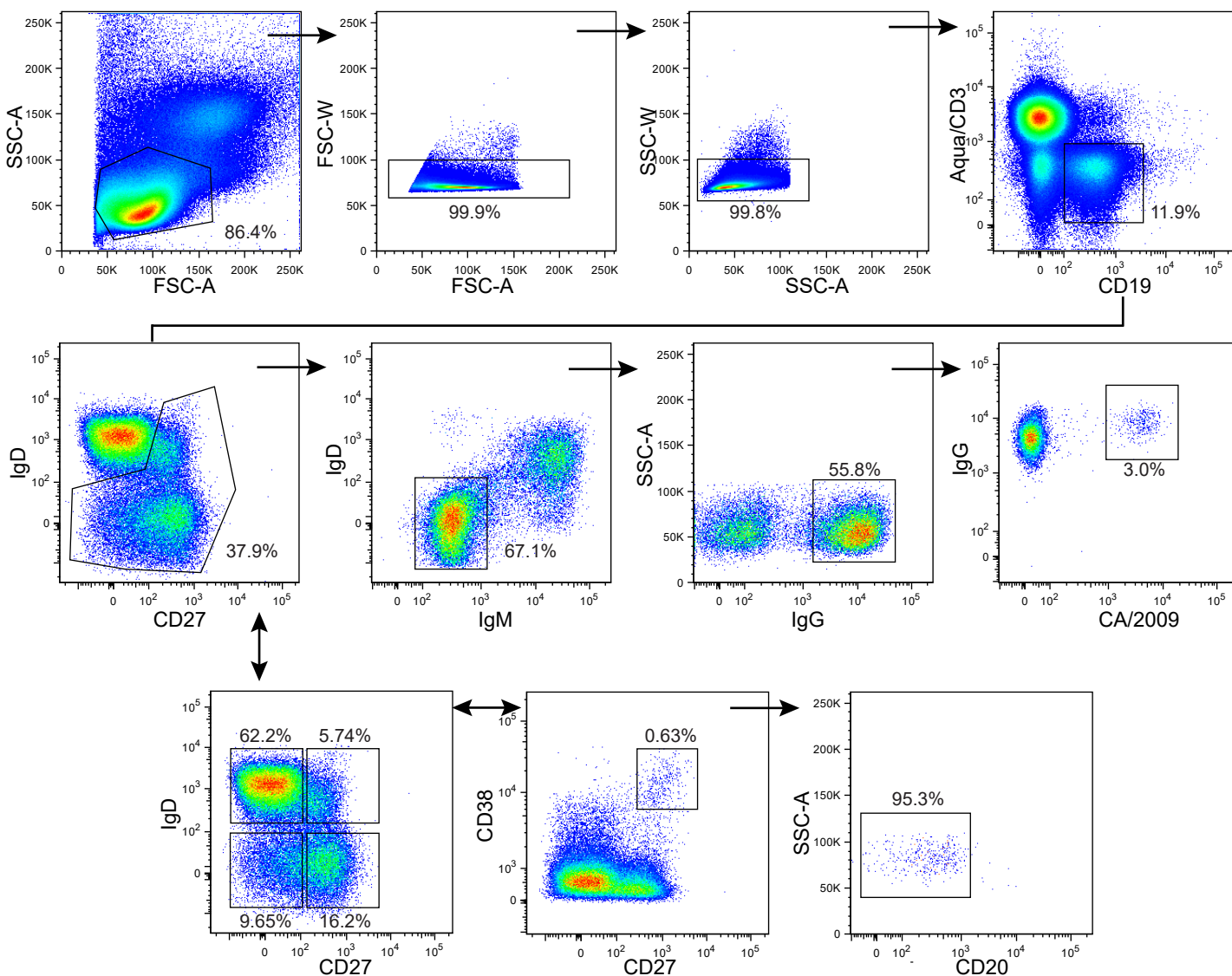


Figure S1. Gating strategy for memory B cell

Representative gating strategy for the detection of CA/2009 antigen-specific IgG switched memory B cells. Total CD19+ B cells were also stratified into naive, unswitched memory, switched memory, and double negative B cell from IgD and CD27 gating as well as CD27+ CD38++ CD20- plasma cells.

Supplemental Figure 3.

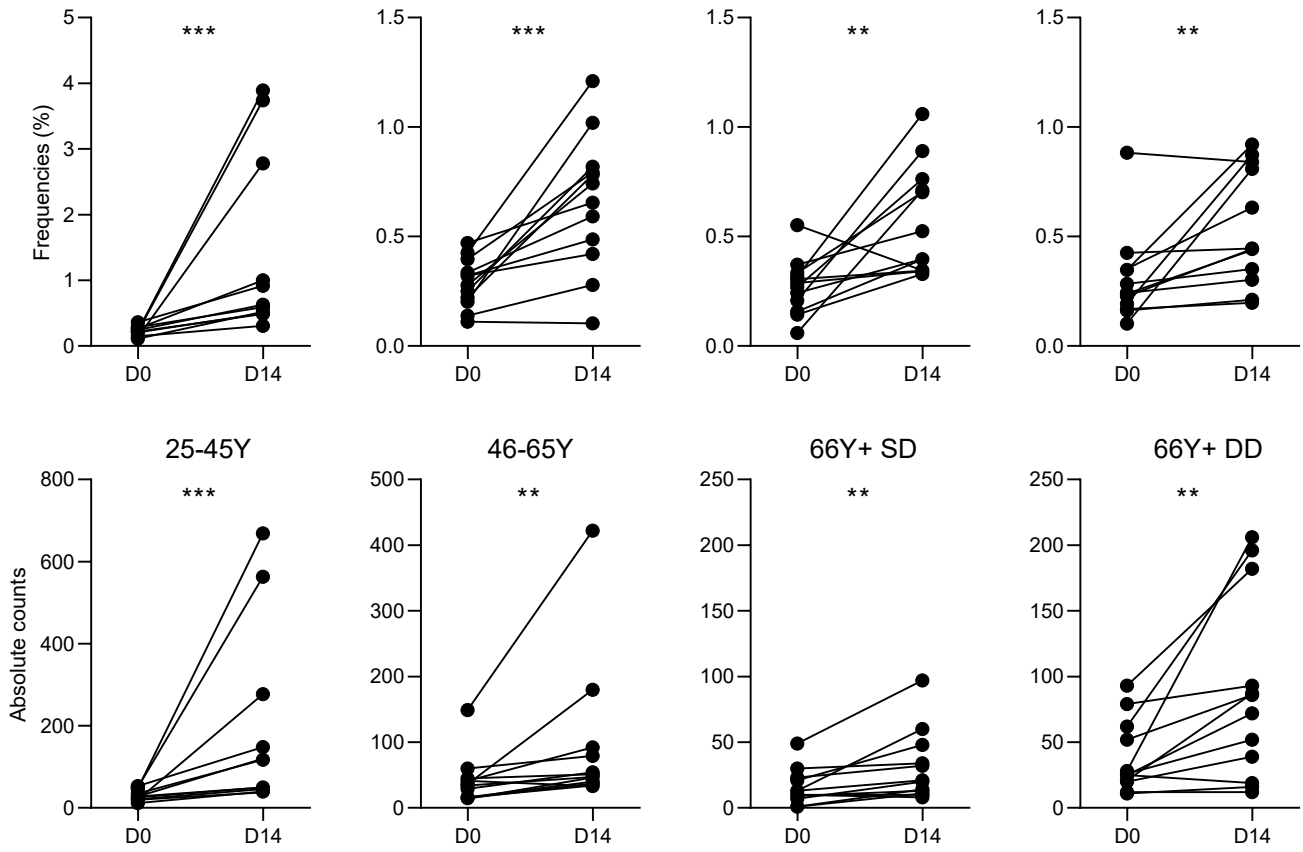


Figure S3. Frequencies and absolute counts of CA/2009-specific IgG+ memory B cells at baseline compared to timepoint for peak expression at 2 weeks. Each individual donor for all age groups were plotted and non-parametric paired t-test was performed.

Supplemental Figure 4.

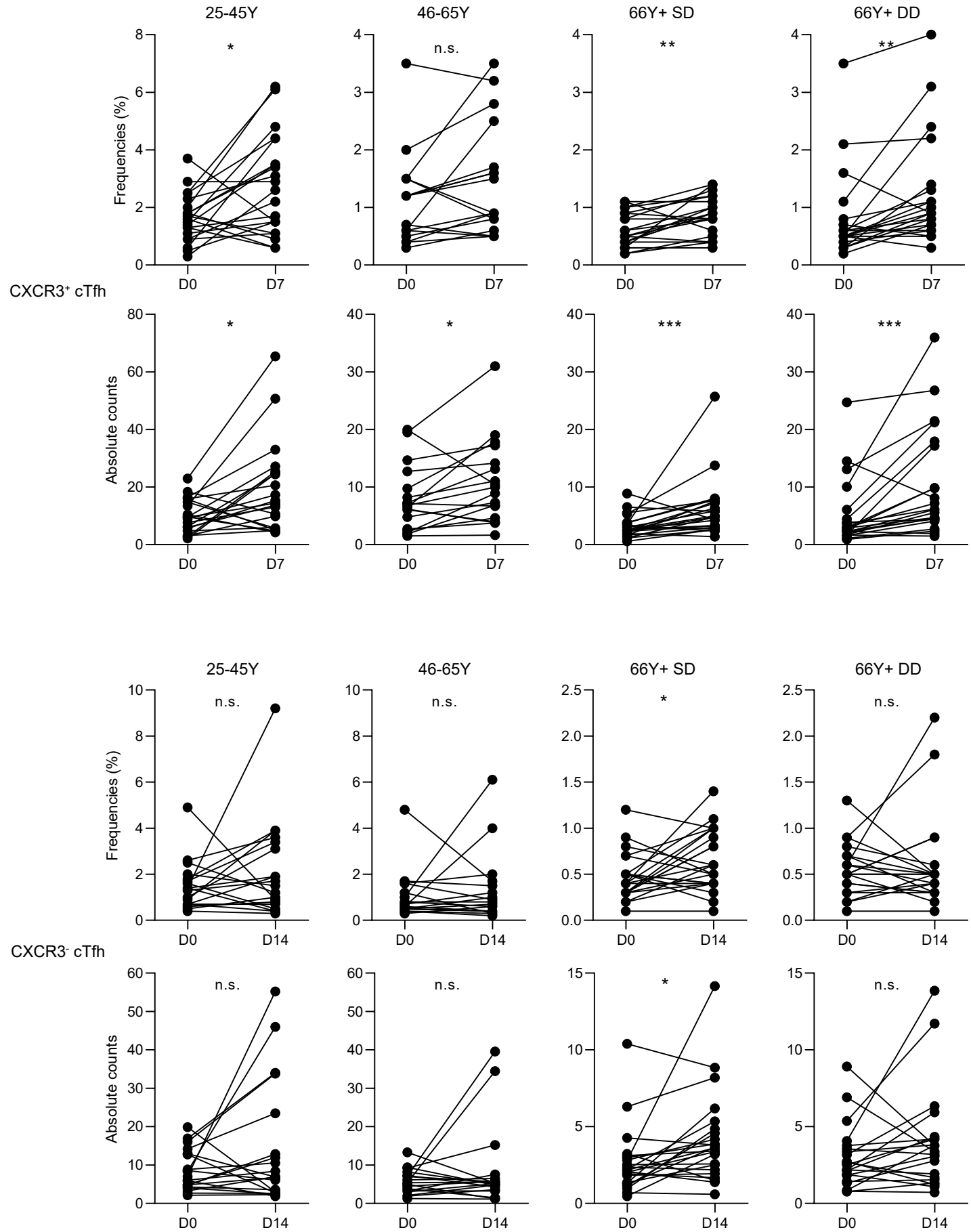


Figure S3. Frequencies and absolute counts of CXCR3+/- cTfh at baseline compared to timepoint for peak expression (1 week for CXCR3+ cTfh and 2 weeks for CXCR3- cTfh). Each individual donor for all age groups were plotted and non-parametric paired t-test was performed.